Wear Measurement of Polyethylene Components in Total Knee Replacement

Wei Jiang

Submitted in accordance with the requirements for the degree of

Doctor of Philosophy

The University of Leeds

Institute of Medical and Biological Engineering, School of Mechanical Engineering

Under supervision of

Professor John Fisher

Professor Zhongmin Jin

Professor Ruth K Wilcox

Dr Claire Brockett

February 2014

The candidate confirms that the work submitted is his own, except where work that has formed part of jointly authored publications has been included. The contribution of the candidate and the other authors to this work has been explicitly indicated below. The candidate confirms that appropriate credit has been given within the thesis where reference has been made to the work of others.

Acknowledgements

I would like to thank my supervisors, Professor John Fisher, Professor Zhongmin Jin, Professor Ruth K Wilcox and Dr Claire Brockett for their great supervision and professional guidance throughout my project.

I would like to acknowledge the financial support I received from the China Scholarship Council. I also wish to thank DePuy International, UK for the provision of the samples and CAD models used in this project.

Special thanks to Dr. Louise Jennings, Mr. Phil Wood, Mr. Lee Wetherill, Mrs. Jane Cardie, Mr. Adrian Eagles, Mrs. Amisha Desal, Mrs. Silvia Carbone, Mr. Keith Dyer and Mr. Irvin Homan, for their technical support throughout my research. Thanks to Mrs. Debra Baldwin and Ms. Cheryl Harris for their administrative support. Many thanks to Dr Ling Wang for her patient guidance with the CMM training. I would like to thank Dr Raman Maiti for his help with the experimental work. Also, thanks to Dr Abdellatif A.Y.Abdelgaied for his help with the computational modelling. Special thanks to 442C guys for their help and invaluable discussions.

Most of all, I would like to thank my family for their continued support. Thanks to my wife, Dr Cuicui Ji, who is the most important person in my life. Thanks for her support and encouragement in the past four years. I would like to dedicate my thesis to my parents.

Abstract

The total knee replacement (TKR) was designed to provide final-stage treatment for patients to replace the damaged biological tissues and help the patient to carry out daily normal activities. Determination of wear of the polyethylene knee inserts has been an important subject in improving the longevity of TKR. Accurate wear measurement methodologies are essential to differentiate between the performance of different materials and designs because the geometry changes can be small and can consist of both wear and creep.

The aim of this study was to develop a coordinate based three-dimensional volumetric determination methodology using CMM and Micro-CT measurement techniques. The validation of the methodology was carried out using a FE model and computational volume removal test. Afterwards, the volumetric determination method was used to calculate the volume loss from computational and experimental tests of volume removal and creep deformation. Finally, the methodology was applied to evaluate both simulator and retrieval specimens. The studies indicated the presented volumetric determination methodology was not dependent on pre-wear data, CAD model or original design drawings and can be used for both simulator and retrieval analysis at relevant levels of wear and creep. It can also be applied to the biotribological study of other polyethylene components, since wear and damage can be assessed visually and volumetrically. The comparison between CMM and Micro-CT methods suggested that the CMM has higher accuracy and better repeatability. Whilst the methods developed in this thesis were suitable for laboratory and computational wear determination, they are not suitable for all specimens in retrieval study due to the greater amount of wear and damage on the surface.

Table of Contents

Acknowledgements ..... **iii**
Abstract ..... **iv**
Table of Contents ..... **v**
List of Figures ..... **ix**
List of Tables ..... **xiii**
Abbreviations ..... **xv**
Nomenclature ..... **xvi**
Chapter 1 Introduction and Literature Review **1**
1.1 Introduction of Total Knee Replacement 1
1.2 The normal knee joint 4
1.2.1 Geometry and structure 5
1.2.2 Loading and Motion in the Knee 8
1.3 Polyethylene 11
1.3.1 Material properties of polyethylene 11
1.3.2 Highly Crosslinked polyethylene 15
1.3.3 Vitamin E polyethylene 17
1.3.4 Polyethylene wear 19
1.4 Laboratory and retrieval study 23
1.4.1 Laboratory testing of polyethylene components in TKR 23
1.4.2 Retrieval analysis of polyethylene component in TKR 27
1.5 Wear Measurement Method 30
1.5.1 Radiographic methods 32
1.5.2 Roentgen stereophotogrammetric analysis (RSA) 34
1.5.3 Micro-CT based methods 37
1.5.4 CMM-based methods 42
1.6 Project aims and objectives 45
1.6.1 Rationale 45
1.6.2 Aims and objectives 46
1.6.3 Thesis outline 47
Chapter 2 Wear Measurement Methodology **48**
2.1 Introduction 48

2.2 Gravimetric measurement 49
2.2.1 Cleaning 50
2.2.2 Weighing 50
2.2.2.1 Calibration 51
2.3 Micro-Computed Topography (Micro-CT) measurement 52
2.3.1 Introduction 52
2.3.2 Micro-CT scanning 53
2.3.2.1 Calibration 55
2.3.3 Micro-CT image analysis 56
2.3.4 Derivation of surface coordinate data 60
2.4 Coordinates Measuring Machine (CMM) measurement 62
2.4.1 Introduction 62
2.4.2 Calibration 64
2.4.3 Sample preparation for measurement 65
2.4.4 The influence of configuration 69
2.4.5 The influence of CMM scan interval 71
2.4.6 Data analysis 74
2.5 Concordance correlations coefficient (CCC) 75
Chapter 3 Coordinate Based Novel Volumetric Determination Methodology for PE Tibial Knee Components 77
3.1 Introduction 77
3.2 Volumetric determination methodology 78
3.2.1 Volumetric determination with a reference 79
3.2.2 Volumetric determination without a reference 80
3.2.2.1 Undeformed region identification 81
3.2.2.2 Polynomial surface curve fitting 83
3.3 Methodology validation 89
3.3.1 Validation with reference 90
3.3.2 Validation without reference 91
3.3.2.1 Validation from FE model 91
3.3.2.2 Validation from computational volume removal 95
3.4 Discussion 97
Chapter 4 Computational and Experimental Studies of Simulated Wear Tests 100
4.1 Introduction 100

4.2 Materials and Methods 101
4.2.1 Computational wear test 101
4.2.2 Experimental wear test 102
4.3 Results 105
4.3.1 Computational wear test results 105
4.3.2 Experimental wear test results 109
4.4 Discussion 112
Chapter 5 Computational and Experimental Studies of Creep Deformation Tests 115
5.1 Introduction 115
5.2 Materials and Methods 116
5.2.1 Computational creep test 116
5.2.1.1 Creep generation using a 22mm ball 116
5.2.1.2 Creep generation using a femoral component 118
5.2.2 Experimental creep test 119
5.2.2.1 Knee simulator 119
5.2.2.2 Creep deformation test 122
5.3 Results 123
5.3.1 Computational creep test results 123
5.3.1.1 Creep results of PFC sigma 22 mm ball test model 123
5.3.1.2 Creep results of PFC sigma test model 126
5.3.2 Experimental creep test results 128
5.3.2.1 Soak control 128
5.3.2.2 Geometrical creep measurements 129
5.4 Discussion 131
Chapter 6 Comparison of CMM and Micro-CT Volumetric Analysis of Laboratory Specimens 137
6.1 Introduction 137
6.2 Materials and Methods 138
6.2.1 CMM 138
6.2.2 Micro-CT 139
6.3 Results 140
6.4 Discussion 143
Chapter 7 Retrieval Analysis 148
7.1 Introduction 148

7.2 Materials and Methods 149
7.3 Results 152
7.3.1 Visual inspection 152
7.3.2 Volumetric determination 155
7.4 Discussion 156
7.5 Conclusion 158
Chapter 8 Overall Discussion, Conclusion and Future Work 159
8.1 Overall discussion 159
8.2 Conclusion 163
8.3 Future work 164
References 165
Appendix (List of Conference Publications) 179
Appendix A 180

List of Figures

Figure 1.1 Components of total knee prosthesis……..…… 2

Figure 1.2 DePuy Low Contact Stress (LCS) Mobile Bearing Total Knee… 3

Figure 1.3 The basic structure of a synovial joint……..5

Figure 1.4 The anatomy of the knee joint. ……6

Figure 1.5 Polyethylene chain…… 14

Figure 1.6 Applied stress and included strain as functions of time over a short period for a viscoelastic material…….. 14

Figure 1.7 Structure of tocopherols……...18

Figure 1.8 Effect of vitamin-E concentration on the crosslink density of 100kGy, gamma irradiated UHMWPE……...19

Figure 1.9 Multifactorial causes of polyethylene wear……20

Figure 1.10 Typical appearance of delamination on a polyethylene tibial insert…… 22

Figure 1.11 ISO standard axial force (AF) [N] and flexion-extension (FE) [degree], for total knee replacement wear test machines…….25

Figure 1.12 Scanning electron microscopy of the polyethylene wear particles…….. 27

Figure 1.13 Patterns of polyethylene surface deformation…… 29

Figure 1.14 A schematic diagram of the imaging system……..33

Figure 1.15 Closest connection line between virtual projection and actural projection……35

Figure 1.16 Three methods used to estimate volumetric loss…….. 37

Figure 1.17 Thresholded image acquiring by changing the threshold scale……39

Figure 1.18 Third body debris embedded in the condyles of a polyethylene component with green colour……41

Figure 1.19 Translation and rotation of the x'-y'-z' reference frame…… 42

Figure 2.1 Mettler XP205 digital balance……. 49

Figure 2.2 Metal Control Pin…….. 51

Figure 2.3 Scanco Micro-CT100……53

Figure 2.4 Photograph of a typical tibial knee component…….53

Figure 2.5 Polyethylene methacrylate (PMMA) specimen holders……..54

Figure 2.6 Greyscale threshold……..57

Figure 2.7 µCT image slices from original greyscale to threshold……...57

Figure 2.8 Example of reconstructed 3D image…… 58

Figure 2.9 Schematic diagram of Micro-CT procedure……..59

Figure 2.10 Three-dimensional image reconstruction using image coordinates…….. 62

Figure 2.11 Mitutoyo Legex 322 Coordinate Measuring Machine……....64

Figure 2.12 CMM probe calibration by measuring the 20mm diameter ceramic master ball……... 65

Figure 2.13 Holder for tibial knee components used in CMM…….. 66

Figure 2.14 Definition of the x-y-z coordinates and the origin…….. 67

Figure 2.15 CAD model of PFC sigma tibial component and origin alignment…….. 68

Figure 2.16 Some styli and extensions used for CMM measurements…...69

Figure 2.17 Ruby silicon nitride zirconia styli with different diameter sizes 70

Figure 2.18 Different extensions used with stylus for greater reach……71

Figure 2.19 Renishaw scanning head used for coordinate measurement..72

Figure 2.20 The influence of CMM scan interval on volume difference….. 73

Figure 2.21 Reconstructed surface of left condyle……. 75

Figure 2.22 Assessing agreement of observed values and target values 76

Figure 3.1 CAD model of a typical tibial knee component as a reference..80

Figure 3.2 Acquiring of surface coordinates of tibial knee component……82

Figure 3.3 The profile in the x-z plane through y=25 mm of wear and the undeformed regions……83

Figure 3.4 Selection of reference line used for surface curve fitting……83

Figure 3.5 Volume difference and RMS error of 2nd to 5th order polynomial fitting……85

Figure 3.6 Residuals of 2nd to 5th order polynomial fitting at Y-Z plane... 86

Figure 3.7 Surface coordinates obtained using CMM and reconstructed original surface for volumetric assessment…….. 88

Figure 3.8 Max linear wear determination using profiles before and after wear……90

Figure 3.9 selection of reference line at different heights of z position…... 92

Figure 3.10 Selection of undeformed area used for curved surface fitting. 92

Figure 3.11 Two-dimensional profiles comparison with different selection of 'undeformed' region at different Y position..... 94

Figure 3.12 Profiles comparison (Y=25 mm, 55% undeformed region as reference, wear region range from 2% to 38%)……96

Figure 4.1 CMM measurement of left condyle of a new tibial knee component……. 102

Figure 4.2 Physical volume removal location on the left condyle… …….103

Figure 4.3 Experimental wear test on tibial knee component……104

Figure 4.4 The wear volume generated with increasing wear area……...107

Figure 4.5 Original surface reconstructed as pre-wear data……...107

Figure 4.6 Three-dimensional and X-Y images of computational wear test……...108

Figure 4.7 Comparison of gravimetric and geometrical wear measurement…….. 110

Figure 4.8 Three-dimensional and X-Y images of experimental wear test……...111

Figure 4.9 Comparison of theoretical and computational wear volume. ..113

Figure 4.10 Comparison of gravimetric and geometrical wear measurement with and without reference……..... 113

Figure 4.11 Plastic deformation was accompanied during the physical volume removal test……...114

Figure 5.1 The PFC sigma creep test model using a 22 mm ball……..117

Figure 5.2 The PFC sigma creep test model using a femoral component... 118

Figure 5.3 The ProSim (Manchester, UK) knee simulator……...120

Figure 5.4 Anatomical mounting of the TKR……..121

Figure 5.5 Contact location analysis to determine optimal positioning of insert for creep study…… 121

Figure 5.6 Flowchart describing the flow for creep test……... 123

Figure 5.7 Creep volume and maximum creep depth versus the test duration for 22 mm ball creep test model……. 125

Figure 5.8 Creep volume and maximum creep depth versus the test duration for PFC sigma creep test model……. 127

Figure 5.9 Weight changes of soak control samples throughout the creep test……...128

Figure 5.10 Creep volume and maximum creep depth versus the test duration for experimental creep test……. 130

Figure 5.11 Surface scar area of each creep test…….131

Figure 5.12 Comparison of FE model (22 mm diameter ball) and surface curve fitting methodology……..... 133

Figure 5.13 Comparison of FE model (femoral component) and surface curve fitting methodology…….. 134

Figure 5.14 Comparison of geometric analysis with and without initial surface geometry…… 135

Figure 6.1 CMM and Micro-CT measurement results of laboratory specimens with 95% confidence limit…….. 142

Figure 6.2 Comparison of CMM and Micro-CT volumetric analysis against gravimetric measurement……... 145

Figure 6.3 CMM and Micro-CT volumetric analysis results of laboratory specimens with 95% confidence limit……... 146

Figure 7.1 Tibial knee component retrievals……..152

Figure 7.2 Wear characteristics for tibial knee retrievals……154

List of Tables

Table 1.1 Reported tibio-femoral joint loads during daily activities……... 9

Table 1.2 Max compressive load and the knee flexion angles at different activities…… 10

Table 1.3 Molecular Weights of common polyethylene resin used in orthopaedic devices……..13

Table 1.4 List of highly crosslinked polyethylene used in total knee replacement……...16

Table 1.5 Measurement of wear rate in total knee replacement…….. 28

Table 1.6 Types of wear from 90 retrieved polyethylene components in knee prostheses…… 30

Table 1.7 Comparison of radiographic method and RSA method on translations and rotations…….. 36

Table 1.8 The changes in mean attenuation and the standard deviation for various parts of the phantom with different gantry angles…..41

Table 1.9 A comparison of CMM method and gravimetric method……..44

Table 2.1 Scanning parameters of Micro-CT100…….55

Table 2.2 IPL commands for volumetric measurement……..60

Table 2.3 The influence of CMM scan interval on volume difference……..73

Table 3.1 Comparison of different polynomial fitting and corresponding volume determination results…… 85

Table 3.2 Comparison of orthogonal and polynomial results…… 87

Table 3.3 Calculation results compared with the finite element model……90

Table 3.4 Surface curve fitting results with different reference coordinates…93

Table 3.5 Comparison of computational volume removal and surface curve fitting results……95

Table 4.1 Physical volume removal test parameters……104

Table 4.2 Computational wear test results……106

Table 4.3 Comparison of gravimetric and geometrical wear measurement. 110

Table 5.1 Creep deformation test results using a 22 mm ball……124

Table 5.2 Creep deformation test results using a femoral component…..126

Table 5.3 Experimental creep deformation tests……...129

Table 6.1 Total wear volume of specimens obtained using gravimetric analysis……..139

Table 6.2 CMM and Micro-CT volumetric measurement results……. 141

Table 7.1 Clinical data of tibial knee component retrievals……. 150

Table 7.2 Occurrence of damage modes in the tibial retrieval specimens…155

Abbreviations

ANOVA	Analysis of variance
AP	Anterior Posterior
BW	Body weight
CAD	Computer Aided Design
CCC	Concordance correlations coefficients
CL	Confidence limit
CMM	Co-ordinate measuring machine
FE	Flexion Extension
IPL	Image processing language
ISO	International Organisation of standardization
Micro-CT	Microscopic computed tomography
MC	Million cycles
PE	Polyethylene
PTFE	Polytetrafluoroethylene
SD	Standard deviation
TKR	Total knee replacement
UHMWPE	Ultra high molecular weight polyethylene
UKP	Unicompartmental Knee Prosthesis

Nomenclature

h	Thickness
t	Time
δ_{creep}	Creep wear depth
δ_{av}	Average pressure

Chapter 1

Introduction and Literature Review

1.1 Introduction of Total Knee Replacement

Total knee replacement (TKR) is being widely used as its successful and effective treatment of degenerative knee joint diseases, and 80 percent of which were carried out because of osteoarthritis of the knee. Every year about 0.5 million patients undergo total knee replacement surgery worldwide, and around 22000 of which take place in UK (National joint registry for England and Wales, 2004). The number of knee replacement operations is increasing every year worldwide (Carr and Goswami, 2009). There exist significant advantages in the type and quality of the metals, ultra high molecular weight polyethylene (UHMWPE), and, more recently, ceramics used in the prosthesis manufacturing process, leading to improved longevity. With modern techniques, more and more patients are receiving the benefits from TKR (Deirmengian and Lonner, 2008; Lee and Goodman, 2008). However, the longevity of TKR is limited due to damage of the articulating surface of tibial knee component (Wright and Bartel 1986; Landy and Walker 1988; Collier *et al*. 1991; Blunn *et al*. 1997; Wright and Goodman 2001), which leads to osteolysis and implant loosening. Determination of wear of the polyethylene knee inserts has been an important subject to improve the longevity of TKR (Krutz *et al*. 2004).

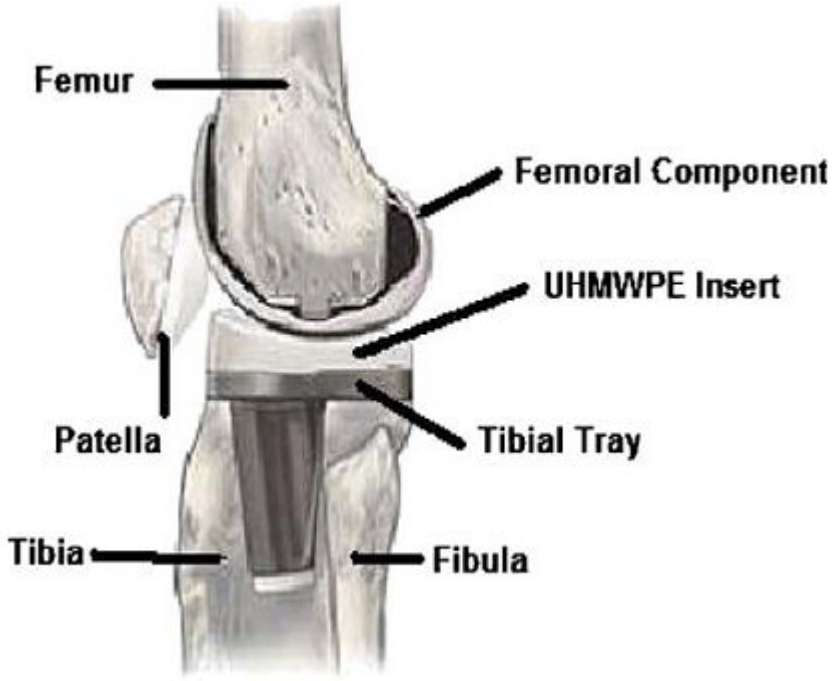

Figure 1.1 Components of total knee prosthesis (Willing and Kim 2009).

Figure 1.1 shows components of total knee prosthesis, which are generally combined with femoral component, tibial bearing component and tibial tray, and in some designs, patellar component, such as the low contact stress (LCS) mobile bearing manufactured by DePuy, which is demonstrated in Figure 1.2(b). The LCS mobile bearing allows the important rotation component to human knee motion, which is not included in many other fixed bearing designs, in which the tibial components are fixed together and result in additional stress on the polyethylene component and underlying bone. While in the LCS mobile bearing total knee replacememt, the metal tibial tray allows the tibial bearing component to rotate, as the femoral component rotates.

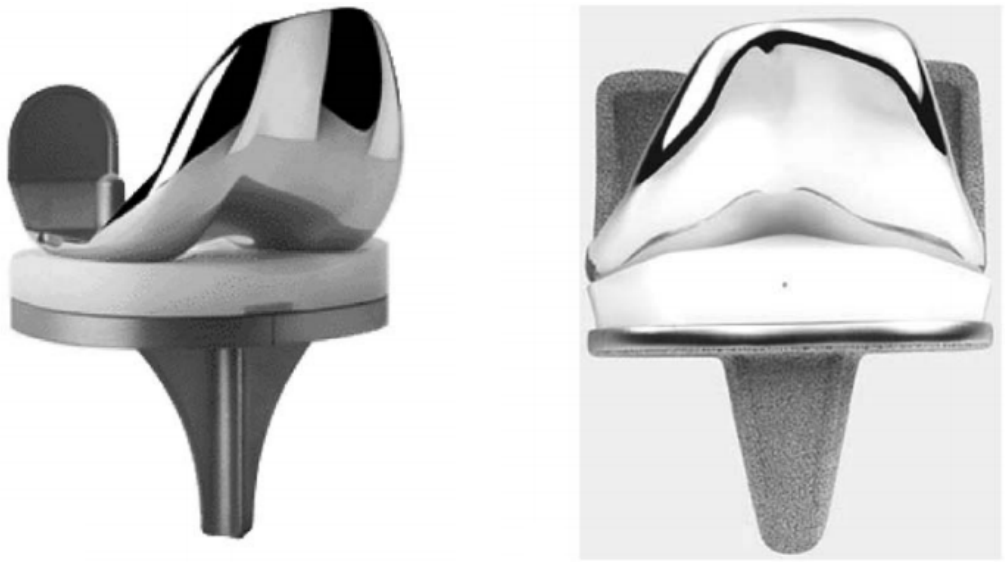

(a) (b)

Figure 1.2 (a) DePuy PFS Sigma; (b) DePuy Low Contact Stress (LCS) Mobile Bearing Total Knee (McEwen *et al*. 2005).

With the time goes by, implants can wear and loosen. It is considered that the main limiting factor to the longevity of TKR is the wear of polyethylene components, as the associated polyethylene wear debris may produce an adverse tissue reaction and subsequent loosening (Mcgloughlin and Kavanagh, 2000), studies show that up to 16% of knees fail due to wear (Engh, 1988). There are currently several kinds of techniques used to evaluate polyethylene wear based on gravimetric, radiographic, micro-computer tomography and more recently coordinates based. All of these measurement techniques have their own unique advantages and disadvantages; some of these have enough accuracy but cannot be used for clinical application, while others can be applied to medical usage, however, lack of accuracy because of roughly image based. In addition, another exist

problem is references are required for some measurement methods, such as gravimetric. As a result, novel measurement methods still need to be developed to evaluate the amount of wear accurately and used for both laboratory and clinical application.

1.2 The normal knee joint

A joint is the location at which two or more bones make contact in the human body, which is constructed to allow various movements and provide mechanical support during daily activities. There are three groups of joints in the human body: fibrous, cartilaginous and synovial. The synovial joints allow more movements than the other two types of joints. Figure 1.3 demonstrates the basic structure of a synovial joint. In the synovial joint, the end of the articulating surfaces is covered with articular cartilage, which reduces friction. The articulating bones are separated by a space called the joint cavity but held together by the synovial membrane, which forms a synovial capsule and secretes synovial fluid into the joint cavity for lubrication. The knee joint belongs to the third type, synovial joints, or can be called diarthrodial, which is the largest joint in human body. A healthy knee moves easily, allowing human to walk, turn, and squat without pain, which combines with a complex network of bones, cartilage, ligaments, muscles, and tendons work together to make a knee flexible. The knee is also one of the most vulnerable joints to both trauma and the development of degenerative lesions (Al-Turaiki, 1986).

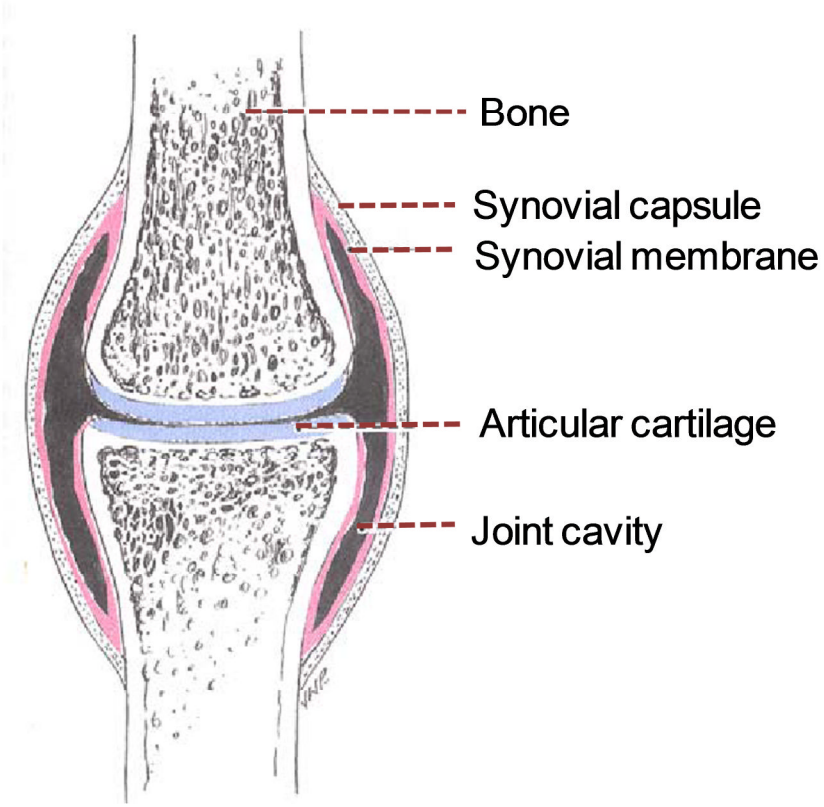

Figure 1.3 The basic structure of a synovial joint (Fisher, 2001).

1.2.1 Geometry and structure

The knee is a complex, compound, condyloid variety of a synovial joint. It actually comprises three functional compartments: the femoropatellar articulation consists of the patella, and the patellar groove on the front of the femur through which it slides; and the medial and lateral femorotibial articulations linking the femur, or thigh bone, with the tibia, the main bone of the lower leg. The joint is bathed in synovial fluid, which is contained inside the synovial membrane called the joint capsule. Figure 1.4 shows the anatomy of the knee joint.

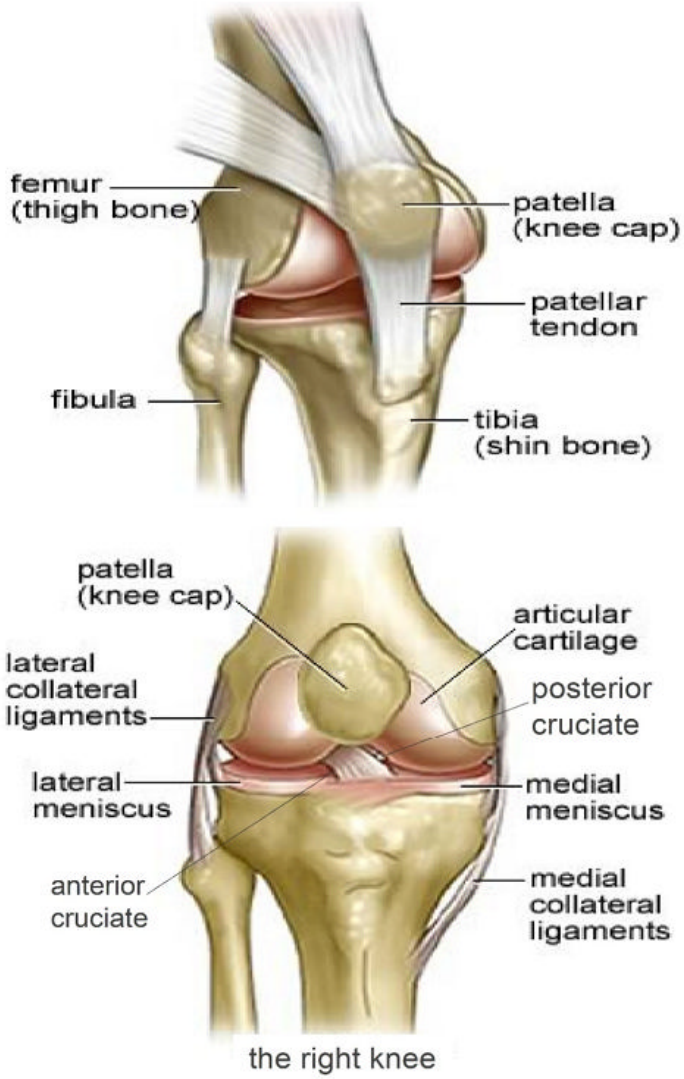

Figure 1.4 The anatomy of the knee joint (ACLSolutions 2012).

The articular bodies of the femur are its lateral and medial condyles. These diverge slightly distally and posteriorly, with the lateral condyle being wider in front than at the back while the medial condyle is of more constant width. The pair of tibial condyles is divided by the intercondylar eminence composed of a lateral and a medial tubercle. The patella is inserted into the thin anterior wall of the joint capsule. On its posterior surface are a lateral and a medial articular surface, both of which communicate with the patellar

surface, which unites the two femoral condyles on the anterior side of the bone's distal end (Werner *et al.* 2004). The articular capsule has a synovial and a fibrous membrane separated by fatty deposits. Anteriorly, the synovial membrane is attached on the margin of the cartilage on both the femur and the tibia, but on the femur, the suprapatellar bursa or recess extends the joint space proximally. While on the behind, the synovial membrane is attached to the margins of the two femoral condyles, which produces two extensions similar to the anterior recess. Cartilage ensures supple knee movement. There are two types of joint cartilage in the knees: fibrous cartilage (the meniscus) and hyaline cartilage. Fibrous cartilage has tensile strength and can resist pressure. Hyaline cartilage covers the surface along which the joints move.

Cartilage has a very limited capacity for self-restoration. The newly formed tissue will generally consist for a large part of fibrous cartilage of lesser quality than the original hyaline cartilage. As a result, new cracks and tears will form in the cartilage over time. The articular disks of the knee joint are called menisci as they only partly divide the joint space. These two disks, the medial meniscus and the lateral meniscus, consist of connective tissue with extensive collagen fibers containing cartilage-like cells. The menisci are flattened in the middle of the knee joint, fused with the synovial membrane laterally, and can move over the tibial surface. The menisci serve to protect the ends of the bones from rubbing on each other and to effectively deepen the tibial sockets into which the femur attaches. They also play a role in shock absorption, and may be cracked or torn when the knee is forcefully rotated and/or bent. The knee is held together by four ligaments: medial collateral

ligament, lateral collateral ligament, anterior cruciate ligament, posterior cruciate ligament. The ligaments surrounding the knee joint offer stability by limiting movements and, together with several menisci and bursae, protect the articular capsule (Werner *et al.* 2004).

1.2.2 Loading and Motion in the Knee

The knee permits flexion and extension about a virtually transversal axis, as well as a slight medial and lateral rotation about the axis of the lower leg in the flexed position. The femur and menisci move over the tibia during rotation, while the femur rolls and glides over the menisci during extension-flexion (Werner *et al.* 2004).

Movements of the knee joint can be classified as having 6 degrees of freedom: three translations (anterior/posterior, medial/lateral, and inferior/superior) and three rotations (flexion/extension, internal/external, and abduction/adduction). Movements of the knee joint are determined by the shape of the articulating surfaces of the tibia and femur as well as the orientation of the four major ligaments of the knee joint, including the anterior and posterior cruciate ligaments and the medial and lateral collateral ligaments as a 4-bar linkage system.

The center of the transverse axis of the extension/flexion movements is located where both collateral ligaments and both cruciate ligaments intersect. This center moves upward and backward during flexion, while the distance between the center and the articular surfaces of the femur changes dynamically with the decreasing curvature of the femoral condyles. The total

range of motion is dependent of several parameters such as soft-tissue restraints, active insufficiency, and hamstring tightness (Thieme, 2006).

Table 1.1 Reported tibio-femoral joint loads during daily activities

Authors	Activity	Tibio-femoral joint load (Body Weight)
Maquet (1975)	Running & jumping	Up to 20
Andriacchi (1980)	Downstairs walking	6.0
Ericson (1986)	Cycling	1.2
Collins (1995)	Level walking	3.9-6.0
Kuster (1997)	Level walking	3.9
	Downstairs walking	8.0

The knee joint is subject to large mechanical loads during daily activities caused by a number of mechanical factors with a large range of motion and is located below the center of gravity of the human body. Besides, the knee joint is not a highly conforming joint, which means loads are distributed over relatively small areas and would result in large loads acting. The tibio-femoral joint bears an average load from 1.2 to 20 times the body weight (Table 1.1). The patello-femoral joint bears a similar degree of loading as the tibio-femoral joint (Matthews *et al.* 1977; Nisell, 1985; Ericson and Nisell, 1987). The present study would focus on the tibio-femoral; therefore, there would be no discussion about the load of the patello-femoral joint.

A large range of flexion angle is required during daily movements. For instance, flexion of about 8.5° is required for walk, flexion of about 72° for stand from a chair, while the flexion is about 75° for sit in a chair. Greater degrees of flexion are required for more strenuous activities such as squatting or kneeling (Dowson and Wright, 1981). As can be seen from Table 1.2, for normal loading, walking, there was moderate load and low flexion angles. Stair activities and golf swing had high load and moderate flexion. At last, chair and squatting activities had moderate load and high flexion. The maximum compressive load occurred during stair ascent, which is 3.6 body weight (BW). The data was obtained by a custom-designed instrumented knee prosthesis, which was implanted in the right knee of an 81 year old male patient (170 cm, 633 N) (Annegret *et al.* 2007).

Table 1.2 Max compressive load and the knee flexion angles at different activities

Activity	Maximum compressive load (Body Weight)	Flexion angle at max compressive load (°)
Walk	2.5	8.5
Stair descent	3.5	30
Stair ascent	3.6	40
Golf swing	3.2	30
Chair stand to sit	2.5	75
Chair sit to stand	1.8	72
Squat	2.2	92

1.3 Polyethylene

As an outstanding material for orthopaedic joint replacement, polyethylene can provide excellent abrasion resistance, low friction, high impact resistance, a self-lubricating surface, insignificant water absorption, good chemical resistance, high-energy absorption, and no temperature sensitivity in the human biological environment. Ultra-high molecular weight polyethylene (UHMWPE) is currently the most commonly used material as a bearing surface in total joint replacements, if well designed and well implanted, products made of this material can function for more than fifteen years or even longer.

1.3.1 Material properties of polyethylene

Polyethylene is a polymer, which consists of only carbon and hydrogen in long CH2-chains (Kikugawa *et al*. 2013). As demonstrated in Figure 1.5, the polymer chain is often shown in two dimensions, but it should be noticed that they have a three dimensional structure. Each bond is at 109° to the next, when stress is applied, these chains stretch and the elongation of polymers can be thousands of times greater than it is in crystalline structures (Picaud *et al.* 2003).. The polymer consists of crystalline lamellae embedded in non-crystalline amorphous regions. The polyethylene used for orthopaedic implants today is ultra-high molecular weight polyethylene (UHMWPE), defined as a linear polyethylene with an average molecular weight higher than 3.1 million g/mol. The molecular weight of UHMWPE is the number of

ethylene groups (C2H4), which makes up one molecular of polyethylene polymer and multiplied by the molecular weight of ethylene. GUR® ultra-high molecular weight polyethylene (UHMW-PE) is a linear polyethylene with a much higher molecular weight than standard PE, which offers outstanding abrasion resistance, superior impact resistance, non-sticking and self-lubricating properties, and excellent mechanical characteristics, even in cryogenic conditions (Kurtz 2009). GUR 1020 and GUR 1050 are the most commonly used resins in orthopaedic implants today. Table 1.3 shows molecular weights of some common polyethylene resins used in current orthopaedic applications.

There are four basic mechanical properties, including stiffness, ductility, strength, and elongation to break. The modulus of elasticity is the ratio between force per unit area and the resulting deformation. The elastic modulus reduces with strain. As a visco-elastic material, polyethylene has the potential for plastic deformation during wearing. Plastic deformation occurs when the stress is sufficient to permanently deform the material, which is irreversible. However, an object in the plastic deformation range will first have undergone elastic deformation, which is reversible; therefore the object will return part way to its original shape. Yield strength is the amount of stress, which makes a plastic deformation in a component, and fatigue strength is the amount of stress below which no failure would occur with regardless of the number of wear cycles. Elongation to break is the load over the elongated length of the polyethylene until it breaks. Creep can occur in polymers which are considered visco-elastic material. Creep is the effect of long polymer chains in polyethylene sliding over each other, which can result in slow

material deformation, however, creep does not result in the production of debris. The σ-ε curve was illustrated in Figure 1.6 (Turner 2001). At a time t0, a viscoelastic material is loaded with a constant stress that is maintained for a sufficiently long time period. The material responds to the stress with a strain that increases until the material ultimately fails. When the stress is maintained for a shorter time period, the material undergoes an initial strain until a time t1 at which the stress is relieved, at which time the strain immediately decreases discontinuity then continues decreasing gradually to a residual strain. As reported in a simulator test, the amount of wear accounted for less than 30% of the change in polyethylene thickness, while the rest was plastic deformation or creep (Rose and Radin, 1982). The amount of polyethylene wear is high in the early period after implant and then decreases with time goes on, on the other hand, creep is important within the first six to twelve months and decreases over time, after that polyethylene wear is considered as linear or can be described as a state stage (Sychterz *et al.* 1999, Kurtz et al. 1999, Kurtz 2004, Kurtz 2009).

Table 1.3 Molecular Weights of common polyethylene resin used in orthopaedic devices

Product	Base Resin	Molecular Weight (g/mol)
1900	1900	2-4 million
GUR 412	GUR 412	4 million
GUR 415	GUR 415	6 million
GUR 1020	GUR 1020	3.5 million
GUR 1050	GUR 1050	5.5-6 million

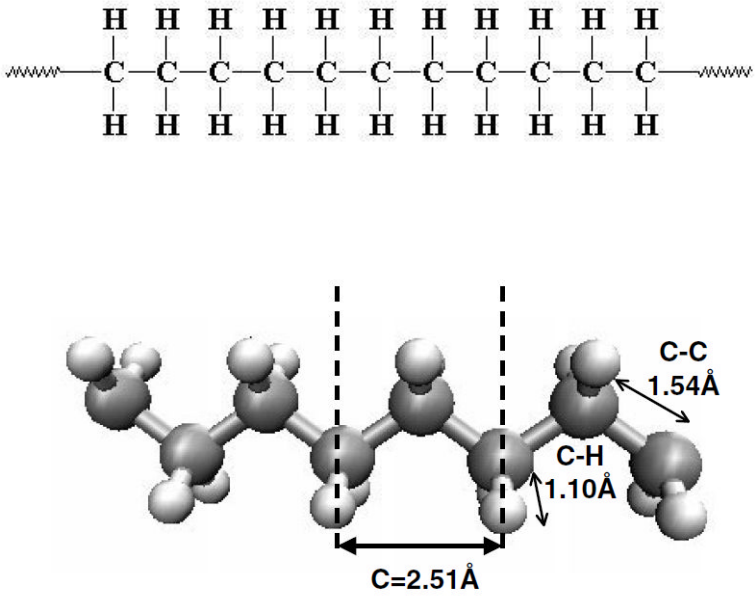

Figure 1.5 Polyethylene chain (Kikugawa *et al.* 2013, Picaud *et al.* 2003).

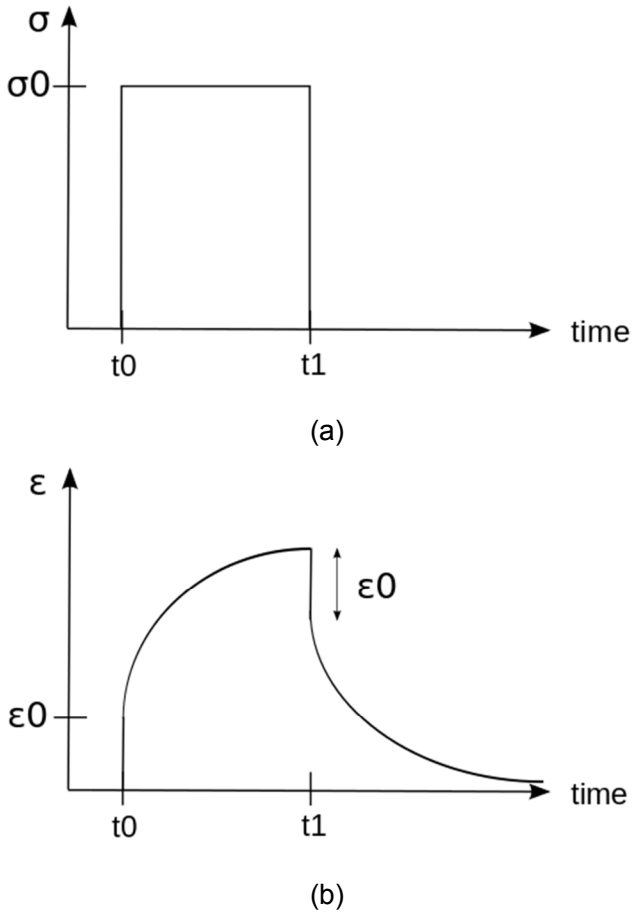

Figure 1.6 (a) Applied stress and (b) induced strain as functions of time over a short period for a viscoelastic material (Turner 2001).

1.3.2 Highly Crosslinked polyethylene

Highly crosslinked UHMWPE was firstly introduced for clinical usage in the 1970s by Oonishi and Grobbelaar and their co-workers (Oonishi and Kadoya, 2000; Atkinson and Cicek, 1984; Grobbelaar and du Plessis, 1978) and then reintroduced by Wroblewski and colleagues (Wroblewski *et al.* 2005) in the 1980s for both hip and knee replacements, and encouraging long-term clinical results were reported at the end of the 1990s. From laboratory studies, there is a remarkable decrease in wear rate with increasing cross-linkage (high to 90%) (Kurtz *et al.* 1999; McKellop *et al.* 1999). For short and mid-term follow-up clinical studies, the wear decreases 50–80% (Digas *et al.* 2003; Rohrl *et al.* 2007).

Cross-linking of polyethylene can be obtained under high loads of irradiation, chemical agents, or peroxides, all of which would result in a higher resistance to wear of the polyethylene (Kurtz *et al.* 1999; Oonishi and Kadoya, 2000). After that, two main types of thermal treatment are used to avoid the oxidation of polyethylene, one is anneal below the melting point of the irradiated polymer and the other is melt after irradiation. By annealing, the mechanical properties are maintained; however, free radicals and the potential for posttreatment oxidation still exist. The oxidation would lead to degradation of the polyethylene and further result in surface fatigue of the components (Mitroka *et al*. 2013). On the other hand, remelting involves heating of the cross-linked polyethylene to temperatures higher than the melting point, which would not only result in free radicals in the crystalline regions accessible for elimination, but also the microstructure of the

polyethylene is changed in the form of reduced crystallinity and mechanical properties are decreased.

The mechanism of cross-linking is that UHMWPE crosslinks when exposed to ionizing radiation through free radical recombination reactions. C-H and C-C bonds were cleaved by the ionizing radiation and then generating free radicals, some of which would recombine to generate crosslinks. The cleavage of C-C bond is chain scission and would lead to a reduction of the molecular weight of the polyethylene. Both electron beam (e-beam) and gamma irradiation can be used for crosslinking of UHMWPE. Table 1.4 listed the irradiated and melted UHMWPEs that are used in total knee replacement (Orhun *et al.* 2003).

Table 1.4 List of highly crosslinked polyethylene used in total knee replacement

Manufacturer	Irradiation temperature (^{o}C)	Radiation dose (kGy)	Radition type	Postirradiation thermal treatment	Sterilization method
Zimmer	~125	65	E-beam	Melted at 150^{o}C	Gas plasma
Sulzer	~120-125	95			Ethylene oxide

The size of wear particles of highly cross-linked polyethylene is smaller; however, it was found recently that the biological activity of crosslinked UHMWPE debris need to be investigated as increased molecular weight increased the biological reactivity of the debris (Ingram *et al.* 2002). Besides, direct cell culture studies of wear debris generated in aseptic multidirectional wear simulators have shown an increase in the biological activity and release of osteolytic cytokines with crosslinked debris compared to non crosslinked debris (Ingram *et al*. 2003)

1.3.3 Vitamin E polyethylene

Polyethylene with the addition of vitamin E has been recently developed. Vitamin E, a natural antioxidant, consists of tocopherols and tocotrienols (Figure 1.7), is the most abundant and effective chain-breaking antioxidant present in the human body (Packer, 1991) with main function of protecting cell membranes from oxidation. Without remelting the irradiated cross-linked polymers, Vitamin E hinders cascade oxidation reactions in the UHMWPE and this results in a reduction in mechanical properties, which caused by a decrease in crystallinity as the remelting process is avoided (Oral *et al.* 2004; Oral *et al.* 2005; Oral *et al.* 2006). It is believed that E-Poly highly cross-linked polyethylene (HXLPE) excees the limitations of first generation remelted and annealed highly cross-linked UHMWPE and can provide both high mechanical strength and oxidative stability (Oral *et al.* 2009). It has been shown from oxidative stability testing that vitamin E has the ability to prevent oxidative degradation of polyethylene without remelting, which has a contribution to the

maintenance of mechanical properties and wear resistance over time (Oral *et al.* 2004; Oral *et al.* 2006; Oral *et al.* 2009).

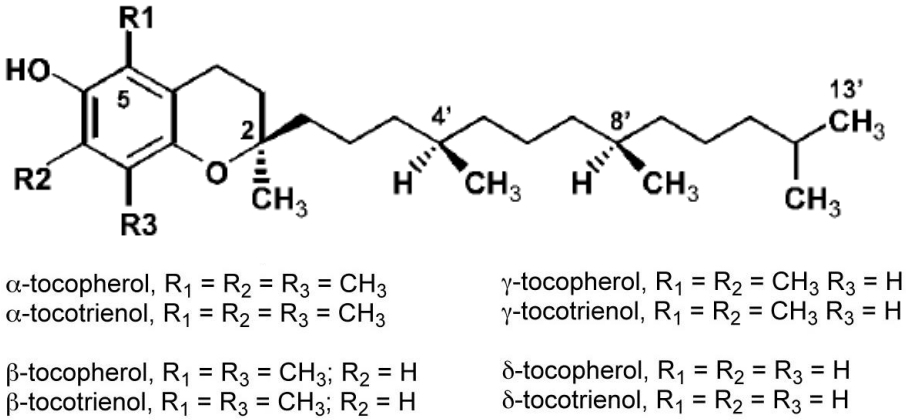

Figure 1.7 Structure of tocopherols (Sontag and Parker 2007).

The use of vitamin-E stabilized, radiation crosslinked UHMWPE is especially important for use in tibial component bearings due to the improved fatigue resistance and oxidation resistance compared to irradiated and melted UHMWPEs. However, currently, the primary disadvantage of vitamin-E UHMWPE is generally considered increased resistance of the material to subsequent radiation crosslinking, which was influenced by the method of irradiation and concentration level of antioxidant (Oral *et al.* 2005; Parth, 2002; Oral *et al.* 2008). As demonstrated in Figure 1.8, the crosslink density decreases with the increasing of vitamin E concentration.

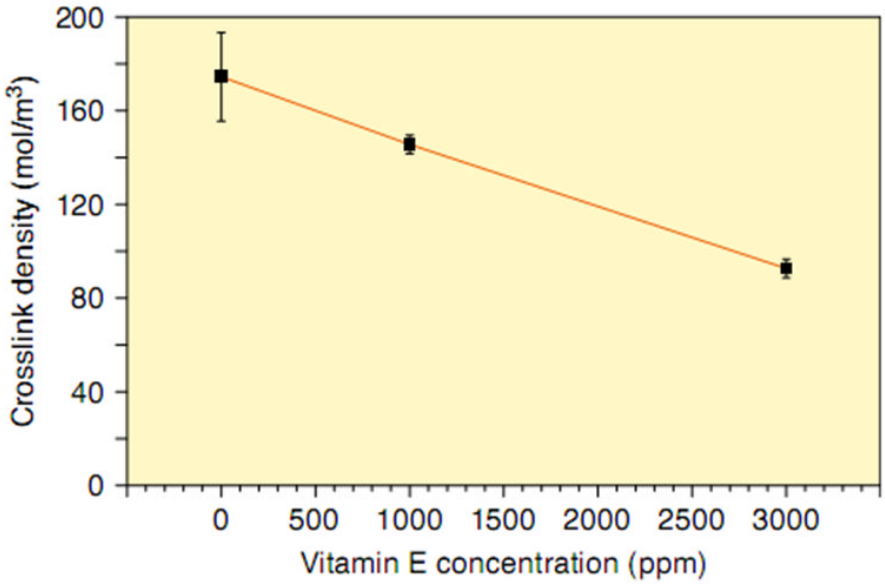

Figure 1.8 Effect of vitamin-E concentration on the crosslink density of 100kGy, gamma irradiated UHMWPE (Oral *et al.* 2005)

1.3.4 Polyethylene wear

Wear is defined as the progressive removal of material from the prosthesis, which would result in particulate debris. The most important wear in a normal total knee replacement would be between the femoral metal component and the polyethylene insert, including tibial inserts and patellar components. There exist many complexity factors of polyethylene wear, for example material properties including hardness, surface finishing, and conformity of the tibial component. Besides, implant design, bone cements, implant surface coatings, operative procedure and component placement, component fixation, the quality and manufacturing of polyethylene, as well as the sterilization technique could affect the polyethylene wear, as shown in Figure 1.9. The patient aspect, such as age, male gender and activity level

would influence the success of total knee replacement, it is known that patients below the age of 60 walk 30% more than patients who were 60 years or older. The average walking activity is 0.9 million cycles per year while the number of most active patients would be an average of 3.2 million cycles per year (Schmalzried *et al.* 1998). As wear is a complex process, many influence aspects probably remain unknown even many contributing factors have been described.

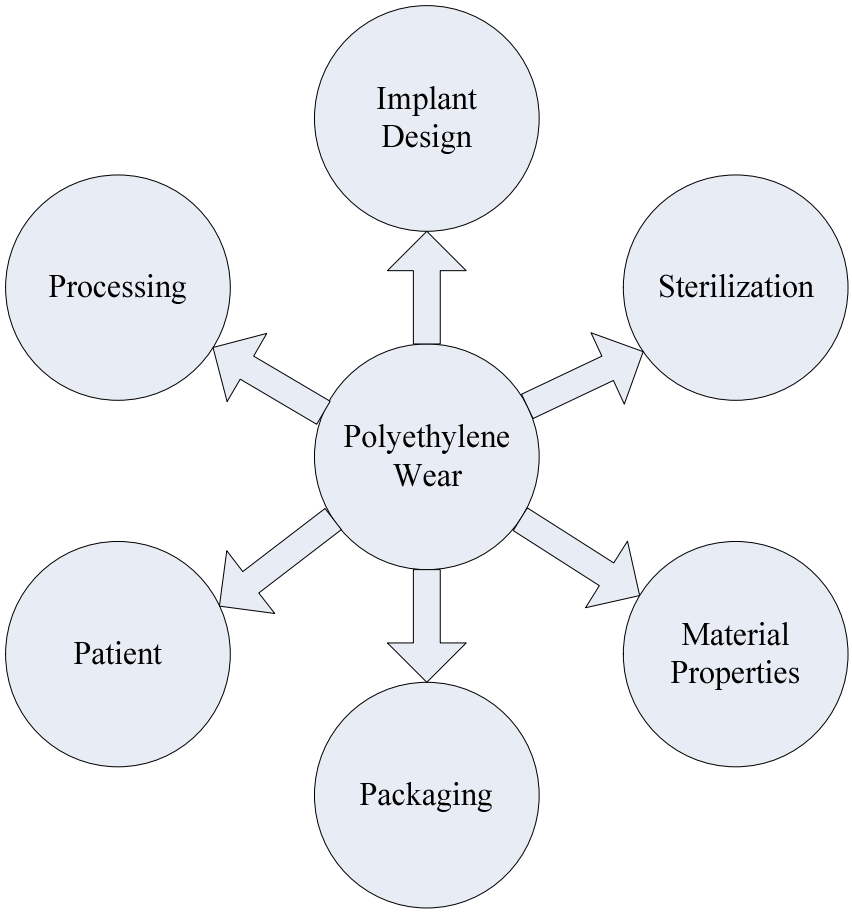

Figure 1.9 Multifactorial causes of polyethylene wear.

Wear mechanisms in laboratory and retrieved implants can be classified into abrasion, cracking, creep, and delamination (Wright and Bartel, 1984; Landy and Walker, 1988), which would result in scar on the articular surfaces of the tibial insert and the patellar component. Abrasive wear occurs when a hard rough surface slides across a softer surface. In TKR, abrasion would occur between the femoral head and the polyethylene components including tibial and patella. Cracking would result in surface fatigue. Both creep and deformation would induce permanent deformation and contribute to the scar on not only the articular surfaces but also on the backside of polyethylene components. In the first two years of *in vivo* use, creep accumulates and then reaches a steady state. Because of the yielding of the polyethylene surface when the joint is loaded, deformation occurs rapidly and this becomes a primary cause of most polyethylene failures in total knee replacement among these wear mechanisms (Bevill *et al*, 2005). Delamination can contribute to the loss of geometric conformity and alteration of load distribution, and finally result in implant failure by fracture of the tibial insert or wear-through. Figure 1.10 demonstrates a typical appearance of delamination on a polyethylene tibial insert from retrieved implant in 1992.

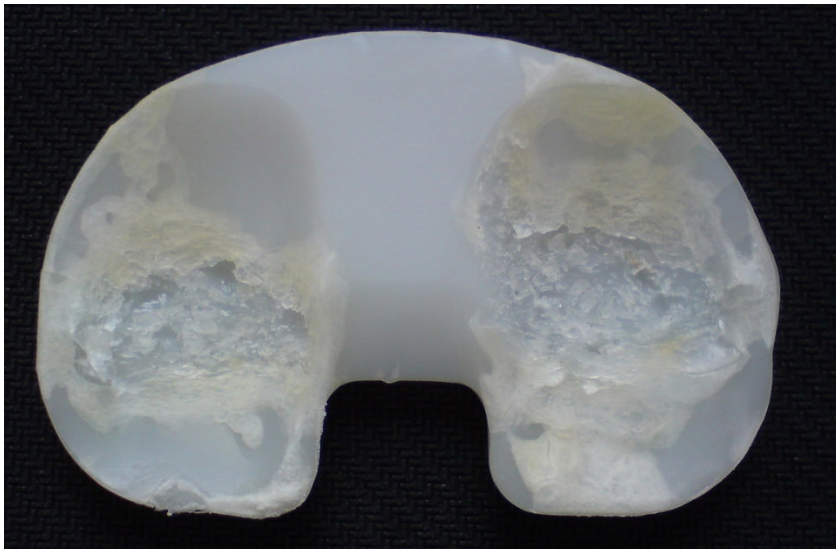

Figure 1.10 Typical appearance of delamination on a polyethylene tibial insert.

It is very important to measure the amount of wear, crystallinity, molecular weight, and deformation of the polyethylene component, which can be evaluated by means of x-ray spectrophotometry, infrared spectrometry, gel permeation chromatography, scanning electron microscopy as well as light microscopy combined with polarized light (Blunn *et al.* 1991; Blunn *et al.* 1992). The wear of polyethylene component depends on molecular weight (Rose *et al.* 1979), homogenicity (Schmotzer and Song, 1991), thickness (Knutson *et al.* 1981), geometry (Bartel *et al.* 1986; Buechel *et al.* 1991; Collier *et al.* 1991), and articular surface irregularities (Milliano and Whiteside, 1991; Elbert *et al.* 1992).

1.4 Laboratory and retrieval study

During the last decades, ultra high molecular weight polyethylene (UHMWPE) has been widely used as bearing components in total knee replacements. Many researchers have taken laboratory and retrieval studies to understand the wear mechanism and the influence of wear, such as polyethylene wear particles, which would result in aseptic loosening of the total knee replacement (Harris, 1995; Kobayashi *et al.* 1997)

1.4.1 Laboratory testing of polyethylene components in TKR

Assessment of the amount of wear *in vitro* is considered as an essential step in the development of a new joint replacement. *In vitro* simulator testing of tibio-femoral joint has been widely carried out over the last 20 years.

Oxidation and delamination fatigue are main causes of failure of total knee replacements (Engh *et al.* 1992; Jones *et al.* 1992), the later has been reported in both simulator (Bell *et al.* 1998; Reeves *et al.* 2000) and clinical studies (Engh *et al.* 1992; Won *et al*. 2000). However, delamination is no longer a problem due to increasing material properties of the polyethylene used in TKR. It is generally considered that in the design of total knee replacements, bearing contact stresses decrease as conformity increases (Jin *et al.* 1995; Bartel *et al.* 1995) which can contribute to delamination fatigue. Galvin and their co-workers compared the wear of fixed-bearing total knee replacements with curved and flat inserts (Galvin *et al.*2009), and results show that the flat inserts that given higher contact stress and smaller contact areas

would result in lower surface wear. Moreover, high contact stress knee with a low-medium level of cross shear would lead to a dramatically lower wear rate. The input profile for the knee joint simulators was demonstrated in Figure 1.11. The ISO standard loading parameters for wear test machines are shown in Figure 1.11(a) and (b), while the AP displacement and IE rotation of the natural knee are shown in Figure 1.11(c). The FE rotation ranges between zero and 58 degrees, while the IE rotation range is ±5 degrees. The AP displacement of the natural knee is in the range of 1 to -10 mm. There are two peaks of flexion, a smaller one, during the stance phase, and the other, larger one, during the swing phase. The maximum axial force act up on the knee during the gait cycle is approximately 2600N, while the AP force is in the range of -262 to 110 N.

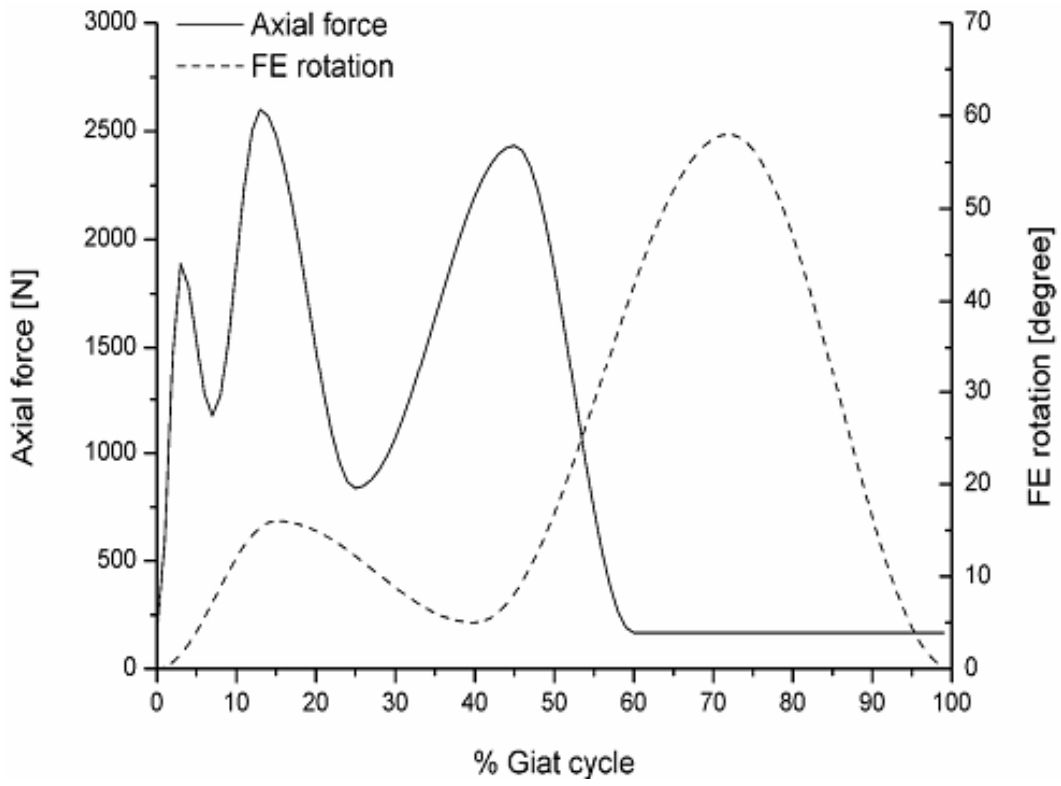

(a) axial force (AF) [N] and flexion-extension (FE) [degree]

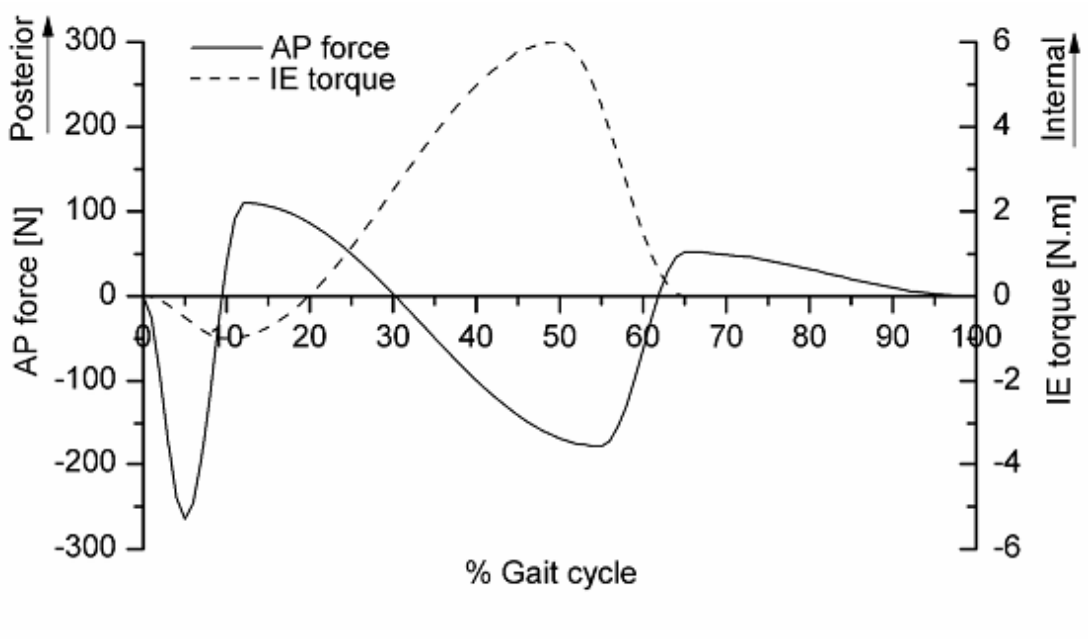

(b) anterior-posterior (AP) force [N] and internalexternal (IE) torque [N.m]

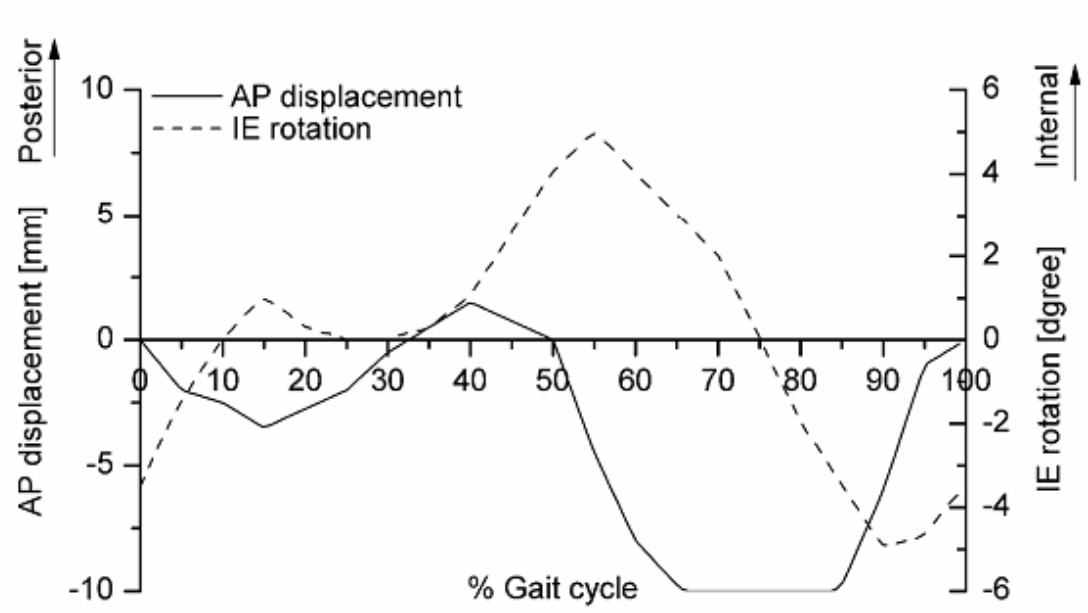

(c) natural knee AP displacement [mm] and IE rotation [degree]

Figure 1.11 ISO standard axial force (AF) [N] and flexion-extension (FE) [degree], for total knee replacement wear test machines (McEwen *et al*. 2005; ISO 14243-1 2009; Lafortune *et al*. 1992; Barnett *et al*. 2002).

Oonishi determined the effect of femoral component materials total knee prostheses and sterilization methods on wear properties by means of a knee simulator and retrieval analysis (Oonishi *et al.* 2009). The simulator test indicate that wear between UHMWPE and ceramic is much lower than that of Co-Cr femoral component, but the retrieval analysis did not show significant difference. A novel tibial post durability test was carried out on a modern posterior-stabilized implant design with both conventional polyethylene (CPE) and highly crosslinked polyethylene (HXPE) materials using a knee simulator (Stoller *et al.* 2010). Results indicate that the amount of wear reduced 67% and 75% separately by comparing with aged CPE and HXPE was proved can be successfully incorporated into a posterior-stabilized total knee replacement.

Patellofemoral joint simulation was carried out using four input degrees of freedom (Ellision *et al.* 2008); this wear method was validated by comparing the functional kinematics and patellar surface damage modes. It seems that creep deformation and geometry changes remain to be influence factors to geometrical measurements of wear.

Polyethylene wear particle is considered one of the most important factors affecting mid- to long-term results of total knee replacements. The size, shape and total amount of polyethylene wear particles have been showed to cause osteolysis (Campbell *et al.* 1996; Fisher *et al.* 2004; Purdue *et al.* 2007). Figure 1.12 shows an electron microscopy photograph of the polyethylene wear particles. The wear volume and the size of debris generated in simulator seem to be similar to early retrieved knee replacements (McEwen *et al.* 2001; Barnett *et al.* 2002; Howling *et al.* 2001).

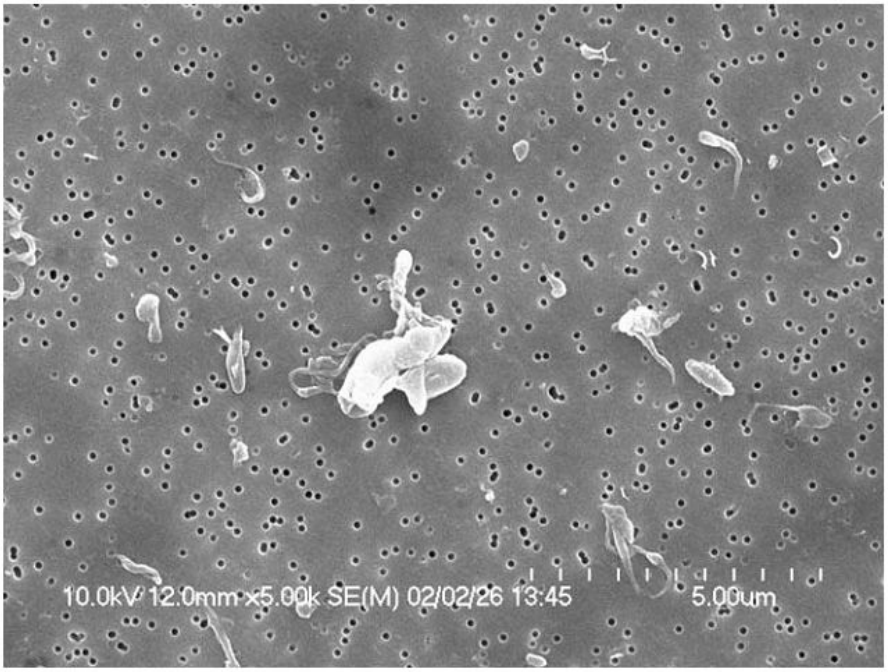

Figure 1.12 Scanning electron microscopy of the polyethylene wear particles (Minoda *et al.* 2005).

1.4.2 Retrieval analysis of polyethylene component in TKR

Retrieval analysis of implant components play an important role in determining the efficacy of new designs and provide an invaluable resource for laboratory investigations (Hailey *et al.* 1994; Williams *et al*. 1998). Osteolysis around the prosthesis can result in pain and loosening of the component and this become a major factor for failure of total joint placements (Goldring *et al.* 1983; Anthony *et al.* 1990; Devane *et al.* 1995; Drown and Ring, 1985). In addition, the osteolysis even causes fracture of the femoral component (Rand, 1994). Table 1.5 demonstrate measurement of wear rate in total knee replacements with different types of implant.

Table 1.5 Measurement of wear rate in total knee replacement

	TKR	Bearing	Wear rate (mm/year)
Argenson *et al* (1992)	Bicompartmental	Fixed	0.026–0.043
Plante *et al* (1993)	Freeman Samuelson	Fixed	0.025
Polyzoides *et al* (1999)	Rotaglide	Mobile	0.046
Benjamin *et al* (2001)	PFC Synatomic	Fixed	0.35
Lavernia *et al* (2001)	Porous Coated	Fixed	0.13
Hoshino *et al* (2002)	Interax	Fixed	0.23
Price *et al* (2005)	Unicompartmental	Mobile	0.02
Gill *et al* (2006)	AGC	Fixed	0.10
Kop *et al* (2007)	LCS	Mobile	0.053

From the table above, the wear rate of mobile bearing components generally shown to be smaller than fixed bearing components of total knee replacement. One of the reasons could be that mobile bearing components allow the rotation of tibial bearing component (McEwen *et al*. 2005). The measurement methods ranging from gravimetric to image based techniques for both *in vivo* and *in vitro* components, such as Roentgen Stereophotogrammetric Analysis (RSA) system used by Price and Gill (Price *et al*. 2005, Gill *et al*. 2006). However, the pre-wear data such as 3D geometry or unworn component are needed for reference to determine the wear.

From 90 retrieved UHMWPE components, Landy and his co–workers summarised the types of wear that are shown in Table 1.6 (Landy *et al*. 1988). No significant difference in overall wear was found from the retrieval analysis. Abrasion occupies the largest percentage (95%), and discoloration is the smallest (8%), delamination, cement particles, cement cavities, burnishing and deformation range from 37% to 90%. Hirakawa described six different types of polyethylene deformation by measuring 75 retrieved implants (Hirakawa *et al*. 1999), as demonstrated in Figure 1.13. The wear region and extent of wear various among the six patterns, including nearly all types of surface deformation of polyethylene wear, which provide a strong basis for evaluation of polyethylene wear.

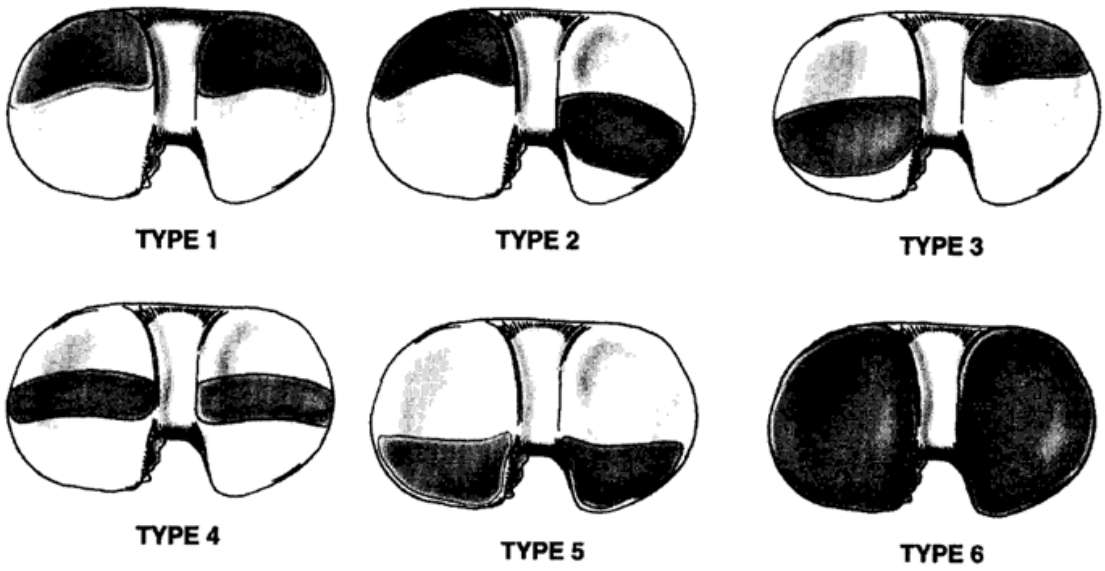

Figure 1.13 Patterns of polyethylene surface deformation (Hirakawa *et al.* 1999)

Table 1.6 Types of wear from 90 retrieved polyethylene components in knee prostheses (Landy *et al.* 1988)

Wear Patten	Percentage
Discoloration	8%
Delamination	37%
Cement panicles	46%
Cement cavities	75%
Burnishing	87%
Deformation	90%
Abrasion	95%

1.5 Wear Measurement Method

Wear of polyethylene bearing component is a major problem in total knee replacement, studies have shown that about 16% of knees fail because of wear (Engh, 1988). Highly crosslinked UHMWPE and vitamin-E were recently introduced clinically in total knee replacement to increase the wear resistance of UHMWPE (Dumbleton *et al.* 2002; Manning *et al.* 2005; Marshall *et al.* 2008). In order to understand historic UHMWPE wear processes and analyze future UHMWPE formulations that attempt to improve the clinical performance, the wear volume and wear patterns of polyethylene components must be evaluated accurately both *in vivo* and *in vitro*, which can provide useful information for design and production of polyethylene bearing components. As a result, a lot of work has been done by many researchers to

evaluate the amount of wear and wear rate based on retrieved polyethylene inserts using statistical methods. However, the amount of wear depends on some aspects mentioned above, such as the implant design, patient, material properties, and biomechanics of the prosthesis, which means the wear rate varies.

Currently there are kinds of methods to evaluate UHMWPE wear, including direct (Pollock *et al.* 2001; Sugano *et al.* 2004), gravimetric (Affatato *et al.* 2002; D'Lima *et al.* 2003), radiographic (Devane *et al.* 1995; Martell and Berdia, 1997; Selvik, 1978; Fukuoka *et al.* 1999; Hoshino *et al.* 2002). Roentgen stereophotogrammetric analysis (RSA) method (Valstar *et al.* 2001; Kaptein *et al.* 2003; Kellett *et al.* 2004; Gill *et al.* 2006), optical (Thomsen, 1999), fluid displacement (Yamamoto *et al.* 2003), microcomputed tomography (Micro-CT) (Bowden *et al.* 2005; Bowden *et al.* 2007; Johnston *et al.* 2009; Lewis *et al.* 2010; McPherson *et al.* 2005; Li *et al.* 2009; Minns *et al.* 2003; Teeter *el al*., 2010; Kinzel *et al.* 2004), and more recently, coordinate measurement machine (CMM) based (Overhoff *et al.* 2001; Veselko *et al.* 1998; Blunt *et al.* 2009; Rouvillain *et al.* 2008; Muratoglu *et al.* 2003; Blunt *et al.* 2008; Spinelli *et al.* 2009). All of these measurement techniques have their own unique advantages and disadvantages. For instance, radiographic, optical, fluid-displacement, and gravimetric methods can provide accurate results; however, they are generally cost a lot of time and have limited value in that they do not identify the scar regions (Affatato *et al.* 2002; D'Lima *et al.* 2003; Thomsen, 1999; Yamamoto *et al.* 2003). Micro CT methods can also provide accurate and relatively fast assessment of wear of polyethylene components (Bowden *et al.* 2005; Bowden *et al.* 2007), however, the main

drawback is that all measurement methods based on micro CT is *in vitro*, which limits their application in clinical. Recently, coordinates based techniques were introduced to evaluate the wear volume of polyethylene components, and had shown to provide more accurate calculation results; nevertheless, this kind of technique is also *ex vivo*.

1.5.1 Radiographic methods

Because of practical issues related to patient's positioning and reproduction of X-ray beam projection, fewer articles on *in vivo* radiographic assessment in total knee replacement have been reported than that of hip. The shortening distance between silhouettes contours of the two components on an X-ray can be identified when wear occurs, which is commonly used because of its simplicity. However, it is difficult to assess the wear volume accurately based on the shortest distance on a two-dimensional image because the radiographic beam is sometimes not parallel to the metal tibial tray. As a result, there are few reports on *in vivo* measurement methods of polyethylene wear. By using arthroscopy, Mints (Mintz *et al.* 1991) observed severe polyethylene wear. Sanzen (Sanzen *et al.* 1996) measured a decrease in the femorotibial distance using a fluoroscopically guided radiograph technique after a certain period. The amount of wear was calculated by subtracting the measured femorotibial distance from the original height of the polyethylene component. Banks (Banks *et al.* 1996), walker and their co-workers (Walker *et al.* 1996.) proposed an algorithm for estimating the 3-D position and orientation of artificial knee implants. Computer technologies are

applied to design to generate three dimensional image easily based on the two dimensional plane by identifying the numerical control of the coordinates. By using this technique, a computer vision technique named 3D/2D matching was introduced to analyze the kinematics in total knee replacement (Lavallee and Szeliski, 1995).

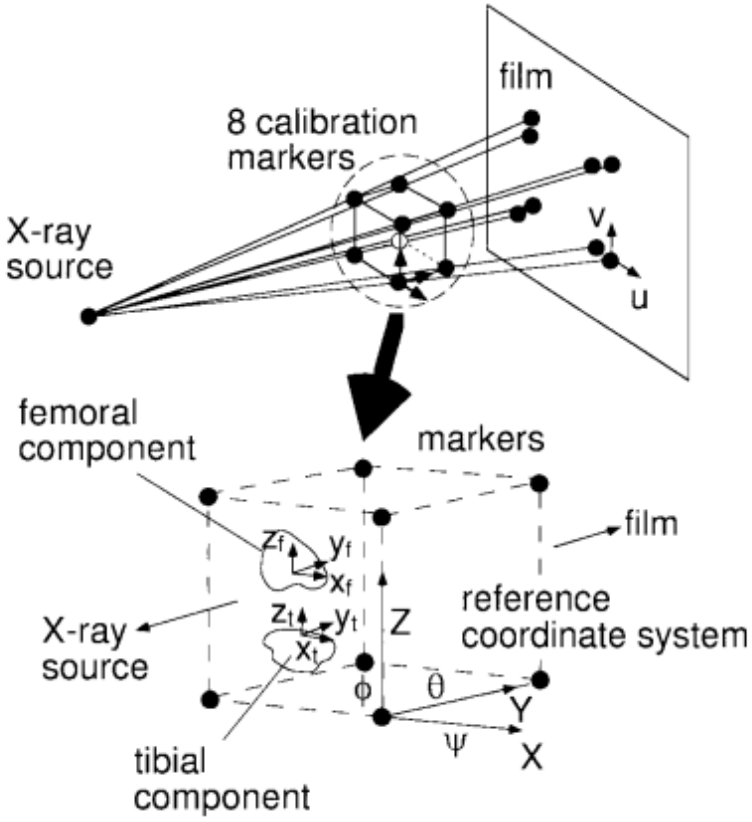

Figure 1.14 A schematic diagram of the imaging system (Yutaka Fukuoka *et al.* 1997).

Based on this 3D/2D matching technique, Yutaka (Yutaka Fukuoka *et al.* 1999;) and Akiho Hoshino (Akiho Hoshino *et al.* 2002) evaluated the polyethylene wear in total knee replacement in both *in vivo* and *in vitro*. They use some points on the edge of the silhouette instead of a closed contour. As

shown in Figure 1.14, four coordinate systems were used, one is a 2-D coordinate system o-uv attached to the X-ray image plane. The three dimensional geometry of the femoral (o_f-$x_f y_f z_f$) and tibial components (o_t-$x_t y_t z_t$) was then described in their own objective coordinate systems. O-XYZ system was defined as the reference coordinate system. Eight calibration points were used to estimate the parameters accurately. By using this technique, experiments were taken both *in vivo* and *in vitro*, the results show that the worst estimation errors of the in-plane/out-of-plane translations was 0.20/1.95 mm and the rotations 0.17/0.29°. The advantages of this technique is that it does not rely on particular points on the implants and requires a calibration marker as well as the three dimensional geometry of the knee implants.

1.5.2 Roentgen stereophotogrammetric analysis (RSA)

Roentgen stereophotogrammetric analysis (RSA) was developed by Selvik and his co-workers (Selvik *et al.* 1978), and the accuracy of RSA reported ranges from 0.05 to 0.5mm for translations with rotations between 0.15° and 1.15° (K. arrholm, 1989; Valstar *et al.* 2000). As a result, RSA is considered the most accurate three dimensional measurement techniques for determining the magnitude of relative displacements from radiographic images, micromotion between the implant and the surrounding bone can be assessed in an early stage (Nagels *et al.* 2002; Valstar *et al.* 2002; Nelissen *et al.* 1998; Ryd, 1992; Selvik, 1989). The RSA method has been used to successfully measure hip replacement wear (Thanner *et al.* 2000), and recently applied to evaluate the wear in knee replacement (Valstar *et al.* 2001;

Kaptein *et al.* 2003; Kellett *et al.* 2004; Gill *et al.* 2006). However, it is difficult to make marks on implants and sometimes even impossible, besides, marking of implants is too expensive for some countries. In order to avoid these disadvantages, Valstar and Kaptein developed a model based RSA method based on minimizing the difference between the virtual projection of a three dimensional surface model with the actual projection of the implant as it appears in a roentgen image, as shown in Figure 1.15. The model was applied to match with actural images and assess the position and rotation of the implant. Both computer aided design (CAD) model and reversed engineering model (RE) were used to investigate the accuracy, the results indicated that RE models is more accurate than the CAD models. The largest standard deviation for any translation was 0.19 mm and rotation was 0.52°.

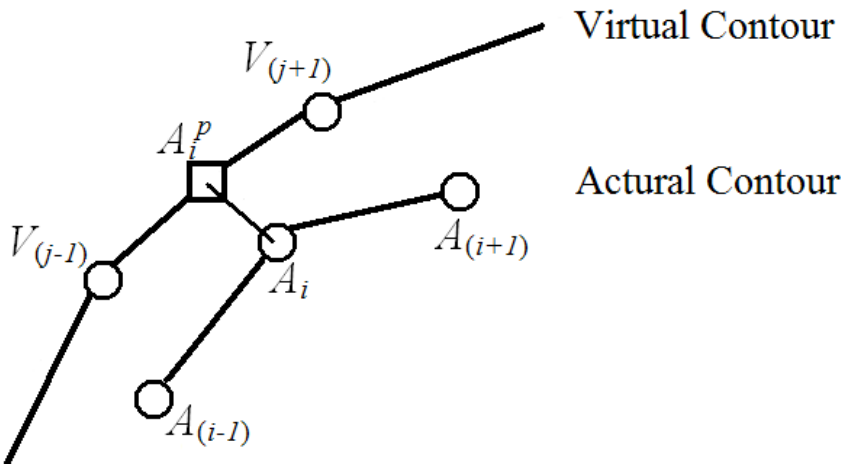

Figure 1.15 Closest connection line between virtual projection and actural projection (Kaptein *et al.* 2003).

Kellett (Kellett *et al.* 2004), Gill (Gill *et al.* 2006) and their co-workers presented a novel RSA system to measure the polyethylene tibial component

in total knee replacement. A comparison was made between a group of six Anatomic Graduated Components (AGC) knee prostheses more than 6 years post-implantation and a control group of six newly implanted AGC prostheses. A CAD model was also applied to estimate both linear penetration and volumetric wear, results show that the linear wear determined to be 0.1 mm/year and the volume wear about 100 mm^3/year. Linear wear is measured in radial direction while wear depth is in vertical. By dividing the surface of both medial and lateral tibial component into 100 equally spaced grid points, the sum of point volumes is considered the wear volume. Three different methods were presented to determine the wear volume from the site, size and depth of the "wear pool": "Average", "Eroded" and "Envelope", as can be seen from Figure 1.16. They believed that a real estimate of the total volume loss would between "Eroded" and "Enveloped" volumes, that is 600-700 mm^3.

The method presented above is suitable for early assessment of wear, which occurs in the first three to six months after implantation (Kellett *et al.* 2004). As a result, by combing the records of RSA measurement, it is possible to estimate the wear volume. Table 1.7 demonstrates the comparison of radiographic method and RSA method on translations and rotations.

Table 1.7 Comparison of radiographic method and RSA method on translations and rotations

Method	Translations (mm)	Rotations ($^\circ$)
Radiographic	0.20-1.95	0.17-0.29
RSA	0.05-0.5	0.15-1.15

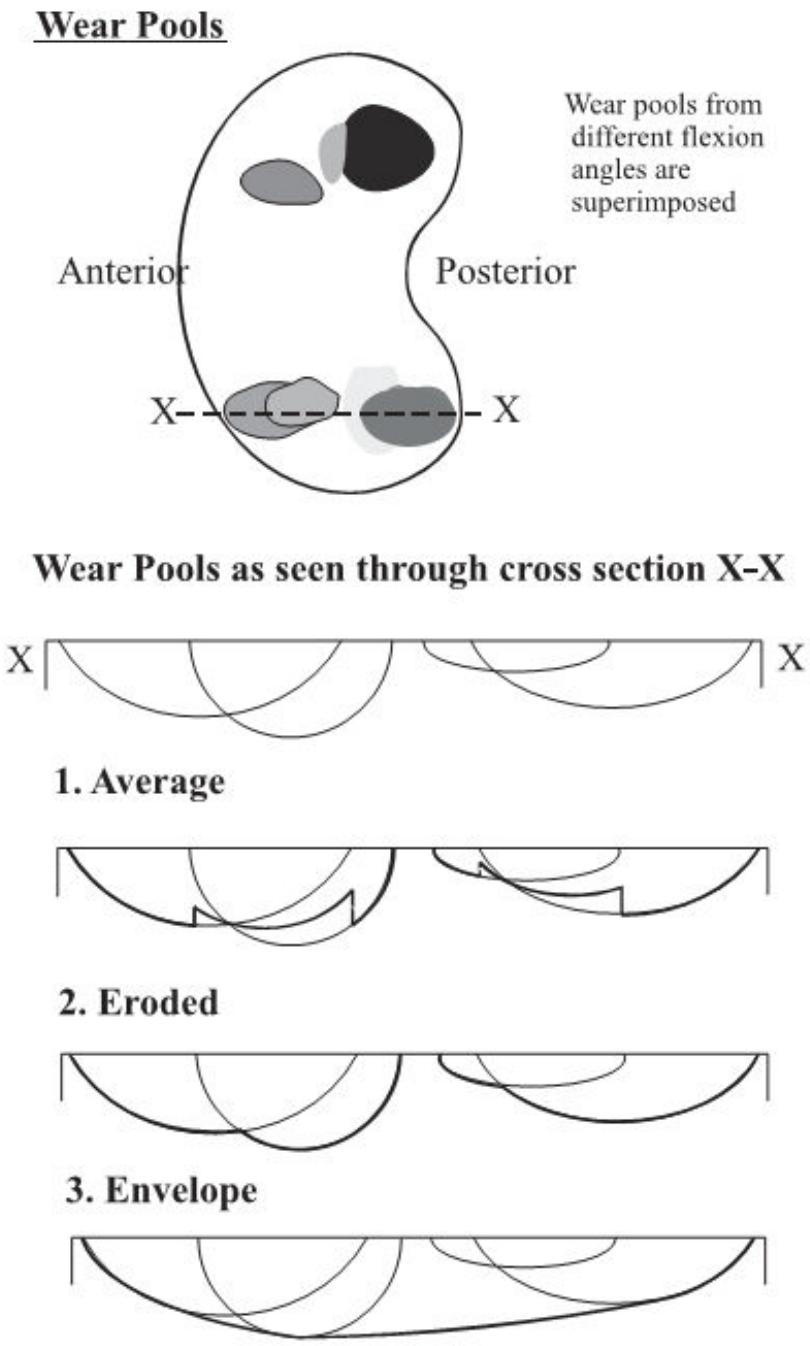

Figure 1.16 Three methods used to estimate volumetric loss (Gill *et al.* 2006).

1.5.3 Micro-CT based methods

Micro-CT is a technique that uses X-rays to generate three-dimensional geometries and can provide information on the internal features of an object

nondestructively. Measurement methods based on Micro-CT can provide reliable, accurate, and relatively fast assessment of wear and damage of polyethylene components (Bowden *et al.* 2005; Bowden *et al.* 2007). Micro-CT can measure surface deviation and the wear volume of retrieved acetabular liners and is applicable for analyzing other polyethylene components, such as tibial inserts. However, creep still cannot be easily distinguished from actual wear, references are required to determine the amount of wear and creep deformation, including a priori knowledge of nominal implant geometry or measured geometric parameters obtained from unworn portions of the components.

One of the major considerations for any Micro-CT scan is resolution versus file size and time consuming. Higher resolution can definitely enhance accuracy; however, with the increasing of resolution, the file size and time cost increase rapidly. After scanning, the amount of wear can be calculated by thresholding the cumulative image slices. Figure 1.17 demonstrates the transmission of greyscale image to thresholded image by setting the right threshold scale. The total number of voxels associated with the particular histogram peak is regarded as the wear volume.

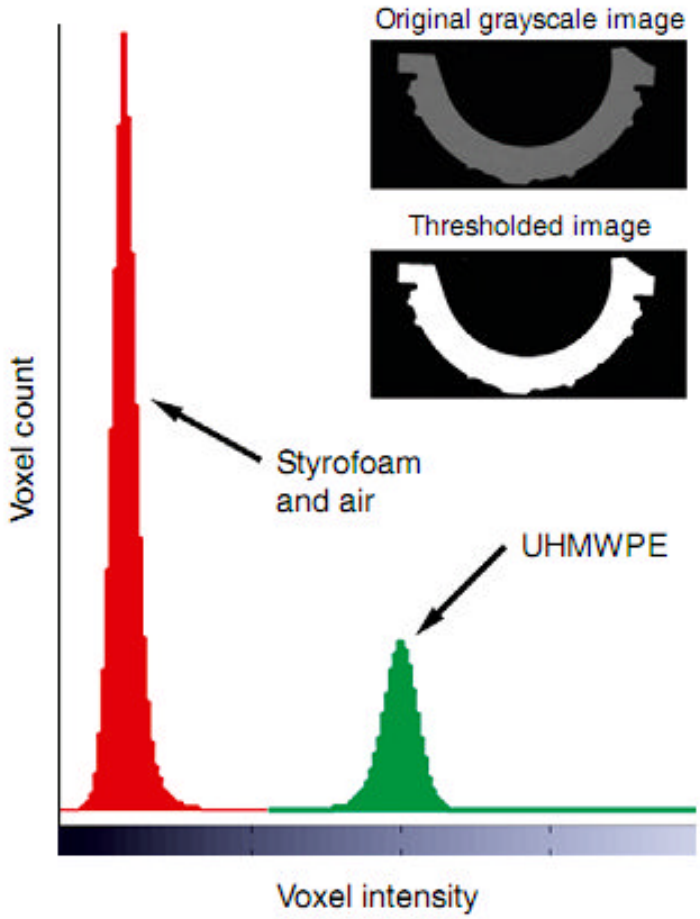

Figure 1.17 Thresholded image acquiring by changing the threshold scale (Kurtz, 2009).

It should be noticed that the metallic particles can result in beam scattering and make it difficult to analyze the polyethylene components using Micro-CT image datasets (Barrett and Keat, 2004). Several kinds of techniques have been introduced to reduce both metallic artefact and beam hardening artefact:

- Improving software reconstruction algorithms (Kalender *et al.* 1987; Wang *et al.* 2000).
- Increasing mAs and KV (Lee *et al.* 2007; Haramati *et al.* 1994).

- Increasing slice thickness (Lee *et al.* 2007),
- Increasing the CT scale (Link *et al.* 2000).

However, CT imaging of total hip replacement has improved using these methods, because of the complex morphology and large volume of metal in total knee replacement, it remains difficult. Lewis (Lewis *et al.* 2010) created a CT phantom in a total knee replacement with angles at 0°, 5°, 10^{o} and 15°, to reduce beam-hardening artefact. Table 1.8 demonstrates the changes in mean attenuation and the standard deviation for various parts of the phantom with different gantry angles. By adding the gantry angle particularly in the antero-inferior to postero-superior direction and then reconstructing images in conventional orthogonal planes, Lewis suggested that CT imaging of total knee replacements may be improved and the measures of artefact in the adjacent tissues can reduced by a 5 to 10 degrees tilt or artefact reduction can be more specifically targeted to the tibial component with an angle of 15°.

In addition, there may outcome third-body wear because of bone or metal particles in total joint replacements. As mentioned above, metallic particles have an influence on scanning; however, bone cement particles and ceramic debris do not exhibit these problems and can be easily visualized (Figure 1.18). By using the same method mentioned above, the volume of third-body particles can be calculated.

Table 1.8 The changes in mean attenuation and the standard deviation for various parts of the phantom with different gantry angles (Lewis *et al.* 2010)

Attenuation (HU)		Gantry angle						
		−15°	−10°	−5°	0°	+5°	+10°	+15°
Whole phantom	Mean	35. 0	44.9	80.3	71.0	44.7	55.5	59.2
	SD	81.7	66.9	64.3	75.8	81.7	75.5	74.9
Tibial component	Mean	33.7	37.6	36.5	16.4	10.5	13.3	1.9
	SD	31.2	34.6	37.9	50.3	43.5	40.5	43.7
Femoral component	Mean	33.9	61.1	119.8	116.2	75.3	91.8	107.4
	SD	122.1	90.2	87.7	95.6	115.1	107.5	105.3

Figure 1.18 Third body debris embedded in the condyles of a polyethylene component with green colour (Kurtz, 2008).

Micro-CT imaging techniques provide an accurate evaluation of wear of retrieved polyethylene insert, however, unlike other radiographic

methodologies; methods based on Micro-CT are all *ex vivo*, which limit its application for clinical usage. Nevertheless, Micro-CT methods are valuable for our knowledge of the relationship between polyethylene components' formulation, loading conditions, mechanical design, and long-term performance because of its three dimensional quantification of wear.

1.5.4 CMM-based methods

A coordinate measuring machine (CMM) is a device for measuring the physical geometrical characteristics of an object, which is widely used in mechanical engineering, aerospace, automotive industries and was applied to study three-dimensional geometry and biomechanics of human joints (Veselko *et al.* 1998). The translation and rotation of the x'-y'-z' reference frame is shown in Figure 1.19.

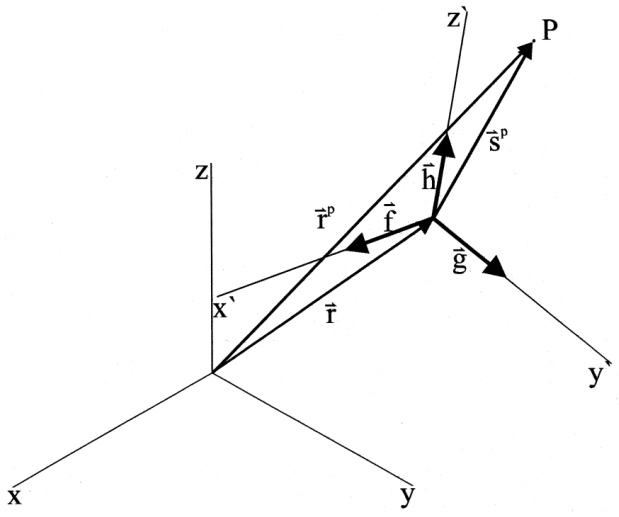

Figure 1.19 Translation and rotation of the x'-y'-z' reference frame (Veselko *et al.* 1998).

Later Muratoglu and his co-workers presented a metrologic method based on CMM to determine the linear penetration and the amount of wear of tibial inserts in total knee replacement (Muratoglu *et al.* 2003). The method was compared with traditional gravimetric method and the results indicate that metrology can clearly calculate reliable volumetric wear measurement, besides; the metrologic method can be applied to determine creep deformation. Based on CAD model and simulator tests, Blunt and his co-workers improved their methodology for determining wear without pre-wear data and compared with gravimetric measurements (Blunt *et al.* 2008), and proved to be an accurate tool combined with an *in vitro* wear model. CMM based procedure was applied to assess the wear of a non-congruous UKP design and also compared with gravimetric method, measurement methods based on CMM shown to have enough accuracy to evaluate the wear of polyethylene in joint replacements. Table 1.9 demonstrates a comparison of CMM method and traditional gravimetric method.

As can be seen from the Table 1.9, the amount of wear calculated by CMM is close to gravimetric measurement; as a result, it is suitable for assessment of wear in both knee replacements and non-congruous UKP. However, geometric measurement of the specimens or designed drawings was required as a reference when calculating. The accuracy would be influenced by uncertainly actual machining tolerance. In addition, like Micro-CT based measurements, CMM provide another accurate solution for polyethylene wear assessment in total knee replacement, nevertheless, methods based on coordinates measurement machine can only be used in

the analysis of retrieved polyethylene components which limit its clinically usage.

Table 1.9 A comparison of CMM method and gravimetric method

	Specimens (Blunt *et al.* 2008)					
	1	2	3	4	5	6
Gravimetric wear (mm^3)	30.9	26.7	46.1	43.7	30.1	43.6
CMM Volumetric wear (mm^3)	34.6	39.9	43.7	47.1	31.0	48.8
	Specimens (Spinelli *et al.* 2009)					
	7	8	9	10	11	12
Gravimetric wear (mg)	1.36	1.61	1.37	1.16	1.63	1.51
CMM Volumetric wear (mg)	1.84	1.82	1.76	1.52	2.02	1.79

Methodologies based on coordinates currently cannot be applied to assess the volume loss without a reference, despite that CAD model can be used as a reference, however, there are over 30 designs of total knee replacement systems and many new designs are being introduced each year (Liow and Murray, 1997), it's not feasible to establish CAD models of all designs. As a result, novel coordinates methodologies need to be developed to determine the amount of wear accurately without pre-wear data or CAD models.

1.6 Project aims and objectives

1.6.1 Rationale

Total knee replacement (TKR) is a common surgical procedure in orthopaedics. The wear of polyethylene inserts is an important cause of aseptic loosening in knee arthroplasty, which is a clinical problem. Detection of significant wear usually happens late on, since available diagnostic techniques are either not sensitive enough or too complicated and expensive for routine use. This becomes a more serious problem when the wear volume measured is small, due to the improvement of highly cross-linked polyethylene and implant designs.

There are two types of damage to polyethylene: one is wear and the other is creep deformation. It is clinically important to measure the amount of wear and creep deformation. Wear measurement methodology becomes critically important if differentiations with respect to materials and design are sought when geometry change is small, which can consist of both wear and creep. Several wear measurement techniques have been developed, ranging from single radiographic techniques to three-dimensional reconstructions. The main method used today is based on gravimetric and maybe difficult to apply in some laboratory studies or clinical practice. As polyethylene wear adversely affects the long-term results of the total knee replacement, reliable techniques are necessary for *in vivo* radiographic evaluation of tibial metal component with the polyethylene liner. Several contemporary computer assisted programme are now available to facilitate this measurement based on three-dimensional reconstruction and advanced instruments such as Micro-CT and

CMM. The underlying hypothesis is that a volume based method may be more applicable to determine the wear of tibial components under various senariors.

1.6.2 Aims and objectives

The aim of the present study is to develop novel three-dimensional methodologies based on three-dimensional geometry to improve the accuracy of wear measurement of the polyethylene tibial insert for the knee implant.

The objectives of the present study were:

- To develop methodologies for acquiring three-dimensional geometry of the components such as Micro-CT and CMM.
- To develop new volumetric determination method based on surface geometry fitting and reconstruction.
- To validate the volumetric determination methodology using a FE model and computational volume removal test.
- To investigate the applicability and accuracy of the volumetric assessment methodology through computational and experimental simulated wear tests and compared to gravimetric measurements.
- To computationally and experimentally validate the volumetric assessment methodology for creep deformation tests.
- To apply the volumetric determination methodology to simulator and retrieved tibial knee inserts.

1.6.3 Thesis outline

Chapter two explains the wear measurement methodology used in the experimental and computational studies. Chapter three presents a novel three dimensional volumetric determination methodology for wear and creep assessment based on coordinates. Chapter four presents experimental studies of artificial wear tests. Computational and experimental studies of creep tests are presented in chapter five. Chapter six and seven present the application of volumetric determination methodology on both laboratory and retrieval analysis. Finally, the overall discussion, conclusion and future work of the project are discussed in chapter eight.

Chapter 2

Wear Measurement Methodology

2.1 Introduction

This chapter describes the materials and methodologies used in the present project. As reported in the Literature Review, there are many methods of determining the volume loss of polyethylene in the hip, knee and spine either using contact or non-contact procedures. Geometric measurements include coordinate measuring machine (CMM) (Raimondi *et al*. 2000; Bills *et al*. 2007) whereas, non-contact procedures include Micro computed topography (Micro-CT) (Vicars *et al*. 2009), Pycnomatic ATC (Pycnometer) (Keng 1970; Viana *et al*. 2002) and gravimetric (Affatato *et al*. 2002; D'Lima *et al*. 2003). Recently, the measurement methods based on CMM and Micro-CT have been developed and validated the repeatability and accuracy (Raimondi *et al*. 2000; Bills *et al*. 2007; Vicars *et al*. 2009; Keng 1970; Viana *et al*. 2002).

In this project, data on the unworn component such as a CAD model, original weight or initial surface coordinates were not always available. A number of techniques were therefore investigated to characterise the volume loss, and these are described in more detail below.

2.2 Gravimetric measurement

The gravimetric measurement technique is the most standard methodology for mass loss measurement of polyethylene in wear simulation (McEwen *et al*. 2001; Affatato *et al*. 2002; D'Lima *et al*. 2003). However, in the case of backside wear involved, gravimetric measurement would be not accurate as reference since geometric measurements were carried out on the superior surface of the component. In this project, Mettler XP201 and XP205 digital balance (Mettler Toledo Inc., Columbus, Ohio, USA) were used to measure the polyethylene loss of tibial components gravimetrically. The maximum weight the Mettler XP205 can measure is 220g and the resolution is 0.01mg. The Mettler XP201 has the same resolution but less maximum measure weight (200g) compared to XP205.

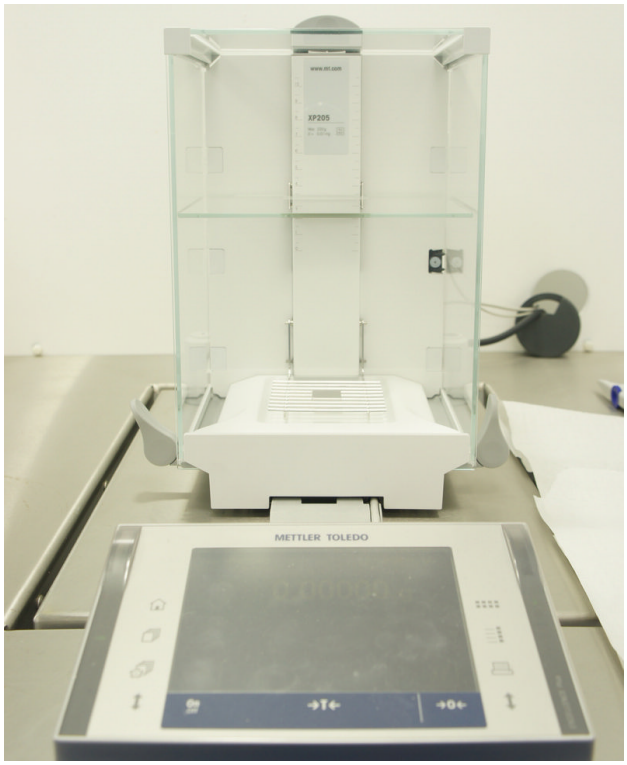

Figure 2.1 Mettler XP205 digital balance.

2.2.1 Cleaning

Trigene (MediChem International Ltd, Seven Oaks, UK) was used to clean the specimen before measurement. After removing from the knee simulator, the polyethylene inserts were cleaned using detergent water then soaked in 1% Trigene solution for 30 minutes to remove all visible serum and contaminants from the surface.

Then, the inserts were soaked in iso-propanol solution (Fisher Scientific, Loughborough, UK) mixed with water (70% iso-propanol: 30% water) and placed in an ultrasonic bath (VWR Labshop, IL, USA) for 10 minutes (IMBE simulator test protocol, Leeds University, UK).

Afterwards, the components were stored in the weighing room, which is temperature and humidity controlled (21^{o}C and 40% respectively) and allowed to stabilise for a period of 48 hours.

2.2.2 Weighing

The tibial components were weighed in the temperature and humidity controlled weighing room. Mettler XP205 digital balance (Mettler Toledo Inc., Columbus, Ohio, USA) was used to weigh the components of weight less than 220g. The components were weighed five times to determine an average weight, and only if the weights were within ±0.00005g were the results accepted.

Volumetric loss was calculated using the following equation, taking the density of polyethylene as 0.931 g/mm^3 (Brockett *et al*. 2011):

$$Volume = \frac{Weight\ change}{density}$$

2.2.2.1 Calibration

The Mettler XP205 digital balance was calibrated annually to United Kingdom Accreditation Service (UKAS) standard. As shown in Figure 2.2, a metallic pin (mass 1.61650g) was used as a control sample, and weighed at each measurement point to verify the balance was functioning correctly. The metal control pin will not account for moisture uptake, and was used purely as a control for each measurement to ensure the balance was operating as expected between the annual calibrations.

Figure 2.2 Metal Control Pin.

2.3 Micro-Computed Topography (Micro-CT) measurement

2.3.1 Introduction

Micro-Computed Topography (Micro-CT) is a technique that uses X-ray imaging to obtain multiple two-dimensional (2-D) images of a specimen in different projections, which can then be reconstructed into three-dimensional (3-D) geometries. The defined region of interest and segmentation parameters, such as greyscale threshold and scaling values, were used for 3D geometry reconstruction as described below. The volume of the object can then be estimated through voxel counting.

Micro-CT is considered a reliable and accurate method for volumetric assessment of retrieved acetabular liners (Bowden *et al*. 2005; Bills *et al*. 2007). The accuracy and precision of volumetric measurement technology based on Micro-CT was investigated using *in-vitro* total disc replacements (Vicars *et al*. 2009) and the Micro-CT was proved to be able to provide qualitative data (wear region) and also quantitative data (height loss). A Scanco Micro-CT100 (Scanco Medical, Brüttisellen, Switzerland) was used for measurement and analysis of tibial knee components in this project (Figure 2.3).

Figure 2.3 Scanco Micro-CT100.

2.3.2 Micro-CT scanning

Figure 2.4 shows a typical specimen of tibial knee component from laboratory test (DePuy Sigma). For retrievals obtained under ethical approval, the components were first sterilised and cleaned, and then stored in a sealed box while not being measured.

Figure 2.4 Photograph of a typical tibial knee component

The tibial component was measured gravimetrically using Mettler XP205 digital balance before Micro-CT measurement for pre-wear data. Due to the size of the tibial knee component, the largest polyethylene methacrylate (PMMA) specimen holder was used (as shown in Figure 2.5) and the component positioned using packaging foam to ensure that there would be no movement during scanning. The scanning protocol for the tibial components used a standard resolution with the use of a 1024×1024 two-dimensional image matrix. An integration time of 300ms was chosen, which took approximately 90 minutes of scan time and required a minimum of 5 GB storage space. A higher resolution was available, but the cost in terms of time and storage would not have been practical for imaging multiple specimens.

Figure 2.5 Polyethylene methacrylate (PMMA) specimen holders.

Using data from previous studies (Vicars *et al.* 2009; Eckhardt *et al*. 2002; Wong *et al*. 2007; Ding *et al*. 2011) where the optimal parameters, such as voltage and current, were determined the parameters shown in Table 2.1 were chosen.

Table 2.1 Scanning parameters of Micro-CT100

Peak voltage	Current	Specimen holder	Integration time	Resolution (pixels)	Gaussian
70 kVp	114 μA	74 mm	300 ms	1024	0.8, 1

2.3.2.1 Calibration

To ensure the accuracy of the Micro-CT measurement, a calibration process was performed every week by the technician using calibration of phantom (QRM Quality Assurance in Radiology and Medicine, Germany), which consists of five cylindrical inserts of different densities of calcium hydroxyapatite (CaHA). The phantom was used to calibrate retrievals and experimental specimens. After scanning, the densities found were compared with manufacturing specifications.

As Micro-CT analysis is based on two-dimensional greyscale image slices, it is important to distinguish the specimen from the background. The threshold is the most important factor in Micro-CT image analysis (Ding *et al*. 1999; Fajardo *et al*. 2002; Hara *et al*. 2002; Kerckhofs *et al*. 2008), and is used to define the greyscale number that differentiates the specimen from the

background. Changing the threshold will result in variation of geometry, which will further influence the volumetric assessment. However, using the phantom calibration alone to derive a fixed value of threshold has been found to be not acceptable based on past investigations (Kuhn *et al*. 1990, Sips *et al*. 2008). In order to determine the accurate threshold for obtaining Micro-CT coordinate data from 2D greyscale image slices, a methodology for calculating the threshold was required for each scan. In this project, a reference specimen of cylindrical polyethylene with a known volume of 936 mm^3 was used for a calibration process with every tibial knee component. The volume of the reference specimen was determined via an in-built image processing programme (Scanco Medical Module, version V5.01a). The threshold was determined based on the polyethylene reference specimen and then used for volumetric assessment of tibial knee components and image digitization.

2.3.3 Micro-CT image analysis

Once the scan was finished, the time to complete the reconstruction and storage of the data was comparable to the scan time (depending on specimen height and image resolution). Two dimensional image slices were then obtained and three-dimensional (3D) images were reconstructed through the following steps:

- Selection of the region of interest on 2D image slices;
- Selection of segmentation parameters using greyscale threshold and scaling values.

Figure 2.6 Greyscale threshold (Vicars *et al.* 2009).

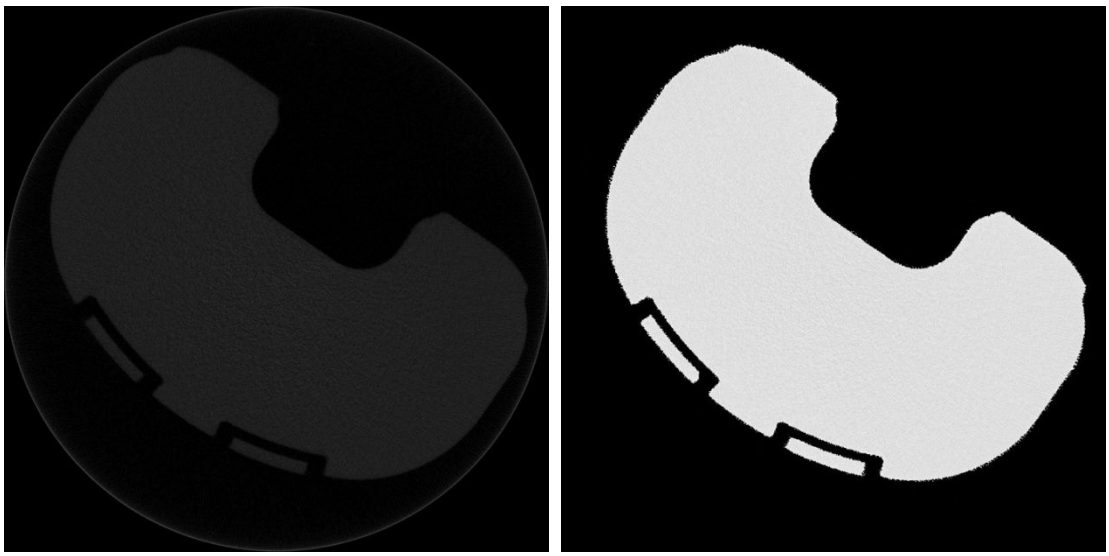

(a) Original greyscale image (b) Thresholded image

Figure 2.7 µCT image slices from original greyscale to threshold.

The threshold was an important parameter, above which which a pixel was distinguished as being part of the object material, and below which it was considered background material. Figure 2.6 shows the greyscale range used by the proprietary software (IPL, Scanco Medical, Brüttisellen, Switzerland) from 0 to 1000, there are two Gaussian scaling values used in the µCT software: sigma and support, which were selected to reduce image noise (Eckhardt *et al*. 2002; Wong *et al*. 2007; Ding *et al*. 2011). Figure 2.7 (a) is an

original greyscale image slice, (b) was obtained by thresholding. The threshold selected in this study was 20, and the Gaussian values of sigma and support were 0.8 and 1, respectively. The choise of the threshold value dramatically influences the volume of the object calculated using the internal IPL software. It was found, for instance, that a threshold value of 21 rather than 20 resulted in over 30 mm^3 volume difference for the tibial knee component. As previous mentioned, a known volume reference specimen was used to determine the threshold in this project. Figure 2.8 demonstrates a three dimensional image of a retrieved tibial knee component reconstructed from 2D greyscale image slices with different angles.

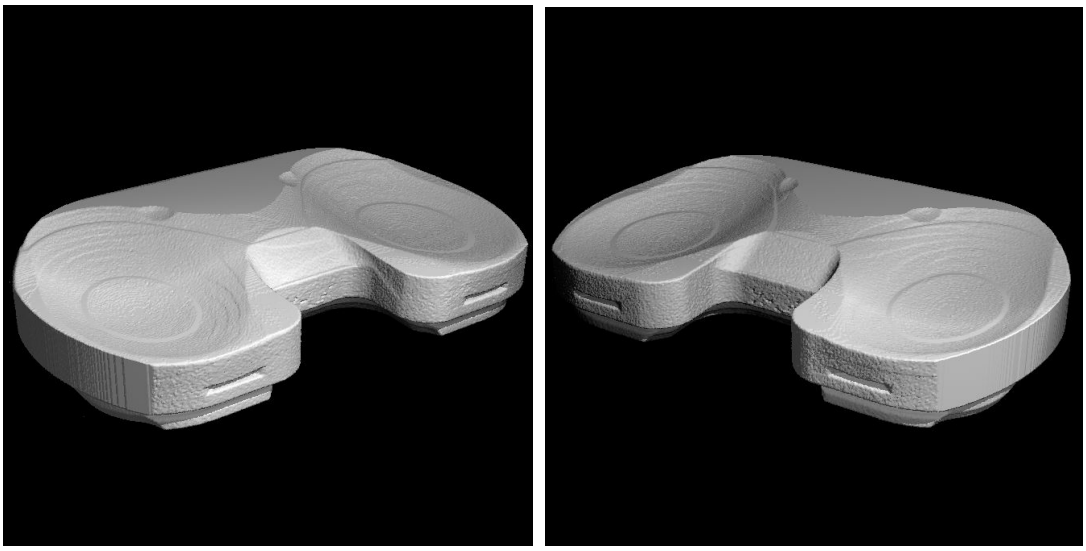

(a) (b)

Figure 2.8 Example of reconstructed 3D image

The in-built software, image processing language (IPL) was used for the volumetric calculation of tibial knee components. By selecting the region of

interest in the 2D image slices, the volume of the specimen can be calculated using the IPL. The Micro-CT scanning and volumetric analysing process are demonstrated in Figure 2.9. Table 2.2 illustrates the IPL commands used for volume calculation.

Gravimetric measurement was used as a reference to Micro-CT measurement, for experimental specimens, the data was obtained before and after the experimental simulation.

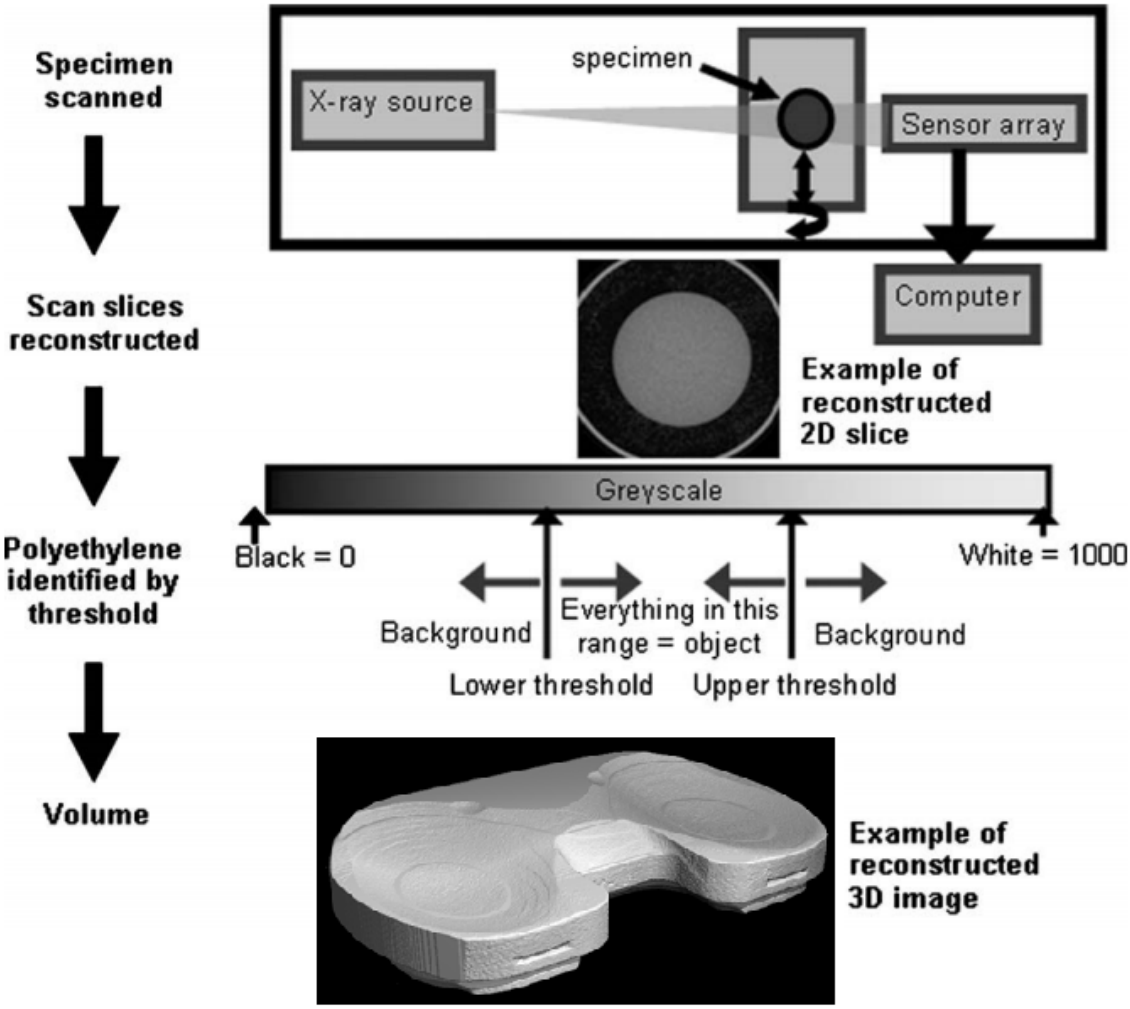

Figure 2.9 Schematic diagram of Micro-CT procedure (Vicars *et al*. 2009).

Table 2.2 IPL commands for volumetric measurement

Step	Command	Description
1	isq_to_aim	Converts *.ISQ to *.AIM file
2	write	creat *.AIM file to disk
3	gobj	Uses a '.gobj' to trim down aim file
4	gauss_seg	Segments the image based on threshold value.
5	cl_ow_rank_extract	Extracts the largest volume.
6	examine	Summarises the output in form of largest volume.

2.3.4 Derivation of surface coordinate data

For those components without pre-wear data (such as original gravimetric and geometrical measurements) or where no CAD model is available for reference, it would be difficult to determine the volume loss directly from the Micro-CT 2D image slices. The coordinate measuring machine (CMM) was considered as a technique for volumetric assessment of retrieved components in this study. Hence, a methodology was required for obtaining Micro-CT surface coordinate data to enable the same volume loss code to be applied to the Micro-CT data as to the CMM.

The 2D image slices were originally stored in proprietary format as an ISQ file. They were first converted into TIF images and then analyzed on a PC. Tapes or ftp software were used to move the data. The mathematical software MATLAB (Version 7.11, Mathworks Inc, USA) was used for image digitization and three-dimensional reconstruction. The original resolution of 2D image slices was 1024X1024, which is too large for calculation as larger image size requires much more memory and storage. An unworn tibial

component was used to investigate the effect of going from 1024X1024 matrix to 512X512. The volume difference of the left condyle of the tibial component was less than 1.0 mm^3. Therefore the images were re-sized to 512X512 to shorten the calculation time without affecting the volumetric analysis significantly.

During the image digitization, a three-dimensional matrix was defined to store initial image data and another 3-D matrix to store image data after binarization. In addition, a 2-D matrix was defined to store surface topography data. The process of image digitization and 3-D reconstruction was:

- Input original image slices and store original image slices data
- Remove image noise and convert to binary
- Store surface coordinates of each image slices
- Three-dimensional reconstruction

Figure 2.10 illustrates a three-dimensional image reconstructed using surface coordinates from 2D Micro-CT greyscale image slices. The blue colour represents the condyles of the tibial component and the shades of the colour represent the height.

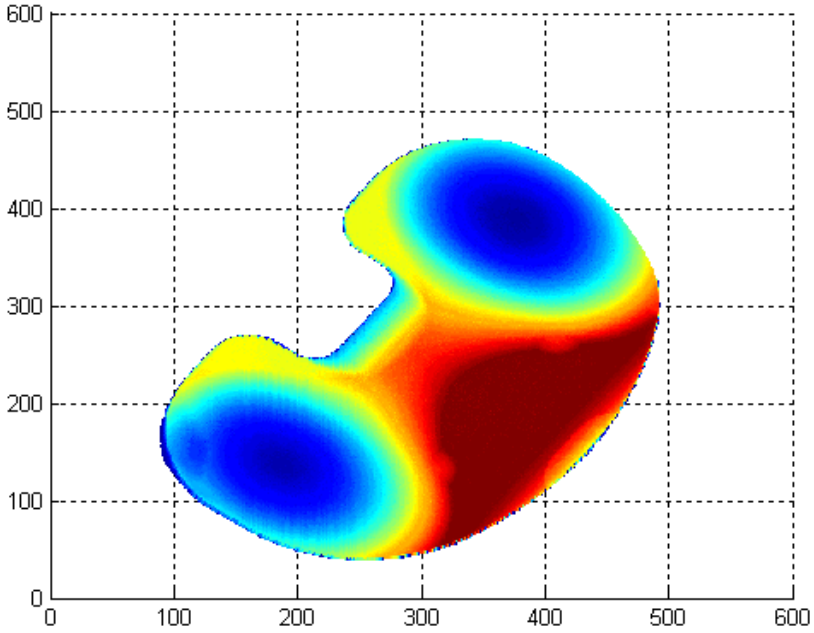

Figure 2.10 Three-dimensional image reconstruction using image coordinates.

2.4 Coordinates Measuring Machine (CMM) measurement

2.4.1 Introduction

The coordinate measuring machine (CMM) (Legex 322, Mitutoyo, UK) was used for geometrical measurement. The manufacturers indicate the resolution of the CMM was 0.8μm. As this technique measures the surface coordinates, both wear and creep deformation on the specimen surface are determined. CMM has been used previously for volumetric wear assessment of hip and knee replacement components from both *in-vitro* and retrieved from patients (Raimondi *et al*. 2000; Bills *et al*. 2007; M.Spinelli *et al*. 2009; J.K.Lord *et al.* 2011).

Compared to gravimetric measurement methodology, coordinate metrology provides a three-dimensional (3-D) construction of the component, which shows the wear area and depth on the component. In addition, CMM techniques do not need the original measurements of the components before test or implantation as an estimate of the original surface can be generated from unworn area of the components. However, only a perfect spherical specimen could be analysed using the post processing software (SR3D, Tribosol, UK), which means a novel three-dimensional volumetric assessment methodology needed to be developed for tibial knee components.

The Legex 322 coordinate measuring machine (Mitutoyo, UK) has a resolution of 0.8μm; however, this value increases with probe/stylus combination and other measurement parameters. The accuracy stated by Mitutoyo is (0.8+2*L*/1000) μm, where *L* is the measurement length in mm. In this study, the largest tibial knee component was 70 mm and the largest value of *L* was 23.6 mm, the corresponding measurement accuracy is 0.85 μm. The machine configuration and set up, as well as the analysis process will affect the accuracy of the measurement. It has been recommended that the minimum accuracy of a coordinate measurement machine used for volumetric wear analysis should be 2 μm (Becker, *et al*., 2006); however, the CMM used in this project is far more accurate than this. As shown in Figure 2.11, the whole system including Mitutoyo Legex 322 Coordinate Measuring Machine, control panel, PC and the printer.

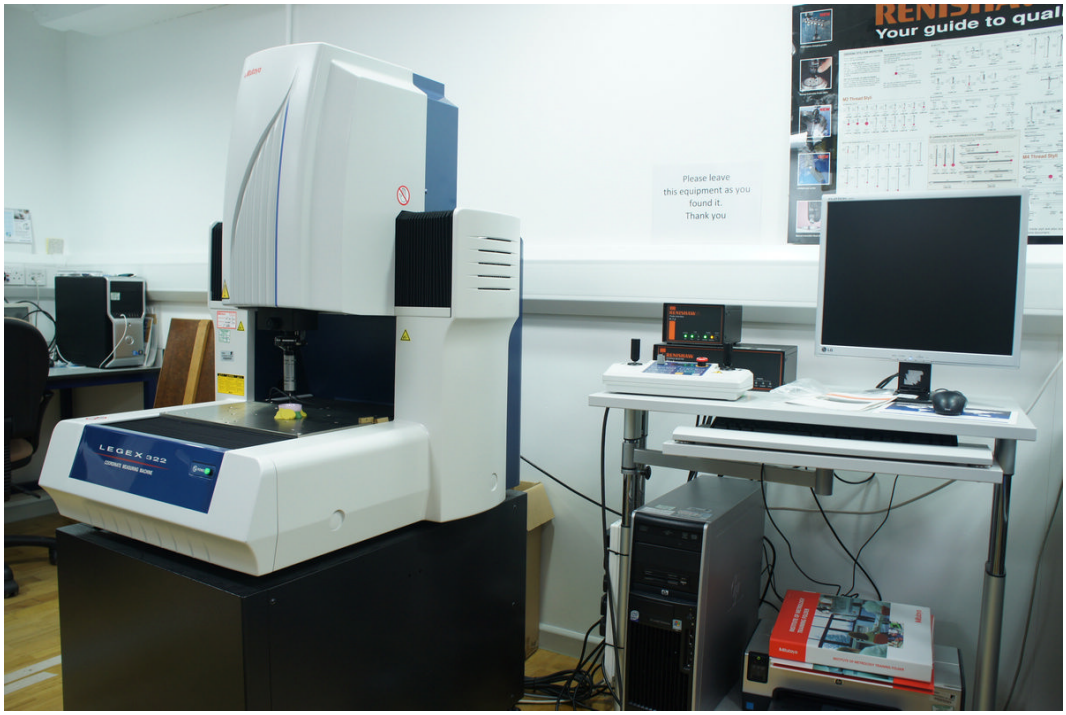

Figure 2.11 Mitutoyo Legex 322 Coordinate Measuring Machine.

2.4.2 Calibration

The probe calibration was performed before every measurement by measuring the 20mm diameter ceramic master ball. The diameter of the master ball is 19.9924mm which falls within the specification detailed in the certificate. Firstly the master ball was mounted on the CMM table and the ruby probe was attached using the specific tools. An initial contact of first top point was measured manually, and then the CMM automatically measures the master ball twice. Figure 2.12 illustrates CMM probe calibration by measuring the 20mm diameter ceramic master ball.

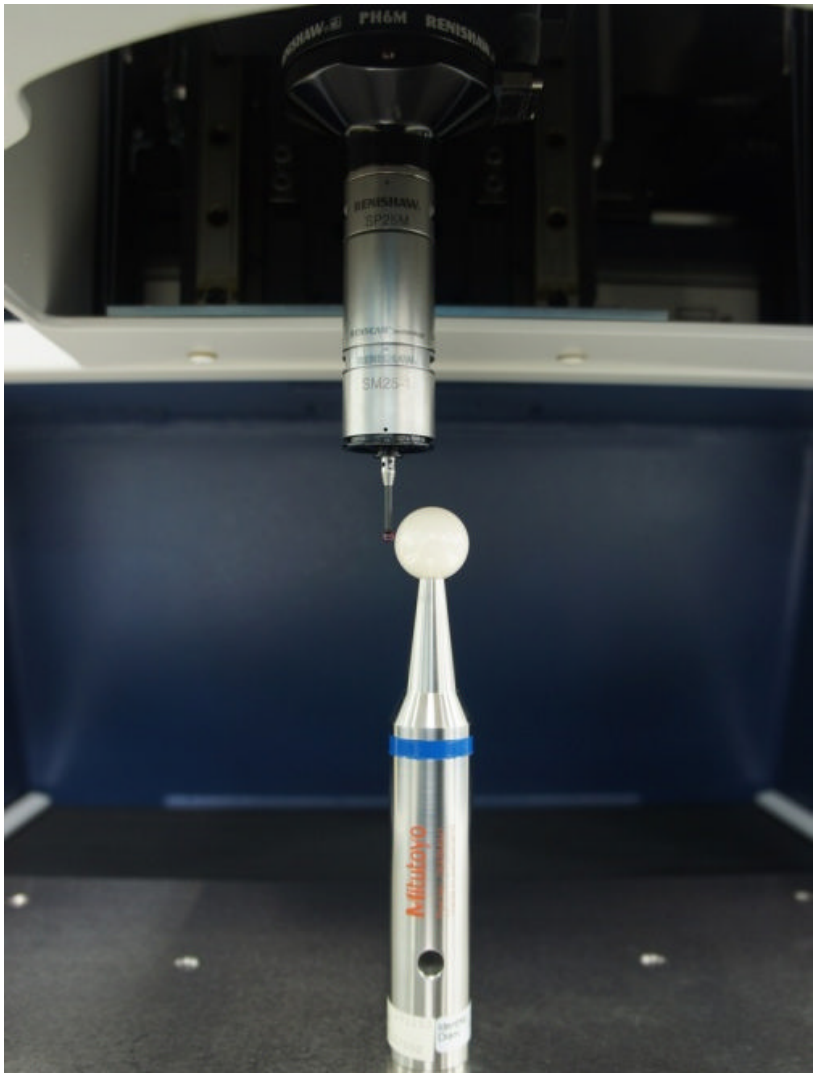

Figure 2.12 CMM probe calibration by measuring the 20mm diameter ceramic master ball.

2.4.3 Sample preparation for measurement

The test components were cleaned with iso-propanol solution and dusted with compressed air to make sure dust particles would not affect the measurement. As shown in Figure 2.13, the specimens were placed on a metallic holder and fixed with plasticine for measurement immediately after cleaning. The specimen holder was fixed to the table with plasticine to make

sure no movements occurred during scanning. Most of the volume change and deformation occur on the left and right condyles of the tibial knee components. In this project, the wear and creep on each condyle were analysed separately and then the volume changes summed for the total. In addition, due to the limitations of the current CMM scan programme, the area scanned was a rectangle rather than a circle, which mean the SR3D analysis code was not appropriate.

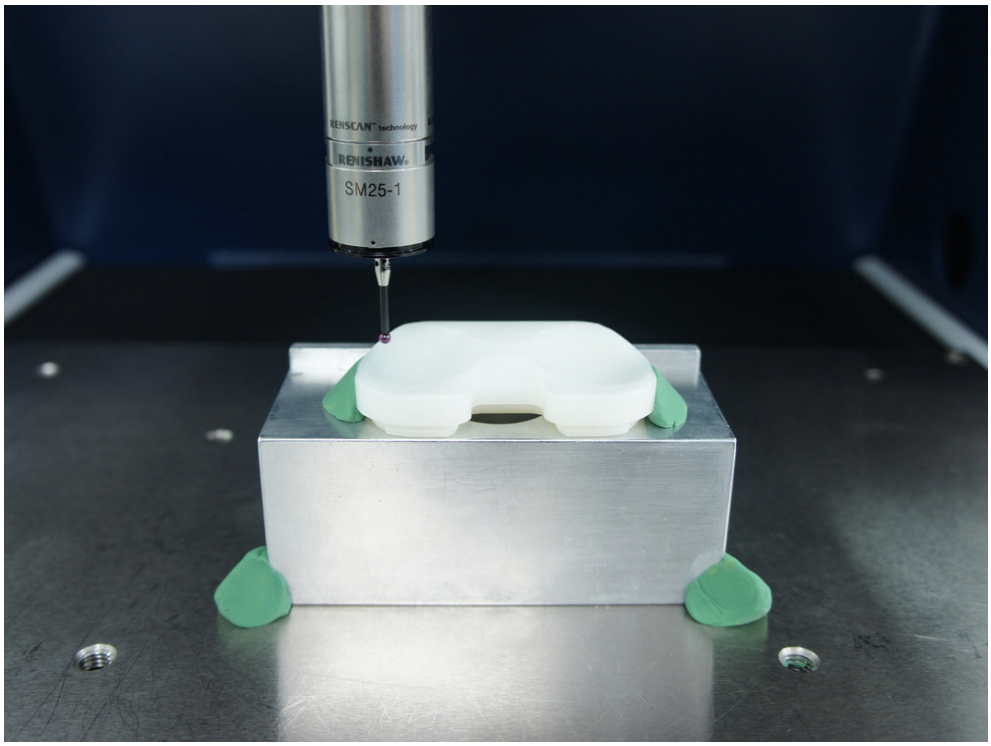

Figure 2.13 Holder for tibial knee components used in CMM.

Before scanning, the axes and the centre of the reference coordinates (x-y-z) were defined and aligned on the tibial insert. The bottom flat surface of the tibial component was considered as the reference x-y plane, the vertical

planes of tibial component were used to find the central plane and determine the y-z plane, and a point in one of the vertical planes was defined as the origin of coordinates. Figure 2.14 shows the x-y-z coordinates and the origin of coordinates. The repeatability of the measurement was investigated by resetting-up the specimen and the result shows that the volume difference was less than 0.5 mm^3.

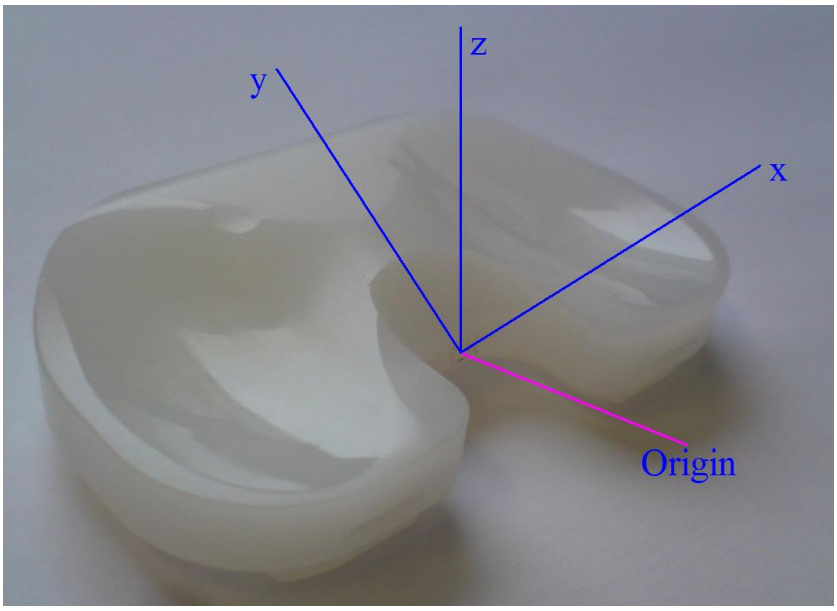

Figure 2.14 Definition of the x-y-z coordinates and the origin.

After the x-y-z coordinate and origin were defined, and the scan area was selected, the surface coordinates of tibial component could be obtained either manually or automatically line by line. However, given a CAD model of the tibial component, the surface coordinates could be obtained by a scan area, which would be more accurate and influence the volume loss measured when severe wear occurs. The coordinate points were stored in a '.dat' text file for analysis. In the project, a DePuy Sigma CAD model was used to obtain

coordinates of both left and right condyles which were measured for volumetric assessment of tibial knee components, as illustrated in Figure 2.15. It is important to align the origins between machine measurement and the CAD model for accurate measurement. Each component was measured three times and an average determined.

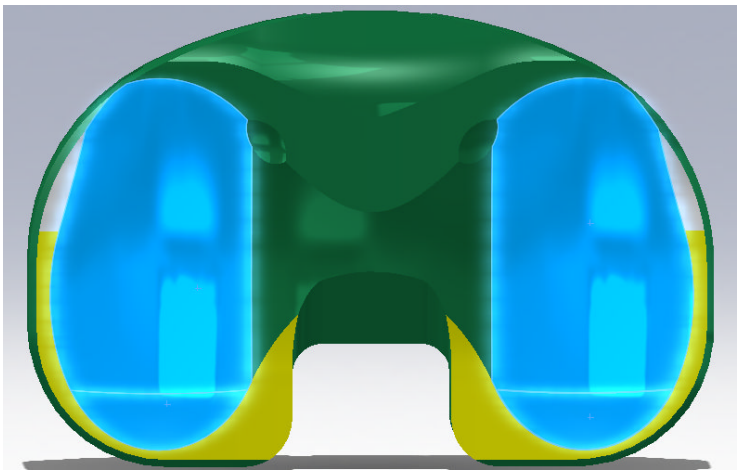

(a)

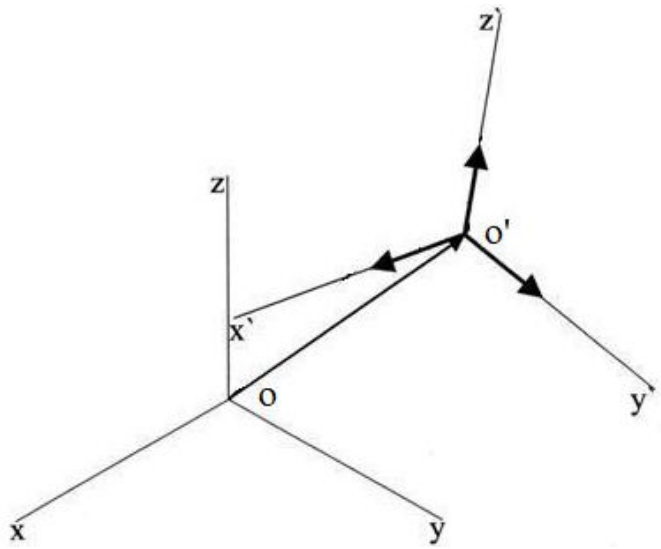

(b)

Figure 2.15 CAD model of PFC sigma tibial component and origin alignment.

2.4.4 The influence of configuration

Prior to the measurement, the machine needed correct configuration and set up, including the size and length of the stylus, and the stylus and probe configurations. As illustrated in Figure 2.16, there are many options for styli and extensions that may be used for CMM measurement. An appropriate configuration for each measurement must be chosen to obtain the best accuracy.

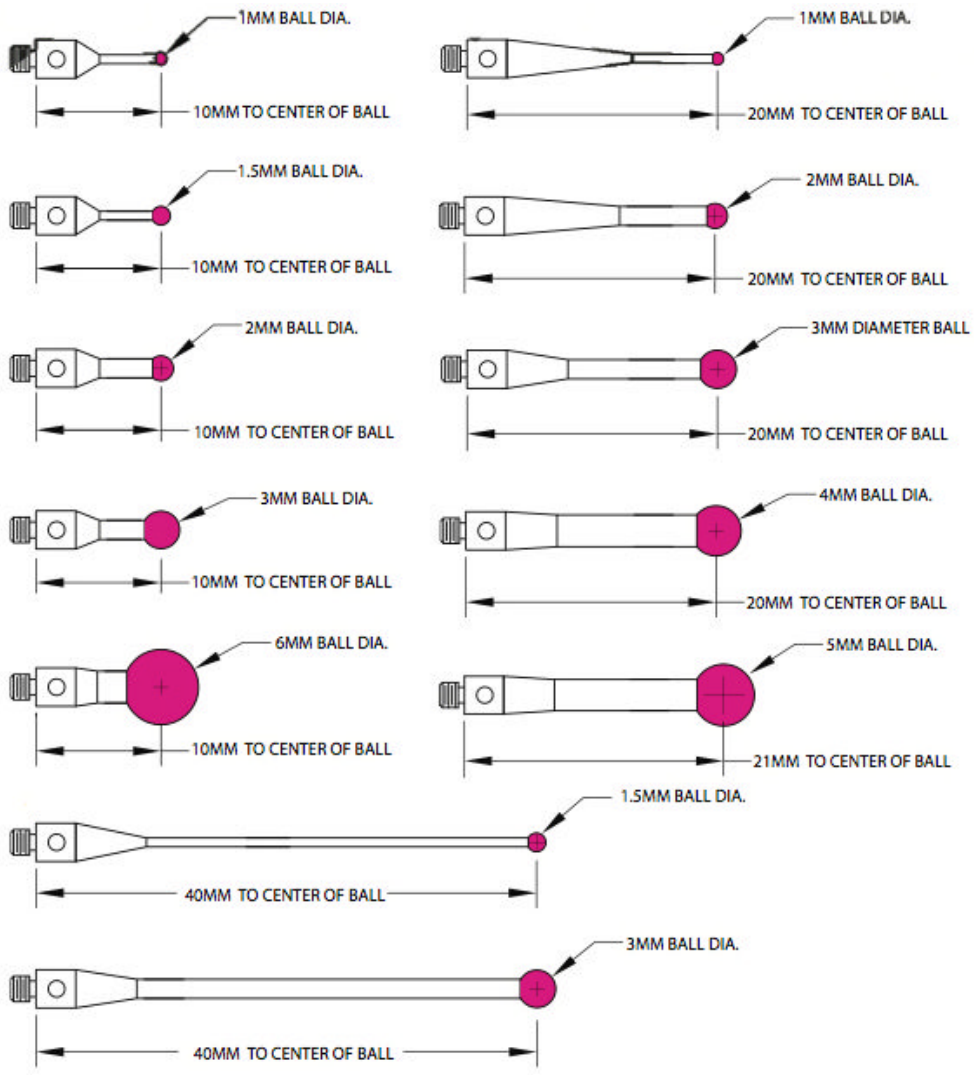

Figure 2.16 Some styli and extensions used for CMM measurements.

A smaller size of stylus means more detail would be measured from the specimen surface (Figure 2.17), which is especially essential when the components have narrow and shallow wear areas. However, the form error increases with the stylus size and the measurement becomes less accurate. The accuracy of the measurement was also affected by the extension (Figure 2.18); a short extension would provide less bending of the tip of the stylus for better accuracy. The 20 mm extension was chosen to ensure the probe would reach the edge of the specimen when establishing the coordinate system. However, a comparison measurement was carried out to investigate the influence of the extension size. The volume difference was less than 0.5 mm^3 with and without the 20 mm extension. In this study, a 1 mm diameter ruby silicon nitride zirconia styli and 20mm extension were chosen for measurement.

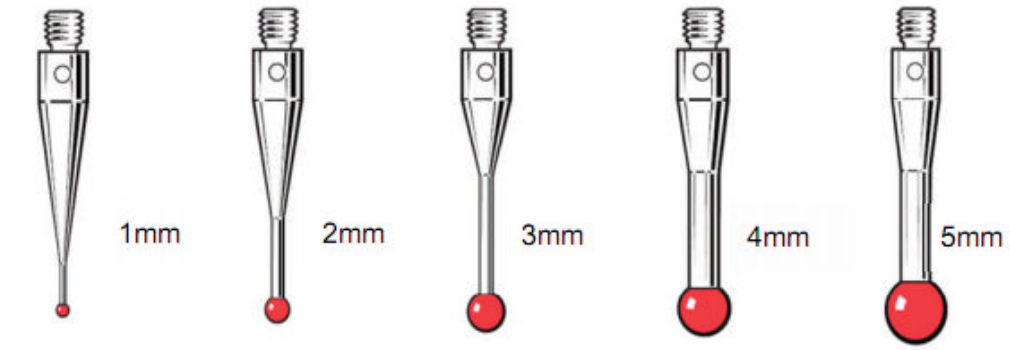

Figure 2.17 Ruby silicon nitride zirconia styli with different diameter sizes.

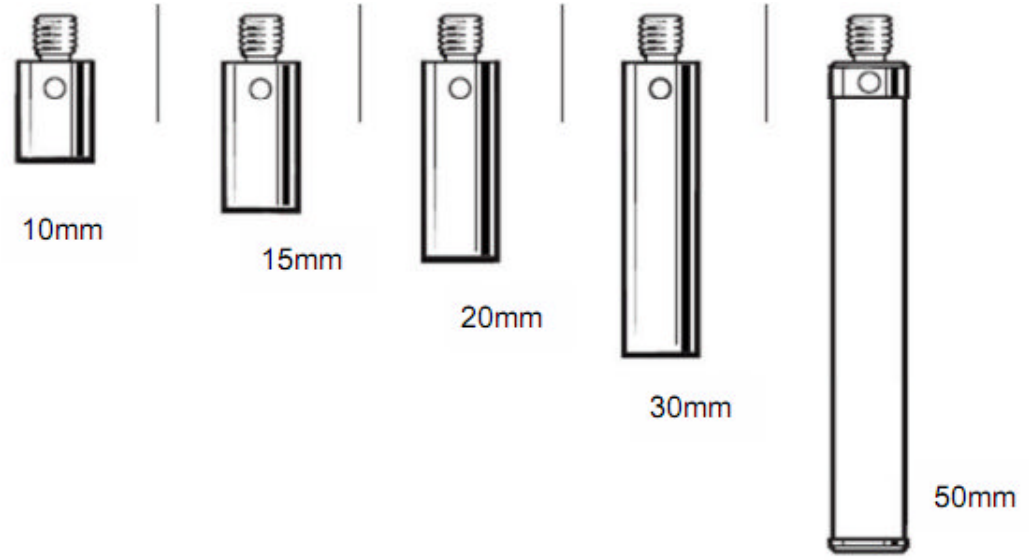

Figure 2.18 Different extensions used with stylus for greater reach.

2.4.5 The influence of CMM scan interval

For wear volume determination, the number of points measured via CMM is very important for volumetric analysis. The smaller the CMM scan interval, the more points taken, and the more surface details for wear assessment. However, smaller scan intervals are more time consuming for measurement and data processing. In contrast to the conventional measurement setup, with a scanning interval, the CMM was also fitted with a SP25M scanning head (Figure 2.19), which allowed continuous contact and data measurement. Comparing to a conventional head, the SP25M reduced measurement time dramatically. For tibial knee components, the measurement time reduced from 4 hours to 20 minutes.

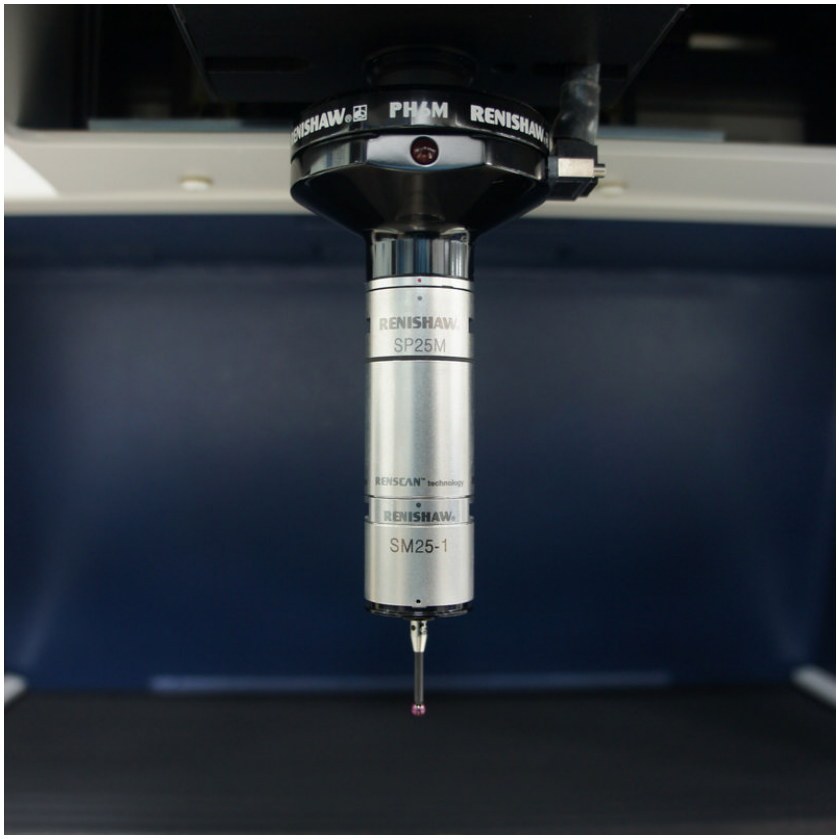

Figure 2.19 Renishaw scanning head used for coordinate measurement.

An unworn tibial knee component was used to investigate the influence of the CMM scan interval. Only the left condyle was measured in this study. As illustrated in Table 2.3 and Figure 2.20, the influence of the CMM scan interval from 0.1 mm to 2.0 mm was investigated and the results showed that, with the increasing interval of the CMM scan, the points measured decreased from 31133 to 90 and the volume difference increased from 0.2514 mm^3 to 8.7372 mm^3, meanwhile the time taken decreased. As a result, the scan interval with 0.2 mm was adopted in this project to balance accuracy and time costs.

Table 2.3 The influence of CMM scan interval on volume difference.

Sample no.	Interval/mm	Matrix	Volume difference/mm^3
I	2	10×9	8.7372
	1.5	13×11	7.5864
	1	20×17	6.1626
	0.5	39×33	1.3008
	0.2	96×82	0.4967
	0.1	191×163	0.2514

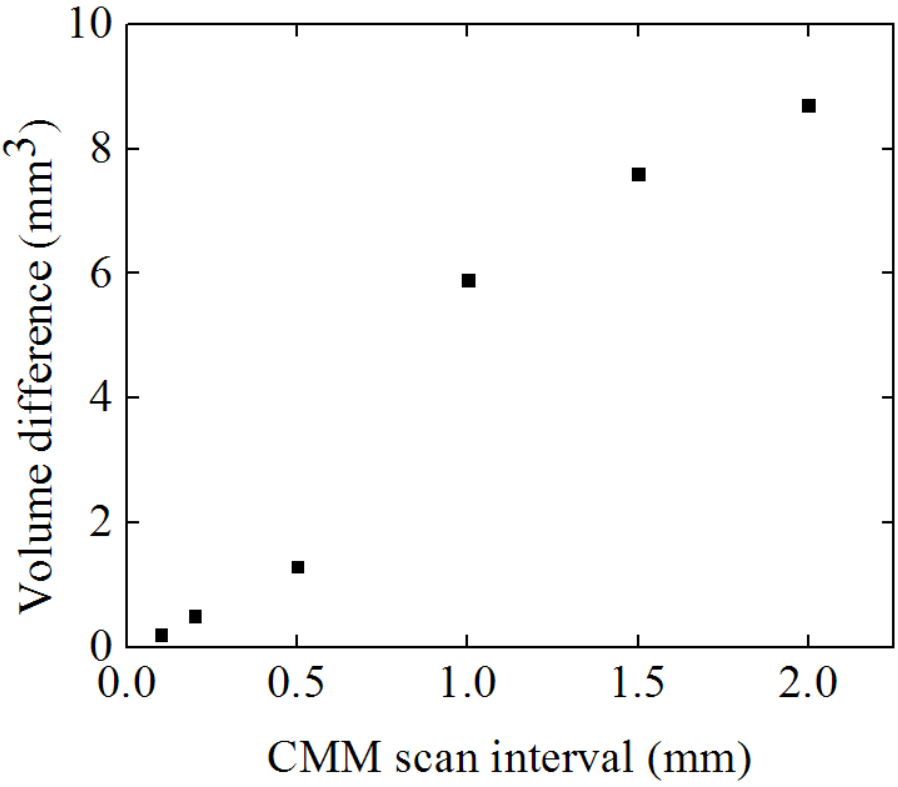

Figure 2.20 The influence of CMM scan interval on volume difference.

2.4.6 Data analysis

The volume measurement analysis was carried out using a Matlab program written by the author. After importing the measurement data from the CMM PC, the coordinate data was read in to Matlab for analysis and used to reconstruct the original surface of the component, which was essential for retrieved specimens and laboratory samples without pre-wear data. A three-dimensional surface curve fitting methodology was developed for reconstruction, which will be detailed in Chapter 3.

For the experimentally tested specimens, the initial surface before wear was measured as reference and compared with the worn specimen in Matlab for volumetric assessment. For explants or retrievals where no pre-wear data was available, the 3-D surface curve fitting method used an unworn region for reference and regenerated the original surface of the tibial knee component; hence the loss in volume was calculated. Figure 2.21 illustrated a reconstructed surface of the left condyle used as the original surface. There were some limitations in this measurement, such as the uncertainly in the actual machining tolerance and other environmental factors.

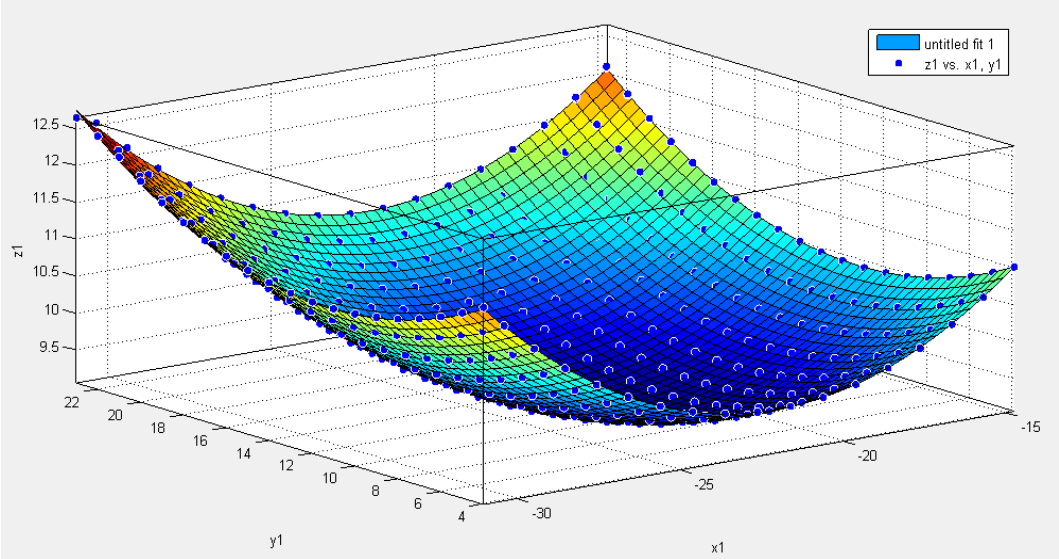

Figure 2.21 Reconstructed surface of left condyle.

2.5 Concordance correlations coefficient (CCC)

Where two measurement of wear volume were compared, the concordance correlations coefficient (CCC) defined by Lin (1989; 2008). In this project, a comparison between reference (gravimetric, FE model) and Micro-CT/CMM measurement was performed using CCC to evaluate the degree to which pairs fall on the 45° line (Lin 1989; Lin 2008). MATLAB (Version 7.11, Mathworks Inc, USA) was used to calculate the CCC following the equation defined by Lin:

$$CCC = \frac{2S_{12}}{S_1^{\,2} + S_2^{\,2} + (\overline{Y}_1 - \overline{Y}_2)^2}$$

where

$$\overline{Y}_j = \frac{1}{n}\sum_{i=1}^{n} Y_{ij}, \quad S_j^{\,2} = \frac{1}{n}\sum_{i=1}^{n} (Y_{ij} - \overline{Y}_j)^2$$

$$S_{12} = \frac{1}{n}\sum_{i=1}^{n}(Y_{i1} - \overline{Y_1})(Y_{i2} - \overline{Y_2})$$

and

If the Y1 and Y2 are in prefect agreement, the value of CCC would be 1, however, always less than 1, which characterises the agreement of the new methodology and the reference measurement. As illustrated in Figure 2.22, observed values from new method were assessed against gold standard method using CCC (Lin 2008).

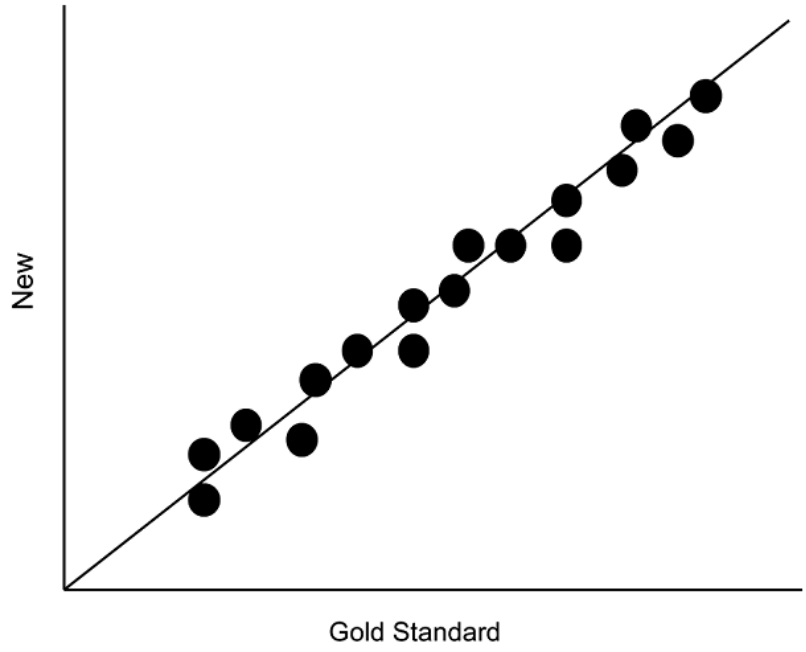

Figure 2.22 Assessing agreement of observed values (new) and target values (gold standard method) (Lin 2008).

Chapter 3

Coordinate Based Novel Volumetric Determination Methodology for PE Tibial Knee Components

3.1 Introduction

This chapter describes the development and validation of a coordinate based three-dimensional (3-D) volumetric determination methodology for polyethylene tibial knee inserts in Total Knee Replacement (TKR).

As discussed in Literature Review, wear is a common problem in TKR. Wear assessment of the polyethylene knee inserts has been an essential part of the process of improving their longevity (Krutz *et al*. 2004). Wear measurement methodologies become critically important if differentiations with respect to materials and design are sought when the geometry changes are small, and are a result of both wear and creep. The coordinate measuring machine (CMM) has been proved to be an accurate technique for volumetric assessment (Blunt *et al*. 2008; Spinelli *et al*. 2009). The aim of this study was to develop a novel methodology based on three dimensional (3-D) geometry to determine volumetric material loss of tibial knee components and validate its effectiveness and accuracy.

3.2 Volumetric determination methodology

This section describes the methods used to determine the volume change. In brief, the approach was as follows. The surface coordinates of tibial knee inserts were acquired using CMM, using a CAD model for accurate coordinate capture (section 2.4). Both initial surface coordinates and gold standard gravimetric measurement were adopted as pre-wear data for later validation. From the captured 3-D coordinates, a three-dimensional surface was established using the methods described in Section 2.4.6. The undeformed region was identified automatically using a MATLAB (Version 7.11, Mathworks Inc, USA) program, which was used as reference for volume loss assessment in the conditions where no pre-wear data was provided (Muratoglu *et al*. 2003). A 5^{th} order polynomial surface curve fitting algorithm was used to generate the original 3D surface based on this undeformed region, which will be detailed in Section 3.2.2.2.

Once the surface coordinates of tibial knee components were acquired, further analysis was undertaken to evaluate both the linear and volumetric wear as well as the creep deformation. Two situations were considered, one with reference, and the other without a reference. For the *in vitro* specimens, the initial surface before wear was measured using Micro-CT and CMM as a reference and compared with the worn specimen for volumetric assessment. Gravimetric measurement was also performed as a gold standard reference for wear volume determination. For explants or retrievals where no pre-wear data was available, the 3-D surface curve fitting method used an unworn

region for reference and regenerated the original surface of the tibial knee component in order to calculate the loss in volume.

3.2.1 Volumetric determination with a reference

A reference surface can be obtained from three approaches: (a) pre-wear data; (b) A CAD model; (c) design drawings. The reference surfaces provide accurate information for analysis, however, the tolerances of a CAD model and measurement errors during pre-wear data acquisition could influence the volume calculation dramatically (Carmignato *et al* 2011).

Using approach (a), unworn tibial knee components were measured using either Micro-CT or CMM before the simulation tests using the methods described in Chapter 2. The amount of wear was calculated by simply subtracting the volume before and after simulation testing. By using CMM, surface coordinates of tibial knee components were obtained as a reference for assessment of linear wear and volume loss. For Micro-CT, an image digitization methodology was used to obtain points in form of coordinates from the image slices for volumetric assessment (section 2.3.4). In addition, using approach (b), a PFC Sigma CAD model was obtained from the manufacturer and used as pre-wear data for reference. Figure 3.1 demonstrates a CAD model of tibial knee component used as a reference.

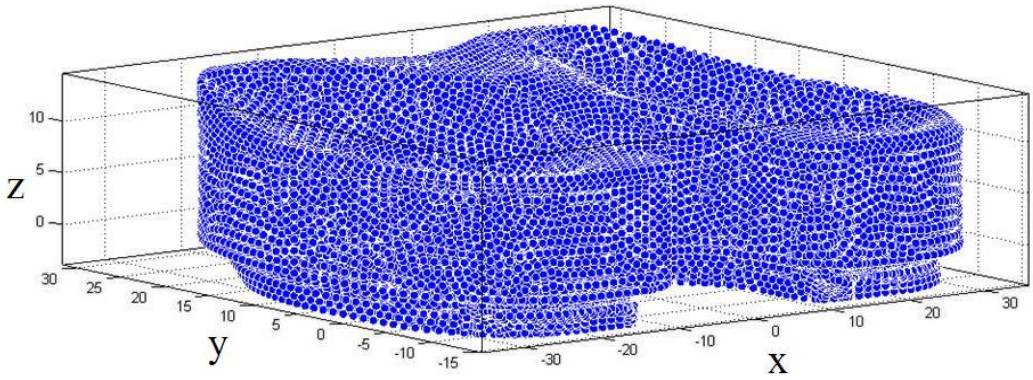

Figure 3.1 CAD model of a typical tibial knee component used as a reference**.**

3.2.2 Volumetric determination without a reference

For cases where it was not possible to obtain a reference surface, an alternative method was developed. This used a 5th order polynomial surface curve fitting algorithm to generate the original 3-D surface, based on the undeformed region of the component. The reconstructed surface was considered as the original surface for the volumetric wear determination. Since two-dimensional image slices obtained from Micro-CT measurement can be digitalized in the form of coordinates (section 2.3.4), the following calculation and discussion were focused on the use of coordinates for volumetric wear assessment of the tibial knee components.

The process of surface curve fitting and wear assessment was as follows:

- surface coordinates acquisition
- undeformed region identification
- surface curve fitting

- reconstruction of original surface
- volume determination

Figure 3.2 shows the acquisition of coordinates of the upper surface from a finite element (FE) model, provided by a colleague within the research institution (A.Abdelgaied). The FE model was used for computational wear simulation with 5 million cycles (MC). The wear volume and maximum linear penetration were provided for comparison of the surface curve fitting methodology.

3.2.2.1 Undeformed region identification

The wear region identification is important for accurate surface curve fitting; since the worn region will be removed from the dataset and just the undeformed region retained to reconstruct the original geometry. Figure 3.3 demonstrates the wear region and undeformed region in form of two-dimensional profile. As the wear region cannot be determined precisely without a reference, several undeformed regions were selected manually as reference surfaces to fit the geometry and then compared with FE models to validate the surface fitting methodology. Figure 3.4 shows selection of different undeformed regions, based on the vertical coordinates. The selection method does have some limitations, since the presented surface curve fitting methodology was based on the undeformed region, the ‘original’ surface reconstruction would not be able to be used as a reference if the undeformed region is not sufficiently large.

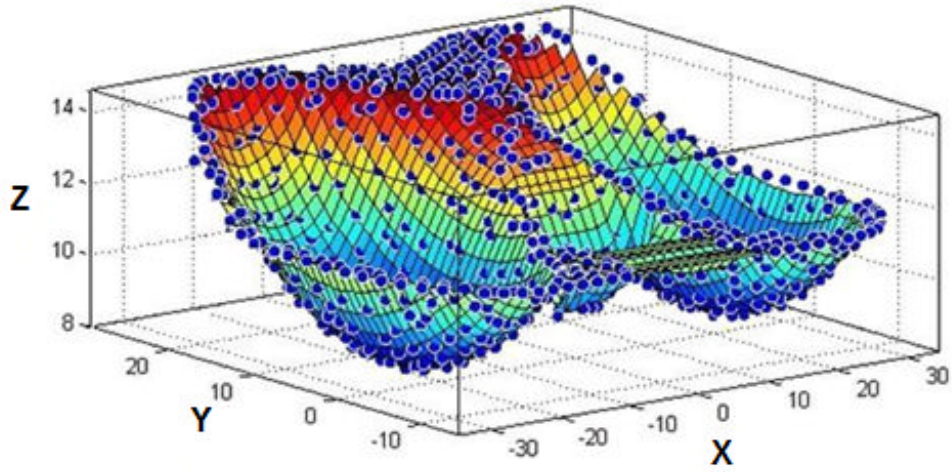

(a)

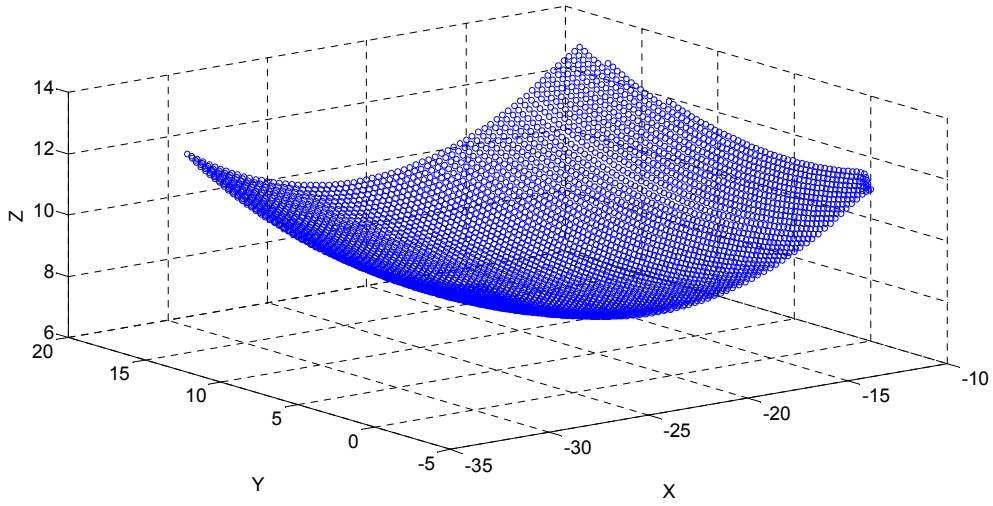

(b)

Figure 3.2 Acquisition of surface coordinates of tibial knee component: (a) coordinates of upper surface from FE model; (b) coordinates of left condyle from an unworn tibial knee component.

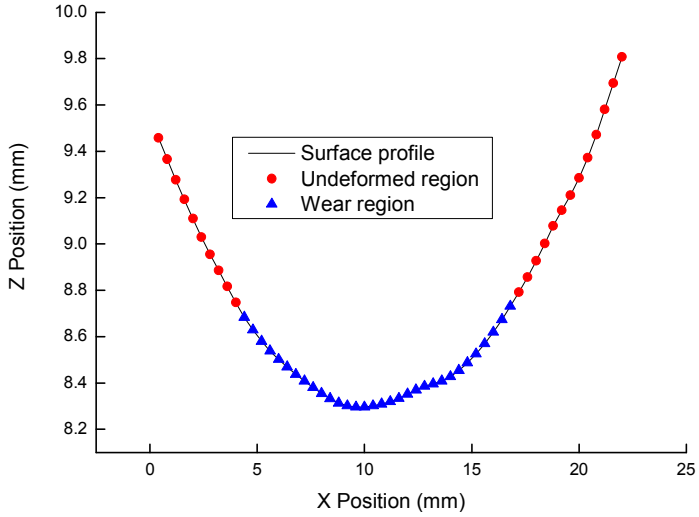

Figure 3.3 The profile in the x-z plane through y=25 mm of wear and the undeformed regions.

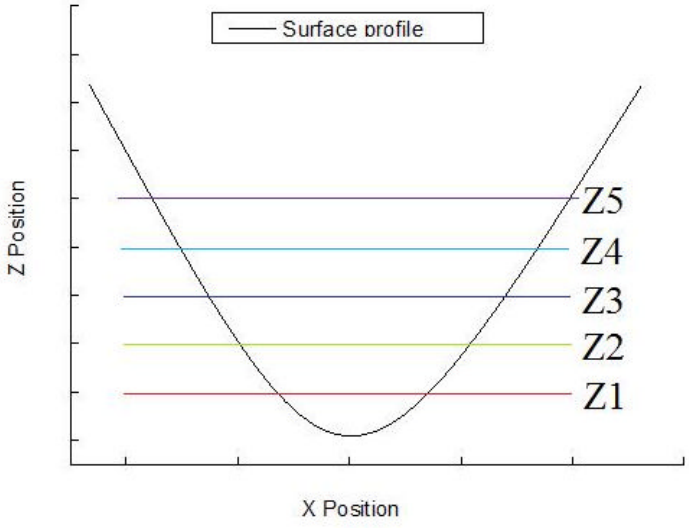

Figure 3.4 Selection of reference line used for surface curve fitting.

3.2.2.2 Polynomial surface curve fitting

An unworn tibial knee component was measured using the coordinate measuring machine to obtain surface coordinates of the left condyle and was used to investigate the volume determination results using different surface

fitting algorithms. The surface was defined by a polynomial, the order of which was varied from a 2nd order ('poly22') to a 5th order ('poly55'). The polynomial model used in this study fitted a polynomial in degree x and y, which means poly55 is poly(x=5, y=5).

For each polynomial considered, the root mean square error (RMSE) between the polynomial surface and the underlying CMM-measured geometry was calculated. As shown in Figure 3.6, the residuals between reconstructed surface coordinates and scanned coordinates at Y-Z plane decreased with the increasing order of the polynomial. The comparison of results from the different polynomial fitting and corresponding volume determination are presented in Table 3.1, including RSME and volume difference. With the increasing order of the polynomial, the volume difference reduced and the corresponding RMSE decreased. Studies show that higher order polynomial fitting would increase the time of analysis and require greater computational power. The solution time was approximately 2 minutes for a 2nd order up to 6 minutes for a 5th order polynomial fitting and volumetric wear analysis when running on a desktop PC (Intel (R) Xeon (R) CPU X5260@3.33GHz, 3.25 GB of RAM).

With increasing of order of polynomial, the volume difference between unworn tibial knee component and the polynomial surface decreased dramatically from 2nd order to 3rd order and then became stable from the 4th degree polynomial and reached the lowest value when the fitting degree increased to a 5th order (Figure 3.5). The RMS error was not affected by the polynomial being odd or even; there was just a general decease in error as the order increased.

Table 3.1 Comparison of different polynomial fitting and corresponding volume determination results

Fitting degree	RMSE	Volume difference/mm^3
2nd	0.0156	1.6358
3rd	0.0102	0.8165
4th	0.0038	0.1096
5th	0.0037	0.0968

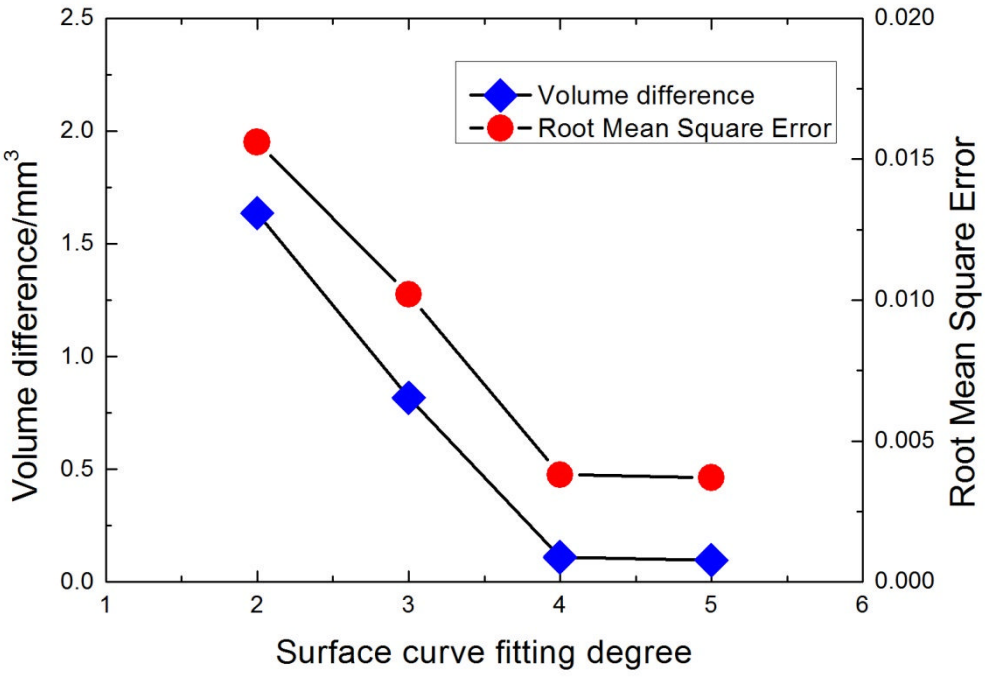

Figure 3.5 Volume difference and RMS error of 2nd order to 5th order polynomial fitting.

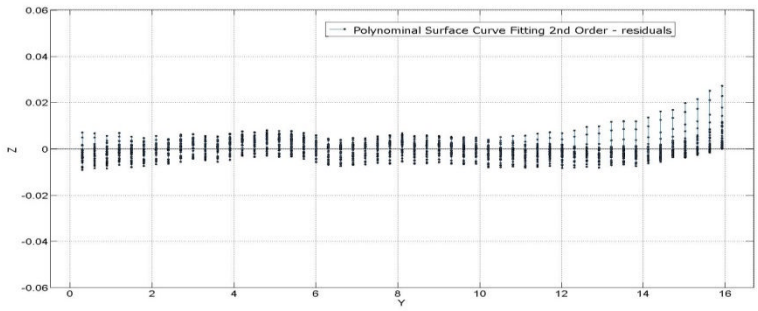

(a) 2nd order polynomial fitting (poly22)

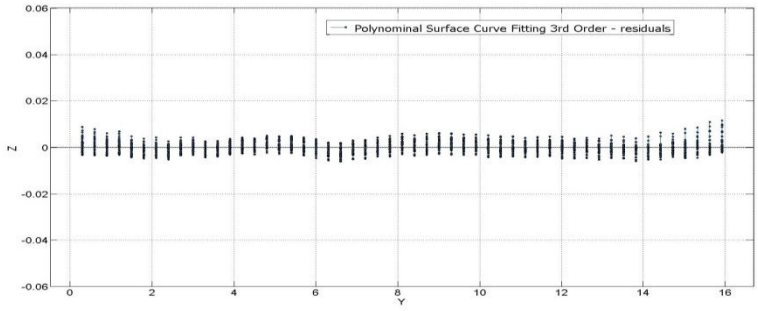

(b) 3rd order polynomial fitting (poly33)

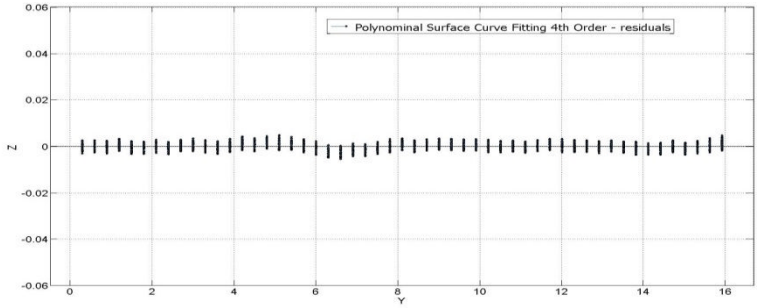

(c) 4th order polynomial fitting (poly44)

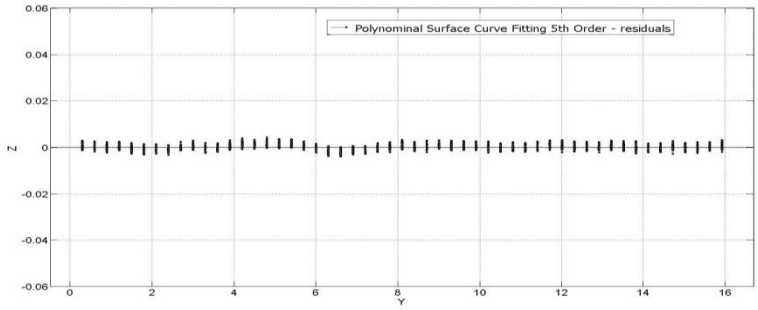

(d) 5th order polynomial fitting (poly55)

Figure 3.6 Residuals of 2nd order to 5th order polynomial fitting at Y-Z plane.

In addition to the polynomials above, an orthogonal polynomial of the form generated by Forsythe (Forsythe 1957) was also investigated using simulated wear data (Section 3.2.2). The results including RMSE and volume difference for orthogonal and polynomial are illustrated in Table 3.2. It is shown that Orthogonal is slighter better then 5^{th} order Polynomial with maximum volume difference of 0.2 mm^3. However, the time consuming for the Orthogonal was greater than Polynomial due to the complexity of the formula (Forsythe 1957, Smith 1965).

Table 3.2 Comparison of orthogonal and polynomial results

Simulated Wear (mm^3)	Orthogonal (mm^3)	RMSE (Orthogonal)	Polynomial (mm^3)	RMSE (Polynomial)
1.3	1.3	0.0018	1.3	0.0018
5.1	5.1	0.0021	5.1	0.0021
11.2	11.2	0.0022	11.1	0.0037
19.7	19.6	0.0036	19.5	0.0049
30.6	30.4	0.0051	30.3	0.0063
42.5	42.2	0.0065	42.1	0.0079

As a result of this study, a 5^{th} polynomial was used for surface curve fitting in this project to reconstruct the original surface as follows for a fifth order, the equation used for generating as below:

$$f(x,y) = P00 + P10x + P01y + P20x^2 + P11xy + P02y^2 + P30x^3 + P21x^2y + P12xy^2 + P03y^2 + P40x^4 + P31x^3y + P22x^2y^2 + P13xy^3 + P04y^4 + P50x^5 + P41x^4y + P32x^3y^2 + P23x^2y^3 + P14xy^4 + P05y^5$$

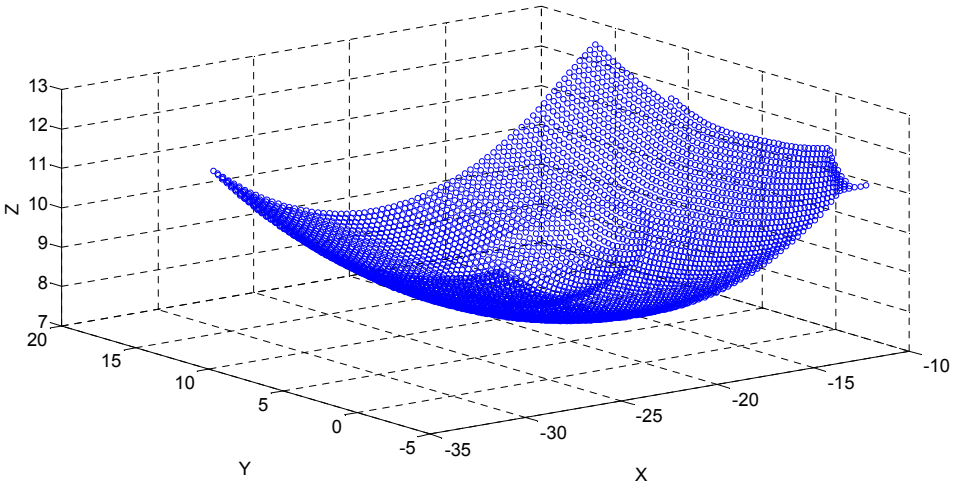

(a) coordinates obtained from a worn surface of left condyle

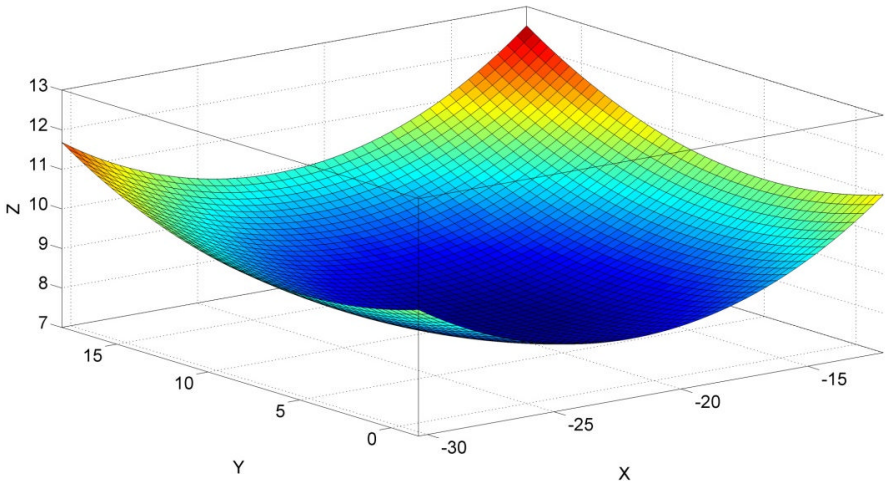

(b) reconstructed surface curve

Figure 3.7 Surface coordinates obtained using CMM and reconstructed original surface for volumetric assessment.

Matlab was used to programme based on the equation above and regenerate original surface curve.

After fitted the surface by programming in mathematical software Matlab, the surface equation was generated. Surface interpolation methodology was applied to generate a regular grid of x and y coordinates if required to assess the amount of wear under the reconstructed surface. The original unworn coordinates were obtained from the reconstructed surface and used for wear volume calculation. This is illustrated in Figure 3.7. Hence, the volume loss can be determined by subtraction of coordinates obtained from worn surface and regenerated ‘original’ surface.

3.3 Methodology validation

A finite element (FE) model was provided by a colleague within the research institution (A. Abdelgaied) for validation with known wear volume and maximum linear penetration. The FE model was used for computational wear simulation. In the current study, it was used to represent the pre-worn geometry and that after five million cycles. The validation of the curve fitting methodology included both with reference and without reference methods, as detailed below. The wear volumes of left and right condyle were calculated separately and then summed together for total wear volume since the whole upper surface of the tibial knee component cannot be characterized using a single equation.

3.3.1 Validation with reference

Since the coordinates from the finite element model were available before and after wear, the wear volume and maximum linear wear were easily calculated. As shown in Table 3.3, the wear volume determined by surface curve fitting was 36 mm^3, which is close to the FE model (35 mm^3). The maximum linear penetration was determined using profiles before and after wear, as demonstrated in Figure 3.8.

Table 3.3 Calculation results compared with the finite element model

	Wear volume (mm^3)	Max linear wear (mm)	Wear rate (mm^3/mc)
Present study using surface curve fitting	36	0.25	7.2
Finite element model	35	0.25	7

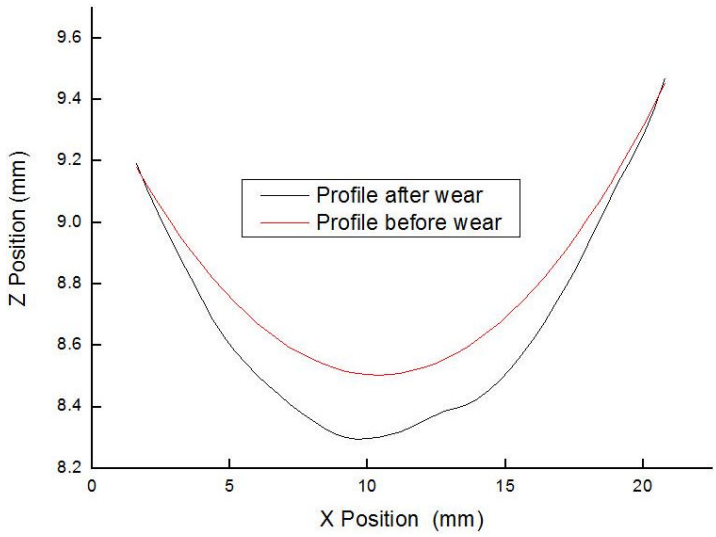

Figure 3.8 Max linear wear determination using profiles before and after wear.

3.3.2 Validation without reference

3.3.2.1 Validation from FE model

For validation of the method without reference, only the coordinates of the surface from the finite element model representing 5 mc were used. The region of wear was not clearly identifiable; and as a result, the curved surface fitting methodology was performed using selection of different reference lines. Five heights of the z position were selected as the reference line ranging from 8.30 mm to 9.25 mm, as shown in Figure 3.9, and were used for the curved surface fitting. Figure 3.10 illustrates the corresponding undeformed area which ranged from 85% to 30% of the whole area of left condyle. The wear area of the left condyle from the FE model is around 50%, as a result, the 55% and 45% selection of the total area appears to be most suitable by comparing with the FE model with wear volume 37 mm^3 and 39 mm^3 respectively. For selection of 85% and 70% of the total area, the selection is not the real undeformed area since part of the worn area is also included. Hence the volumetric wear determination would not be accurate if part of the worn region was used in the curved surface fitting. For selection of an undeformed region less than 45%, there is not enough area used as reference for accurate original surface reconstruction, as demonstrated in Figure 3.10.

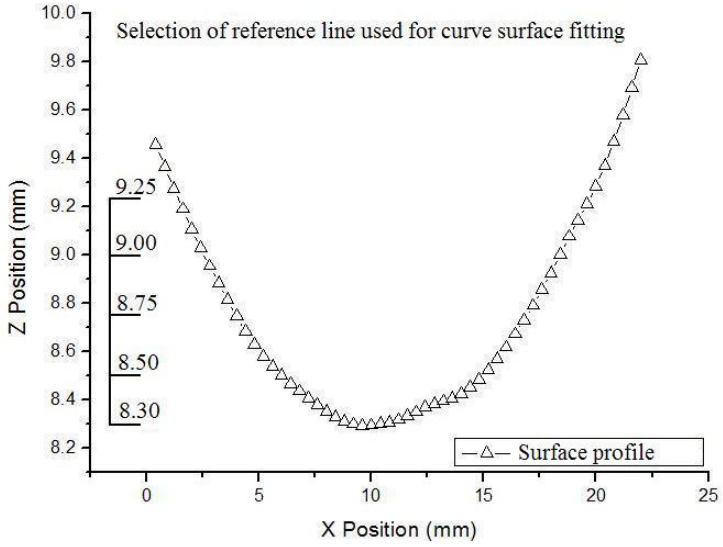

Figure 3.9 Selection of reference line at different heights of z position.

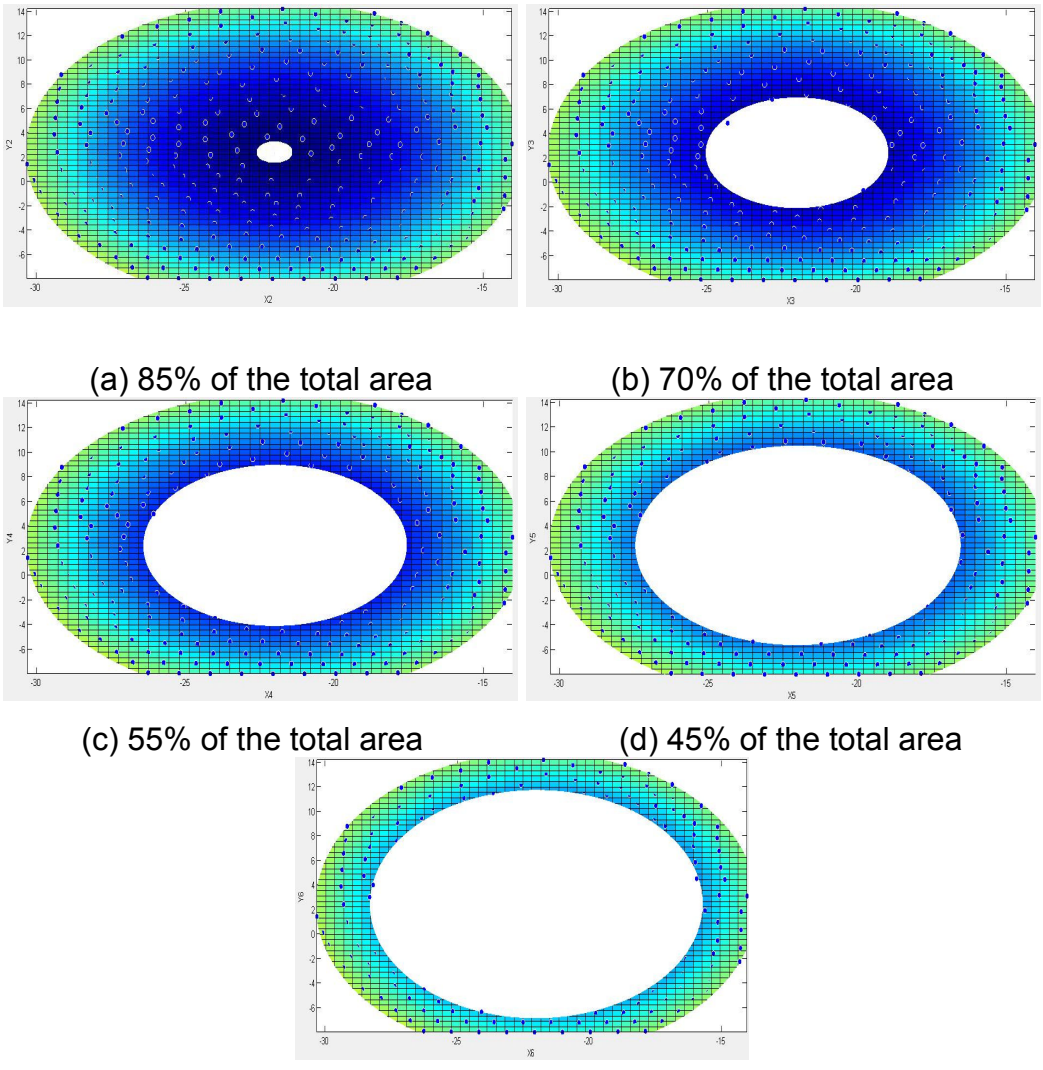

(a) 85% of the total area (b) 70% of the total area

(c) 55% of the total area (d) 45% of the total area

(e) 30% of the total area

Figure 3.10 Selection of undeformed area used for curved surface fitting.

The linear wear and volumetric wear as well as wear rate were calculated with different selections of the 'undeformed' region. The results are presented in Table 3.4. With the increasing percentage of undeformed region selected as reference coordinates for curved surface fitting, the wear volume and maximum linear wear as well as wear rate increased. Detailed comparison of the worn and reconstructed two-dimensional profiles at different Y-positions range from -25 mm to 75 mm of left condyle are shown in Figure 3.11.

Table 3.4 Surface curve fitting results with different reference coordinates

Z/mm	Undeformed region (%)	Wear volume (mm^3)	Max linear wear (mm)	Wear rate (mm^3/mc)
8.30	85	16	0.08	3.2
8.50	70	28	0.19	5.6
8.75	**55**	**37**	**0.26**	**7.4**
9.00	45	39	0.27	7.8
9.25	30	51	0.31	10.2

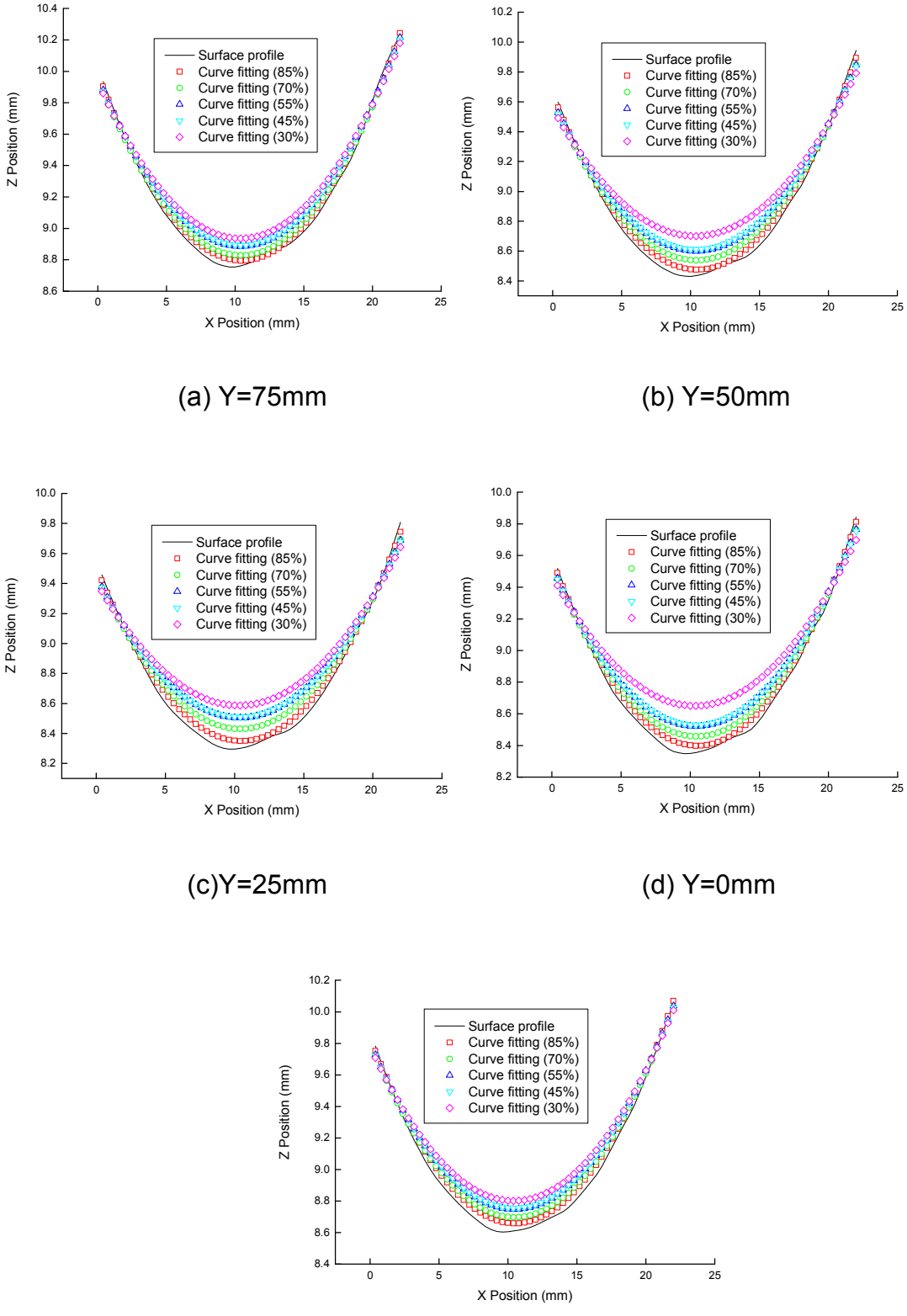

(a) Y=75mm

(b) Y=50mm

(c)Y=25mm

(d) Y=0mm

(e) Y=-25mm

Figure 3.11 Two-dimensional profiles comparison with different selection of 'undeformed' region at different Y position.

3.3.2.2 Validation from computational volume removal

From the methodology above, surface fitting was shown to be reliable for evaluating wear volume of polyethylene components when the amount of wear is not severe. In addition, undeformed region selected from 55% of the total area used as a reference appears to be the best. A computational volume removal test was performed to further validate the coordinate based three-dimensional volumetric assessment methodology. In the present study, the surface was generated with different wear areas range from 2% to 38%, which were manually removed from the original surface based on coordinates provided by the finite element model. The maximum linear wear penetration was 0.15 mm and the wear volume removed range from 1.3 mm^3 to 42.5 mm^3.

Table 3.5 Comparison of computational volume removal and surface curve fitting results

Wear region (%)	Wear volume cut (mm^3)	Maximum linear wear cut (mm)	Wear volume calculated (mm^3)	Maximum linear wear calculated (mm)
2	1.3	0.15	1.3	0.15
5	5.1		5.1	
10	11.2		11.1	
16	19.7		19.6	
25	30.6		30.3	
38	42.5		42.1	

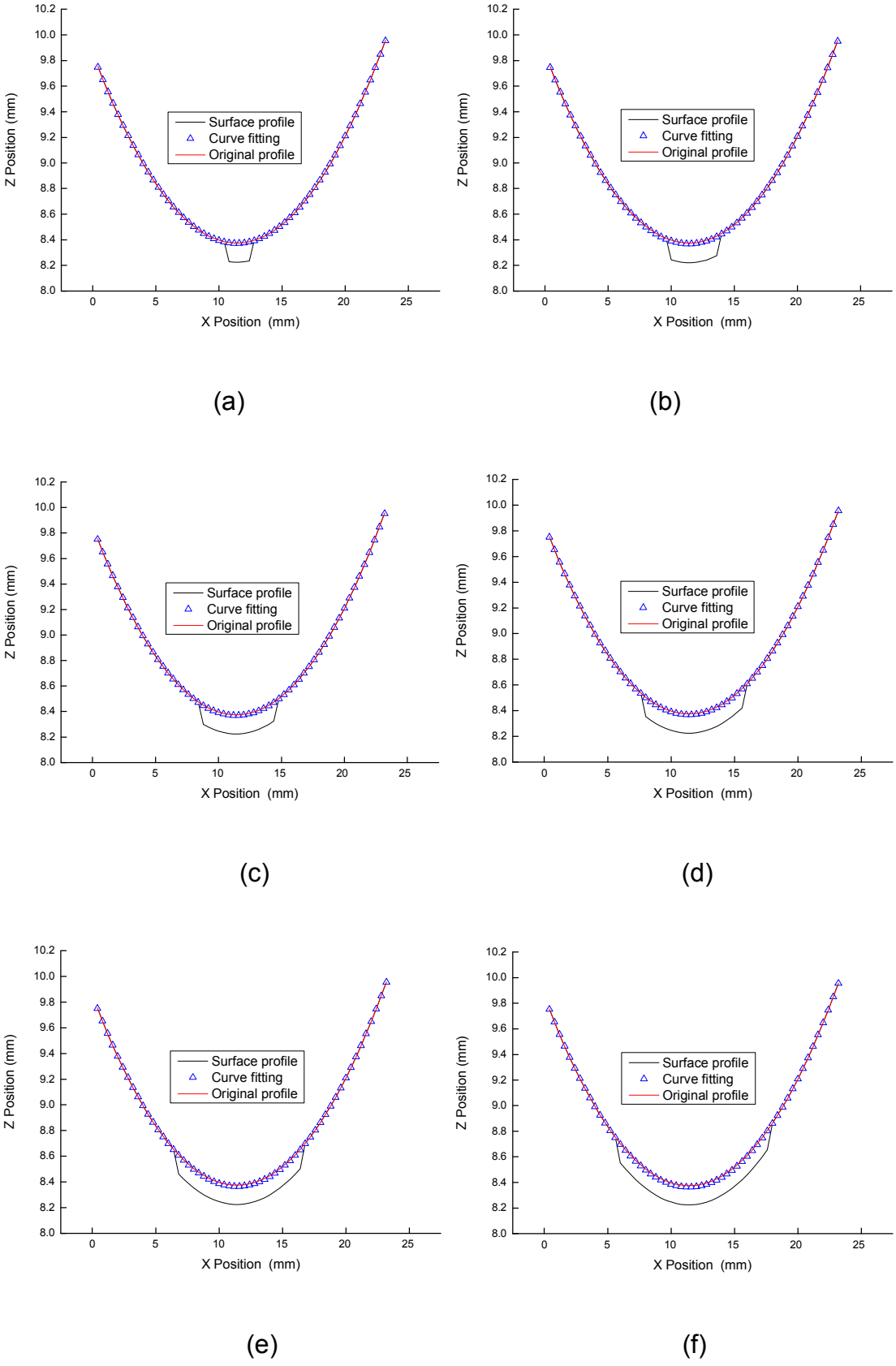

Figure 3.12 Profiles comparison (Y=25 mm, 55% undeformed region as reference, wear region range from 2% to 38%).

The surface fitting algorithm was then applied using the undeformed coordinates from 55% of the total area. The known volume removed and the volume calculated from the surface fitting algorithm were compared and the results are shown in Table 3.5. The wear volume calculated was close to the wear volume removed and the maximum linear wear calculated was the same as the computational result. Therefore, the surface fitting methodology is reliable and feasible for estimating the relevant amount of wear. Detailed comparison of surface profile and curve fitting as well as original profile are shown in Figure 3.12.

3.4 Discussion

Initial geometric measurement of specimens or design drawings would be ideal as a reference for volumetric wear assessment; however, these are not always available (Liow *et al*. 1997). Assessment of amount of wear with and without references was carried out by three-dimensional voxels counting and surface curve fitting respectively. For the curved surface fitting, the results were shown to be accurate with an undeformed region of around 50% of the condyle surface as reference coordinates for surface fitting. The presented coordinate based methodology was used to determine volumetric material loss based on 3-D surface curve fitting and the validation results indicated that the methodology is adequate for tibial knee components where no pre-wear data, CAD models or original design drawings are available.

It should be noted that the damaged area is mainly located at the concave surface of the tibial knee bearing components and the amount of

wear from the finite element model used in this study was relatively small. As a result, the curve fitting methodology based on coordinates was able to generate the surface before wear. However, when the amount of wear increases and the border of tibial knee inserts are damaged, the method presented above may be no longer suitable, in this situation, novel procedures are required to evaluate the amount of wear based on drawing of worn tibial knee components.

CAD models, pre-wear data and design drawings can provide references for assessment of wear; however, the accuracy of original drawings may be affected by the tolerance, which would result in over- or under-estimate of the amount of wear. Besides, because many kinds of polyethylene bearing components exists and the number is increasing year by year, there is a variation in the shape of components in the patient population, as a result, it is not feasible to establish all the CAD models to be used as references.

In conclusion, methodologies based on coordinates from Micro-CT two-dimensional greyscale image slices and coordinate measuring machine have been developed to reconstruct the surface geometry of a tibial knee insert. For the wear model considered, where the tibial knee insert was obtained from a wear simulator study under ideal conditions, and wear was moderate, the methodology for reconstruction of the unworn surface was adequate. This was particularly true when roughly 50% of area was selected for surface fitting, even without references, such as pre-wear data, CAD model or original design of drawings. However, only one FE model with a 5 MC simulation duration was used for validation in this project as shorter simulation time would result in smaller wear area and lower volume change. The currently used volumetric

determination methodology requires 50% unworn area for reference to reconstruct the original surface, which means the worst condition was considered in the FE model. In addition, compared to experimental studies, computational model would provide idealized repeated results. There were some limitations in this methodology, such as the uncertainly in the actual machining tolerance and measurement during CMM scanning (S.Carmignato *et al*. 2011). However the general high levels of agreement indicate that this method is appropriate to measure clinically relevant levels of wear. This technique can also be used for the biotribological study of other polyethylene components, since wear and damage can be assessed visually and volumetrically.

Chapter 4

Computational and Experimental Studies of Simulated Wear Tests

4.1 Introduction

This chapter examines tibial knee components that have undergone simulated wear testing to further investigate the applicability and accuracy of the three-dimensional volumetric assessment methodology presented in Chapter 3. These studies will include both computational and experimental volume removal tests.

Computational wear test: A computational investigation was conducted on the left condyle of tibial knee component measured using coordinate measuring machine (CMM) with different wear area. Since the original surface coordinates were obtained as pre-wear data, the wear volume of each step was then calculated as reference for validation of surface curve fitting methodology. Both wear volume and maximum linear wear were determined via surface curve fitting and compared with the coordinated before and after computational wear test.

Experimental wear test: An experimental investigation was performed on the left condyle of a new DePuy Sigma tibial knee component provided by the manufacturer. The original surface of the tibial knee component was measured using CMM to obtain surface coordinates as pre-wear data. As gravimetric is the standard method of wear determination (Dowson and

Jobbins 1988; Barnett 2002; Liao *et al*. 2003; McEwen *et al*. 2005), the method was used as a reference in addition to the CMM methodology. Coordinates of the worn surface were captured using CMM after each physical volume removal test. The wear volume was calculated both with and without initial surface coordinates and compared to the gravimetric measurement.

4.2 Materials and Methods

An unworn Sigma tibial knee component was provided by the manufacturer (DePuySynthes, UK). The original surface coordinates of the left condyle were obtained using a coordinate measuring machine (Section 2.4). these coordinates (illustrated in Figure 4.1) were considered as the pre-wear data and used as reference for both computational and experimental wear tests.

4.2.1 Computational wear test

The coordinates from the left condyle were used for the development of a computational program to artificially generate different wear areas and depths. MATLAB (Version 7.11, Mathworks Inc, USA) was used to programme wear area generation. The wear region of the left condyle range from 0.29% to 38.55% and the maximum wear depth was 0.2 mm.

The volume loss was calculated by comparing the coordinates before and after a computational wear test. This study was used as a reference to investigate the result of surface curve fitting methodology. As demonstrated in Chapter 3, the 'original' surface of the left condyle was reconstructed based on the undeformed region. Hence, a regenerated surface with corresponding coordinates was used as reference to determine the amount of wear volumetrically.

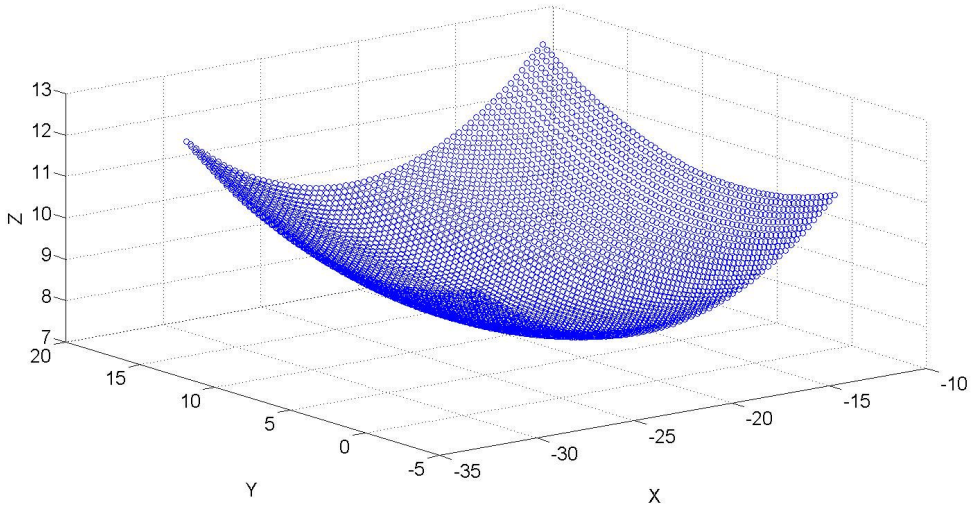

Figure 4.1 CMM measurement of left condyle of a new tibial knee component.

4.2.2 Experimental wear test

Prior to the measurement, the specimens were placed in a temperature and humidity (20^{o}C and 40% respectively) controlled room for 48 hours to dry after cleaning (section 2.2). The initial coordinates of the surface were obtained using coordinate measuring machine (CMM), which were used as

pre-wear data in addition to gravimetric measurement. The surface of the condyle after each experimental wear test was measured again using CMM to capture coordinates for volumetric assessment. In this study, a 24 mm diameter ball-ended cutter was used to remove the polyethylene from the left condyle of a tibial knee component. Figure 4.2 demonstrates the location of the material removal. The requested maximum linear wear depth on left condyle range from 0.10 mm to 1.00 mm (Table 4.1), however, the actual depths were found to be smaller when returned from the technician. The actual maximum linear wear depths were determined using coordinates before and after each physical volume removal test. Another physical volume removal test was performed near the previous one to increase the wear region (Figure 4.3).

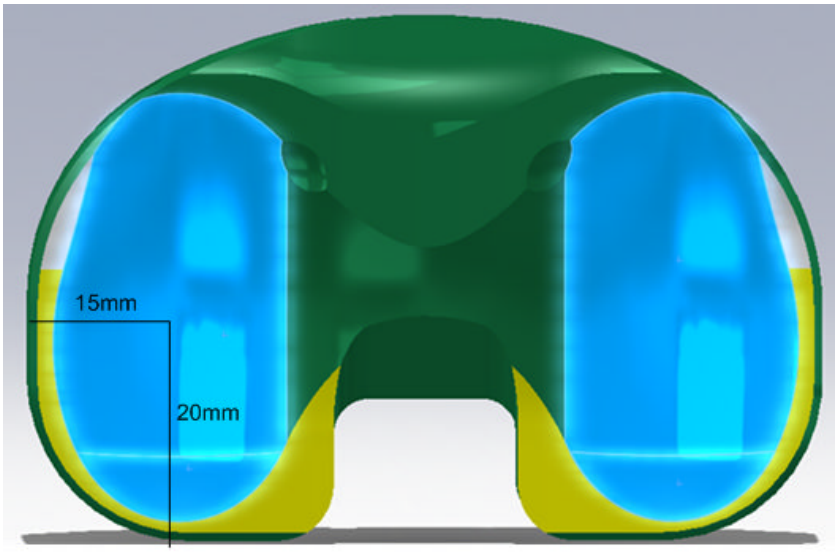

Figure 4.2 Physical volume removal location on the left condyle.

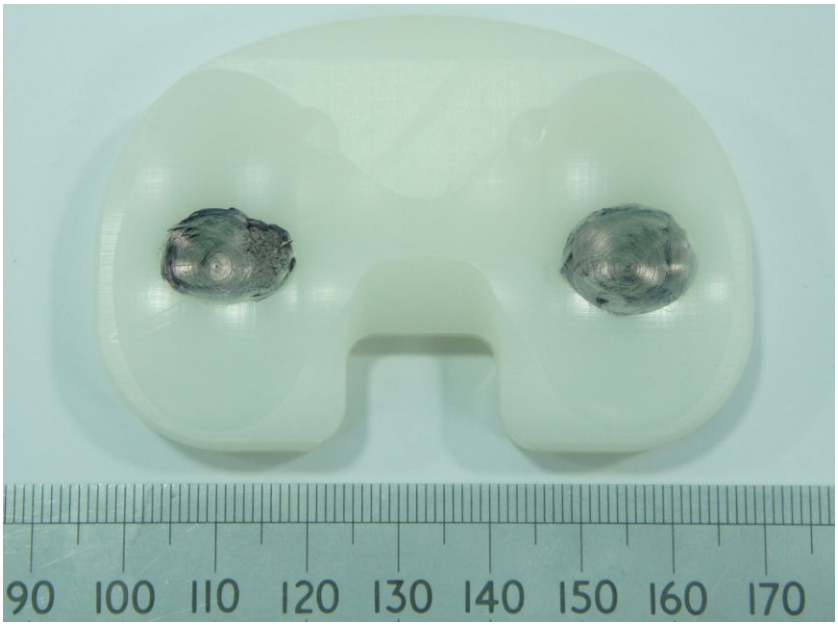

Figure 4.3 The black area with ink painting is the worn region generated using the 24 mm diameter ball-ended cutter.

Table 4.1 Physical volume removal test parameters

Test no.	Diameter of cutter (mm)	Requested maximum linear wear depth (mm)	Calculated maximum linear wear depth (mm)
1		0.10	0.07
2		0.20	0.10
3		0.30	0.15
4		0.40	0.19
5	24	0.50	0.22
6		0.60	0.27
7		0.70	0.31
8		0.80	0.35
9		0.90	0.38
1		1.00	0.43

Based on the surface coordinates obtained from CMM measurement, the undeformed region was determined and used as reconstruction reference to generate the ‘original’ surface with corresponding coordinates to determine the amount of wear. The gold standard gravimetric measurement was performed as a reference for investigation of the surface curve fitting (Section 2.2). Both volume loss and maximum wear depth were calculated based on the coordinates measured by CMM and generated via surface curve fitting.

4.3 Results

The results of both computational and experimental studies of wear tests are detailed below.

4.3.1 Computational wear test results

A total of 17 computational wear tests were performed on the left condyle of the tibial knee component to generate different volumes of wear with increasing wear area. The results are shown in Table 4.2. Three-dimensional volumetric assessment methodology was used to determine the volume loss after each test. A comparison of theoretical wear volume calculated using coordinates before and after wear test and determined wear volume calculated using surface curve fitting was performed and the concordance correlations coefficient (CCC) was determined (Section 2.5).

With the process of computational wear test, the wear volume increases with the increasing of wear area (Figure 4.4), however, the maximum wear region is less than 50% of the left condyle. Hence, there is enough 'undeformed' region for regeneration of the 'original' surface with corresponding coordinates to determine the amount of wear volumetrically.

Table 4.2 Computational wear test results

Test no.	Wear area /%	Theoretical wear volume/mm^3	Determined wear volume/mm^3
1	0.29	0.12897	0.1136
2	2.93	1.30147	1.3276
3	5.51	2.41377	2.5016
4	7.84	3.4452	3.4733
5	10.37	4.64443	4.8269
6	12.89	5.7165	5.9361
7	15.56	6.82333	6.7135
8	17.94	8.069	8.014
9	20.44	9.02967	8.9207
10	22.78	10.146	10.1979
11	25.49	11.3106	11.0616
12	27.99	12.54343	12.5421
13	30.13	13.34993	13.5709
14	32.23	14.14673	14.1682
15	34.61	15.5364	15.6107
16	36.51	16.16287	16.3121
17	38.55	17.35093	17.4182

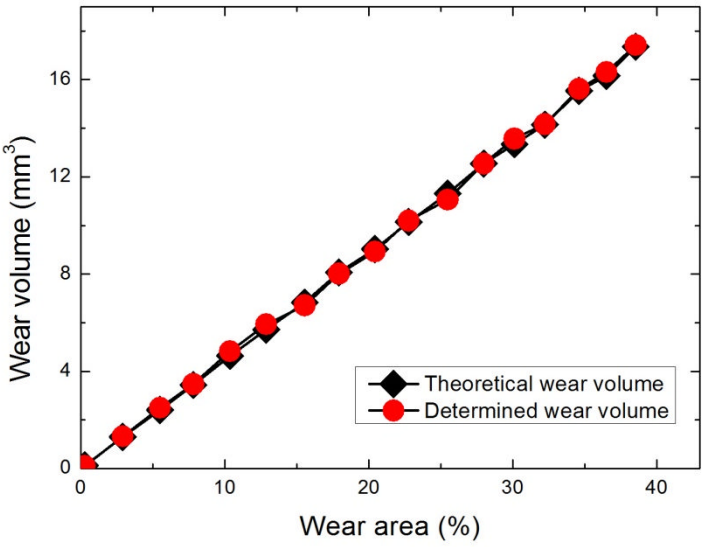

Figure 4.4 The wear volume generated with increasing wear area.

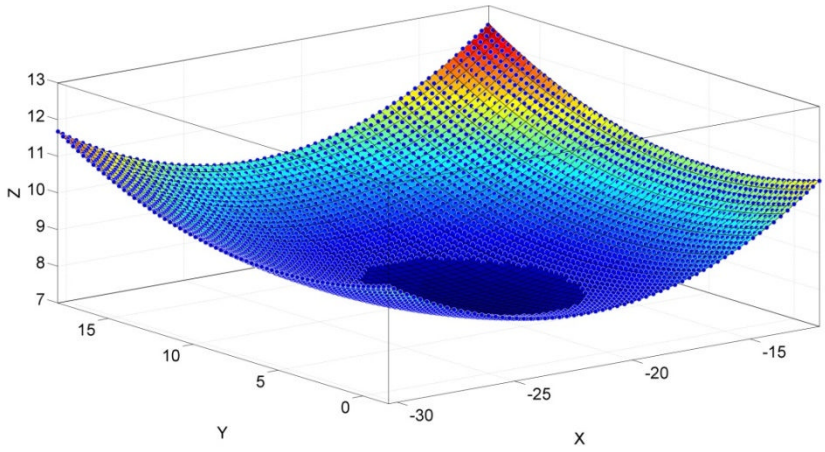

(a) 3D

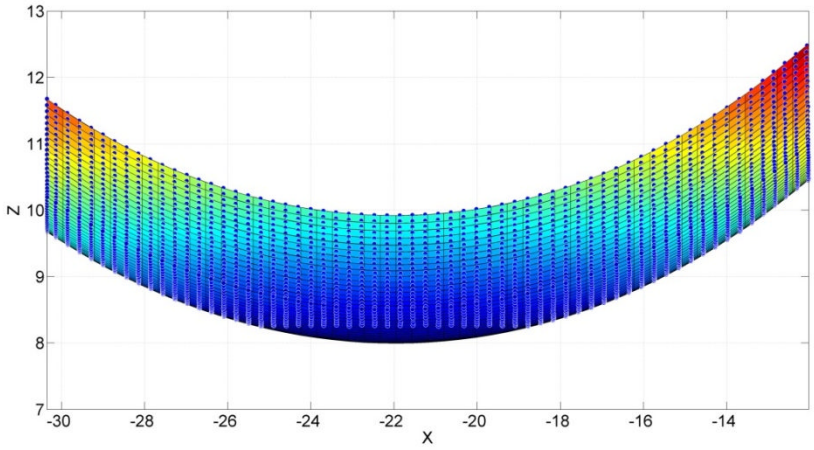

(b) X-Z

Figure 4.5 Original surface reconstructed as pre-wear data.

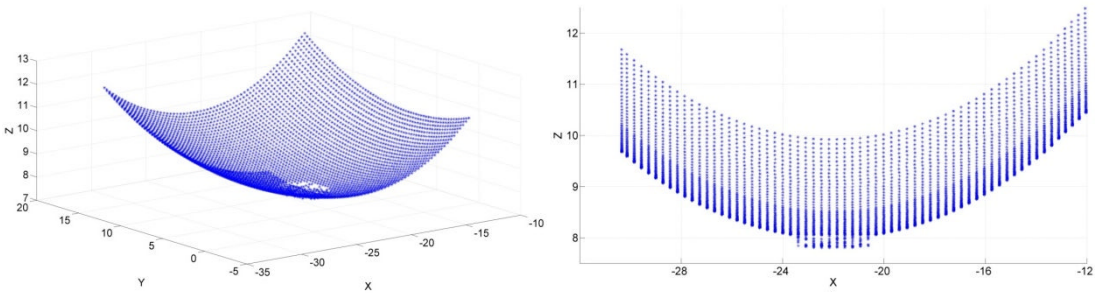

wear area 2.93%

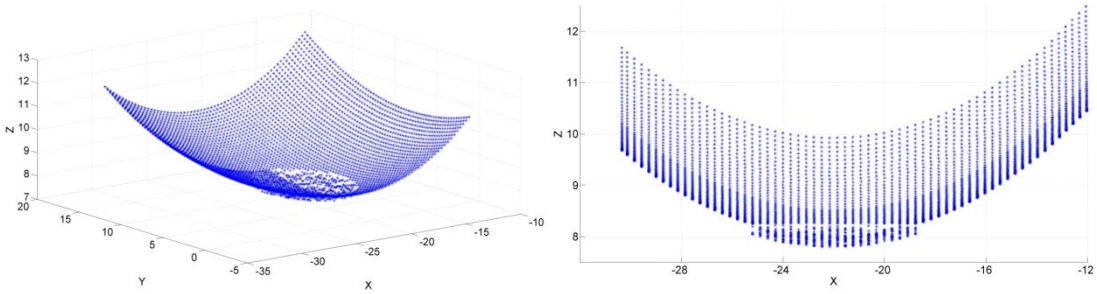

wear area 12.89%

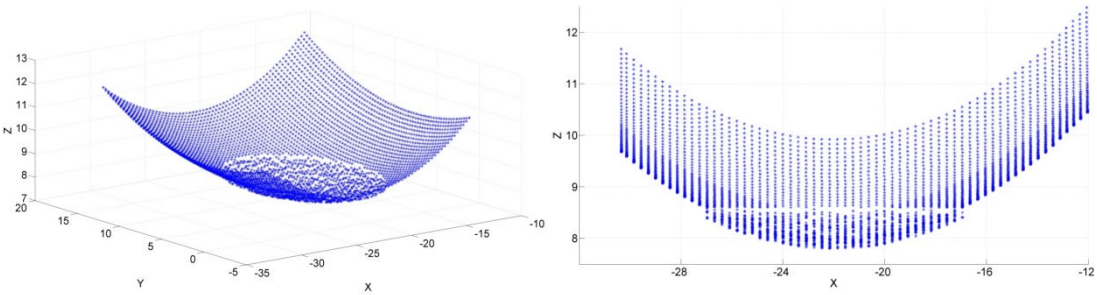

wear area 30.13%

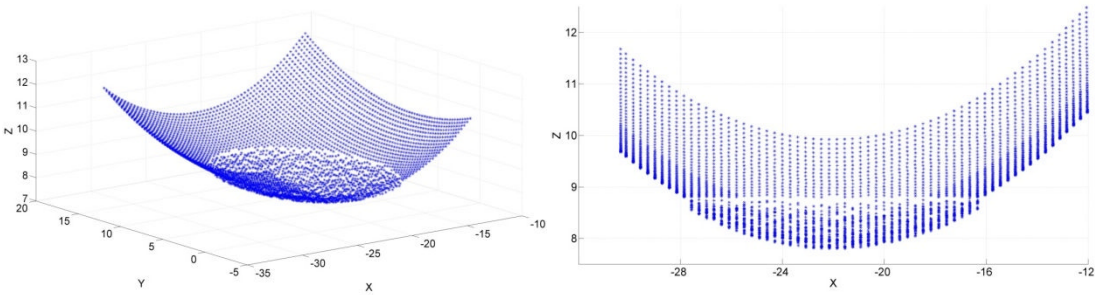

wear area 38.55%

Figure 4.6 Three-dimensional and X-Y images of computational wear test.

Figure 4.5 demonstrates the reconstruction of original surface. The coordinates of the undeformed region were used as reference to regenerate the initial surface using three-dimensional surface curve fitting methodology (Section 3.2.2.2). With the equation provided (Section 3.2.2.2), the original coordinates of the left condyle were then obtained and used to determine the wear volume. Part of three-dimensional (3-D) and X-Z images of computational wear test is shown in Figure 4.6 and the detailed images are illustrated in Appendix A-Figure A for visually investigation to show the simulated wear area.

4.3.2 Experimental wear test results

Gravimetric measurement of the tibial component was performed before and after the experimental wear test. The determination of volume loss with and without initial coordinates is shown in Table 4.3. For volume determination with reference, it is easily to calculate the amount of wear by subtracting the coordinates before and after each test. For volume determination without reference, the 'undeformed' region was first identified and then used to reconstruct the 'original' surface with corresponding coordinates using surface curve fitting method. The volume loss measured gravimetrically ranged between 0.9 mm^3 and 19.3 mm^3, depending on the test condition. The amount of wear determined with and without initial surface coordinates ranged from 1.0 mm^3 – 19.5 mm^3 and 0.8 mm^3 – 18.2 mm^3 with corresponding maximum linear wear from 0.07 mm to 0.43 mm (Figure 4.7).

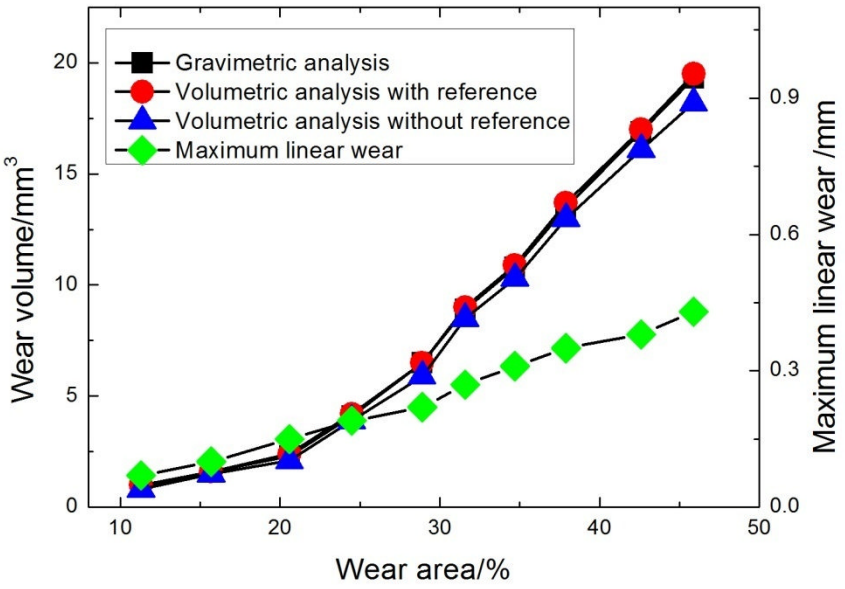

Figure 4.7 Comparison of gravimetric and geometrical wear measurement.

Table 4.3 Comparison of gravimetric and geometrical wear measurement

Test no.	Wear area/%	Gravimetric analysis/ mm^3	Volumetric analysis with reference/mm^3	Volumetric analysis without reference/mm^3	Max linear wear /mm
1	11.3	0.9	1.0	0.8	0.07
2	15.7	1.6	1.6	1.5	0.10
3	20.6	2.3	2.4	2.1	0.15
4	24.5	4.1	4.2	3.9	0.19
5	28.9	6.5	6.5	5.9	0.22
6	31.6	8.9	9	8.5	0.27
7	34.7	10.8	10.9	10.3	0.31
8	37.9	13.5	13.7	13	0.35
9	42.6	16.9	17	16.1	0.38
10	45.9	19.3	19.5	18.2	0.43

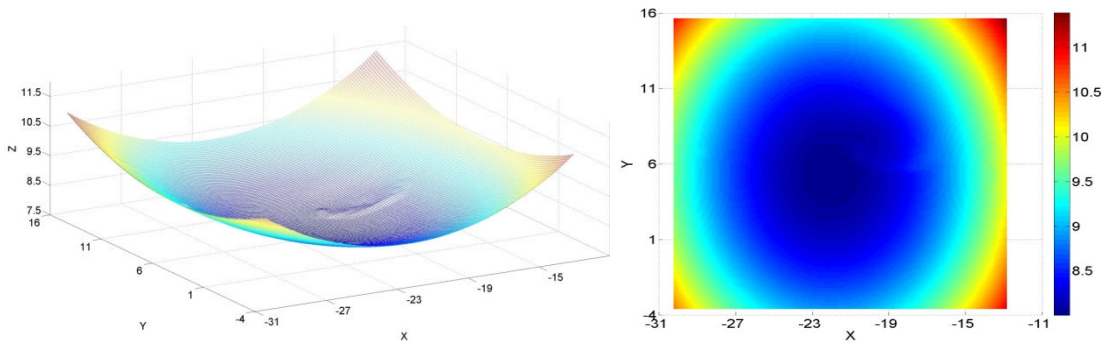

physical volume removal test 1

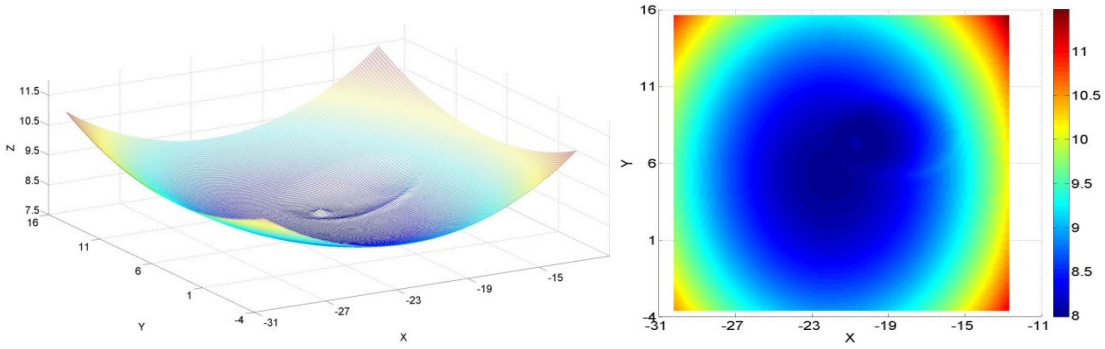

physical volume removal test 3

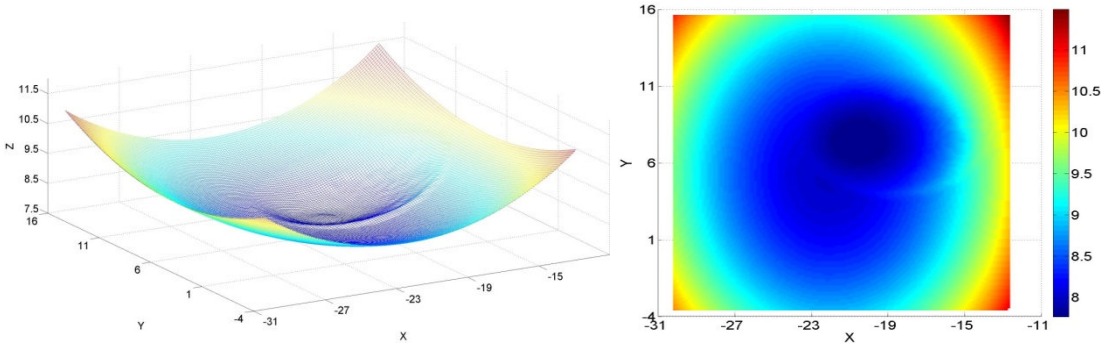

physical volume removal test 6

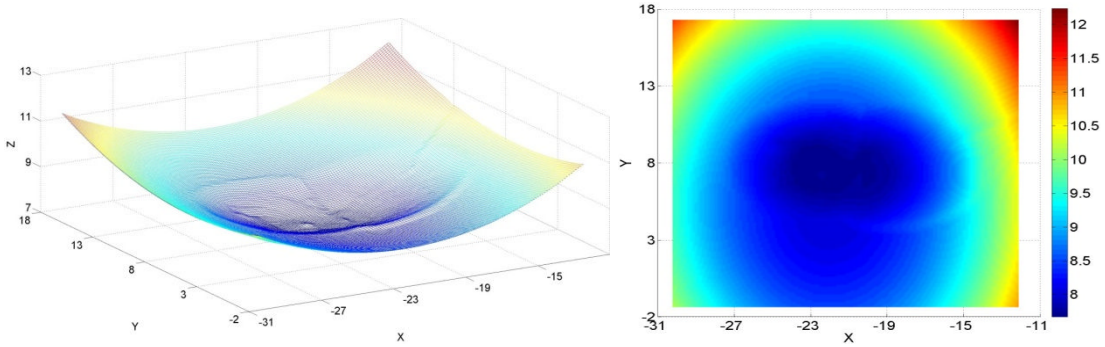

physical volume removal test 10

Figure 4.8 Three-dimensional and X-Y images of experimental wear test.

Part of three-dimensional (3-D) and X-Z images of experimental wear test is shown in Figure 4.8 and the detailed images are illustrated in Appendix A-Figure B.

4.4 Discussion

Chapter 3 presented a three-dimensional coordinate based volumetric assessment methodology and validated its high accuracy for wear volume determination especially when wear area is small. In this chapter, both computational and experimental wear tests were performed to generate different amounts of wear to investigate the applicability and accuracy of the presented methodology. For the computational wear test, the amount of volumetric wear was generated mathematically with the increase of wear area. Since the maximum wear area is less than 50%, there was enough 'undeformed' region for reconstruction of the reference surface. The volumetric assessment was compared to theoretical calculation and shows very high levels of agreement (Figure 4.9). The CCC calculated was 0.9997, which means high accuracy of the surface curve fitting methodology.

The maximum wear area generated experimentally was larger than computational wear test (45.9% and 38.6% of the total area respectively). The corresponding amount of wear simulated was 19.3 mm^3 and 17.4 mm^3 respectively. As illustrated in Figure 4.10, with initial coordinates of the condyle provided, the amount of wear determined is close to the gravimetric measurement (CCC = 0.9998). For volumetric assessment without initial surface data, the volume loss determined using surface curve fitting was

slightly underestimated, however, it still shows high level of agreement (CCC = 0.9960), which indicates the presented three-dimensional geometry based volumetric assessment methodology is appropriate to measure relevant levels of wear.

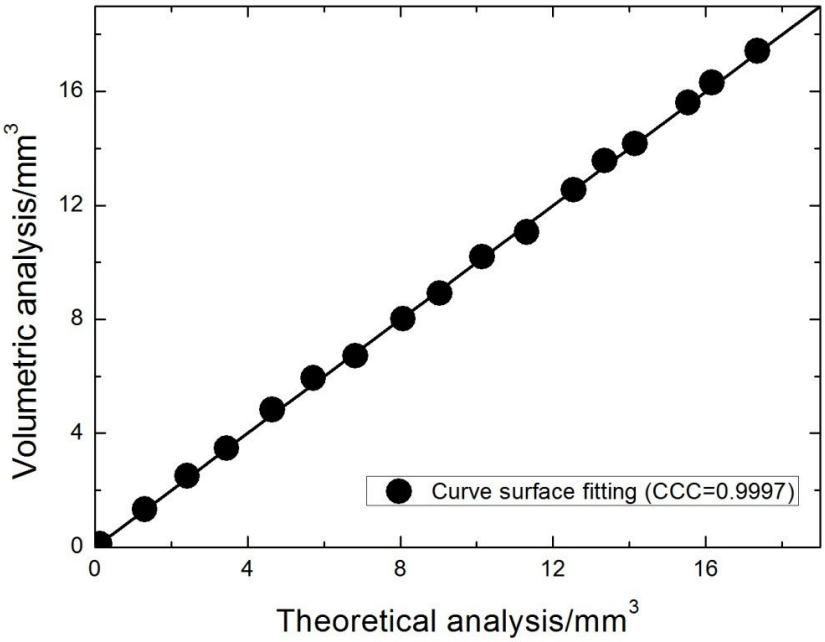

Figure 4.9 Comparison of theoretical and computational wear volume.

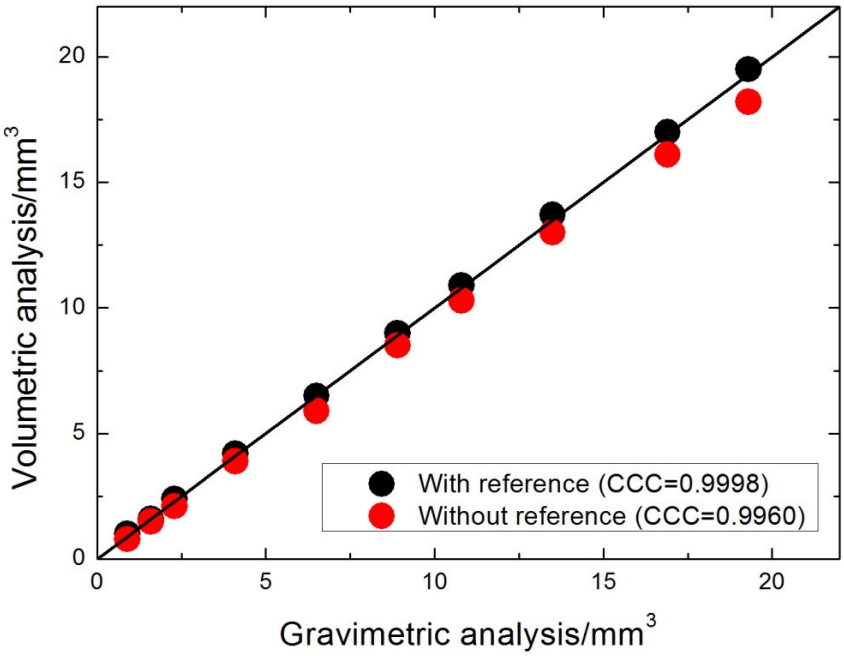

Figure 4.10 Comparison of gravimetric and geometrical wear measurement with and without reference.

However, there are some limitations to the experimental volume removal test. Plastic deformation was found accompanied during the test (4.11), which is likely due to the vibration. As a result, the ‘undeformed’ region selected as reference for regenerating ‘original’ surface was not accurate, which could influence the accuracy of volumetric wear assessment especially when no initial surface geometry is available. The wear region and volume loss generated using both computational and experimental simulated wear tests were smaller than simulator and retrieval specimens. In addition, the surface morphology of simulator and retrieval specimens is much more complicated. As a result, further investigations should be carried out on laboratory and retrieval analysis using the presented volumetric determination methodology, which will be detailed in next chapters.

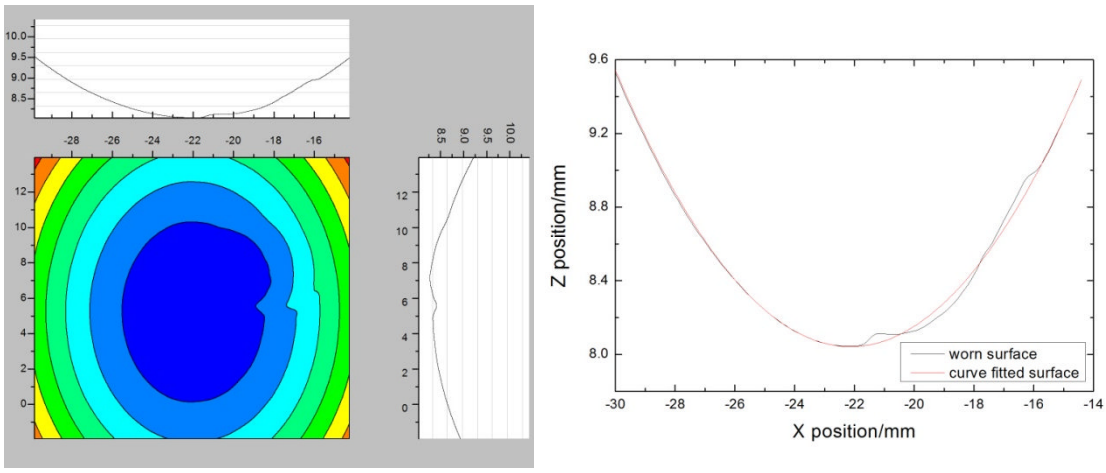

(a) (b)

Figure 4.11 Plastic deformation was accompanied during the physical volume removal test: (a) 2-D profile of left condyle after physical volume removal, (b) 2-D profile comparison of worn surface and curve fitted surface.

Chapter 5

Computational and Experimental Studies of Creep Deformation Tests

5.1 Introduction

Polyethylene is a viscoelastic material which deforms under applied load. The changes in geometry of a loaded polyethylene total joint component include both wear and creep. From the literature, the creep has a significant effect on contact area and wear in total joint replacements (Fregly *et al*. 2005; Penmetsa *et al*. 2006; Zhao *et al*. 2008; Willing and Kim 2009). In addition, creep would quickly increase the contact area up to 50% during the first few hundred thousand gait cycles (Bevill *et al*, 2005). Thus, determination of the amount of creep is important for more accurate assessment of the true in vivo/vitro wear rate.

The purpose of the current chapter was to computationally and experimentally validate the volumetric assessment methodology (Chapter 3) for creep deformation tests. Computational modelling is an alternative solution to *in-vitro* wear simulation and may dramatically shorten the time consuming and associated costs for long-term simulator tests. Two methods of computational modelling were developed by Abdelgaied *et al* (2011) to simulate creep deformation for wear prediction, and this data was provided for analysis.

5.2 Materials and Methods

5.2.1 Computational creep test

The finite element (FE) models of the TKRs were developed using ABAQUS to simulate experimental testing conditions under displacement control. This work was undertaken by A.Abdelgaied in a parallel study. A compressive creep model with appropriate parameters for conventional UHMWPE was adapted from the curve-fitted experimental data reported by Lee and Pienkowski (Lee and Pienkowski, 1998a). The creep was modelled using the following equation (A. Abdelgaied *et al*, 2011):

$$\delta_{creep} = [3.491 \times 10^{-3} + 7.966 \times 10^{-4}(\log(\mathrm{t}) - 4)]\sigma_{av}\mathrm{h} \qquad (5.1)$$

Where t is the time (min), σ_{av} is the average pressure (MPa), and h is the thickness of the polyethylene (mm). The creep recovery was assumed to be 0.5 (Lee and Pienkowski, 1998b).

5.2.1.1 Creep generation using a 22mm ball

DePuy Sigma fixed bearing TKRs (DePuy International, UK) were tested with a size 3, 10 mm thick curved insert (Abdelgaied *et al*, 2011). In this modelling, true stress-strain data (Godest *et al*. 2002) was used and the UHMWPE was considered as an elastic-plastic material. The modulus of elasticity and Poisson's ratio selected in the model were 463 MPa (Kurtz *et al*. 2002; Zhao *et al*. 2008) and 0.46 (Bartel *et al*. 1995; Fregly *et al*. 2003; Zhao

et al. 2008) respectively. The tibial component was meshed using the quadratic tetrahedral elements (C3D10M).

In this model, a 22 mm diameter rigid ball was used to generate creep on the right condyle of the tibial component under a constant load of 2600N (Figure 5.1(a)), to represent the maximum axial force acting up on the knee during the gait cycle. The tibial component was fixed on a plate and the contact pressure generated is shown in Figure 5.1(b). The solution technique described in Section 3.2 was used to calculate the linear and the volumetric creep deformation and compared to the FE model for validation of the surface curve fitting methodology.

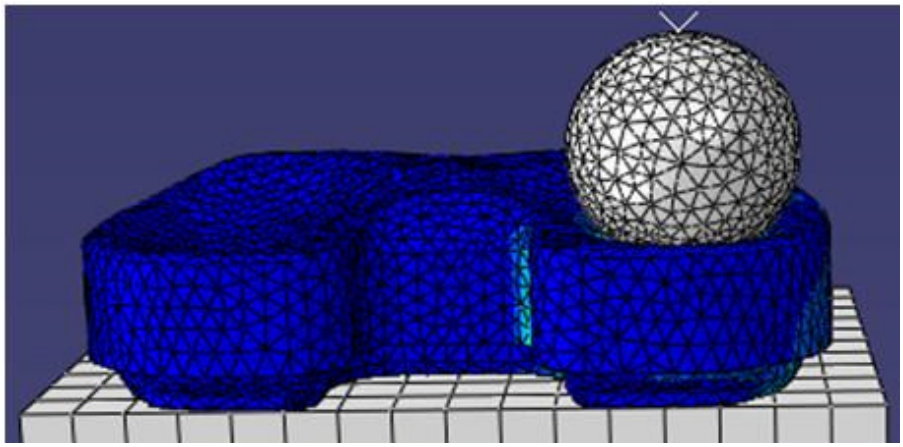

(a)

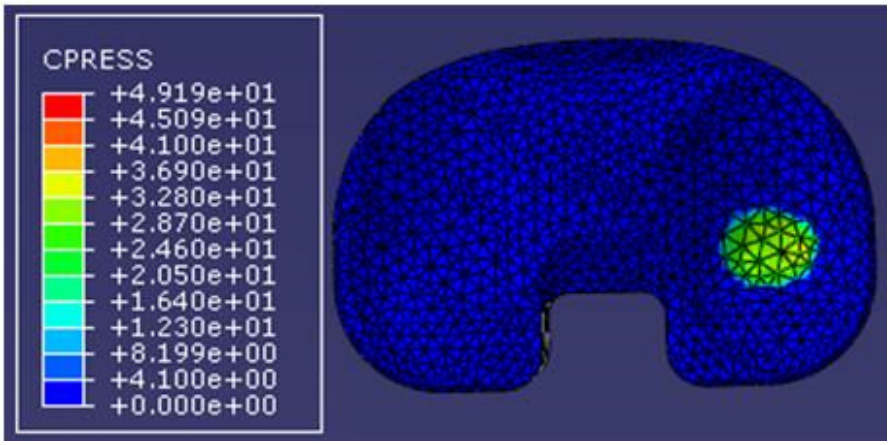

(b)

Figure 5.1 The PFC sigma creep test model using a 22 mm ball.

5.2.1.2 Creep generation using a femoral component

The parameters and mesh type used in this modelling were the same as used in Section 5.2.1.1 except the 22 mm diameter ball was replaced with a femoral component, which was modelled as a rigid body (Figure 5.2 (a)). The isotropic coefficient of friction was assumed as 0.04 (Godest *et al*. 2002; Willing and Kim 2009) in a penalty contact formulation to describe the contact between the tibial and the femoral contact surfaces. According to the experimental setup, the axial load was applied on a reference node (Abdelgaied *et al*, 2011) of the femoral component, which was located at a 5 mm offset to the medial direction (Figure 5.2 (a)).

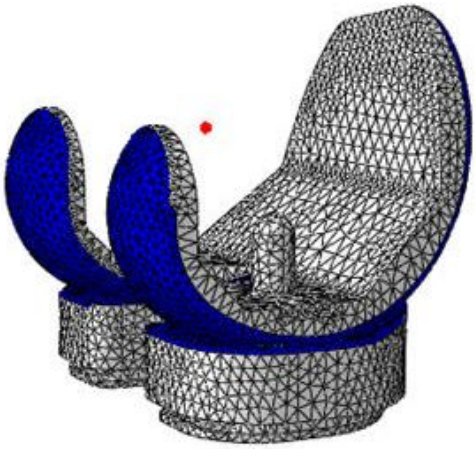

(a)

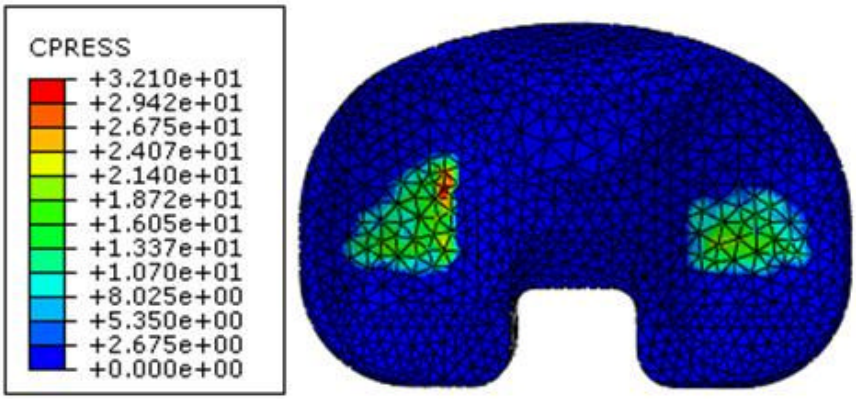

(b)

Figure 5.2 The PFC sigma creep test model using a femoral component.

As illustrated in Figure 5.2(b), the contact area on medial condyle was slightly larger than on the lateral side. Since the initial geometry of the tibial component was provided, the amount of creep and maximum linear depth were determined by subtracting the coordinates before and after the computational test (3.2.1). The surface curve fitting methodology (section 3.2.2) was used to reconstruct the 'original' surface geometry for determination of the amount of creep and compared to the FE models.

5.2.2 Experimental creep test

A six-station knee simulator designed by ProSim (Manchester, UK) was used to carry out creep deformation tests. Prior to the test, the tibial components were cleaned using the solution presented in Section 2.2.1.

5.2.2.1 Knee simulator

As described by Barnett *et al*. (2001), the ProSim knee simulator (Figure 5.3) used in the University of Leeds has six stations in two groups with three stations per group. Every station has six degrees of freedom, which are either pneumatically or electro-mechanically controlled. The axial load, flexion-extension (F-E), internal-external (I-E) rotation and the anterior-posterior (A-P) displacement were dynamically controlled through defined input profiles. The abduction-adduction (A-A) rotation was unconstrained but not controlled, and the medial-lateral position was defined during pre-test and constant throughout the study.

As demonstrated in Figure 5.4, each station has a separate pneumatic actuator for the axial load, anterior-posterior displacement and internal-external rotation. The axis of load was offset 5 mm medially from the knee prosthesis central axis, as recommended in the ISO standard (ISO 14243-1 2009) for the knees of the dimensions used in the current study (McEwen *et al*. 2005). Due to the limitations of the CMM measurement area of tibial knee component, a contact location analysis to determine optimal positioning of insert was performed (Figure 5.5) to ensure the creep deformation area was roughly in the centre of each condyle. The medial-lateral position d (Figure 5.5) was chosen in this study in order to provide the maximum measurement area for CMM scanning (Section 2.4.3) and ensure the creep area was included in the region for analysis.

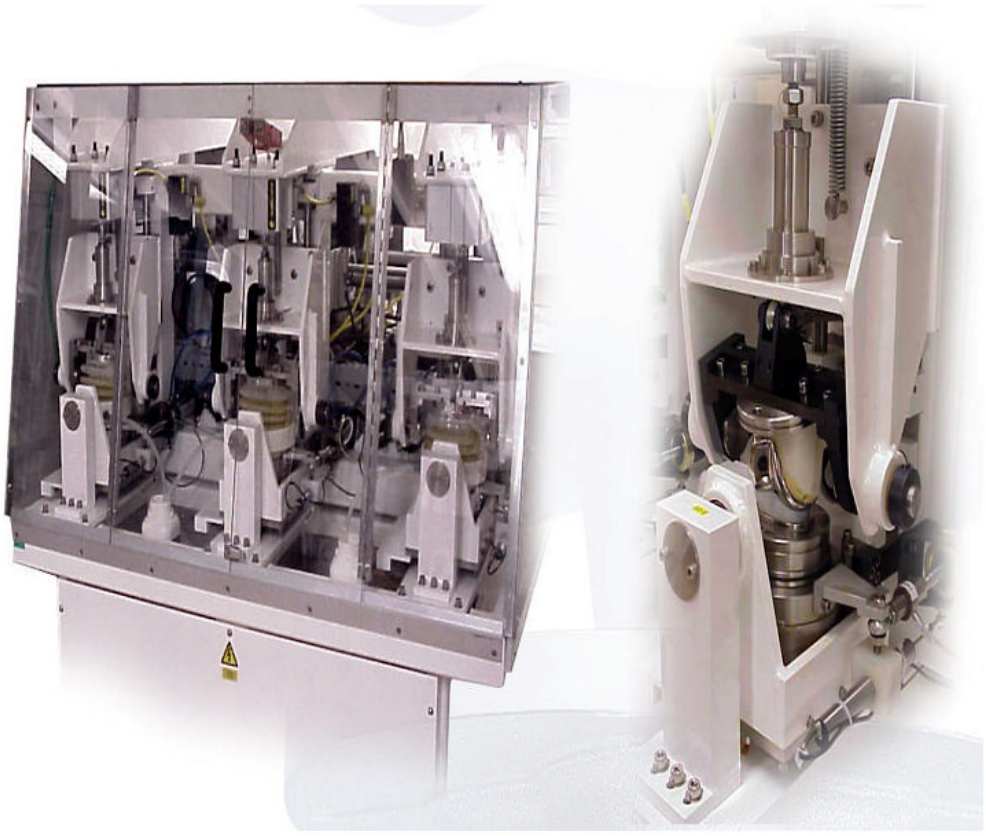

Figure 5.3 The ProSim (Manchester, UK) knee simulator.

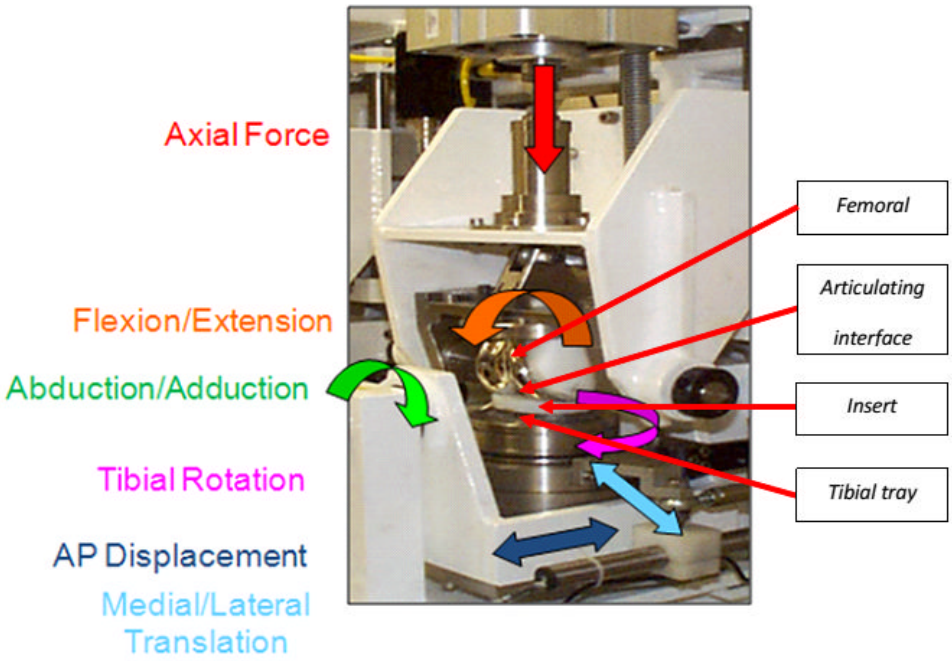

Figure 5.4 Anatomical mounting of the TKR.

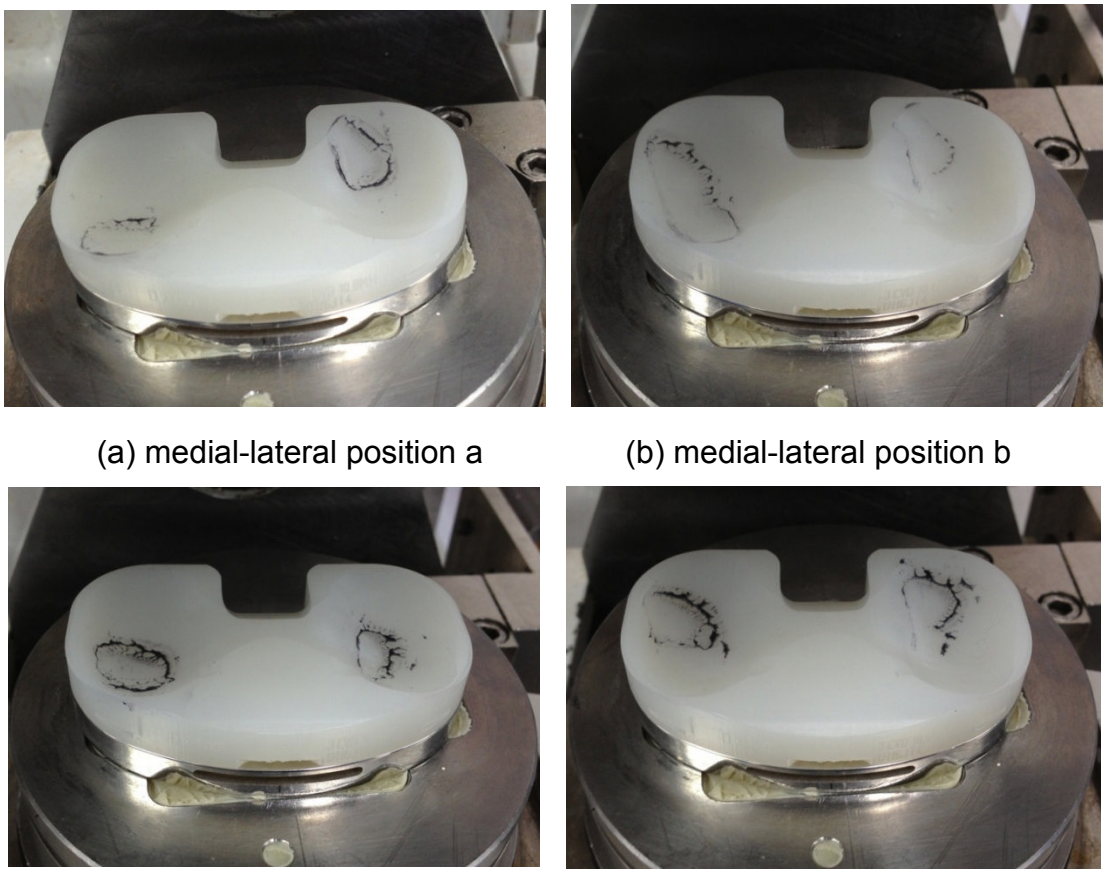

(a) medial-lateral position a (b) medial-lateral position b

(c) medial-lateral position c (d) medial-lateral position d

Figure 5.5 Contact location analysis to determine optimal positioning of insert for creep study.

5.2.2.2 Creep deformation test

Four new DePuy Sigma curved polyethylene inserts were used to carry out the creep test under dynamic axial load (Section 1.4.1, Figure 1.11(a)), each with different loading duration. The time durations for each component were 0.25, 0.50, 0.75 and 1.00 million cycles (MC). One new specimen was placed in to a container with serum for the test duration as a soak control to minimise the error arising from the absorption of fluid in polymers, which has been identified in tibia-femoral wear testing in ISO 14243-3 (2009) when measuring gravimetrically. The soak control was not under any action of displacement or load. The creep volume was determined using a geometric method using a coordinate measuring machine (CMM) to obtain the surface coordinates before and after every test. As gravimetric measurement is considered as the standard method for wear determination (Dowson and Jobbins 1988; Barnett 2002; Liao *et al*. 2003; McEwen *et al*. 2005), the method was used to measure the soak control after each test to investigate the influence of absorption of fluid to the tibial knee component. As demonstrated in the flowchart (Figure 5.6), the creep test started with calibration of the simulator, after setting the simulator, it was then started. The serum was changed after every 1/3 MC and a geometrical measurement technique (CMM) was used to obtain surface coordinates after each test.

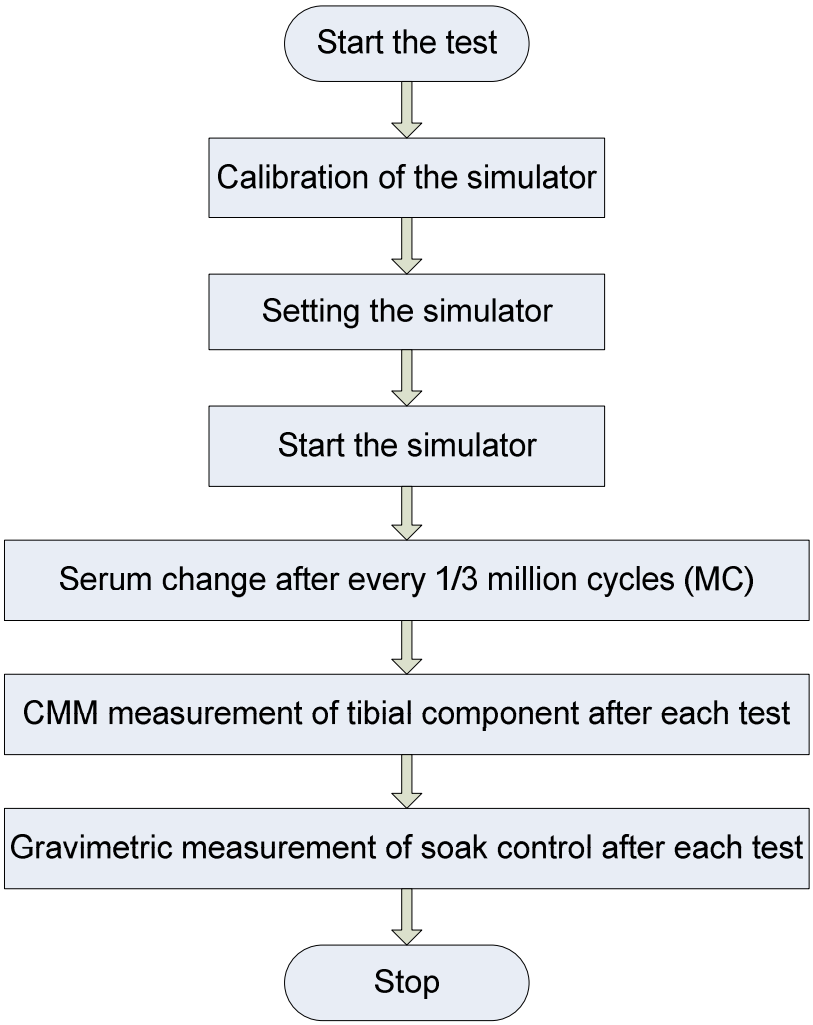

Figure 5.6 Creep test flowchart.

5.3 Results

5.3.1 Computational creep test results

5.3.1.1 Creep results of PFC sigma 22 mm ball test model

The computational model for creep predicted an increasing creep depth and volume with increasing duration. With the increasing of the creep time duration up to 3000 minutes, the creep volume increased to 60.47 mm^3 and the maximum creep depth to 0.87 mm, which were determined using the

surface data before and after each test (Table 5.1). Based on the three-dimensional volumetric determination methodology (Section 3.2.2), an 'original' surface was reconstructed as pre-wear data and used to calculate the creep volume and maximum creep depth, with maximum values of 69.66 mm^3 and 0.90 mm respectively. A comparison of the results is shown in Figure 5.7. The creep deformation increased rapidly during the first 1000 minutes, and then slowly increased thereafter (Figure 5.7).

Table 5.1 Creep deformation test results using a 22 mm ball.

Creep time/min	Creep Volume I/mm^3	Max creep depth I/mm	Creep Volume II/mm^3	Max creep depth II/mm
0	0	0	0	0
100	37.33	0.56	39.52	0.57
200	42.04	0.63	44.14	0.65
300	44.82	0.66	46.84	0.67
400	46.73	0.69	48.76	0.72
500	48.26	0.71	52.25	0.73
1000	53.07	0.76	57.88	0.79
1500	55.71	0.79	59.59	0.80
2000	57.75	0.82	63.51	0.84
2500	59.23	0.85	66.99	0.87
3000	60.47	0.87	69.66	0.90

*Creep volume/max creep depth I—Finite Element (FE) model

Creep volume/max creep depth II—Surface curve fitting

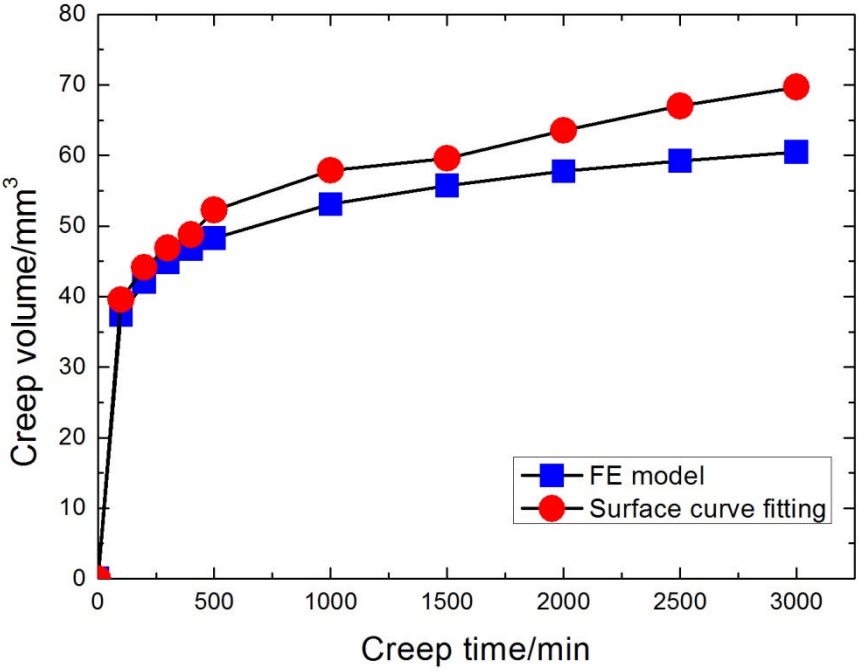

(a)

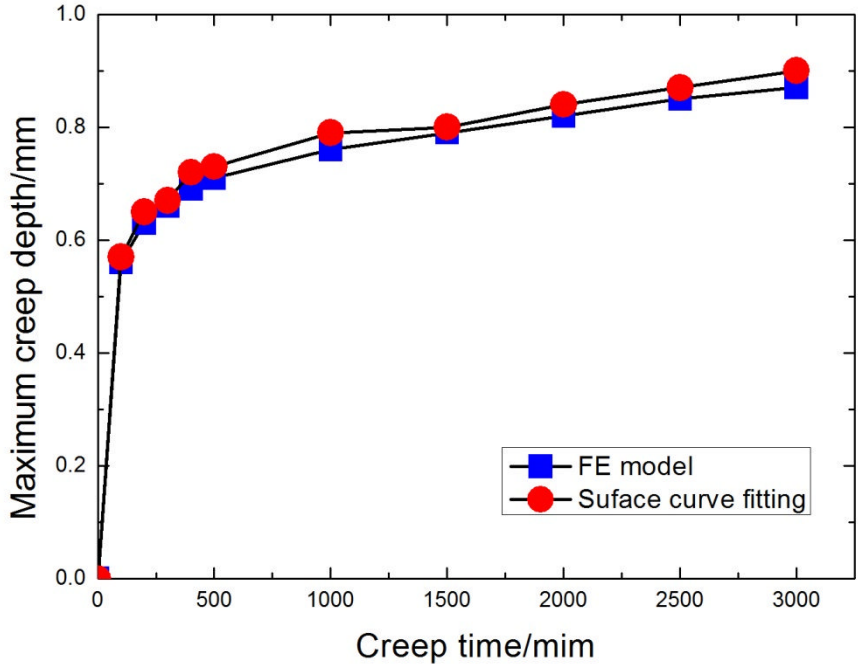

(b)

Figure 5.7 (a) Creep volume and (b) maximum creep depth versus time for the 22 mm ball creep test model.

5.3.1.2 Creep results of PFC sigma test model

The total amount of creep generated using the PFC sigma test model was 75.58 mm^3 at a creep time duration of 3000 mins. The variation of the maximum creep deformation was similar to the previous creep modelling (Figure 5.8(b)), rising to 0.65 mm. The creep volume of each condyle of the tibial knee component was calculated separately and then summed up as total creep volume (Table 5.2). The maximum creep depth was determined based on the surface data after each test and the reconstructed surface using surface curve fitting method (Section 3.2.2). the results are presented in Table 5.2 and Figure 5.8

Table 5.2 Creep deformation test results using a femoral component.

Creep time/min	Total Creep Volume I/mm^3	Max creep depth I/mm	Total Creep Volume II/mm^3	Max creep depth II/mm
0	0	0	0	0
100	46.65	0.39	47.52	0.39
200	52.55	0.46	53.85	0.46
300	55.99	0.49	57.26	0.49
400	58.44	0.50	59.68	0.50
500	60.34	0.52	62.45	0.53
1000	66.23	0.57	69.63	0.58
1500	69.68	0.60	73.21	0.61
2000	72.13	0.62	75.36	0.63
2500	74.03	0.64	77.83	0.65
3000	75.58	0.65	79.98	0.67

*Total creep volume/max creep depth I—Finite Element (FE) model

Total creep volume/max creep depth II—Surface curve fitting

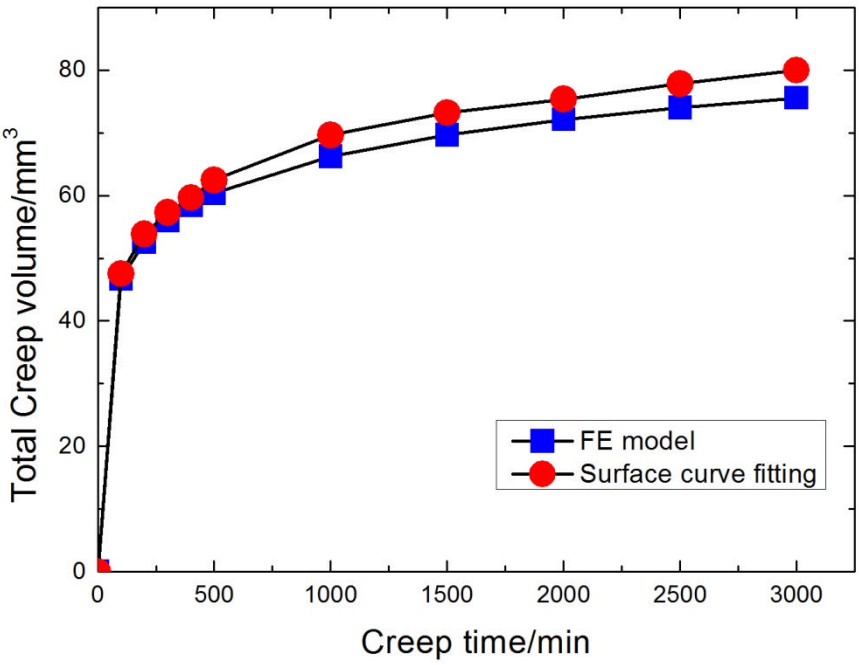

(a)

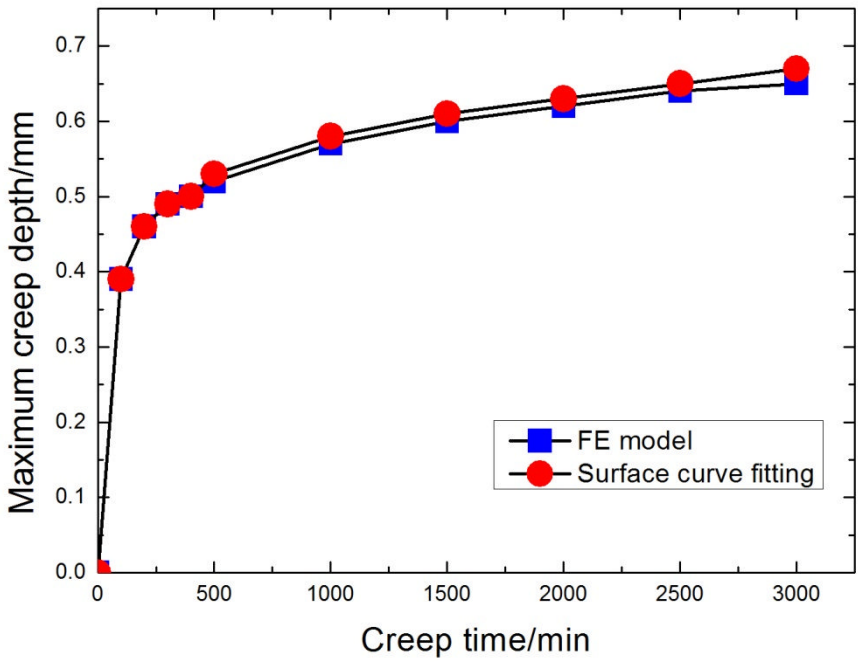

(b)

Figure 5.8 (a) Creep volume and (b) maximum creep depth versus time for the PFC sigma creep test model.

5.3.2 Experimental creep test results

5.3.2.1 Soak control

The cumulative weight changes of the soak specimen during the creep test are presented in Figure 5.9 for the soak control. The cumulative weight gain changes increase up to 0.8 mg when the creep test reaches 1 million cycles. Figure 5.9 illustrates the cumulative weight change of the soak specimen during the creep test.

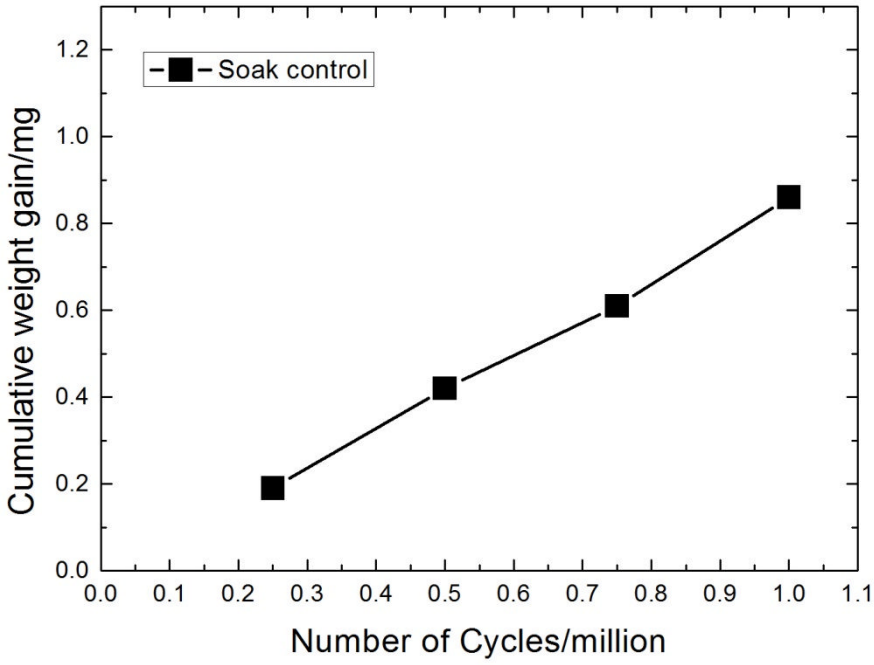

Figure 5.9 Weight changes of soak control sample throughout the creep test.

5.3.2.2 Geometrical creep measurements

The volume change from the creep test was determined using geometrical volumetric techniques – CMM. Since the surface geometry of the specimens was initially measured, the total amount of creep and maximum creep depth were then determined using the coordinates obtained after each creep test. With the increasing time duration, the surface scar area increased and reached a maximum at 1 million cycles (Figure 5.11). The scar area on medial side was a little larger than on the lateral side. The area that was measured on each condyle is overlaid on Figure 5.11 (d).

The total creep volume and maximum creep depth calculated with the coordinates before and after each creep test are illustrated in Table 5.3. It can be seen that both followed a similar trend, with a difference of 3.91 mm^3 and 0.02 mm after one million cycles. The creep volume and maximum creep depth determined using surface curve fitting methodology were slightly larger (Figure 5.10).

Table 5.3 Experimental creep deformation tests.

No of cycles/Million	Total Creep Volume I/mm^3	Max creep depth I/mm	Total Creep Volume II/mm^3	Max creep depth II/mm
0.25	67.32	0.59	66.47	0.60
0.50	77.56	0.63	79.85	0.64
0.75	79.28	0.65	82.19	0.67
1.00	86.61	0.73	90.52	0.75

*Total creep volume/max creep depth I—with initial geometry

Total creep volume/max creep depth II—Surface curve fitting

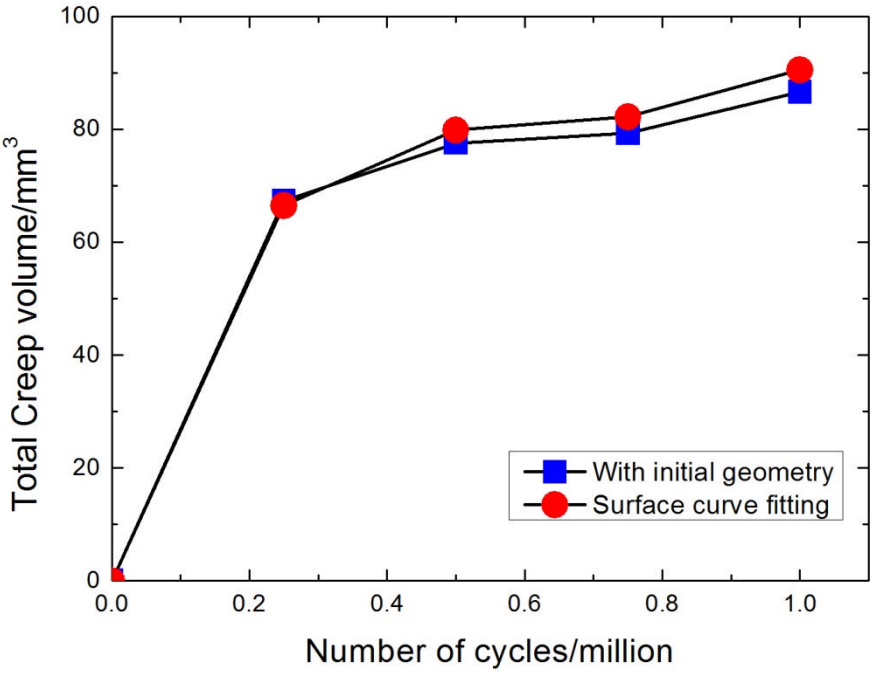

(a)

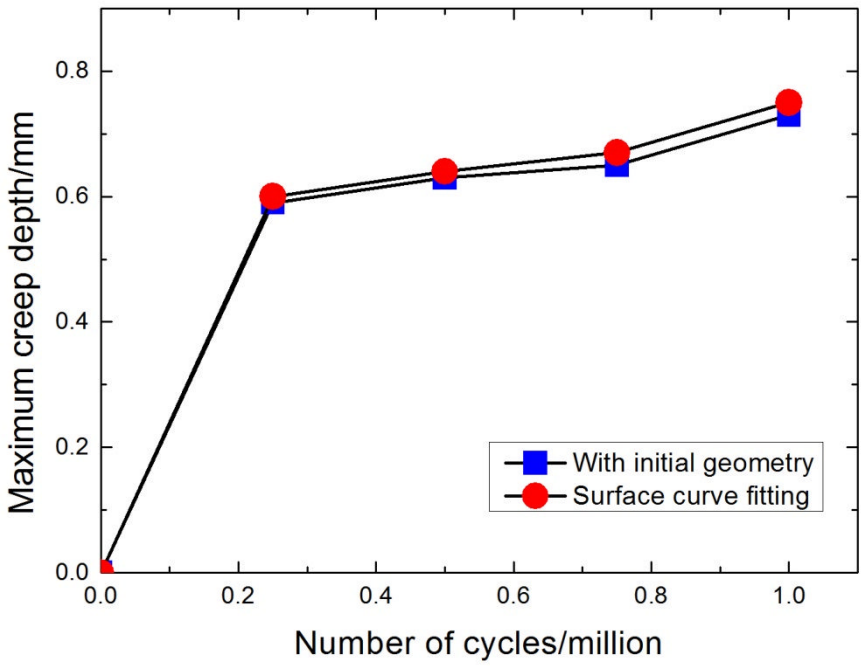

(b)

Figure 5.10 (a) Creep volume and (b) maximum creep depth versus the test duration for experimental creep test for the two measurement methods.

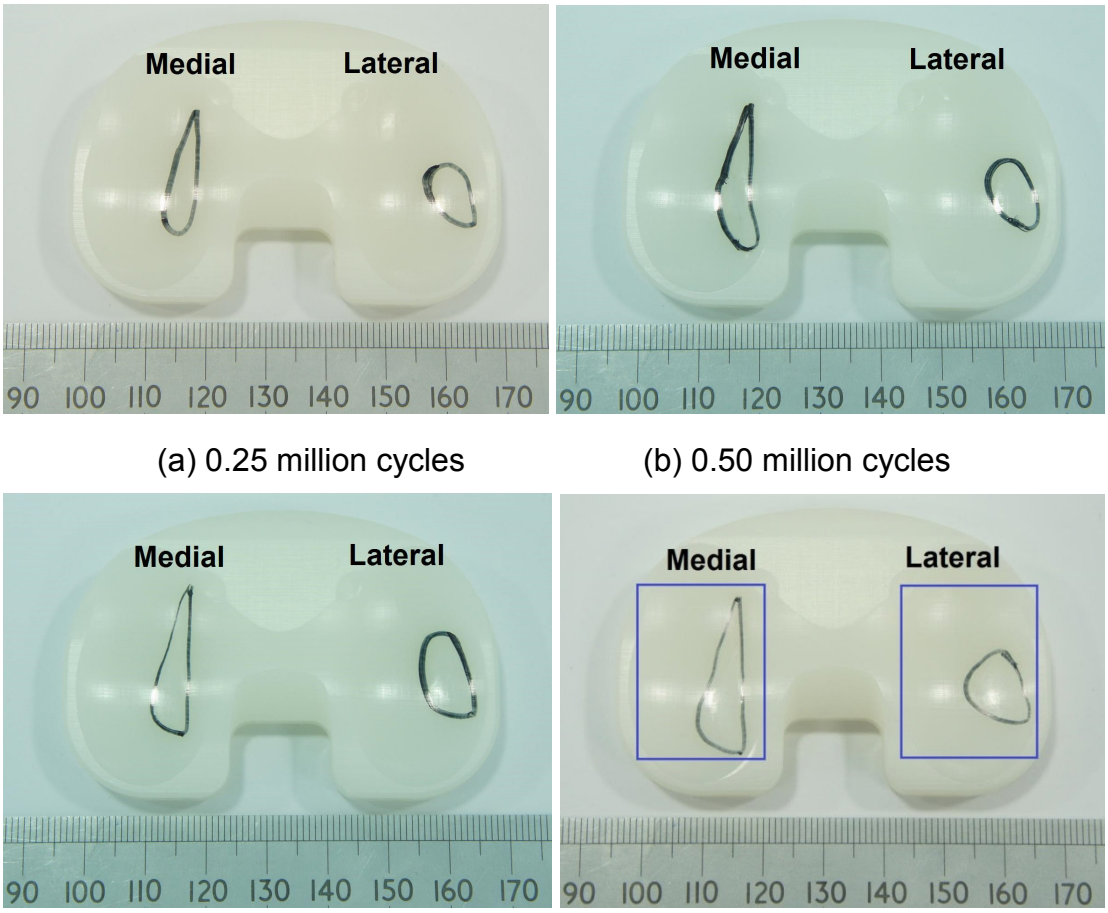

(a) 0.25 million cycles (b) 0.50 million cycles

(c) 0.75 million cycles (d) 1.00 million cycles

Figure 5.11 Surface scar area of each creep test.

5.4 Discussion

The changes in geometry of a loaded articulating polyethylene total joint component include both wear and creep. Creep analysis is therefore important as the true amount of wear would be more accurate by subtraction of the creep deformation from the total penetration. The aim of this study was to validate the volumetric assessment methodology described in Chapter 3 for creep deformation tests. There are some factors that would affect the creep, such as the magnitude and direction of the load, the geometry of the contact

surfaces, the duration of the load and the temperature (E. G. Little, 1985, S. S. Sternstein *et al*, 1988; J. A. Davidson *et al*, 1987; A. Cigada *et al*, 1993).

Finite element model comparison

The maximum creep volume and creep depth generated using a 22 mm diameter ball were 60.47 mm^3 and 0.87 mm with the creep time up to 3000 minutes. The creep was only generated on the right condyle of the tibial knee component. In this study, surface curve fitting was compared to the known amount of volume change that can be derived from the nodes on the FE model. Therefore, the accuracy of the FE model is not important because it is only the initial and final node positions that are used in this study. Compared to the creep volume calculated by finite element (FE) model, the surface curve fitting method appeared to be an overestimate. The corresponding maximum creep volume and creep depth calculated using surface curve fitting method were 69.66 mm^3 and 0.90 mm. To evaluate the agreement between the surface curve fitting method and the FE model, the two datasets were plotted against each other and the concordance correlations coefficients (CCC) (Section 2.5) were calculated. As demonstrated in Figure 5.12(a), the creep volume calculated using surface curve fitting was close to the FE model initially, but became larger with increasing creep duration (CCC=0.8516). This was due to inaccurate reconstruction of the ‘original’ surface geometry, as there was less undeformed region left as reference (section 3.3). The determined maximum creep depth using surface curve fitting was close to the FE model with CCC=0.9764 (Figure 5.12(b)).

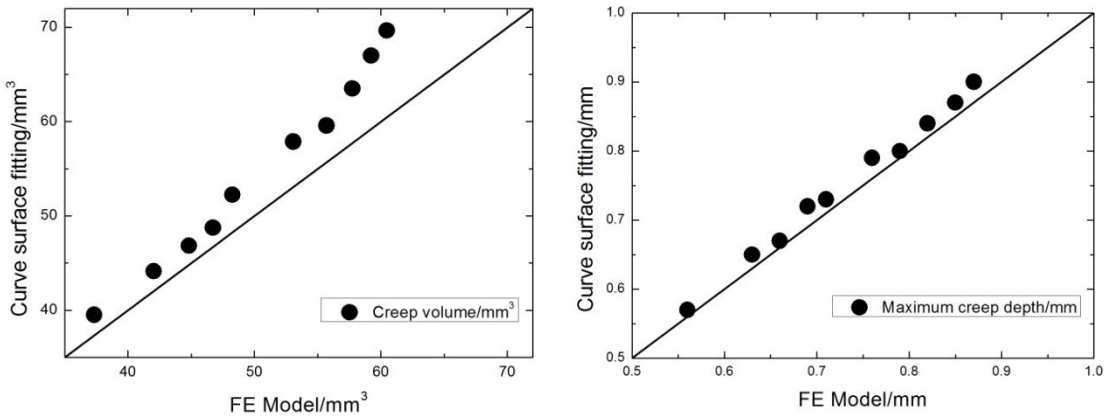

(a) (b)

Figure 5.12 Comparison of PFC Sigma 22 mm diameter ball test creep measurement taken from the FE model and the surface curve fitting methodology: (a) creep volume (CCC=0.8516), (b) maximum creep depth (CCC=0.9764).

The total creep volume generated using the PFC sigma test FE model (up to 75.58 mm^3) was a little larger than the 22 mm ball test model (up to 60.47 mm^3), however, the load was applied on both condyles of the tibial knee component and the creep volume calculated on each condyle was less. The maximum creep depth generated in the PFC sigma test model (up to 0.65 mm) was smaller than the 22 mm ball test model (up to 0.87 mm). This was due to the differences in the contact surfaces between the two computational models. Similar to the previous result, the total creep volume determined using surface curve fitting method was also overestimated (Figure 5.13). However, due to the undeformed region being sufficient for relatively accurate reconstruction of

the ‘original’ surface, the CCC was better than for the 22 mm ball test model (0.9616 and 0.9937 respectively).

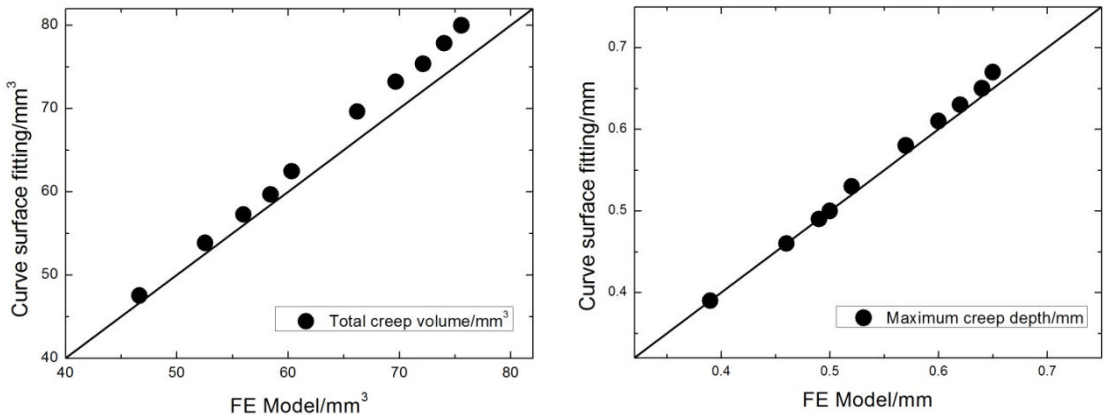

(a) (b)

Figure 5.13 Comparison of PFC Sigma femoral test model and surface curve fitting methodology: (a) total creep volume (CCC=0.9616), (b) maximum creep depth (CCC=0.9937).

Experimental data comparison

Due to the incapability of the group two motor for supporting higher loads in all three stations, the motor tripped at the beginning of the creep test. To avoid damaging the motor, two stations were run as dummies with no motion and with Vaseline used as lubrication during the test.

In the experimental creep test, four samples with one soak control sample was used. The soak control sample was used to determine the amount of fluid absorbed during the test. The volume change of the soak

control was deducted from the creep volume to determine the actual creep volume. The maximum volume gained due to soak was 0.92 mm^3, which was much lower when compared to 86.61 mm^3 generated during the creep test.

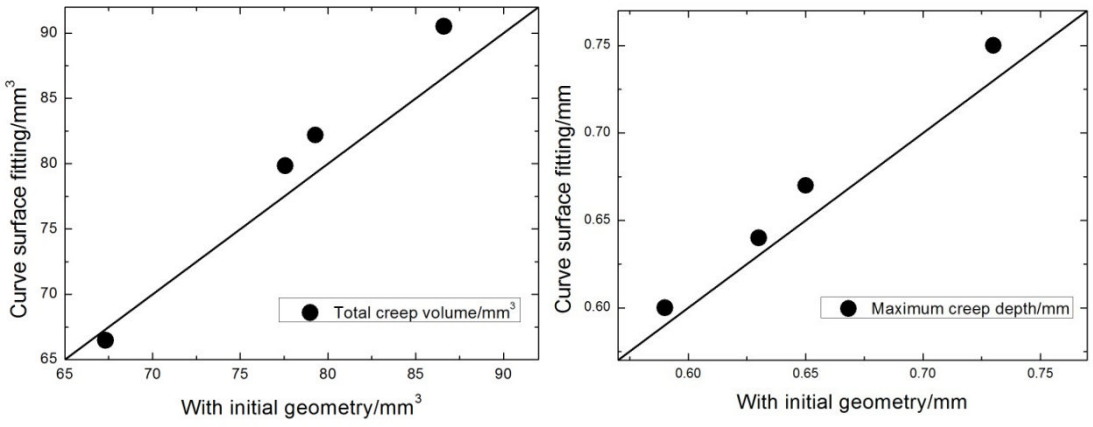

(a) (b)

Figure 5.14 Comparison of geometric analysis with and without initial surface geometry: (a) total creep volume (CCC=0.9411), (b) maximum creep (CCC=0.9573).

Due to the limitations of the current CMM program, the measurement area on the tibial knee component cannot extend to the whole condyle. Thus the predefined medial-lateral position was important as it would affect the contact area between the femoral and tibial components (Figure 5.11). The maximum total creep volume generated at 1 MC was 86.61 mm^3; the corresponding creep depth was 0.73 mm. The volume calculated using the surface curve fitting method was an overestimate for the specimens with initial geometry provided (Figure 5.14). However, a good correlation was observed

(CCC=0.9411 for total creep volume, CCC=0.9573 for maximum creep depth) using the surface curve fitting methodology. In summary, the results presented in this chapter demonstrate that the surface curve fitting methodology can accurately measure the creep volume and maximum creep for both FE creep models and experimental data.

Chapter 6

Comparison of CMM and Micro-CT Volumetric Analysis of Laboratory Specimens

6.1 Introduction

Wear measurement is very important for accurate determination of wear rate and volume loss in total knee replacements. The most standard method is gravimetric analysis (Affatato *et al*. 2002; D'Lima *et al*. 2003). However, the fundamental issue with gravimetric measurement is it needs a reference from which to calculate the wear. In addition, gravimetric measurement has limitations such as inclusion of wear debris in the polyethylene component, transfer of materials into the tibial tray, changes in mass of the polyethylene due to fluid uptake, and the cementation of the components (Bills *et al*. 2005; Bills *et al*. 2007), which may result in inaccurate volumetric determination from gravimetric analysis (Blunt *et al*. 2007). Since it is necessary to have a reference measurement for gravimetric analysis, it is not possible to use this method for retrieved samples. Therefore, in order to avoid these disadvantages, advanced volumetric measurement techniques such as coordinate metrology (CMM) (Raimondi *et al*. 2000; Bills *et al*. 2007) and Micro computed topography (Micro-CT) (Vicars *et al*. 2009; Anneli *et al*. 2011) have been used to determine the volume change of polyethylene in hip, knee and spinal replacement devices and validated for accuracy and repeatability.

In this chapter, CMM (Legex 322, Mitotoyo) and Micro-CT 100 (Scanco Medical, Busserdorf, Switzerland) were used for volumetric measurement of laboratory specimens. The measurement principles are detailed in Chapter 2: Sections 2.3 and 2.4. The purpose of this chapter is to compare CMM and Micro-CT measurement techniques using gravimetric measurement of volume loss as reference.

6.2 Materials and Methods

A total of 12 UHMWPE tibial knee components (DePuy, UK), which were tested in six station knee simulator (University of Leeds, UK) were used for measurement. The wear tests were carried out by a colleague within the research institution (C.Brockett) in 2009 and 2011. Two input profiles were used for the specimens, one is the ISO setup and the other is a standard CR150. The specimens were divided into two groups according to the total wear volume measured gravimetrically (Table 6.1). The group of specimens with smaller volume loss was graded as Group1 and the other group with greater volume loss was then graded as Group2. The methodologies of CMM and Micro-CT for volumetric measurements are detailed in Chapter 2 and Chapter 3: section 2.3.5 and section 3.2.2.

6.2.1 CMM

The specimen was cleaned and prepared for measurement as detailed in Section 2.2.1. The change in mass was assessed using the AT 201 balance

(Mettler Toledo Inc., Columbus, Ohio, USA). The samples were measured using CMM (Legex 322, Mitutoyo, UK) with known wear volume determined using gravimetric analysis. Since there was no initial surface data provided, the coordinates of each condyle surface were measured and surface curve fitting methodology was used for volumetric analysis based on the reconstructed 'original' surface (section 3.2.2.2). The results obtained were compared against gravimetric measurements.

Table 6.1 Total wear volume of specimens obtained using gravimetric analysis

Group 1		Group 2	
Specimen No.	Total wear volume/mm^3	Specimen No.	Total wear volume/mm^3
1	20.12	1	45.74
2	18.41	2	38.87
3	**9.12**	**3**	**49.92**
4	9.96	4	47.44
5	14.90	6	37.47
6	11.02	7	40.06

6.2.2 Micro-CT

As detailed in Chapter 2: section 2.3.3, an accurate threshold was the key parameter for volumetric analysis using Micro-CT (Scanco Medical, Busserdorf, Switzerland). There are two methods to determine the threshold; one is based on gravimetric analysis (Vicars *et al*. 2009), the other is

reference to a known volume cylindrical reference specimen. Known volumetric difference from gravimetric measurement was essential for the first method to calculate the amount of wear in Micro-CT. However, the specimens before wear were not available. Hence, the latter method was used in this study to determine the threshold based on a cylindrical reference specimen with known volume (936 mm^3). The threshold was determined in the image processing language (IPL), which was in-built in the Micro-CT scanner. With the obtained threshold, two-dimensional greyscale image slices were transferred from original ISQ file and stored in the form of TIFF images. Based on the image digitization method (section 2.3.5), the surface coordinates of the specimens were obtained for determination of the volume loss of the polyethylene specimens using surface curve fitting methodology (section 3.2.2).

All measurements were performed three times on each specimen to determine an average volume change and 95% confidence limits calculated, to determine the repeatability of the measurement method.

6.3 Results

The methodology used for volumetric determination using CMM and Micro-CT was surface curve fitting based on unworn area (section 3.2.2). At lower volumes, the volume calculated using CMM and Micro-CT measurement was close to gravimetric analysis. The comparison of CMM and Micro-CT methodologies against gravimetric are shown in Table 6.2. At higher volumes, both CMM and Micro-CT measurement overestimated wear

compared to gravimetric volume and the volume loss determined using Micro-CT was higher than CMM. The measurement times for the CMM and Micro-CT were approximately 40 minutes and 90 minutes per scan respectively. The 95% confidence limit of the Micro-CT methodology was higher than CMM; $\pm$3.26 mm^3 and $\pm$0.89 mm^3 respectively. Hence, the repeatability of CMM was better than Micro-CT. However, the repeatability of both methodologies was less than the gravimetric measurement ($\pm$0.02 mm^3). It can be seen from the Figure 6.1; both CMM and Micro-CT measurement appear to be an overestimate compared to gravimetric measurement.

Table 6.2 CMM and Micro-CT volumetric measurement results

Specimen No.	Gravimetric measurement/mm^3	CMM measurement/mm^3	Micro-CT measurement/mm^3
Group 1-1	20.12	22.85	23.31
Group 1-2	18.41	19.52	21.15
Group 1-3	**9.12**	**10.05**	**11.16**
Group 1-4	9.96	10.87	11.86
Group 1-5	14.90	16.78	16.18
Group 1-6	11.02	12.16	13.35
Group 2-1	45.74	49.39	51.56
Group 2-2	38.87	41.76	45.47
Group 2-3	**49.92**	**52.57**	**55.95**
Group 2-4	47.44	51.26	53.68
Group 2-6	40.06	43.65	42.54
Group 2-7	37.47	39.61	41.39

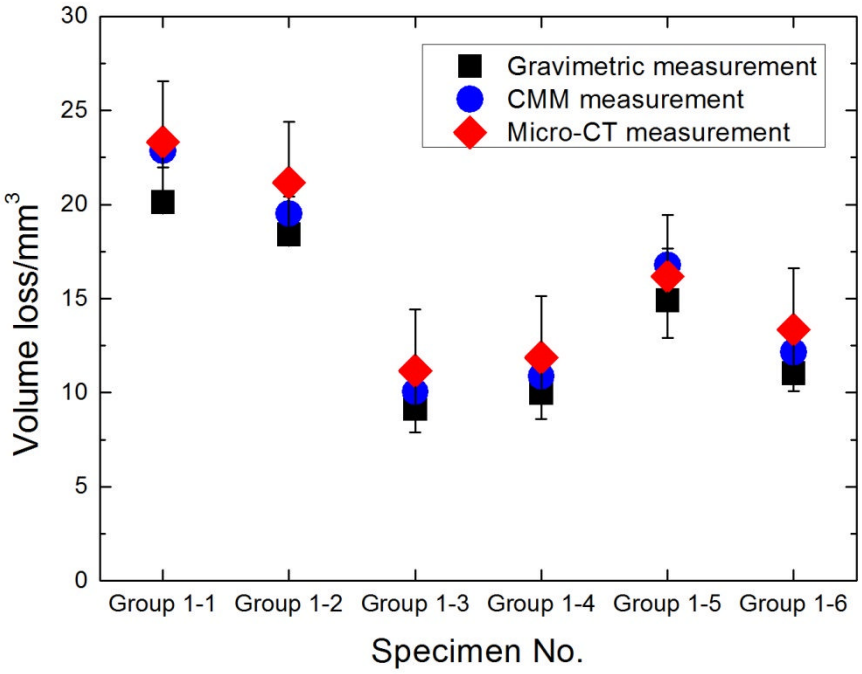

(a)

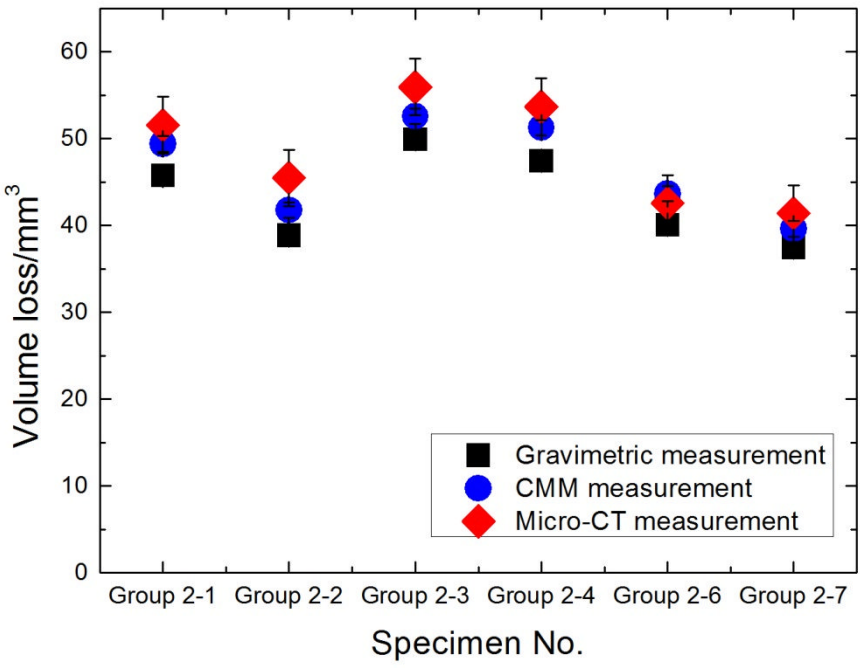

(b)

Figure 6.1 CMM and Micro-CT measurement results of laboratory specimens with 95% confidence limit.

6.4 Discussion

Gravimetric measurement methodology is the standard method used in the determination of volume loss (Affatato *et al*. 2002; D'Lima *et al*. 2003). However, fluid absorption and metallic debris inclusion may affect the measurement. Methodologies with greater accuracy and repeatability without these limitations are required. CMM and Micro-CT measurement techniques were used in this project to determine the volume loss of polyethylene tibial knee specimens and compared against gravimetric analysis, which was considered as the reference. However, it should be noticed that gravimetric measurement does not include creep whereas CMM and Micro-CT do as they are geometry based measurement techniques. Besides, backside wear will be included in gravimetric measurement but not in CMM/Micro-CT in this project since geometry changes only in left and right condyles of the tibial knee components were considered.

In this project, both CMM and Micro-CT analysis were based on the coordinates of the articulating surface. For CMM measurement, the coordinates were obtained directly from the scanning probe and stored on the PC in the form of txt file for analysis. For the Micro-CT, an image digitization method was used to transfer the two-dimensional greyscale images into coordinates for volumetric analysis. It has been reported that differences in the measured volumetric wear may be due to errors in thresholding and in the scanner which affect the intensity of the image (Ding *et al*. 1999; Fajardo *et al*. 2002; Hara *et al*. 2002; Kerckhofs *et al*. 2008). In order to obtain accurate surface geometry, a known volume reference specimen was used to

determine the threshold, which was the most important parameter for image digitization. However, even with the determined threshold, the average repeatability of Micro-CT ($\pm$3.26 mm^3) was still higher than of gravimetric measurement ($\pm$0.02 mm^3). The CMM ($\pm$0.89 mm^3) had better repeatability than Micro-CT, but still higher than gravimetric.

Concordance correlations coefficients (CCC) (Section 2.5) were used to evaluate the two measurement techniques against gravimetric measurement. As demonstrated in Figure 6.2, both CMM and Micro-CT measurement indicated higher wear compared to gravimetric analysis. Both CMM and Micro-CT measurements showed greater agreement with the gravimetric analysis when the volume loss was low (Figure 6.2(a)) and less agreement when volume loss became higher (Figure 6.2(b)). From the figure, CMM (CCC=0.9400 and 0.8188 respectively) provided a higher concordance than Micro-CT measurement (CCC=0.8770 and 0.6363 respectively) with the gravimetric analysis, this is more likely due to the thresholding in Micro-CT and image digitization from two-dimensional greyscale image slices. In addition, as demonstrated in Figure 6.3, the minimum and maximum volume difference of CMM analysis was 0.91 mm^3 and 3.82 mm^3. The corresponding volume difference of Micro-CT analysis was 1.90 mm^3 and 6.60 mm^3. These studies indicated that CMM had better accuracy compared to Micro-CT analysis.

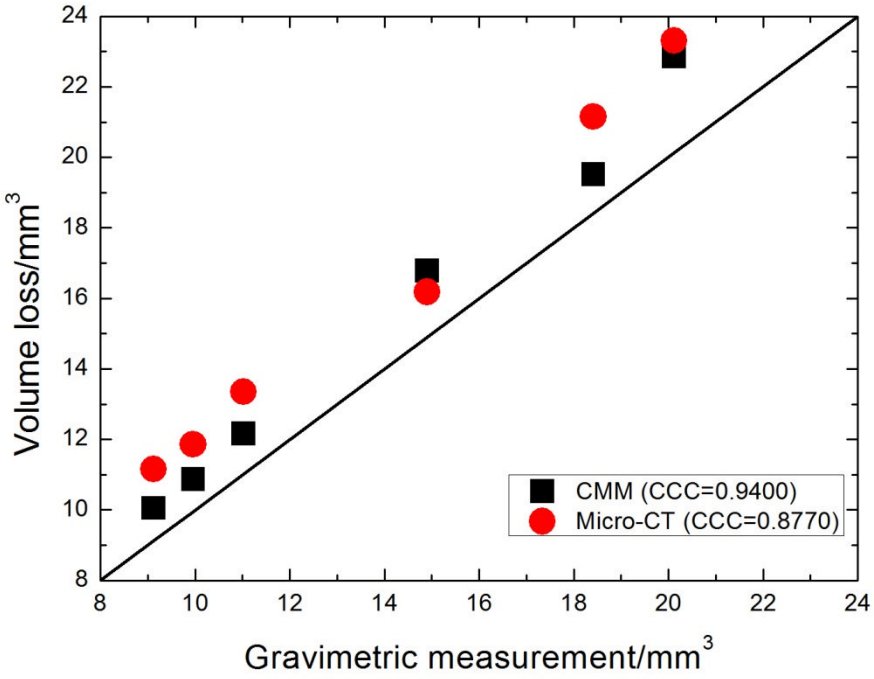

(a)

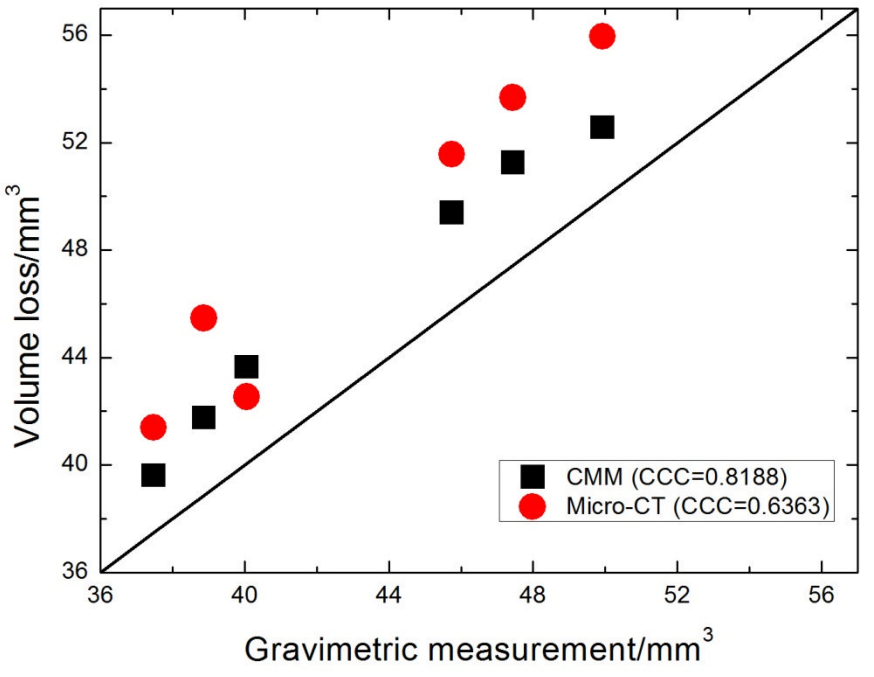

(b)

Figure 6.2 Comparison of CMM and Micro-CT volumetric analysis against gravimetric measurement.

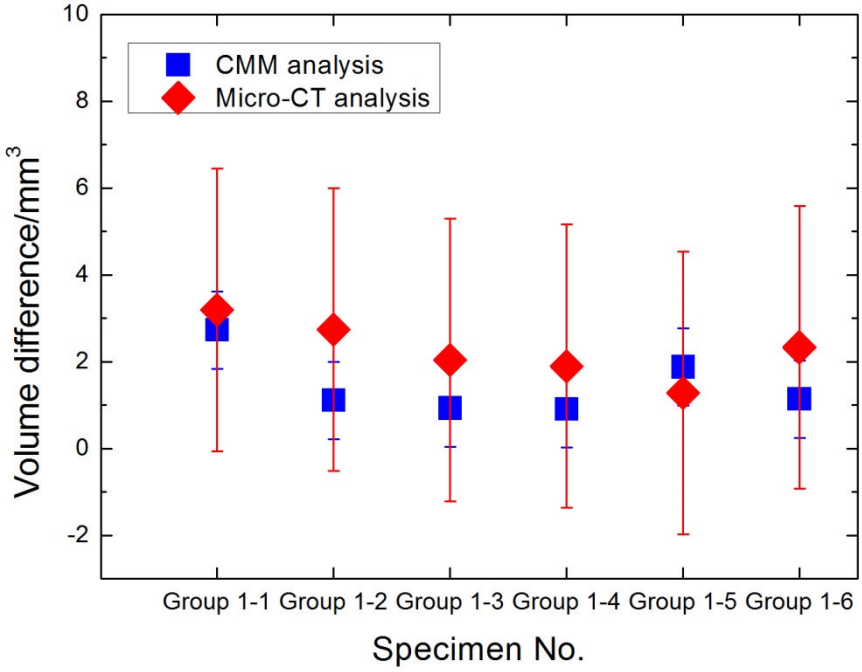

(a)

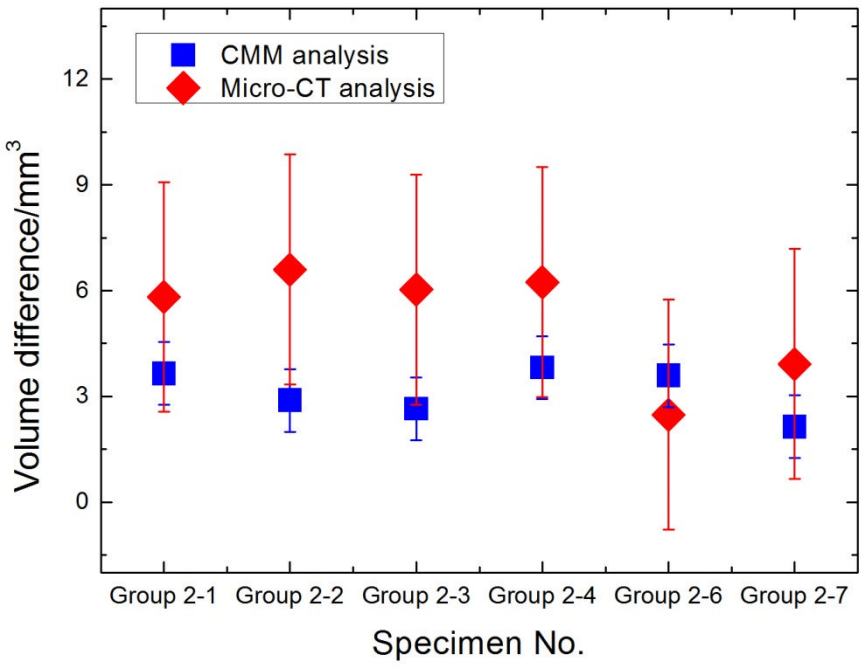

(b)

Figure 6.3 CMM and Micro-CT volumetric analysis results of laboratory specimens with 95% confidence limit.

Since the IPL software can determine the volume of the specimen (Vicars *et al*. 2009), Micro-CT can also be used to determine the volume loss with pre-wear data provided, which is similar to gravimetric measurements. However, for retrievals or cases similar to the present study, due to the absence of pre-wear data, the reference surface is not available, surface curve fitting methodology based on CMM coordinates and image digitization would be more appropriate to determine the volume loss. Gravimetric measurement was used as reference in this study to investigate the surface curve fitting methodology based on CMM and Micro-CT measurement techniques. Both CMM and Micro-CT can be used for retrievals when no pre-wear data exists, however, more specimens should be measured to investigate the applicability and accuracy of the method at higher volume loss, especially when no unworn area was available as reference for surface fit, which will be explained in the next chapter.

In summary, gravimetric volume analysis remains the most accurate and easiest method to determine the volume loss of polyethylene specimens. However, gravimetric analysis cannot be used at all for retrieval studies, which is an important area of interest in clinical performance. CMM and Micro-CT are alternative measurement techniques used for volume loss determination. In the study, since no pre-wear data available for reference, surface curve fitting methodology was used to create a nominal ‘original’ surface based on the unworn surface. CMM and Micro-CT techniques could determine the back side wear of tibial knee inserts, which is not available for gravimetric measurement. The CMM measurement took less time and had better accuracy and repeatability compared to Micro-CT measurement technique.

Chapter 7

Retrieval Analysis

7.1 Introduction

For several decades, ultra high molecular weight polyethylene (UHMWPE) has been widely used in total knee replacement (TKR) as a bearing material (Santavirta *et al*. 1998). The longevity of TKR is limited due to damage of articulating surface of tibial knee component (Wright and Bartel 1986; Landy and Walker 1988; Collier *et al*. 1991; Blunn *et al*. 1997; Wright and Goodman 2001), which may lead to osteolysis and implant loosening. Abrasive and adhesive mechanisms or fatigue processes that lead to pitting and delamination also result in damage. Polyethylene wear of the tibial knee component is considered a major factor that limits the clinical longevity of TKR (Whaley *et al*. 2003; O'Rourke *et al*. 2011). Several methods have been developed in the past to evaluate clinical retrievals (Hood *et al*. 1983; Raimondi *et al*. 2000; Bowden *et al*. 2005; Rawlinson *et al*. 2006; Bills *et al*. 2007; Kurtz *et al*. 2007). Gravimetric and Micro-CT analysis has been used for volume loss measurement when pre-wear data was available. CMM is considered the only option for volumetric assessment where no pre-wear data available.

The absence of pre-wear data for retrievals presents difficulties when comparing with *in-vitro* tested total knee replacements, where the pre-wear measurements are known. Volumetric measurement using gravimetric

analysis is only possible when volume before the wear process is measured. However, without pre-wear data, it would be difficult to determine the volume loss accurately. The purpose of the current chapter was to quantitatively determine the volume loss from retrievals using CMM and Micro-CT techniques. However, the presented coordinate based volumetric assessment methodology does have limitations as it requires unworn area for reconstruction of the initial geometry (section 3.2).

7.2 Materials and Methods

Eight retrieved tibial knee component specimens were collected from different hospitals under an NRES approved procedure (09/H1307/60) and are detailed in Table 7.1. The manufacturer of the tibial knee specimens was DePuy 75% of the implants were PFC and PFC Sigma designs, while the remaining 25% data was not known. The division of specimens in terms of gender was 75% female and 25% male. The average years *in situ* was 11.4±6.3 years with 37.5% left knees and 62.5% right knees. The reasons for the revision were aseptic loosening (25%), instability (12.5%), wear (12.5%), infection (12.5%) and autopsy (25%). The reason for failure in 1 specimen (F) was unknown. The average weight and height was 74.9±28.4 kg and 162.7±8.2 cm respectively.

According to the method by Hood *et al*. (1983), retrievals were graded based on intensity, area and type of wear scars. The wear scar measurements were captured using a high zoom camera (SONY DSLR NEX 5C). Wear characteristics were evaluated using visual inspection. The details

of methodologies are presented in chapter 2 and chapter 3. As illustrated in Figure 7.1, specimen A has the tibial tray attached and it was not possible to remove the tibial component due to cement.

Table 7.1 Clinical data of tibial knee component retrievals (Retrieval database, University of Leeds)

Patient No.	Prosthesis type	Gender	Weight/kg	Height/cm	Time in situ/years	Side	Reason for revision
A	PFC	M	80	165	15	R	Aseptic loosening
B	PFC-Sigma posterior stabilised	M	64	173	2	L	Aseptic loosening
C	PFC	F	66	164	18	R	Instability
D	PFC	F	143	167	18	R	Wear
E	-	F	64	165	9	L	Infection
F	-	F	58	-	-	R	-
G	PFC	F	67	158	13	L	Autopsy
H	PFC	F	57	147	5	R	Autopsy

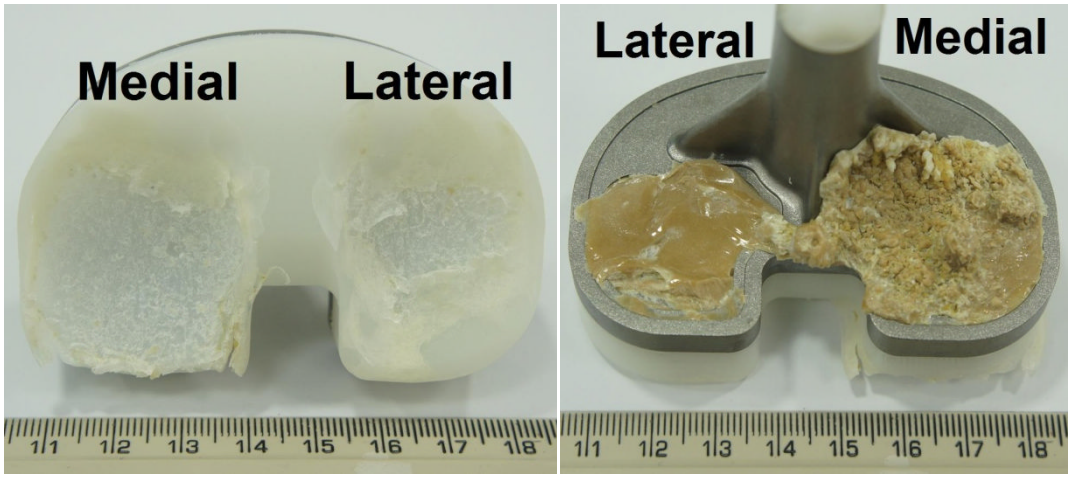

A (Patient code: SP-MHS-1005-002)

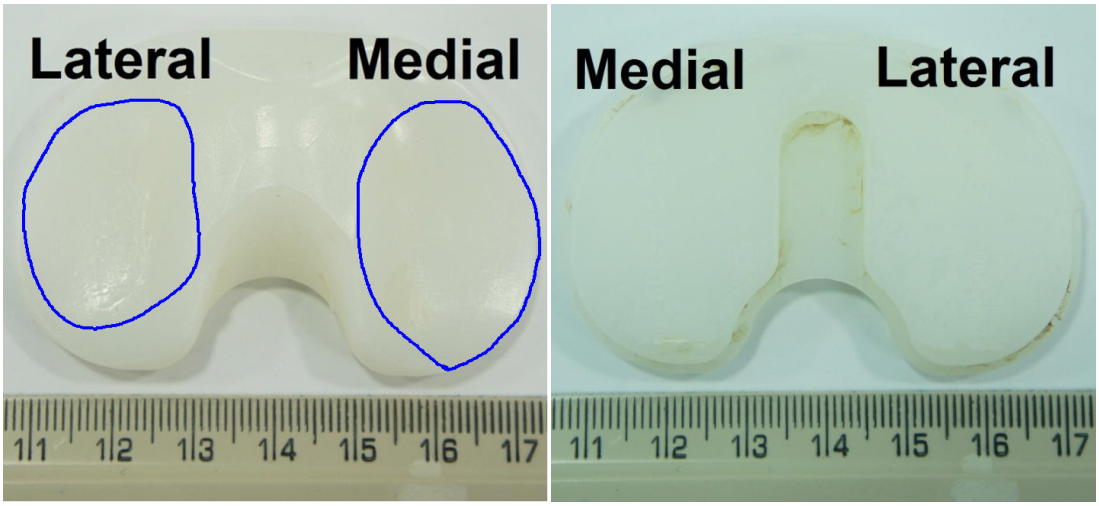

B (Patient code: CB-NL-1109-002)

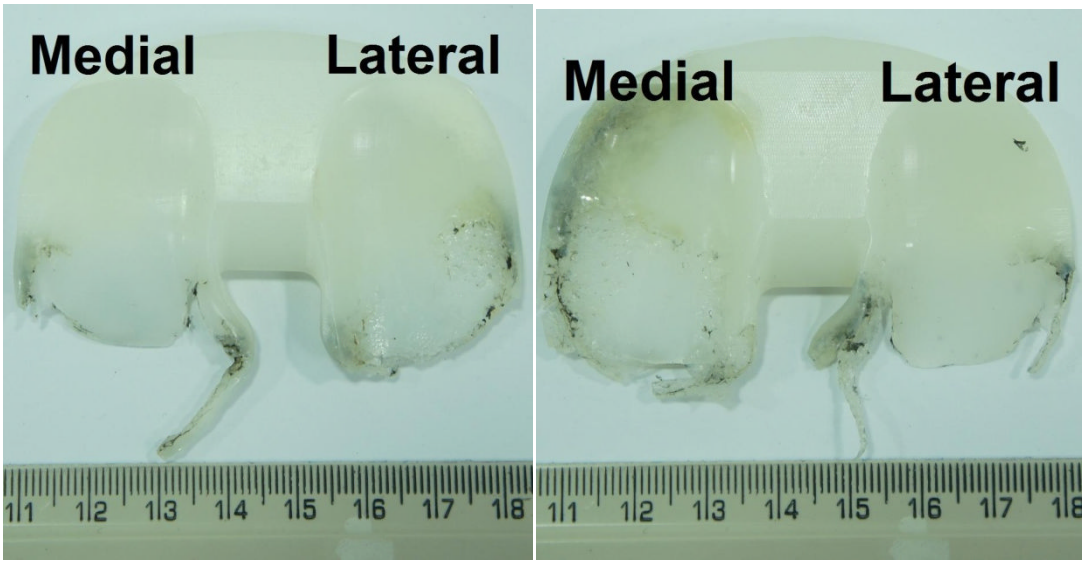

C (Patient code: SP-MHS-1109-001) D (Patient code: SW-MHS-1204-001)

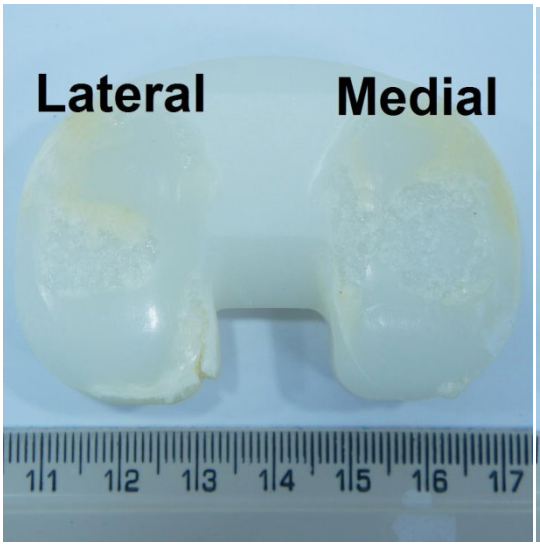

E (Patient code: K4401)

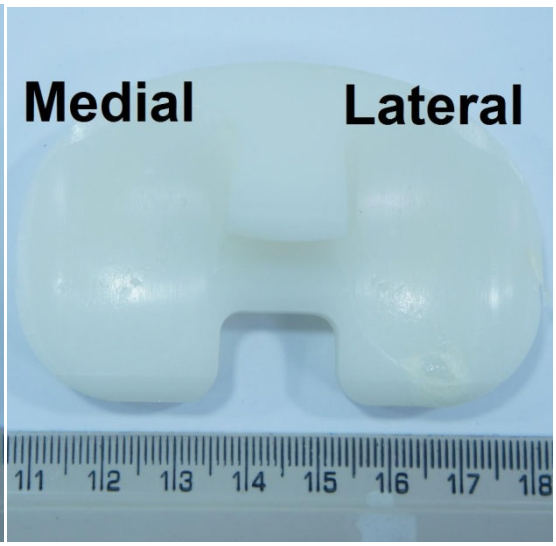

F (Patient code: K4410)

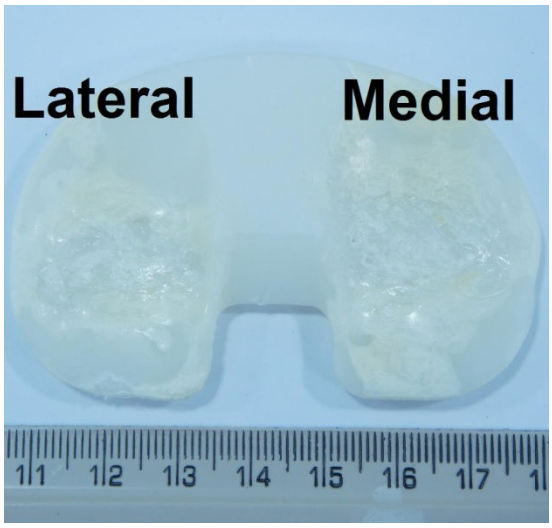

G (Patient code: K4411)

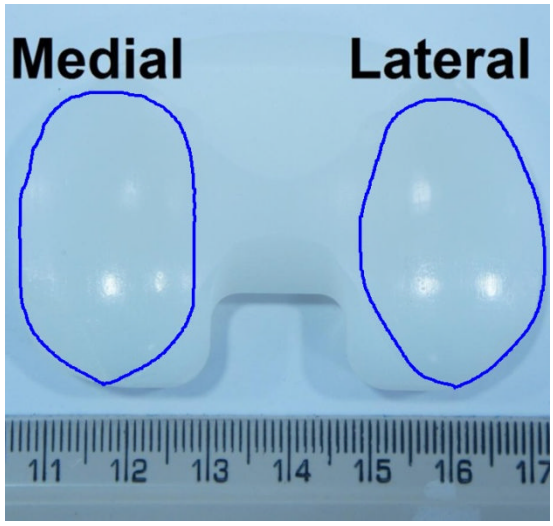

H (Patient code: K4413)

Figure 7.1 Tibial knee component retrievals.

7.3 Results

7.3.1 Visual inspection

The various types of wear found in the tibial retrievals were pitting, scratching, burnishing, delamination, surface deformation and cement debris as shown in Figure 7.2. The retrievals F and H were the least damaged

specimens according to the varied regimes found. The specimens which appeared to show the greatest extent of wear were specimens C and D with large wear areas posteriorly on the insert. Samples A and G appeared to have the most significant regions of delamination. Some scratching was observed on retrievals B, C, D, E and H. It appeared that scratching on retrievals B and H were due to third body wear particles, however, scratches on retrievals C, D and E were due to handing and revision process.

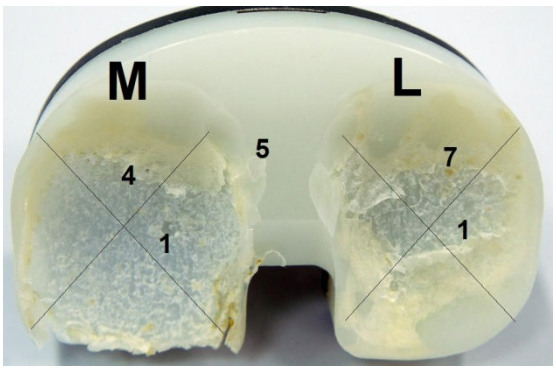

A

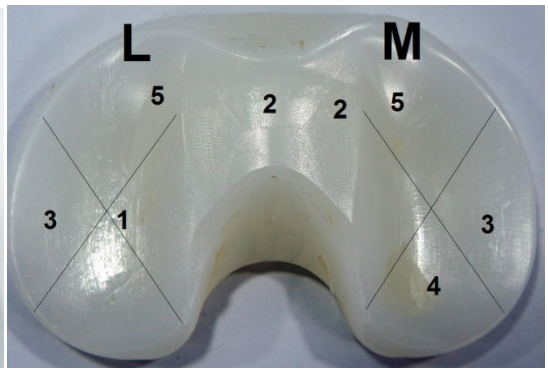

B

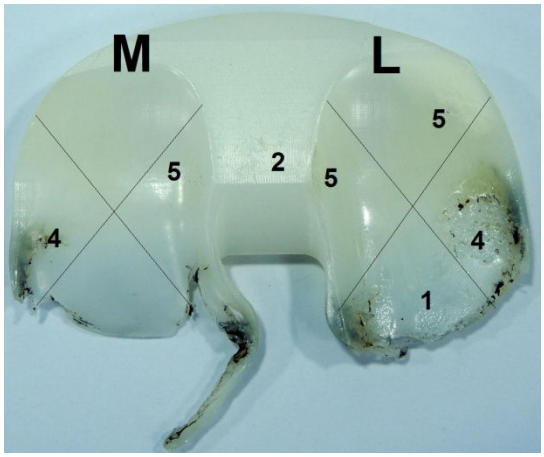

C

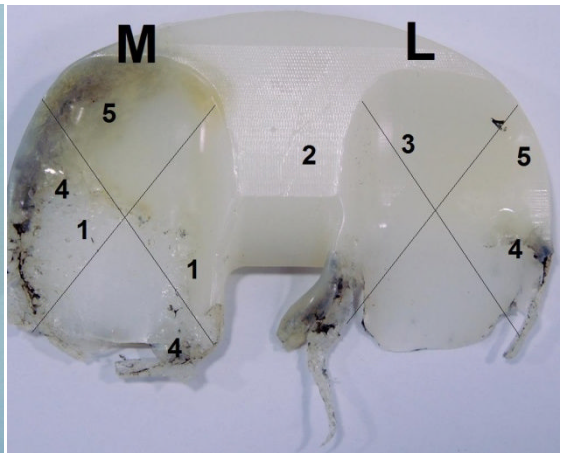

D

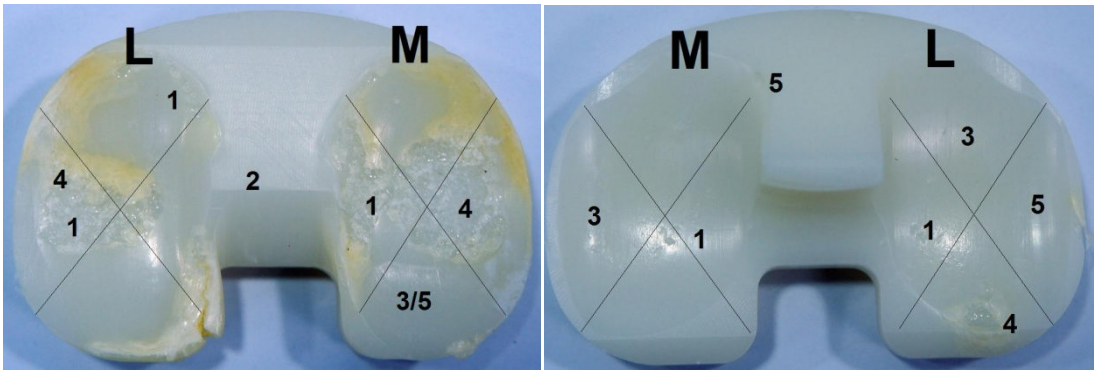

E F

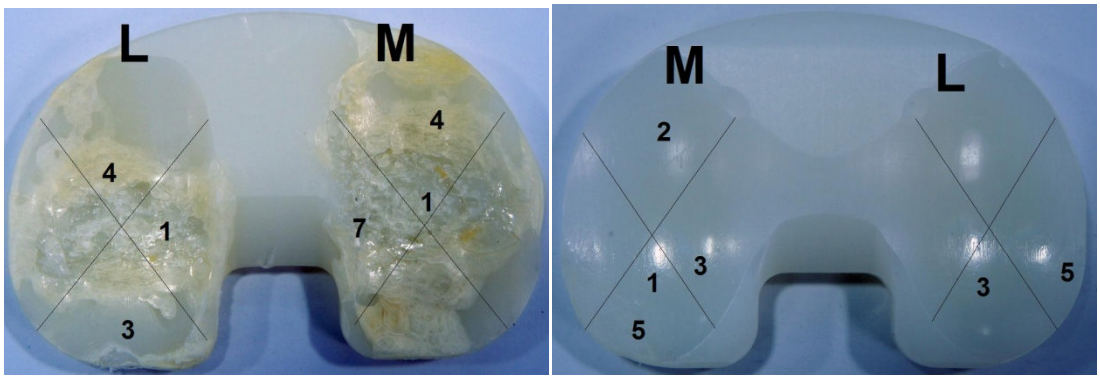

G H

Figure 7.2 Wear characteristics for tibial knee retrievals (Specimen A to H). 1: pitting, 2: scratching, 3: burnishing, 4: delamination, 5: surface deformation, 6: adhesive, 7: cement debris.

As demonstrated in Table 7.2, analysis of the surfaces showed some wear mechanisms occurring in all retrievals analysed. The frequency of damage modes were analysed as a percentage of the dataset (n=8). Pitting was observed on all samples, with delamination and deformation also occurring frequently amongst the samples. There was no adhesive wear found in the tibial retrievals.

Table 7.2 Occurrence of damage modes in the tibial retrieval specimens

Type of wear	8 Tibial components
Pitting	100%
Scratching	62.5%
Burnishing	75%
Delamination	87.5%
Deformation	87.5%
Adhesive	0%
cement debris	25%

7.3.2 Volumetric determination

Initially, it was intended that CMM and Micro-CT measurement techniques would be used for volumetric assessment of the tibial retrievals based on the presented surface curve fitting methodology (section 3.2) in this study. The volumetric assessment methodology is coordinate based, which can be obtained from the CMM measurement and two-dimensional greyscale image slices. However, the current scanning probe used for the CMM methodology measures the surface continuously (section 2.4). As illustrated in Figure 7.2, 87.5% of the retrievals had delamination on the surface, which would limit the measurement of CMM as the scanning would stop with measurement errors due to the bend of CMM probe. Both the CMM and Micro-CT volumetric determination methodologies presented in this thesis require an unworn area to reconstruct the ‘original’ surface for reference. However, none of the retrievals had sufficient unworn area for accurate

regeneration of the original surface. Thus, neither CMM nor Micro-CT measurement was carried out to determine the volume loss of the retrievals.

7.4 Discussion

Hood *et al*. (1983) found that there are seven wear damage modes on the articulating surface of retrieved tibial knee components, including surface deformation, pitting, cement debris, scratching, burnishing, abrasion and delamination. In the present study, the most common damage mode found on the articulating surface of the retrieved polyethylene tibal insert was pitting (100%); followed by delamination (87.5%), surface deformation (87.5%), burnishing (75%), scratching (62.5%) and cement debris (25%). There was no abrasion found in this study.

Pitting and delamination have been reported as the most common damage modes for total knee replacement (Bradford *et al*. 2004), which is similar to the present study. Collier *et al*. (1996) investigated the correlation between implantation time and occurrence of delamination. For implantation duration of less than 4 years, 17-27% of the retrieval tibial knee components demonstrated sings of delamination. For implantation duration of more than 4 years, delamination damage was found in 65% of the retrievals. In the present study, one specimen had an implantation duration of less than 4 years and delamination was found, however, the major damage mode to this specimen was burnishing. Delamination occurred in 85.7% of the retrieval tibial knee inserts implanted for more than 4 years in the present study, greater than previously reported (Collier *et al*. 1996). Pitting and delamination damage are

related to fatigue wear and according to the research by Medel *et al*. (2011), fatigue wear was the dominant damage mode in knee replacement, and was caused by low conformity and high contact stress between the femoral and tibial knee components.

Pre-wear measurement is essential for accurate determination of volume loss, however, pre-wear data is not always provided. Since CMM and Micro-CT do not depend on the pre-wear data, these techniques have been used for volumetric analysis of retrievals (Bowden *et al*. 2005; Bills *et al*. 2005; Bills *et al*. 2007). In the present study, volumetric assessment methodology was planned based on coordinates and intended to evaluate the retrievals quantitatively in the form of volume loss and linear penetration.

CMM and Micro-CT were initially intended to obtain the surface geometry of the retrieval tibial knee component and later analyse using the surface curve fitting method. However, due to the delamination on most of the specimens (87.5%), it was not possible to use the CMM method, as the probe is in continuous contact with the surface. The delamination on the surface of the inserts, and regions of material that were not removed from the insert may cause the CMM probe to bend and the programme to stop with measurement errors. Thus, those retrieval specimens (A, C, D, E and G) cannot be measured using CMM methods. Furthermore, the edge of several retrieved specimens was significantly worn (B, C, D F and H), meaning there was no unworn region available to use as a reference surface. It would be difficult and impractical to obtain the coordinates from either CMM or two-dimensional greyscale image slices. As illustrated in Figure 7.1, it seems that the superior surfaces of retrieval specimens B and H were smooth and can be used for

CMM analysis, however, the worn area were too large on both left and right condyle. Which means no sufficient undeformed area can be used as reference to reconstruct the original surface for volume loss determination. As a result, none of the retrieval specimens were measured using CMM and Micro-CT for volumetric analysis.

7.5 Conclusion

Eight tibial knee component retrievals were analysed visually and the articulating surface of the retrievals showed a variety of wear mechanisms, such as pitting (100%), delamination (87.5%), surface deformation (87.5%), burnishing (75%), scratching (62.5%) and cement debris (25%). No adhesive wear was found in the retrievals.

The presented volumetric assessment methodology based on surface curve fitting was not applicable for the retrievals in this study due to the limitation of the measurement and no unworn area left for ‘original’ surface geometry reconstruction.

Chapter 8

Overall Discussion, Conclusion and Future Work

8.1 Overall discussion

The total knee replacement (TKR) was designed to provide final-stage treatment for patients to replace the damaged biological tissues and help the patient to carry out daily normal activities. The requirement for knee replacement operations is increasing every year worldwide (Carr and Goswami 2009). The longevity of TKR is limited due to damage of the articulating surface of tibial knee component (Wright and Bartel 1986; Landy and Walker 1988; Collier *et al*. 1991; Blunn *et al*. 1997; Wright and Goodman 2001), which leads to osteolysis and implant loosening. Determination of wear of the polyethylene knee inserts has been an important subject in improving the longevity of TKR (Krutz *et al*. 2004). Accurate wear measurement methodologies are essential to differentiate between the performance of different materials and designs because the geometry changes can be small and can consist of both wear and creep. Gravimetric analysis is the standard method of wear measurement (Affatato *et al*. 2002; D'Lima *et al*. 2003). However, gravimetric methods have limitations due to fluid intake, backside wear, the mass of fixturing attached to the specimens and the absence of pre-wear data in retrievals (Bills *et al*. 2005; Bills *et al*. 2007). Coordinate measuring machine (CMM) and Micro computed tomography (Micro-CT) have been recently used for volumetric measurement of wear and provide a

potential alternative to gravimetric methods (Keng 1970; Raimondi *et al*. 2000; Bills *et al*. 2007; Vicars *et al*. 2009).

The aim of this study was to develop a coordinate based three-dimensional volumetric determination methodology using CMM and Micro-CT measurement techniques. The validation of the methodology was carried out using a FE model and computational volume removal test. Afterwards, the volumetric determination method was used to calculate the volume loss from computational and experimental tests of volume removal and creep deformation. Finally, the methodology was applied to evaluate both simulator and retrieval specimens.

The initial geometric measurements of specimens or design drawings are not always available (Liow *et al*. 1997), which are ideal as reference for accurate volumetric wear assessment. In this study, it was found that the presented coordinate based methodology is adequate for tibial knee components where no pre-wear data is provided. However, the surface curve fitting requires a selection of an undeformed region of about 50% of the area to use as reference coordinates for accurate ‘initial’ geometry reconstruction. As the wear processes, the amount of wear increases and the border of tibial knee inserts can be damaged. In this situation, the presented method may be no longer suitable and CAD models or original design drawings are essential to evaluate the amount of wear.

The Micro-CT measurement technique provides two-dimensional greyscale image slices for analysis and can also be used to determine the volume change (Vicars *et al*. 2009; Anneli *et al*. 2011). The most important parameter used in Micro-CT image analysis is the threshold (Ding *et al*. 1999;

Fajardo *et al*. 2002; Hara *et al*. 2002; Kerckhofs *et al*. 2008), which is used to define the specimen from the background. In order to determine the threshold accurately and repeatably, a cylindrical polyethylene reference specimen with known volume was used in this study as a control. With the determined threshold, the two-dimensional greyscale image slices were then digitized in the form of coordinates for analysis.

The maximum worn area generated from computational and experimental volume removal tests was less than 50%. Thus, the reconstruction of the 'initial' geometry was relatively accurate. The volume loss determined using surface curve fitting was slightly underestimated compared to gravimetric measurement, however, the agreement was high (CCC=0.9960). The difference between computational and experimental tests is that the edge of the wear scar generated computationally was more clear, which makes it easier to distinguish the wear area from the condyle leading to higher agreement in the volumetric determination (CCC=0.9997). Furthermore, plastic deformation was found to occur in the volume removal tests, which resulted in inaccurate identification of the undeformed region. This was due to mechanical vibration during the experimental tests.

Determination of the amount of creep is important for more accurate assessment of true in vivo/vitro wear rate because creep can increase the contact area by up to 50% during the first few hundred thousand gait cycles (Bevill S *et al*, 2005). A computational creep deformation test was undertaken as part of a wear prediction modelling study (Abdelgaied *et al*, 2011), which was used to provide surface geometry before and after creep. Two types of contact surface were considered, one was with a 22 mm ball and the other

was with a femoral component. The Leeds/ProSim knee simulator was used to perform creep tests on four new tibial knee components for up to 1 million cycles. The amount of creep determined using the surface curve fitting method was greater than FE model (CCC=0.8516 for 22mm ball model and CCC=0.9616 for PFC sigma test model respectively). The creep depth determined had higher level of agreement (CCC=0.9764 for 22mm ball model and CCC=0.9937 for PFC sigma test model respectively). Both total creep volume and maximum creep depth determined for the experimental creep tests were overestimated, however, a good correlation was observed (CCC=0.9411 and CCC=0.9573 respectively).

The surface curve fitting method was also applied to analyse *in vitro* test specimens and retrievals. For *in vitro* specimens, gravimetric analysis was used as reference. The repeatability of the CMM ($\pm$0.89 mm^3) was better than Micro-CT ($\pm$3.26 mm^3), however, it was still higher than that of the gravimetric measurement ($\pm$0.02 mm^3). Both results from CMM and Micro-CT were overestimates and with the increasing of volume loss, the error becomes greater. The volumetric analysis against gravimetric indicated that the CMM (CCC=0.9400 and 0.8188 respectively) has higher accuracy than Micro-CT measurement (CCC=0.8770 and 0.6363 respectively), which is most likely due to the thresholding in the Micro-CT and image digitization from two-dimensional greyscale image slices. Eight retrieval polyethylene tibial knee components were analysed and the wear mechanisms present in the retrievals were pitting (100%), delamination (87.5%), surface deformation (87.5%), burnishing (75%), scratching (62.5%) and cement debris (25%). Adhesive wear were absent in this study. Due to the absence of pre-wear data,

the existence of worn edges and delamination damage in most of the retrieval specimens, the volume determination using surface curve fitting methodology was not appropriate. Hence, neither CMM nor Micro-CT was performed to obtain surface coordinates for volumetric analysis. Pitting and delamination were found the most common damage modes for the retrievals in this study, which is the same as reported previously (Bradford *et al*. 2004).

8.2 Conclusion

A novel three-dimensional coordinate based volumetric determination methodology was developed for CMM and Micro-CT analysis. It was found that the 'original' surface geometry of the tibial knee component could be reconstructed based on the 'undeformed' region using a 5^{th} order polynomial surface curve fitting, provided an unworn area of approximately 50% was used as reference for the surface fitting. Since coordinates can be obtained from CMM directly and Micro-CT two-dimensional greyscale image slices using image digitization, the presented volumetric determination methodology was not dependent on pre-wear data, CAD model or original design drawings and can be used for both simulator and retrieval analysis at relevant levels of wear and creep. It can also be applied to the biotribological study of other polyethylene components, since wear and damage can be assessed visually and volumetrically.

When the surface curve fitting method was applied to analyse both experimental and computational wear data, it was found to have high levels of agreement compared to gravimetric analysis, and it was also possible to use

the method to determine the amount of creep. The comparison between CMM and Micro-CT methods suggested that the CMM is more accurate and therefore this is recommended for future studies. Whilst the methods developed in this thesis were suitable for laboratory and computational wear determination, they are not suitable for all specimens in retrieval study due to the greater amount of wear and damage on the surface.

8.3 Future work

The study considered development of three-dimensional coordinate based volumetric assessment methodology and its application for laboratory and retrieval analysis. Further investigations and efforts should focus on the following:

- Apply the methodology to different types of tibial knee components.
- Investigate the use of the methodology for retrievals where lower levels of wear are present.
- Develop a Graphical User Interface (GUI) based on the presented methodology to enable the methods to be more easily applied.
- Improve the methodology for high volume loss determination by considering the use of CAD models and drawings of the tibial component to determine the wear volume.

References

Abdelgaied, A., Liu, F., Brockett, C., Jennings, L., Fisher, J. and Jin, Z. (2011) Computational wear prediction of artificial knee joints based on a new wear law and formulation. J Biomech, 44: 1108-1116.

ACLSolutions. (2012). "http://www.aclsolutions.com/default.php." Retrieved March, 2012.

Affatato, S., Bordini, B., Fagnano, C., Taddei, P., Tinti, A., Toni, A. (2002) Effects of the sterilisation method on the wear of UHMWPE acetabular cups tested in a hip joint simulator. Biomaterials, 23:1439-1446.

Affatato, S., L. Cristofolini, W. Leardini, P. Erani, M. Zavalloni, D. Tigani, M. Viceconti (2008). A New Method of In Vitro Wear Assessment of the UHMWPE Tibial Insert in Total Knee Replacement. Artificial Organs 32(12): 942-948.

Al-Turaiki, M. H. S. (1986) The Human Knee-Functional Anatomy, Biomechanics, and Instabilities & Assessment Techniques.

Andriacchi, P. T., Andersson, G. B. J, Fermier, R. W., Stern, D., Galante, J. O. (1980) A study of lower-limb mechanics during stair-climbing. J Bone Joint Surg [Am], 62:749-757.

Annegret, M., Chris, O., Dyrby, Darryl, D., D'Lima, Clifford, W., Colwell, Jr., Thomas, P., Andriacchi. (2007) In Vivo Knee Loading Characteristics during Activities of Daily Living as Measured by an Instrumented Total Knee Replacement. Journal of Orthopaedic Research, 26: 1167-1172.

Anthony, P. P., Gie, G. A., Howie, C, R., Ling, R. S. (1990) Localised endosteal bone lysis in relation to femoral components of cemented total hip arthroplasties. J Bone Joint Surg Br, 72: 971.

Argenson, J. N., O'Connor, J. J. (1992) Polyethylene wear in meniscal knee replacement. A one to nine-year retrieval analysis of the Oxford knee. J Bone Joint Surg (Br), 74: 228-232.

Atkinson, J. R., Dowling, J. M., Cicek, and R. Z. (1980) Materials for internal prostheses: The present position and possible future developments, Biomaterials, 1, 89–96.

Atkinson, J. R., Cicek, R. Z. (1984) Silane crosslinked polyethylene for prosthetic applications. II. Creep and wear behaviour and a preliminary moulding test. Biomaterials, 6: 326-335.

Atkinson, J. R., Dowson, D., Isaac, J. H., and Wroblewski B. M. (1985) Laboratory wear tests and clinical observations of the penetration of femoral heads into acetabular cups in total replacement hip joints: III. The measurement of internal volume changes in explanted Charnley sockets after 2–16 years in vivo and the determination of wear factors, Wear, 104, 225–244.

Banks, S. A., Hodge, W. A. (1996) Accurate measurement of three- dimensional knee replacement kinematics using single-plane fluo- roscopy. IEEE Trans. Biomed. Eng, 43: 638-649.

Bartel, D. L., Bicknell, V. L., Wright, T. M. (1986) The effect of conformity, thickness, and material on stresses in ultra high molecular weight components for total joint replacement. J Bone Joint Surg (Am), 7: 1041-1051.

Bartel, D. L., Rawlinson, J. J., Burstein, A. H., Ranawat, C. S., Flynn, W. F., (1995) Stresses in polyethylene components of contemporary total knee replacements. Clinical Orthopaedics and Related Research, 317: 76-82.

Barnett, P. I., McEwen, H. M. J., Auger, D. D., Stone, M. H., Ingham, E., Fisher, J., (2002) Investigation of wear of knee prostheses in a new displacement/force-controlled simulator. Proceedings of the Institution of Mechanical Engineers Part H-Journal of Engineering in Medicine, 216: 51-61.

Barrett, J. F., Keat, N. (2004) Artifacts in CT: recognition and avoidance. Radiographics, 24: 1679-1691.

Becker, A., Schollhorn, K., Dirix, Y., and Schmotzer, H. (2006) Metal-on-metal bearings I: The influence of 3D measurement accuracy on the calculated wear of a ball head using a new mathematical approach.

Bell, C. J., Walker, P. G., Blunn, G. W. (1998) The effect of oxidation on delamination of UHMWPE tibial components. J Arthroplasty, 13: 280-290.

Benjamin, J., Szivek, J., Dersam, G., Persselin, S., Johnson, R. (2001) Linear and volumetric wear of tibial inserts in posterior cruciate retaining knee arthroplasties. Clin Orthop, 392: 131-138.

Blunn, G. W., Walker, P. S., Joshi, A., Hardinge, K. (1991) The dominance of cyclic sliding in producing wear in total knee replacements. Clin Orthop, 273: 253-60.

Blunn, G. W., Joshi, A., Hardinge, K., Engelbrecht, E., Walker, P. S., Lidgren, L., Ryd, L. (1992) The effect of bearing conformity on the wear of polyethylene tibial components. Trans of the 38th Annual Meeting Orthop Res Soc.

Blunn, G. W., Joshi, A. B., Lilley, P. A., Engelbrecht E, Ryd L, Lidgren L. (1992) Polyethylene wear in unicondylar knee prostheses. 106 Retrieved Marmor, PCA, and St. Georg tibial components compared. Acta Orthop Scand, 63(3):247–55

Blunn, G., Joshi, A., Minns, R. (1997). Wear in retrieved condylar knee arthroplasties. A comparison of wear in different designs of 280 retrieved condylar knee prostheses. J Arthoplasty, 12:281–290.

Blunt, L. A., Bills, P. J., Jiang, X. Q., Charkrabarty, G. (2008) Improvement in the assessment of wear of total knee replacements using coordinate-measuring machine techniques. Proc. IMech, 222: 309-318.

Blunt, L., Bills, P. J., Jiang, X.,Hardaker, C., Charkrabarty, G. (2009) The role of tribology and metrology in the latest development of bio-materials. Wear, 266: 424-431.

Bills, P., Brown, L., Jiang, X. and Blunt, L. (2005) A metrology solution for the orthopaedic industry Journal of Physics, 13: 316-319

Bills, P., Blunt, L. & Jiang, X. (2007) Development of a technique for accurately determining clinical wear in explanted total hip replacements. Wear, 263: 1133-1137.

Bowden, A. E., Kurtz, S. M., Edidin, A. A. (2005) Validation of a micro-CT technique for measuring volumetric wear in retrieved acetabular liners. J Biomed Mater Res, 75: 205-209.

Bowden, A. E., Shkolnikov, Y., MacDonald, D., Kurtz, S. M. (2007) Development and validation of an automated microCT-based technique for mapping damage of explanted polymeric components for TDR. 7th Annual Meeting of the Spine Arthroplasty Society, Berlin, Germany.

Bradford, L., Baker, D. A., Graham, J., Chawan, A., Ries, M. D., Pruitt, L. A. (2004) Wear and surface cracking in early retrieved highly cross-linked polyethylene acetabular liners. J Bone Joint Surg Am., 86:12 71–82.

Brockett, C. L., Jennings, L. M., Fisher, J. (2011) The wear of fixed and mobile bearing unicompartmental knee replacements. Proceedings of the Institution of Mechanical Engineers Part H-Journal of Engineering in Medicine 225(H5): 511-519.

Buechel, F. F., Pappas, M. I., Malois, G. (1991) Evaluation of contact stress in metal backed patellar replacements. A predictor of survivorship. Clin Orthop, 273: 190-197.

Campbell, P., Doorn, P., Dorey, F., Amstutz, H. C. (1996) Wear and morphology of ultra-high molecular weight polyethylene wear particles from total hip replacements. Proc Inst Mech Eng, 210: 167-174.

Carr, B. C. and Goswami, T. (2009). "Knee implants - Review of models and biomechanics." Materials & Design 30(2): 398-413.

Cigada, A., Brunella, M. F., and Pezzi, D. (1993) Wear and creep of UHMWPE by hip joint simulator tests, inTransactions of the 19th Annual Meeting of the Society for Biomaterials, 333.

Collier, J. P., McNamara, J. L., Surprenant, V. A., Jensen, R. E., Surprenant, H. P. (1991) All polyethylene patellar components are not the answer. Clin Orthop, 273: 198-203.

Collier, J., Mayor, M., McNamara, J. (1991). Analysis of the failure of 122 polyethylene inserts from uncemented tibial knee components. Clin Orthop, 273:232–242.

Collins, J. J. (1995) The redundant nature of locomotor optimization laws. J Biomech, 28: 251-267.

Collier, J. P., Sperling, D. K., Currier, J. H., Sutula, L. C., Saum, K. A., Mayor, M. B. (1996) Impact of gamma sterilization on clinical performance of polyethylene in the knee. J Arthroplast, 11(4):377–89.

Davidson, J. A., and Schwartz, G., (1987). Wear, creep, and frictional heat of femoral implant articulating surfaces and the effect on long-term performance—Part I, review, J. Biomed. Mater. Res., 21,261–285

Deirmengian, C. A., Lonner, J. H. (2008) What's new in adult reconstructive knee surgery. J Bone Joint Surg Am., 11: 2556-2565.

Devane, P. A., Bourne, R. B., Rorabeck, C. H., Hardie, R. M., Horne, J. G. (1995) Measurement of polyethylene wear in metal-backed acetabular cups. I. Three-dimensional technique. Clin Orthop Relat Res, 319: 303-316.

Dowson, D. & Wright, V., (1981) Introduction to the Biomechanics of Joints and Joint Replacement, Tribology International.

Dowson, D. and B. Jobbins (1988). Design and development of a versatile hip joint simulator and a preliminary assessment of wear and creep in Charnley total replacement hip joints. Engineering in medicine 17(3): 111-7

Digas, G., Karrholm, J., Thanner, J., Malchau, H., Herberts, P. (2003) Highly cross-linked polyethylene in cemented THA: randomized study of 61 hips. Clin , 417: 126-138.

Drown, I. W., Ring, P. A. (1985) Osteolytic changes in the upper femoral shaft following porous coated hip replacement. J Bone Joint Surg Br, 67: 218.

D'Lima, D. D., Hermida, J. C., Chen, P. C., Colwell, C. W. (2003) Polyethylene cross-linking by two different methods reduces acetabular liner wear in a hip joint wear simulator. J Orthop Res, 21:761-766.

Dumbleton, J. H., Manley, M. T., Edidin, A. A. (2002) A literature review of the association between wear rate and osteolysis in total hip arthroplasty. J Arthroplasty, 17: 649-661.

Elbert, K. E., Wright, T., Rimnac, C. M., Ingraffea, A., Klein, R. W. (1992) Mixed mode fatigue crack propagation in ultra high molecular weight polyethylene: experimental tests and numerical analyses. Trans of the 38th Annual Meeting, Orthop Res Soc.

Ellison, P., Barton, D. C., Esler, C., Shaw, D. L., Stone, M. H., Fisher, J. (2008) *In vitro* simulation and quantification of wear within the patellofemoral joint replacement. Journal of Biomechanics, 41: 1407-1416.

Engh, G. A. (1988) Failure of the polyethylene bearing surface of a total knee replacement within four years. A case report. Journal of Bone and Joint Surgery, 7: 1093-1096.

Engh, G. A., Dwyer, K. A., Hanes, C. K. (1992) Polyethylene wear of metal backed tibial components in total and unicompartmental knee prostheses. J Bone Joint Surg (Br), 1: 9-17.

Ericson, M.O., Nisell, R. (1986) Tibiofemoral joint forces during ergometer cycling. Am J Sports Med, 14:285-90.

Ericson, M.O., Nisell, R. (1987) Patellofemoral joint forces during ergometric cycling. Phys. Ther.; 67:1365-1369.

Endo, M., Tipper, J.L., Barton, D. C., Stone, M. H., Ingham, E., Fisher, J., (2002) Comparison of wear, wear debris and functional biological activity of moderately crosslinked and non-crosslinked polyethylenes in hip prostheses. Proc Inst Mech Eng, 2: 111-122.

Fisher, J. (1994) Wear of ultra high molecular weight polyethylene in total artificial joints. Curr Orthopaed, 8: 164-169.

Fisher, J. (2001) Biomedical applications. In Modern tribology handbook, Volume II, CRC Press, NewYork.

Fisher, J., McEwen, H. M., Tipper, J. L., Galvin, A. L., Ingram, J., Kamali, A., Stone, M. H., Ingham, E., (2004) Wear, debris, and biologic activity of cross-linked polyethylene in the knee: benefits and potential concerns. Clinical Orthopaedics and Related Research, 428: 114-119.

Fregly, B. J., Sawyer, W. G., Harman, M. K. and Banks, S. A. (2005) Computational wear prediction of a total knee replacement from in vivo kinematics. Journal of Biomechanics, 38(2): 305-314.

Forsythe, G. E. (1957) Generation and use of orthogonal polynomials for data-fitting with a digital computer. Journal of the Society for Industrial and Applied Mathematics, 5(2): 74-78.

Fukuoka, Y., Hoshino, A., Ishida, A. (1999) A Simple Radiographic Measurement Method for Polyethylene Wear in Total Knee Arthroplasty. TRANSACTIONS ON REHABILITATION ENGINEERING, 7: 228-233.

Galvin, A. L., Lu K., Itoro U., Louise M. J., Hannah M. J., McEwen, Zhongmin, J., Fisher, J. (2009) Effect of conformity and contact stress on wear in fixed-bearing total knee prostheses. Journal of Biomechanics, 42: 1898-1902.

Gill, H. S., Waite, J. C., Short, A., Kellert, C. F., Price, A. J., Murray, D. W. (2006) *In vivo* measurement of volumetric wear of a total knee replacement, The Knee, 13: 312-317.

Goldring, S. R., Schiller, A. L., Roelke, M., Rourke, C. M., Neil, D. A., Harris, W. H. (1983) The synovial like membrane at the bone cement interface in loose total hip replacements and its proposed role in bone lysis. J Bone Joint Surg Am., 65: 575-584.

Grobbelaar, C. J., du Plessis, T. A., Marais, F. (1978) The radiation improvement of polyethylene prostheses. A preliminary study. J Bone Joint Surg Br, 3: 370-374.

Hailey, J. L., Fisher, J., Dowson, D., Sampath, J. R., Elloy, M. (1994) A tribological study of a series of retrieved Accord knee explants. Med Eng Phys 16th edition, 16: 223-228.

Harris, W. H. (1995) The problem is osteolysis. Clin Orthop, 311: 46.

Haramati, N., Staron, R. B., Mazel-Sperling, K., Freeman, K., Nickoloff, E. L., Barax, C. (1994) CT scans through metal scanning technique versus hardware composition. Comput Med Imaging Graph, 18: 429-434.

Hirakawa, K., Bauer, T. W., Yamaguchi, M., Stulberg, B.N., Wilde, A. H. (1999) Relationship Between.Wear Debris Particles and Polyethylene Surface Damage in Primary Total Knee Arthroplasty. The Journal of Arthroplasty, 14:165-171.

Hoshino, A., Fukuoka, Y., Ishida, A. (2002) Accurate *in vivo* measurement of polyethylene wear in total knee arthroplasty. The journal of arthroplasty, 17: 490-496.

Howling, G. I., Barnett, P. I., Tipper, J. L., Stone, M. H., Fisher, J., Ingham, E. (2001) Quantitative characterization of polyethylene debris isolated from periprosthetic tissue in early failure knee implants and early and late failure Charnley hip implants. J BiomedMater Res, 58: 415-420.

Ingram, J., Matthews, J. B., Tipper, J. L., Stone, M. H., Fisher, J. and Ingham, E. (2002) Comparison of the biological activity of grade GUR 1120 and GUR 415 HP UHMWPE wear debris. BioMedical Materials and Engineering 12, 177-188.

Ingram, J., Fisher, J. and Ingham, E. (2003) Biological activity of wear debris from crosslinked polyethylene. Transactions of the Orthopaedic Research Society.

ISO 14243-1 (2009). Implants for surgery—wear of total knee joint prostheses. Part 1: Loading and displacement parameters for wear testing machines with load control and corresponding environmental conditions for test.

Jin, Z. M., Dowson, D., Fisher, J. (1995) Contact pressure prediction in total knee joint replacements. Part 1: general elasticity solution for elliptical layered contacts. Proc Inst Mech Engrs Part H, 209: 1-8.

Jin, Z. M., Stewart, T., Auger, D. D., Dowson, D., Fisher, J. (1995) Contact pressure prediction in total knee joint replacements. Part 2: Application to the design of total knee joint replacements. Proc Inst Mech Engrs Part H, 209: 9-15.

Jones, S. M. G., Pinder, I. M., Moran, C. G., Malcolm, A. J., (1992) Polyethylene wear in uncemented knee replacements. Journal of Bone and Joint Surgery—British, 74: 18-22.

Johnston, J. D., Masri, B. A., Wilson, D. R. (2009) Computed tomography topographic mapping of subchondral density (CT-TOMASD) in osteoarthritic and normal knees: methodological development and preliminary findings. Osteoarthritis and Cartilage, 17: 1319-1326.

Kalender, W. A., Hebel, R., Ebersberger, J. (1987) Reduction of CT artifacts caused by metallic mplants. Radiology, 164: 576–577.

Kaptein, B. L., Valstar, E. R., Stoel, B, C., Rozing, P. M., Reiber, J. H. C. (2003) A new model-based RSA method validated using CAD models and models from reversed engineering. Journal of Biomechanics, 36: 873-882.

Kellett, C. F., Short, A., Price, A., Gill, H. S., Murray, D. W. (2004) *In vivo* measurement of total knee replacement wear. The Knee, 11: 183-187.

Keng, E. Y. H. (1970). Air and Helium Pycnometer. Powder Technology, 3(3): 179-185.

Kinzel, V., Scaddan, M., Bradley, B., Shakespeare, D. (2004) Varus/valgus alignment of the femur in total knee arthroplasty. Can accuracy be improved by pre-operative CT scanning? The Knee, 11: 197-201.

Knutson, K., Jonsson, G., Langer Andersen, J., Larusdottir, H., Lidgren, L. (1981) Deformation and loosening of the tibial component in knee arthroplasty with unicompartmental endoprostheses. Acta Orthop Scand, 6: 667-73.

Kobayashi, A., Freeman, M. A., Bonfield, W. (1997) Number of polyethylene particles and osteolysis in total joint replacements. A quantitative study using a tissue-digestion method. J Bone Joint Surg Br, 79: 844.

Kop, A. M., Swarts, E. (2007) Quantification of polyethylene degradation in mobile bearing knees: A retrieval analysis of the Anterior-Posterior-Glide (APG) and Rotating Platform (RP) Low Contact Stress (LCS) knee. Acta Orthopaedica, 78: 364-370.

Kuster, M. S., Wood, G. A., Stachowiak, G. W., Gachter, A. (1997) Joint load considerations in total knee replacement. J. Bone Joint Surg. Br, 79 (1): 599-604.

Kurtz, S. M., Muratoglu, O. K., Evans, M., Edidin, A. A. (1999) Advances in the processing, sterilization, and crosslinking of ultra-high molecular weight polyethylene for total joint arthroplasty. Biomaterials, 18: 1659-1688.

Kurtz, S. M., Parvizi, J., Purtill, J., Sharkey, P., MacDonald, D., Brenner, E. (2008) *In vivo* oxidation is a primary contributor to delamination in TKA. 75th Annual Meeting of the American Academy of Orthoopaedic Surgeons, San Francisco.

Kurtz, S. M. (2004) The UHMWPE Handbook: Ultra-High Molecular Weight Polyethylene in Total Joint Replacement. Academic Press.

Kurtz, S. M. (2009) UHMWPE Biomaterials Handbook: Ultra High Molecular Weight Polyethylene in Total Joint Replacement and Medical Devices. Academic Press.

Lafortune, M. A., P. R. Cavanagh, H. J. Sommer, A. Kalenak (1992). 3-Dimensional kinematics of the human knee during walking. Journal of Biomechanics, 25(4): 347-357.

Landy, M. M., Walker, P. S. (1988) Wear of ultra high molecular weight polyethylene components of 90 retrieved knee prostheses. J Arthroplasty (Suppl), 3: 73-85.

Lavallee, S., Szeliski, R. (1995) Recovering the position and orientation of reeform objects from image contours using 3D distance maps. IEEE Trans. Pattern Anal. Machine Intell., 17:378-390.

Lavernia, C. J., Sierra, R. J., Hungerford, D. S., Krackow, K. (2001) Activity level and wear in total knee arthroplasty. J Arthroplasty, 16: 446-453.

Lee, M., Kim, S., Lee, S., Song, H., Huh, Y., Kim, D. (2007) Overcoming artifacts from metallic orthopedic implants at high-field-strength MR imaging and multi-detector CT. Radiographics, 27: 791-803.

Lee, K., Goodman, S. B. (2008) Current state and future of joint replacements in the hip and knee. Expert Rev Med Devices, 3: 383-393.

Lewis, M., Toms, A. P., Reid, K., Bugg, W. (2010) CT metal artefact reduction of total knee prostheses using angled gantry multiplanar reformation. The Knee, 17: 279-282.

Li, K., O'Farrell, M., Martin, D., Kopf, S., Harner, C., Zhang, X. (2009) Mapping ligament insertion sites onto bone surfaces in knee by co-registration of CT and digitization data. Journal of Biomechanics, 42: 2624-2626.

Liao, Y. S., H. McKellop, Z. Lu, P. Campbell, P. Benya (2003). The effect of frictional heating and forced cooling on the serum lubricant and wear of UHMW polyethylene cups against cobalt-chromium and zirconia balls. Biomaterials, 24(18): 3047-59.

Lin, L. I. (1989). A concordance correlation coefficient to evaluate reproducibility. Biometrics, 45(1): 255-268.

Lin, L. I. (2008). Overview of agreement statistics for medical devices. Journal of Biopharmaceutical Statistics, 18(1): 126-144.

Link, T. M., Berning, W., Scherf, S., Joosten, U., Joist, A., Engelke, K. (2000) CT of metal mplants: reduction of artifacts using an extended CT scale technique. J Comput Assist Tomogr, 24: 165-72.

Little, E. G. (1985) Compressive creep behavior of irradiated ultra high molecular weight polyethylene at 37°C, Eng. Med.,14, 85–87.

Liow, R. Y., Murray, D. W. (1997) Which primary total knee replacement? A review of currently available TKR in the United Kingdom. Ann Roy Coll Surg Engl, 79: 335-340.

Manning, D. W., Chiang, P. P., Martell, J. M., Galante, J. O., Harris, W. H. (2005) *In vivo* comparative wear study of traditional and highly cross-linked polyethylene in total hip arthroplasty. J Arthroplasty, 20: 880-886.

Maquet, P. G., Van de Berg, A. J., Simonet, J. C. (1975) Femorotibial weight-bearing areas. Experimental determination. J Bone Joint Surg Am, 57:766-771.

Marshall, A., Ries, M. D., Paprosky, W. (2008) How prevalent are implant wear and osteolysis, and how has the scope of osteolysis changed since 2000? J Am Acad Orthop Surg, 16: 1-6.

Martell, J. M., Berdia, S. (1997) Determination of polyethylene wear in total hip replacements with use of digital radiographs. J Bone Joint Surg, 79: 1635-1641.

Matthews, L. S., Sonstegard, D. A., Henke, J. A. (1977) Load bearing characteristics of the patello-femoral joint. Acta Orthop Scand, 48:511-516.

McEwen, H. M. J., Fisher, J., Goldsmith, A. A. J., Auger, D. D., Hardaker, C., Stone, M. H., (2001) Wear of fixed bearing and rotating platform mobile-bearing knees subjected

to high levels of internal and external tibial rotation. Journal of Materials Science—Materials in Medicine, 12: 1049-1052.

McEwen, H. M. J., Barnett, P. I., Bell, C. J., Farrar, R., Auger, D. D., Stone, M. H., Fisher, J., (2005) The influence of design, materials and kinematics on the *in vitro* wear of total knee replacements. Journal of Biomechanics, 38: 357-365.

Mcgloughlin, T. M. & Kavanagh, A. G. (2000). Wear of ultra-high molecular weight polyethylene (UHMWPE) in total knee prostheses: a review of key influences. Proc Inst Mech Eng. Engineering in Medicine, 214: 349-359.

McKellop, H., Shen, F. W., Lu, B., Campbell, P., Salovey, R. (1999) Development of an extremely wear-resistant ultra high molecular weight polyethylene for total hip replacements. J Orthop Res, 2: 157-167.

McPherson, A., Karrholm, J., Pinskerova, V., Sosna, A., Martelli, S. (2005) Imaging knee position using MRI,RSA/CT and 3D digitisation. Journal of Biomechanics, 38: 263-268.

Medel FJ, Kurtz SM, Parvizi J, Klein GR, Kraay MJ, Rimnac CM. In vivo oxidation contributes to delamination but not pitting in polyethylene components for total knee arthroplasty. J Arthroplast; 2011; 26:5 802-810.

Minns, R. J., Bibb, R., Banks, R., Sutton, R. A. (2003) The use of a reconstructed three-dimensional solid model from CT to aid the surgical management of a total knee arthroplasty: a case study. Medical Engineering & Physics, 25: 523-526.

Milliano, M. T., Whiteside, L. A. (1991) Articular surface material effect on metal backed patellar components. A microscopic evaluation. Clin Orthop, 273: 204-214.

Mintz, L., Tsao, A. K., McCrae, C. R., Stulberg, S. D., Wright, T. (1991) The arthroscopic evaluation and characteristics of severe polyethylene wear in total knee arthroplasty. Clin Orthop, 273: 215-222.

Minoda, Y., Kobayashi, A., Iwaki, H., Miyaguchi, M., Kadoya, Y., Ohashi, H., Takaoka, K. (2005) Polyethylene wear particle generation *in vivo* in an alumina medial pivot total knee prosthesis. Biomaterials, 26: 6034-6040.

Muratoglu, O. K., Perinchief, R. S., Bragdon, C. R., O'Connor, D. O., Konrad, R., Harris, W. H. (2003) Metrology to quantifywear and creep of polyethylene tibial knee inserts, Clin. Orthop. Rel. Res, 410: 155-164.

Nagels, J., Valstar, E. R., Stokdijk, M., Rozing, P. M. (2002) Patterns of glenoid componentloosening. Journal of Bone and JointSurgery, 84: 83-87.

National joint registry for England and Wales, (2004) First Annual Report.

Nelissen, R. G., Valstar, E. R., Rozing, P. M., (1998) The effect of hydroxyapatite on the micromotion of total knee prostheses. A prospective, randomized, double-blind study. Journal of Bone and JointSurgery, 80: 1665-1672.

Nisell, R. (1985) Mechanics of the knee: a study of joint and muscle load with clinical applications. Acta Orthop Scand, 56: [Supp] 216.

Oonishi, H., Kadoya, Y. (2000) Wear of high-dose gamma-irradiated polyethylene in total hip replacements. J Orthop Sci , 3: 223-228.

Oonishi, H., Ueno, M., Chol Kim, S., Oonishi, H., Iwamoto, M., Kyomoto, M. (2009) Ceramic Versus Cobalt-Chrome Femoral Components; Wear of Polyethylene Insert in Total Knee Prosthesis. The Journal of Arthroplasty, 24: 374-382.

Oral, E., Wannomae, K. K., Hawkins, N., Harris, W. H., Muratoglu, O. K. (2004) Alpha-tocopherol-doped irradiated UHMWPE for high fatigue resistance and low wear. Biomaterials, 24: 5515-5522.

Oral, E., Greenbaum, E. S., Malhi, A. S., Harris, W. H., Muratoglu, O. K. (2005) Characterization of irradiated blends of alpha-tocopherol and UHMWPE. Biomaterials, 33: 6657-6663.

Oral, E., Christensen, S. D., Malhi, A. S., Wannomae, K. K., Muratoglu, O. K. (2006) Wear resistance and mechanical properties of highly cross-linked, ultrahigh-molecular weight polyethylene doped with vitamin E. J Arthroplasty, 4: 580-591.

Oral, E., Godleski Beckos, C. A., Lozynsky, A. J., Malhi, A. S., Muratoglu, O. K. (2009) Improved resistance to wear and fatigue fracture in high pressure crystallized vitamin E-containing ultra-high molecular weight polyethylene. Biomaterials, 10: 1870-1880.

Orhun, K., Muratoglu, Arthur, M., David, A., Vittetoe, William, H., Harris and Harry, E., Rubash. (2003) Polyethylene Damage in Total Knees and Use of Highly Crosslinked Polyethylene. THE JOURNAL OF BONE AND JOINT SURGERY, 85: 7-13

Overhoff, H. M., Lazovic, D., Liebing, M., Macher, Ch. (2001) Total knee arthroplasty: coordinate system definition and planning based on 3-D ultrasound image volumes. International Congress Series, 1230: 292-299.

O'Rourke, M. R., Callaghan, J. J., Goetz, D. D., Sullivan, P. M., Johnston, R. C. (2002) Osteolysis associated with a cemented modular posteriorcruciate-substituting total knee design: five to eight years follow up. J Bone Joint Surg Am,;84: 1362–1422.

Liza, S., Haseeb, A. S. M. A., Abbas, A. A., Masjuki, H .H. (2011) Failure analysis of retrieved UHMWPE tibial insert in total knee replacement. Engineering Failure Analysis, 18 (6): 1415-1423.

Packer, L. (1991) Protective role of vitamin E in biological systems. Am J Clin Nutr, 53:1050-1055.

Parth, M., Aust, N, Lederer, K. (2002) Studies on the effect of electron beam radiation on the molecular structure of ultra-high molecular weight polyethylene under the influence of alpha-tocopherol with respect to its application in medical implants. J Mater Sci, 10: 917-921.

Picaud, F., Smogunov, A., Corso, A. D., and Tosatti, E. (2003). Complex band structures and decay length in polyethylene chains. Journal of Physics Condensed Matter. 15(22): 3731–3740.

Plante-Bordeneuve, P., Freeman, M. A. (1993) Tibial high density polyethylene wear in conforming tibiofemoral prosthesis. J Bone Joint Surg (Br), 75: 630-636.

Pollock, D., Sychterz, C. J., Engh, C. A. (2001) A clinically practical method of manually assessing polyethylene liner thickness. J Bone Joint Surg, 83:1803-1809.

Polyzoides, A. J., Tsakonas, A., Brooks, S., Pickford, M. (1999) Design characteristics experimental studies and ten years of clinical experience with a fully conforming mobile bearing knee prostheses. Proc of the Intl Symp on the Knee, Inst Mech Eng London.

Price, A. J., Short, A., Kellert, C., Beard, D., Gill, H., Pandit, H., Dodd, C. A., Murray, D. W. (2005) Ten-year *in vivo* wear measurement of a fully congruent mobile bearing unicompartmental knee arthroplasty. J Bone Joint Surg (Br), 87: 1493-1497.

Purdue, P. E., Koulouvaris, P., Potter, H. G., Nestor, B. J., Sculco, T. P. (2007) The cellular and molecular biology of periprosthetic osteolysis. Clin Orthop Relat Res, 454: 251-261.

Rand, J. (1994) Supracondylar fracture of the femur associated with polyethylene wear after total knee arthroplasty. J Bone Joint Surg Am, 76:1389.

Reeves, E. A., Barton, D. C., FitzPatrick, Fisher, J. (2000) Comparison of gas plasma and gamma irradiation in air sterilization on the delamination wear of the ultra-high molecular weight polyethylene used in knee replacements. Proc Inst Mech Engrs Part H, 214: 249-255.

Rohrl, S. M., Li, M. G., Nilsson, K. G., Nivbrant, B. (2007) Very low wear of non-remelted highly cross-linked polyethylene cups: an RSA study lasting up to 6 years. Acta Orthop, 786: 739-745.

Rose, R. M., Radin, E. L. (1982) Wear of polyethylene in the total hip prosthesis. Clin Orthop Relat Res, 170: 107-115.

Rose, R. M., Crugnola, A., Ries, M., Cimino, W. R., Paul, I., Radin, E. L. (1979) On the origins of high *in vivo* wear rates in polyethylene components of total joint prostheses. Clin Orthop, 145: 277-286.

Rose, R. M., Nusbaum, H. J., Schneider, H., Ries, M., Paul, I., Crugnola, A., Simon, S. R. and Radin, E. L. (1980) On the true wear rate of ultra high-molecular-weight polyethylene in the total hip prosthesis, J. Bone Joint Surg. Am, 62: 537–549.

Rouvillain, J. L., Pascal Mousselard, H., Favuto, M., Kanor, M., Garron, E., Catonne, Y. (2008) The level of the joint line after cruciate-retaining total knee replacement: A new coordinate system. The Knee, 15: 31-35.

Ryd, L. (1986) Micromotion in knee arthroplasty: A roentgen stereophotogrammetric analysis of tibial component fixation. Acta Orthopaedica Scandinavica, 57: 1-80.

Santavirta S, Konttinen YT, Lappalainen R, Anttila A, Goodman SB, Lind M, *et al*. Materials in total joint replacement. Curr Orthop 1998;12:51–7.

Sanz´en, L., Sahlstrom, A., Gentz, C-F., Johnell, I. R. (1996) Radiographic wear assessment in a total knee prosthesis. J. Arthroplasty, 11: 738-742.

Selvik, G. (1978) A stereophotogrammetric system for the study of human movements. Scand J Rehabil Med, 6: 16-20.

Selvik, G. (1989) Roentgen stereophotogrammetry: a method for the study of kinematics of the skeletal system. Acta orthopaedic Scandinavica, 60: 1–51.

Schmalzried, T. P., Dorey, F. J., McKellop, H. (1998) The multifactorial nature of polyethylene wear *in vivo*. J Bone Joint Surg Am, 8: 1234-1242.

Schmotzer, H., Song, J. (1991) Parametric analysis of the polyethylene stresses in tibial components using a finite element model. Combined Meeting of the Orthopaedic Research Societies of USA, Japan and Canada, Banff, Alberta.

Smith, F. J. (1965) An algorithm for summing orthogonal polynomial series and their derivatives with application to curve-fitting and interpolation. Mathematics of Computation, 19(89): 33-36.

Sontag, T. J. and Parker, R. S. (2007) Influence of major structural features of tocopherols and tocotrienols on their ω-oxidation by tocopherol-ω-hydroxylase. The Journal of Lipid Research, 48: 1090-1098.

Spinelli, M., Carmignato, S., Affatato, S., Viceconti, M. (2009) CMM–based procedure for polyethylene non-congruous unicompartmental knee prosthesis wear assessment. Wear, 267:753-756.

Sternstein, S. S., and Van Buskirk, C. S.(1988) Polymer creep, in Encyclopedia of Polymer Science and Engineering,H. F. Mark, N. M. Bikales, C. G. Overberger, and G. Menges (eds.), Wiley-Interscience, 12: 470–486.

Stoller, A. P., Todd, S., Johnson, Oludele, O., Popoola, Steven, M. H., and Cheryl, R. B. (2010) Highly Crosslinked Polyethylene in Posterior-Stabilized Total Knee Arthroplasty. The Journal of Arthroplast, article in press.

Sugano, N., Saito, M., Yamamoto, T., Nishii, T., Yau, S. S., Wang, A. (2004) Analysis of a retrieved UHMWPE acetabular cup crosslinked in air with 1000 kGy of gamma radiation. J Orthop Res, 22: 828-831.

Sychterz, C. J., Engh, C. A. Jr., Yang, A., Engh, C. A. (1999) Analysis of temporal wear patterns of porous-coated acetabular components: distinguishing between true wear and so-called bedding-in. J Bone Joint Surg Am; 6: 821-830.

Teeter, M. G., Naudie, D. D. R., Charron, K. D., Holdsworth, D. W. (2010) Three-Dimensional Surface Deviation Maps for Analysis of Retrieved Polyethylene

Acetabular Liners Using Micro-Computed Tomography. The journal of arthroplasty, 25: 330-331.

Thanner, J., Karrholm, J., Herberts, P., Malchau, H. (2000) Hydroxyapatite and tricalcium phosphate-coated cups with and without screw fixation: a randomized study of 64 hips. J Arthroplasty, 15:405-412.

Thieme. (2006) Atlas of Anatomy: General Anatomy and Musculoskeletal System.

Thomsen, M., Burandt, C., Gortz, A., Dathe, H., Meesenburg, D. K., Spiering, S. (1999) An optical method for determining deformation and form changes in polyethylene surfaces of explanted acetabular cups of hip endoprostheses. Biomed Tech, 44 : 247-254.

Turner, S. (2001) Creep of Polymeric Materials. Oxford: Elsevier Science Ltd. 1813–1817.

Valstar, E. R., Garling, E. H., Rozing, P. M. (2002) Micromotion of the Souter-Stratchclyde total elbow prosthesis in patients with rheuma-toid arthritis. Acta Orthopaedica Scandinavica, 73: 264-272.

Valstar, E. R., de Jong, F. W., Vrooman, H. A., Rozing, P. M., Reiber, J. H. C. (2001) Model-based Roentgen stereophotogrammetry of orthopaedic implants. Journal of Biomechanics, 34: 715-722.

Veselko, M., Jenko, M., Lipuscek, I. (1998) The use of the co-ordinate measuring machine for the study of three-dimensional biomechanics of the knee. Computers in Biology and Medicine, 28: 343-357.

Viana, M., P. Jouannin, C. Pontier, D. Chulia (2002). About pycnometric density measurements. Talanta, 57(3): PII S0039-9140(02)00058-9.

Walker, S. A., Hoff, W., Komistek, R., Dennis, D. (1996) *In vivo*' pose stimation of artificial knee implants using computer vision. Biomed. Sci. Instrum, 32: 143-150.

Wang, G., Frei, T., Vannier, M. W. (2000) Fast iterative algorithm for metal artifact reduction in X-ray CT. Acad Radiol, 7: 607-614.

Werner, P. (2004). Color Atlas of Human Anatomy, Vol. 1: Locomotor System (5th edition). 206–213.

Whaley, A. L., Trousdale, R. T., Rand, J. A., Hanssen, A. D. (2003) Cemented long-stem revision total knee arthroplasty. J Arthroplast,18:592–599.

Williams, I. R., Mayor, M. B., Collier, J. P. (1998) The impact of sterilization method on wear in knee arthroplasty. Clin Orthop, 356: 170-180.

Willing, R. and Kim, I. Y. (2009).Three dimensional shape optimization of total knee replacements for reduced wear Structural and Multidisciplinary Optimization 38(4): 405-414.

Wright, T. M., Bartel, D. L. (1984) Surface damage in polyethylene total knee components. American Society of Mechanical Engineers Winter Annual Meeting New Orleans, Louisiana 9-14.

Wright, T, M., Bartel, D.L. (1986) The problem of surface damage in polyethylene total knee components. Clin Orthop 205: 67–74.

Wright, T., Goodman, S. B. (2001). Implant wear in total joint replacements: clinical and biologic issues, materials and design considerations. Rosemont, IL: American Academy of Orthopaedic Surgeons.

Wroblewski, B. M , Siney, P. D., Fleming, P. A. (2005) Low-friction arthroplasty of the hip using alumina ceramic and cross-linked polyethylene. A 17-year follow-up report. J Bone Joint Surg Br, 9: 1220–1221.

Yamamoto, K., Imakiire, A., Masaoka, T., Shishido, T., Mizoue, T., Clarke, I. C. (2003) Wear mode and wear mechanism of retrieved acetabular cups. Int Orthop, 27: 286-290.

Zhao, D., Sakoda, H., Sawyer, W. G., Banks, S. A. and Fregly, B. J. (2008) Predicting knee replacement damage in a simulator machine using a computational model with a consistent wear factor. Journal of Biomechanical Engineering 130(1).

Appendix (List of Conference Publications)

Wei Jiang, Zhongmin Jin, Claire Brockett, Ruth Wilcox, John Fisher and Ling Wang

CMM-based methodology for wear and creep assessment of polyethylene tibial knee inserts

International Conference on BioTribology, September 2011, London, UK

Wei Jiang, Zhongmin Jin, Claire Brockett, Ruth Wilcox and John Fisher

Coordinate Measuring Machine - based methodology for wear and creep assessment of polyethylene tibial knee inserts

Orthopaedic Research Society, January 2013, San Francisco, USA

Appendix A

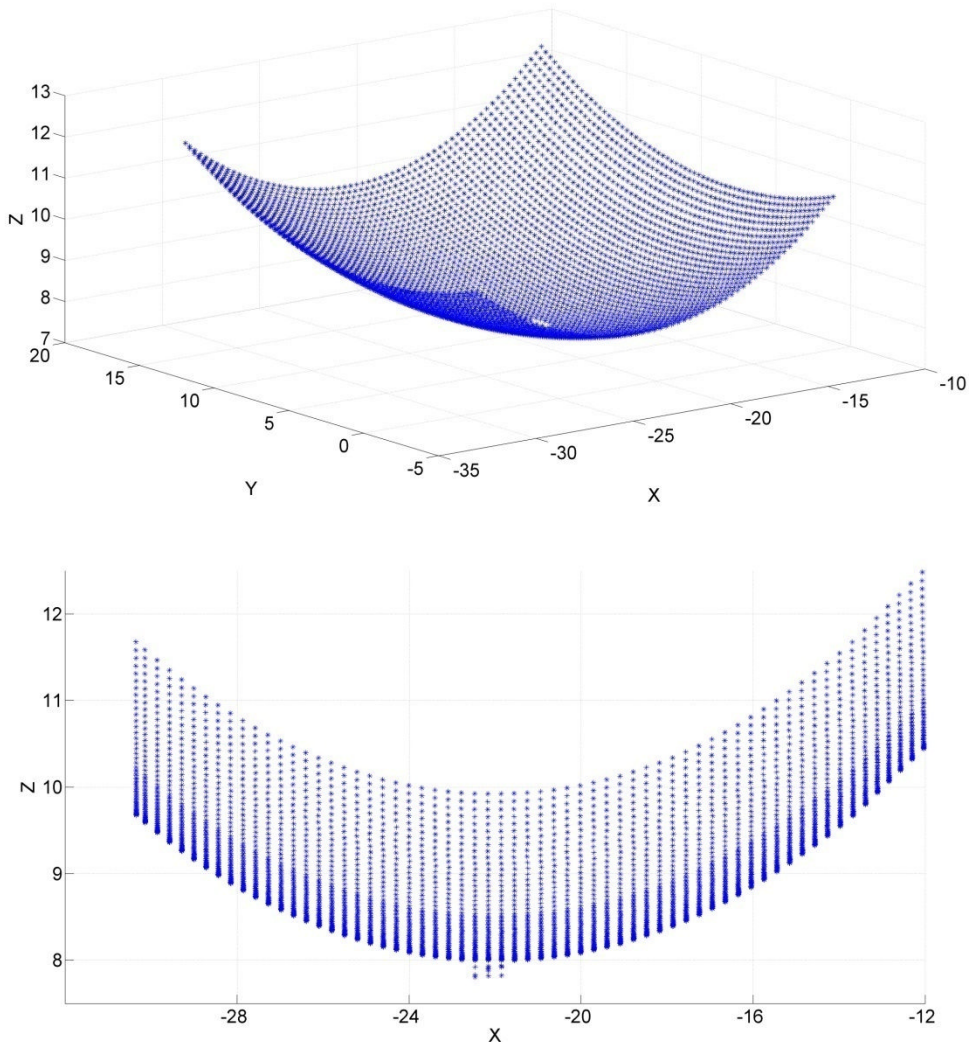

(a) wear area 0.29%

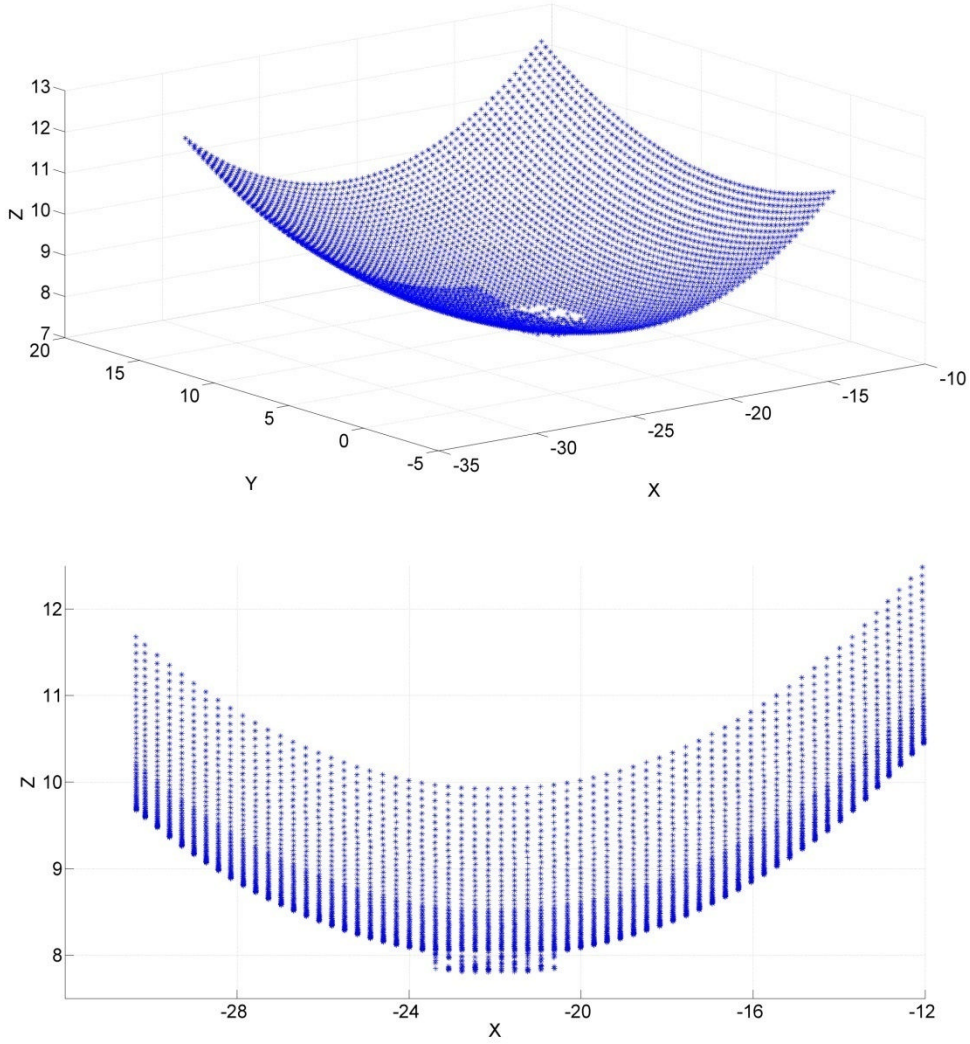

(b) wear area 2.93%

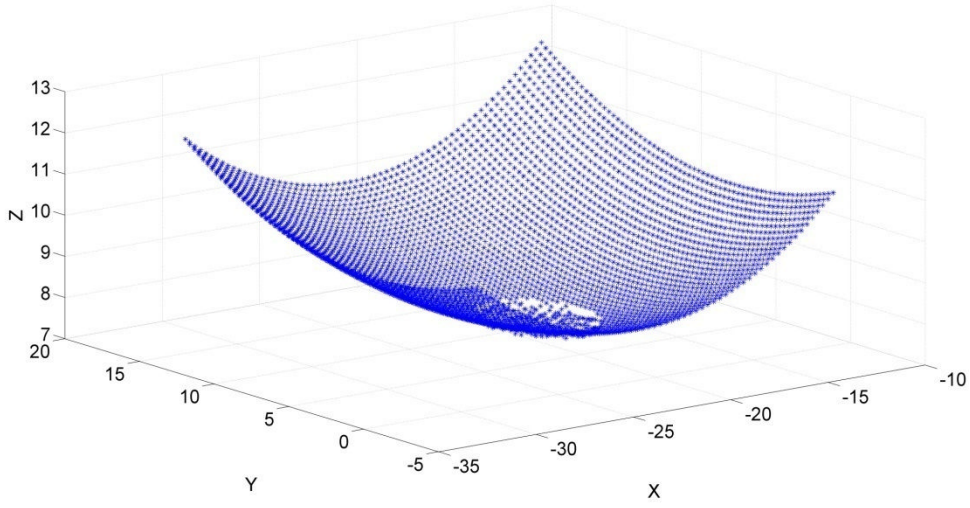

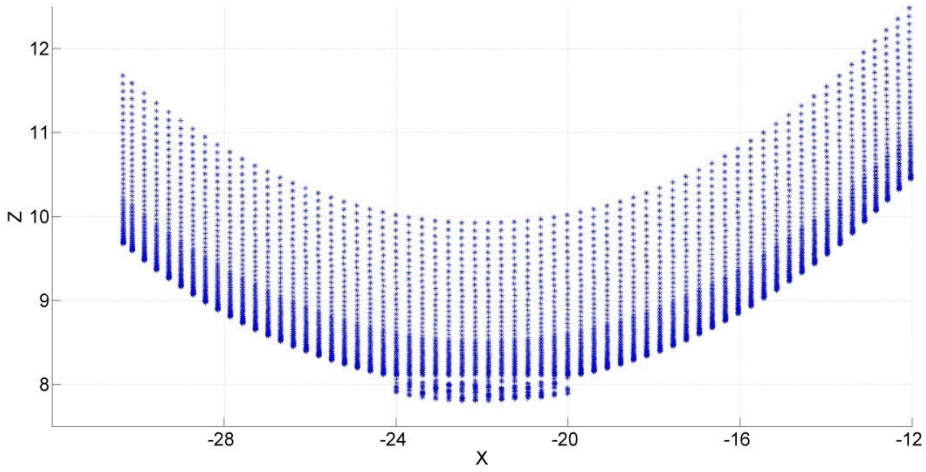

(c) wear area 5.51%

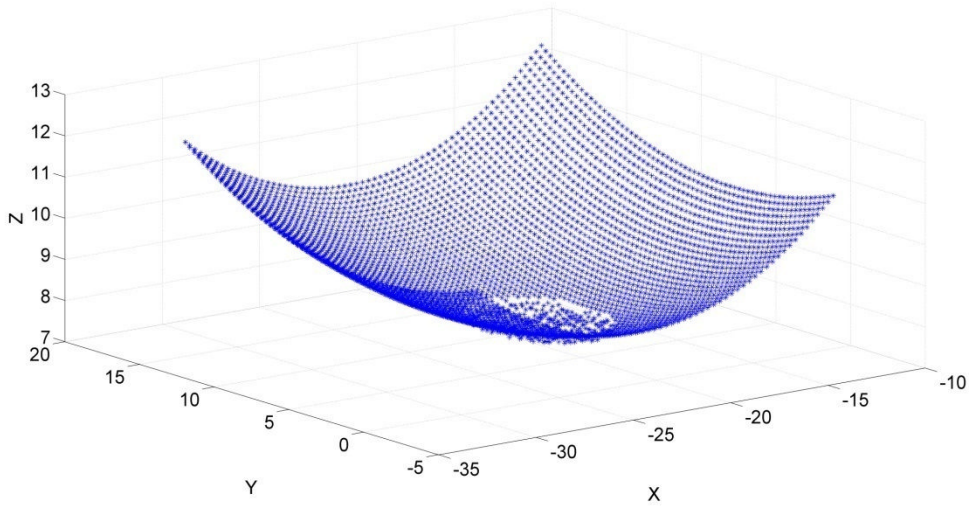

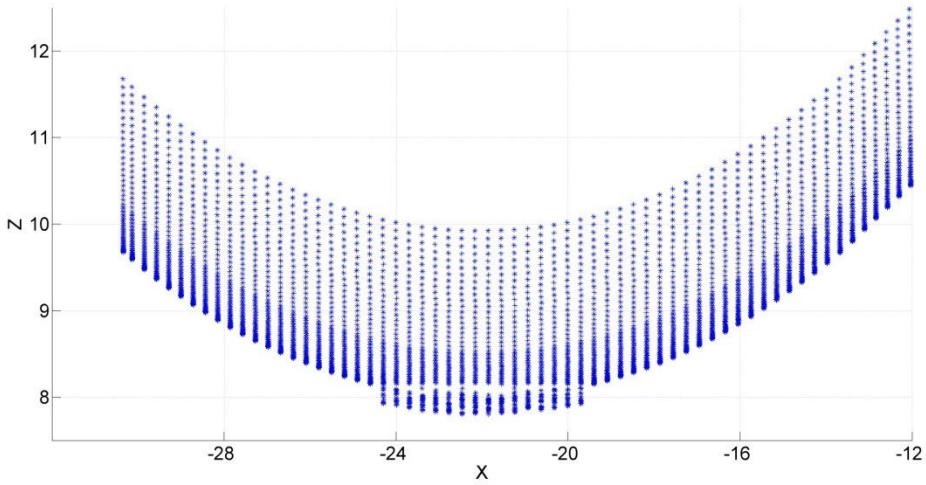

(d) wear area 7.84%

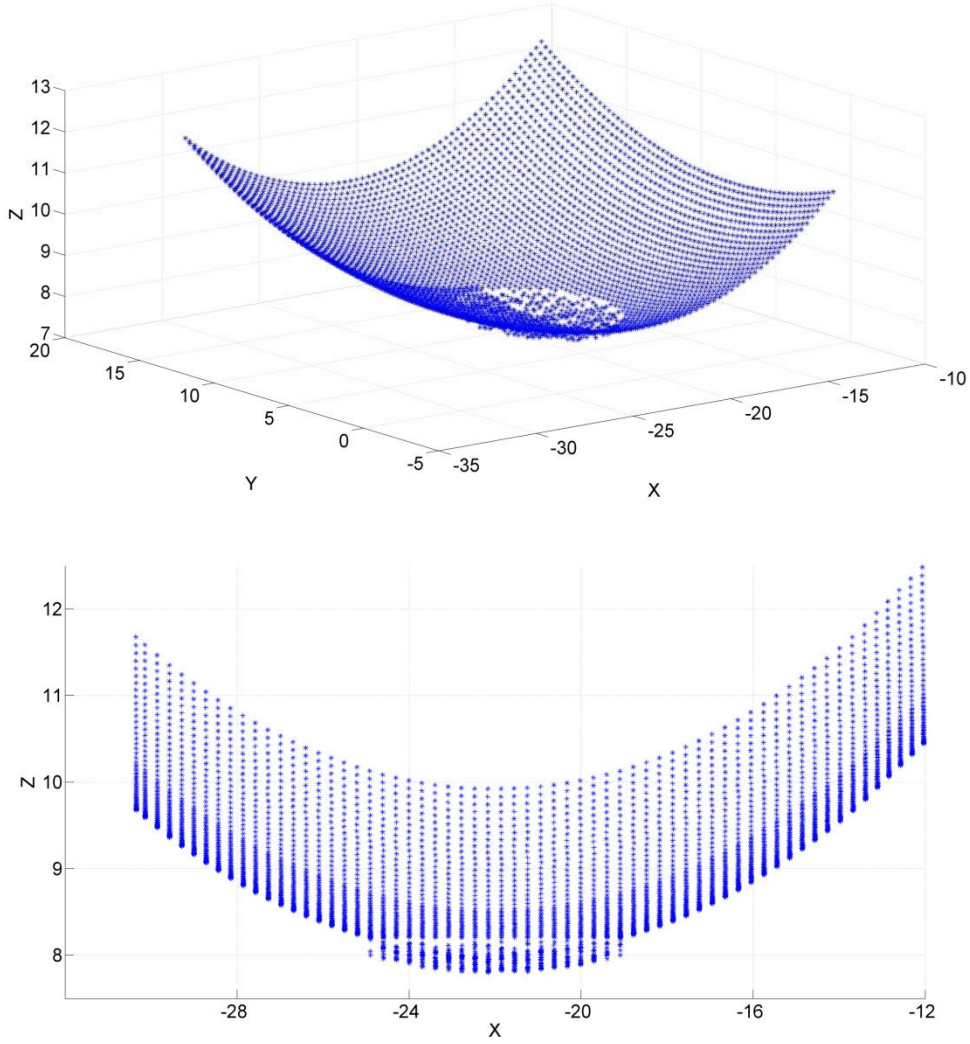

(e) wear area 10.37%

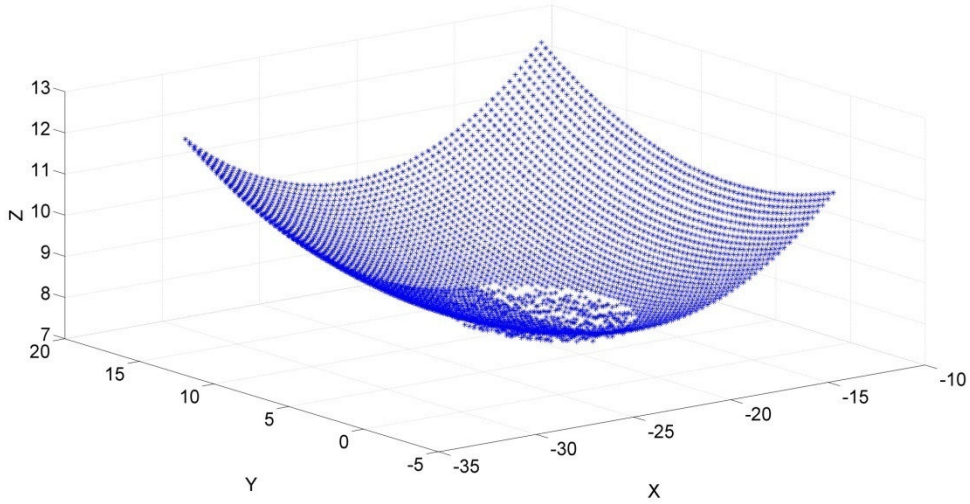

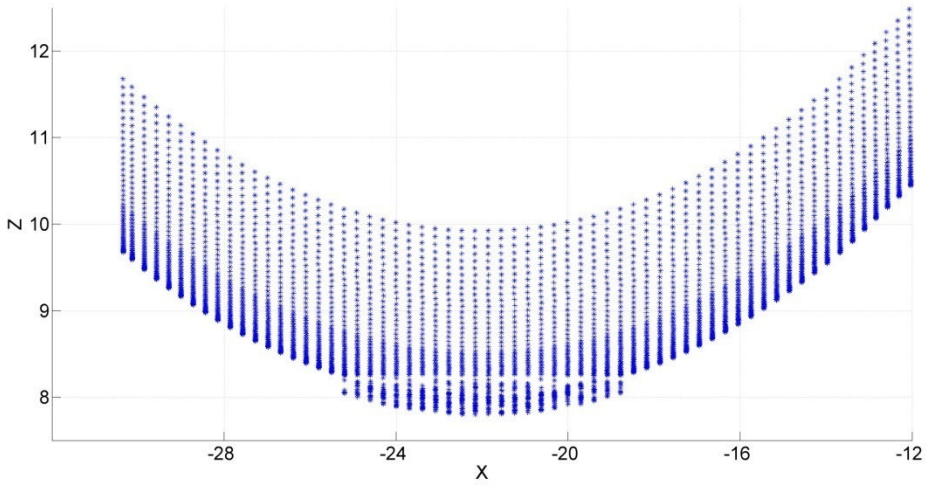

(f) wear area 12.89%

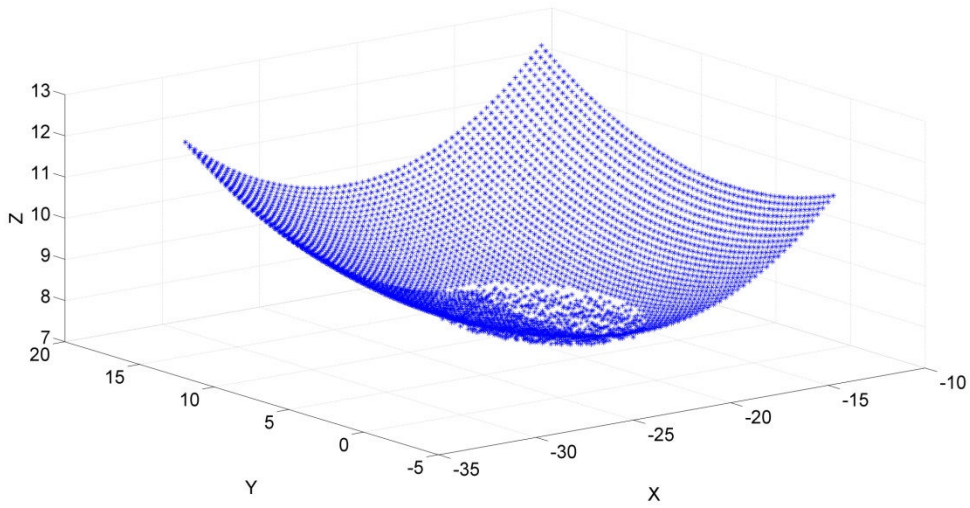

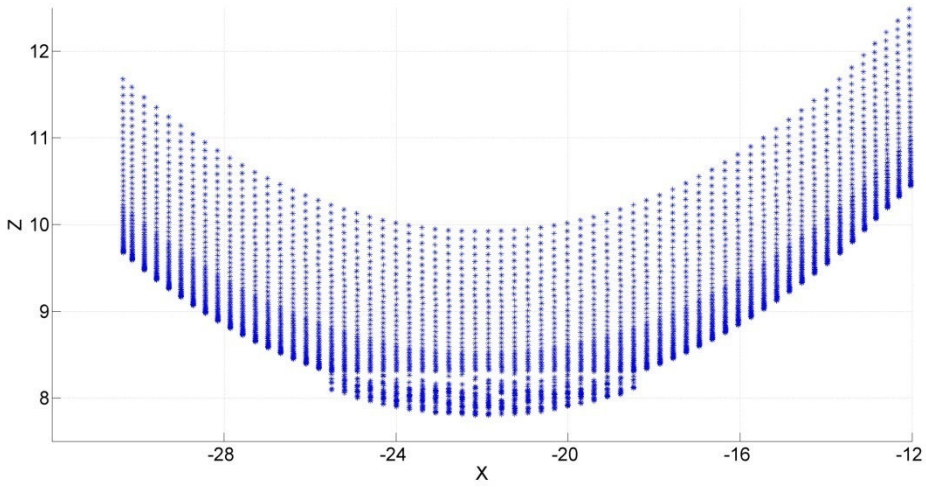

(g) wear area 15.56%

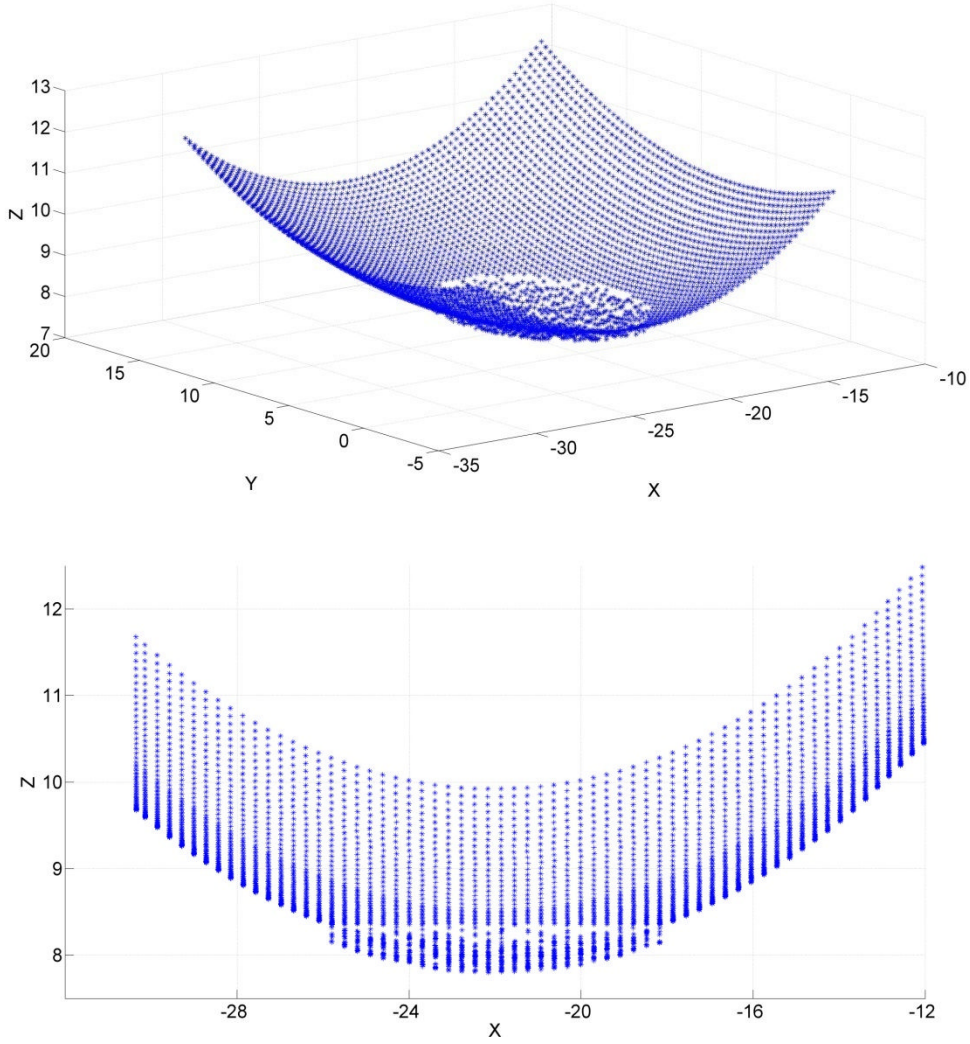

(h) wear area 17.94%

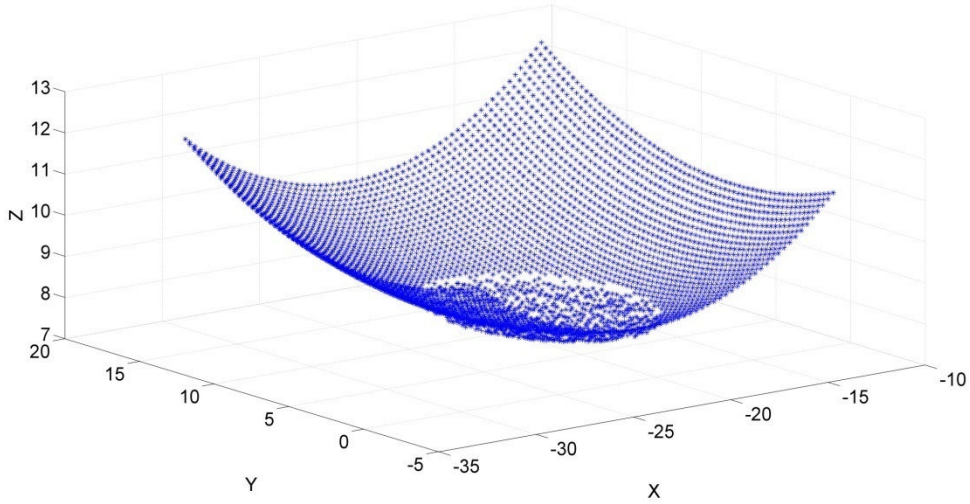

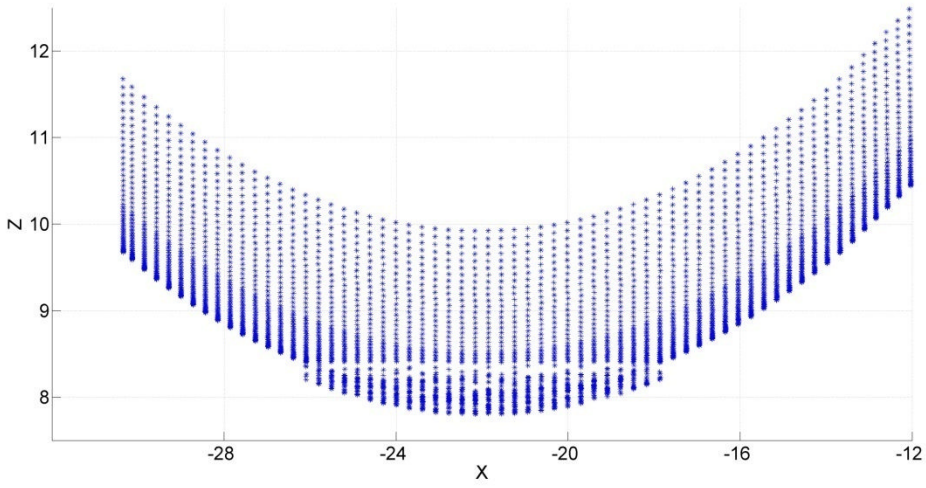

(i) wear area 20.44%

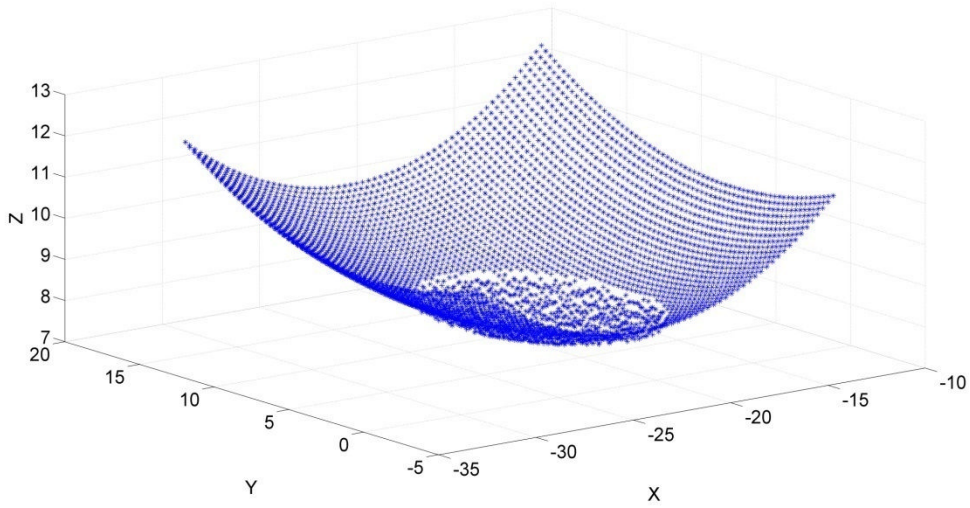

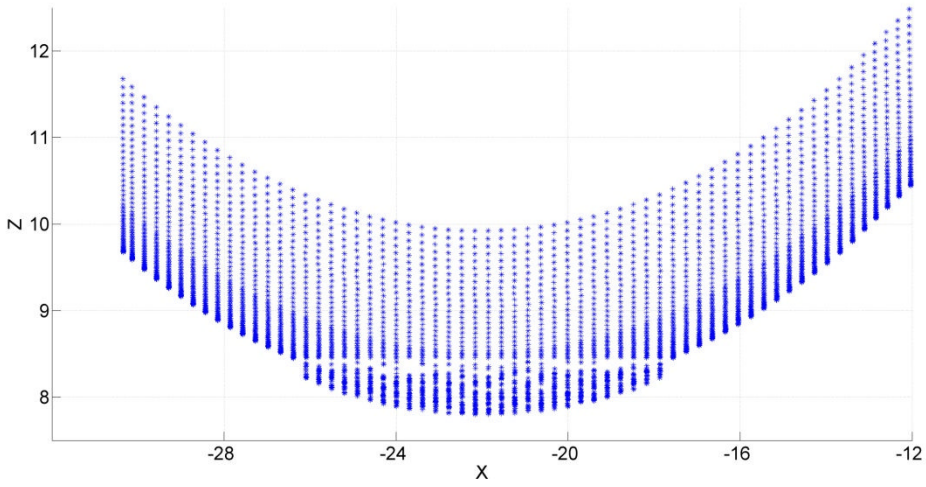

(j) wear area 22.78%

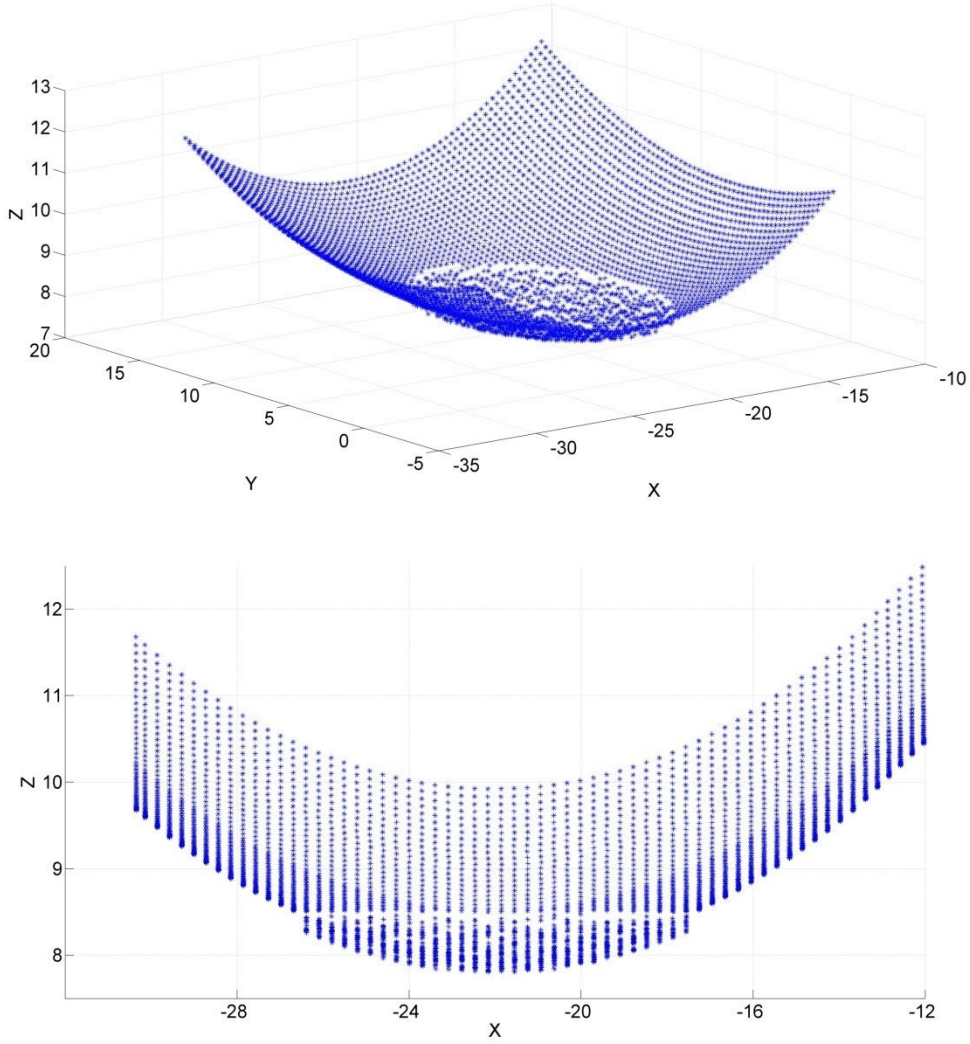

(j) wear area 25.49%

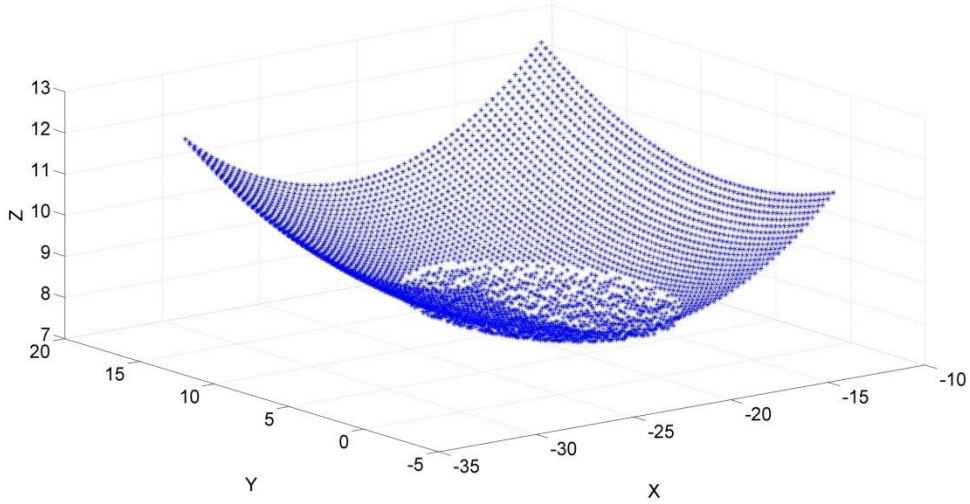

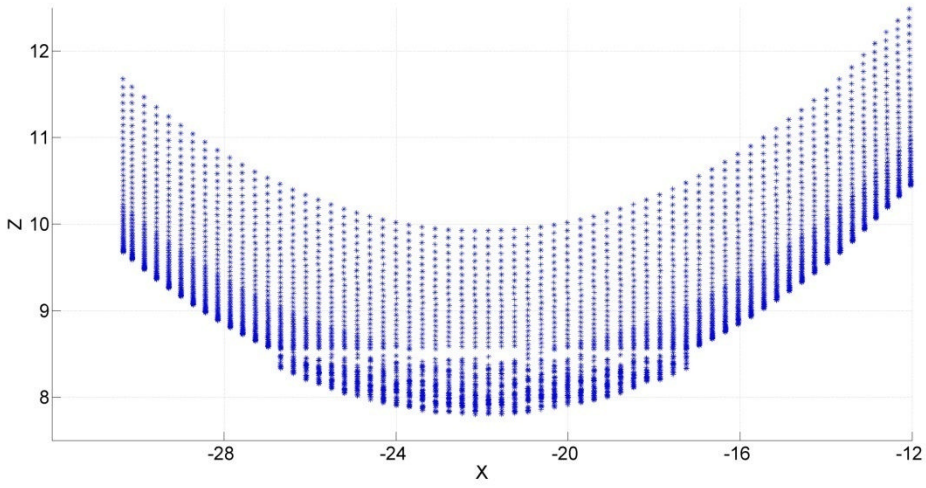

(l) wear area 27.99%

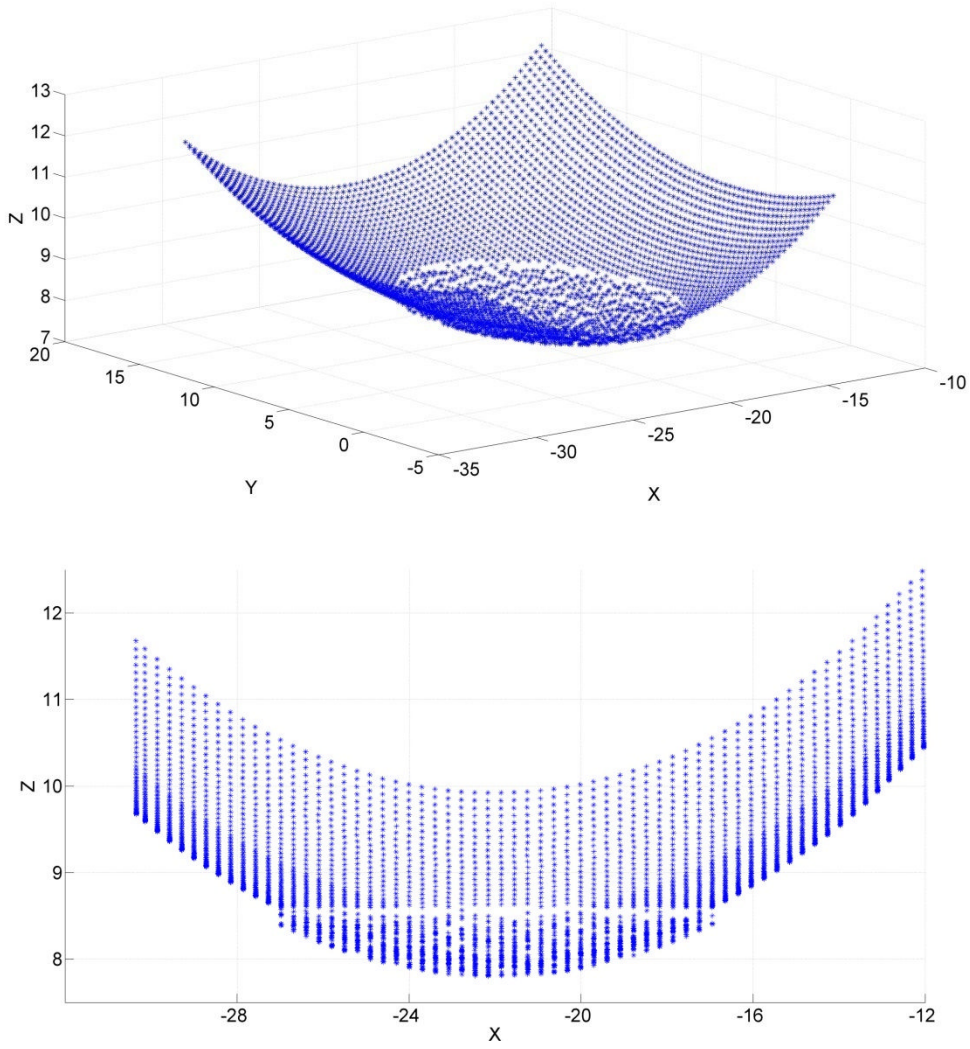

(m) wear area 30.13%

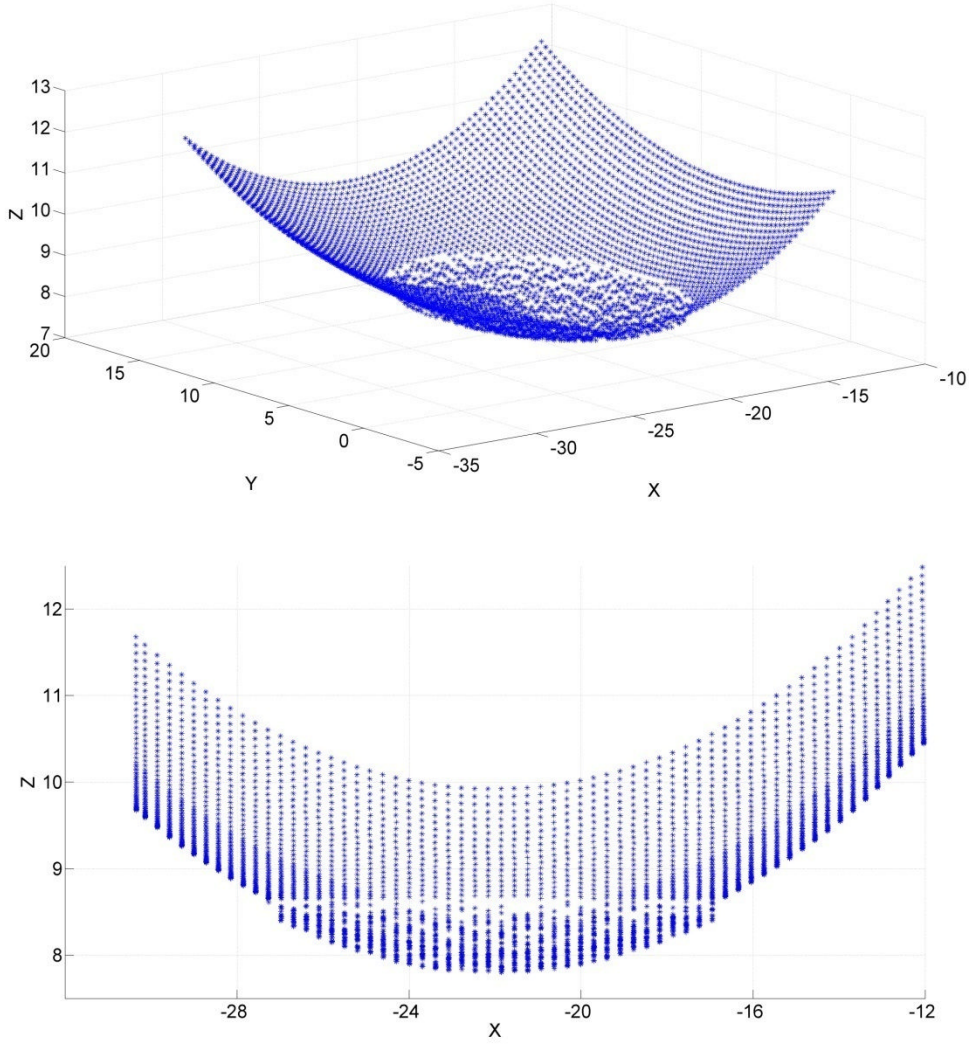

(n) wear area 32.23%

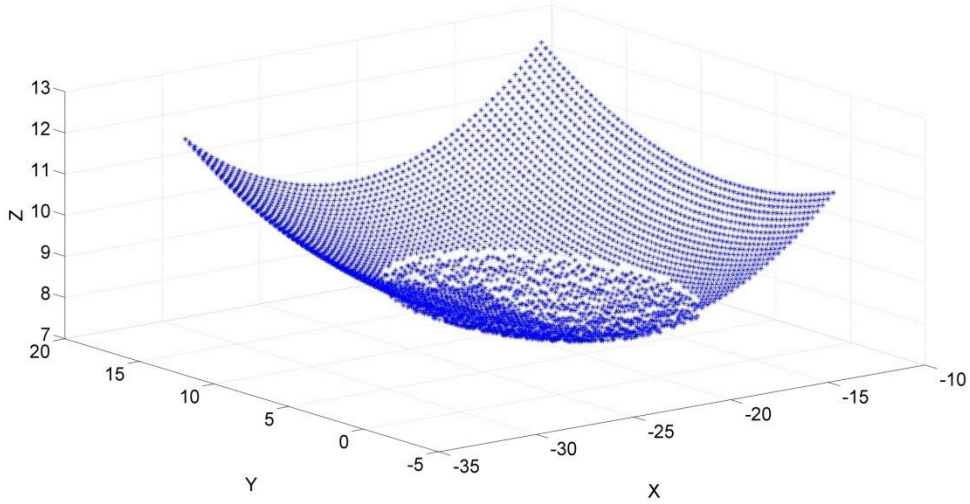

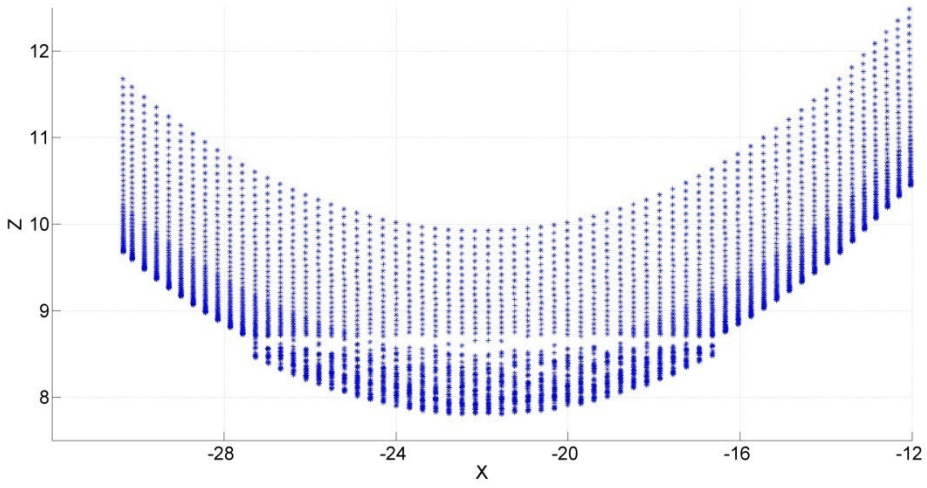

(o) wear area 34.61%

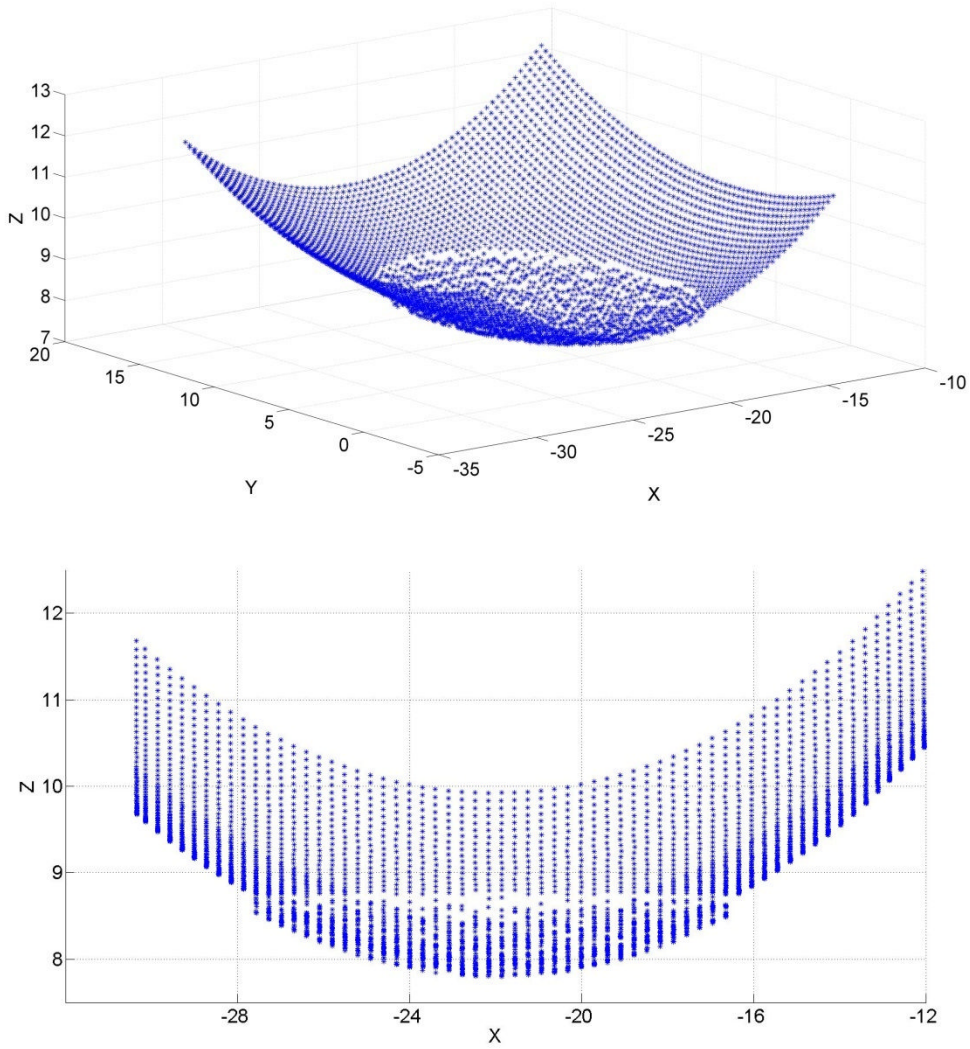

(p) wear area 36.51%

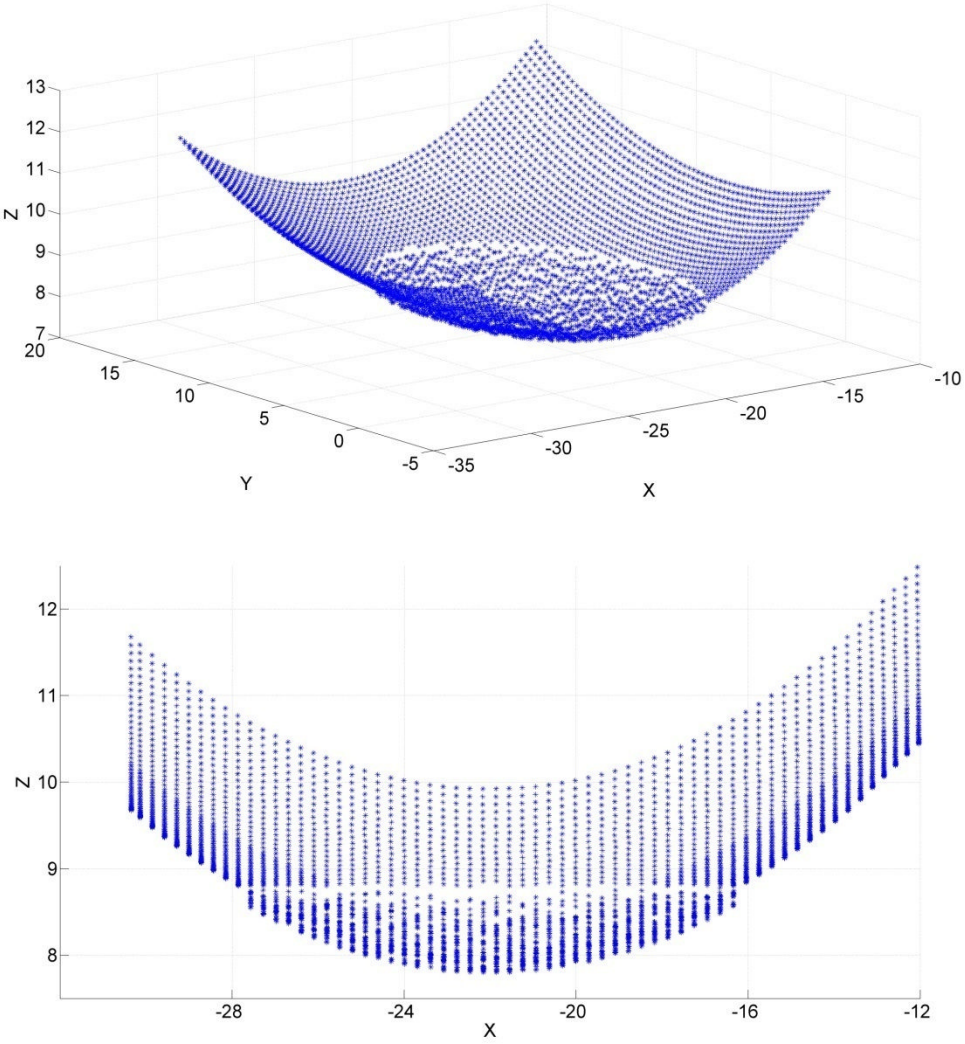

(q) wear area 38.55%

Figure A Three-dimensional and X-Z coordinates images of each computational wear test step.

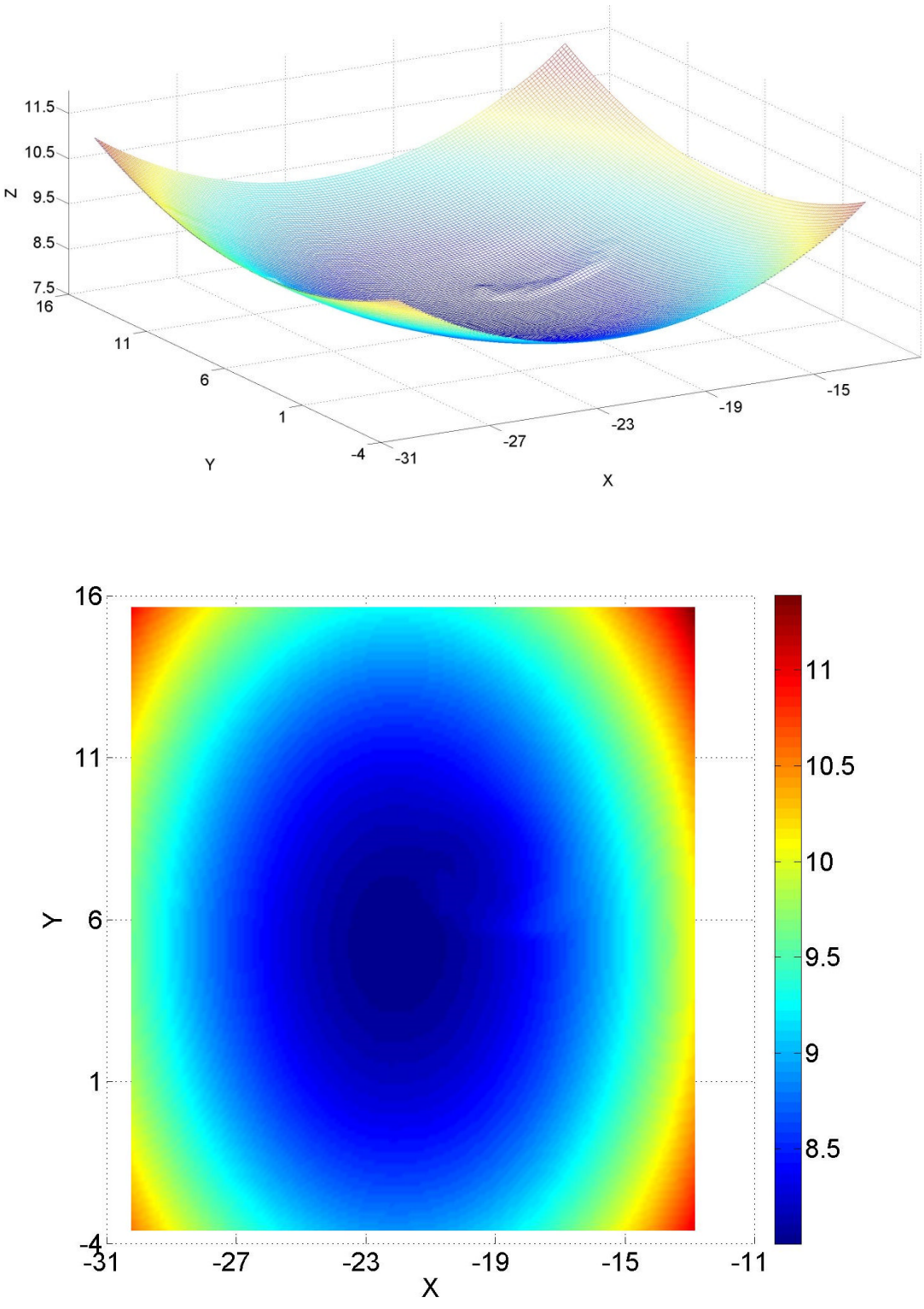

(a) physical volume removal test 1

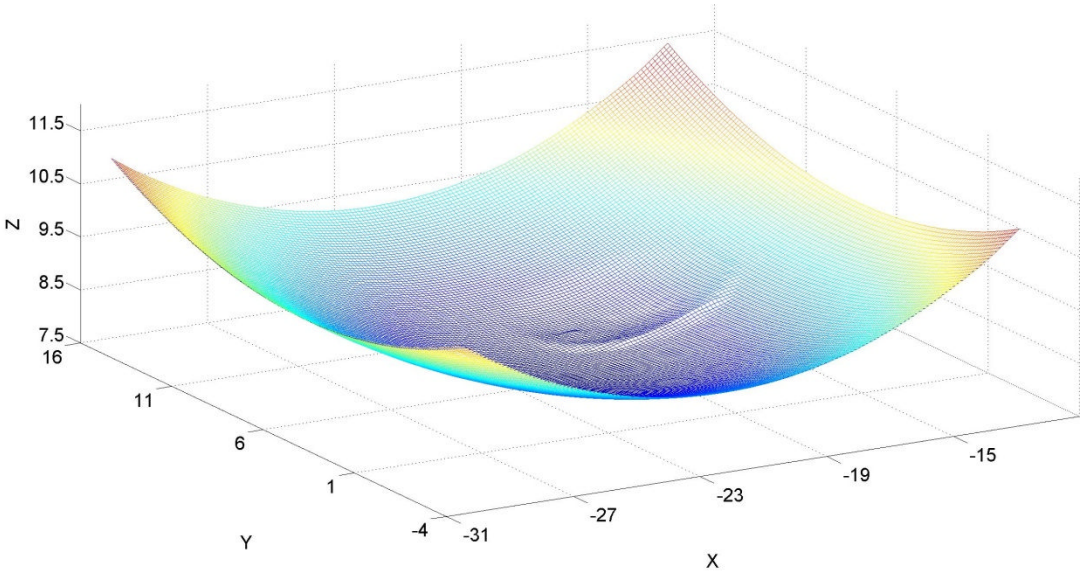

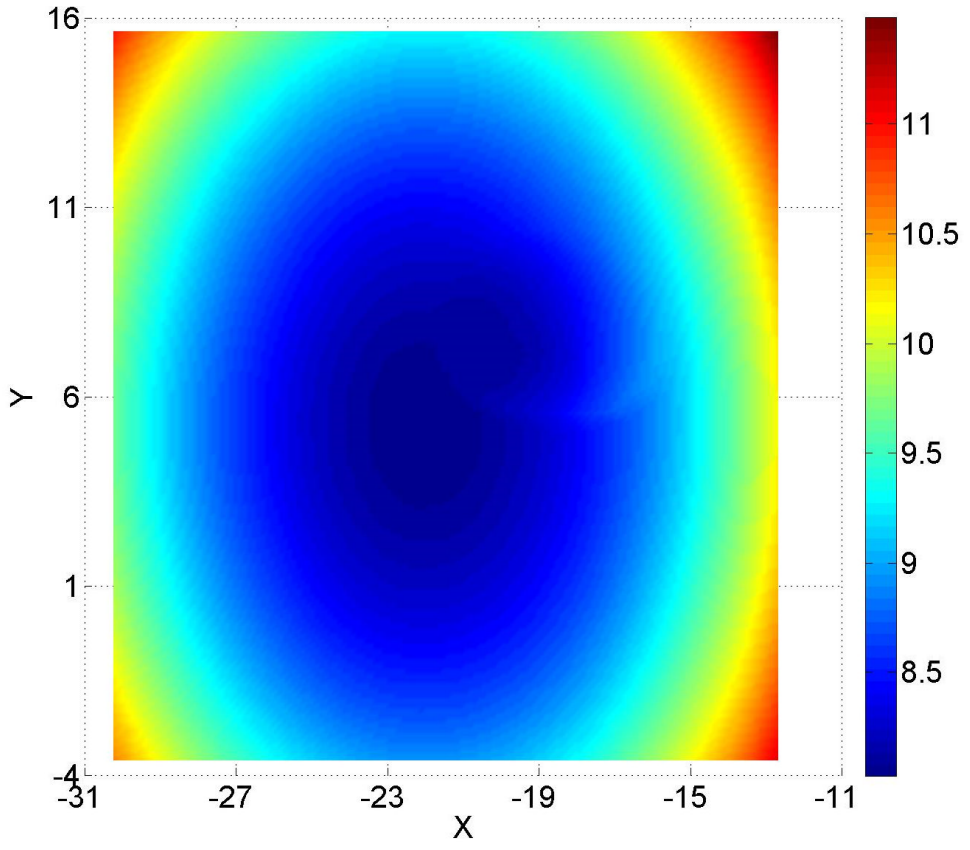

(b) physical volume removal test 2

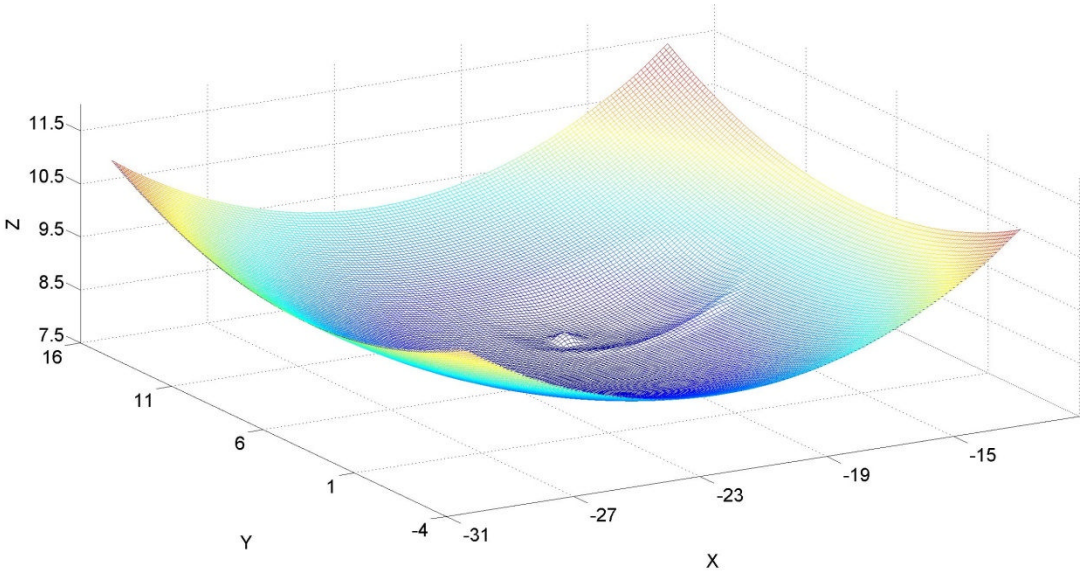

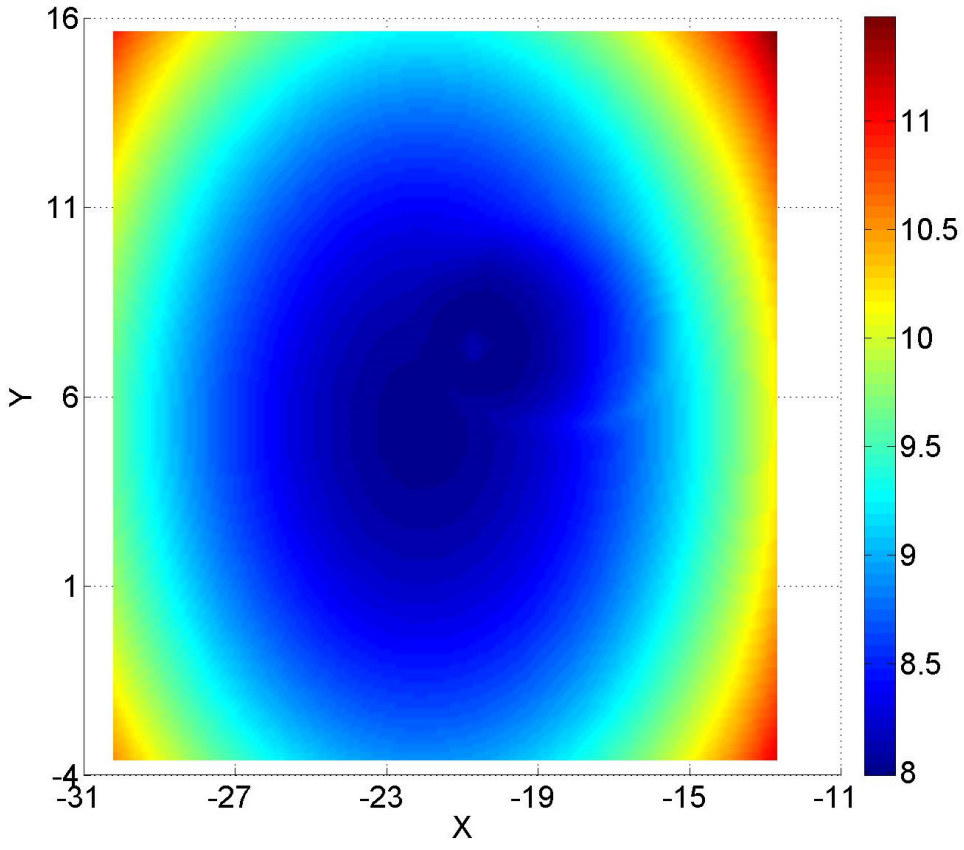

(c) physical volume removal test 3

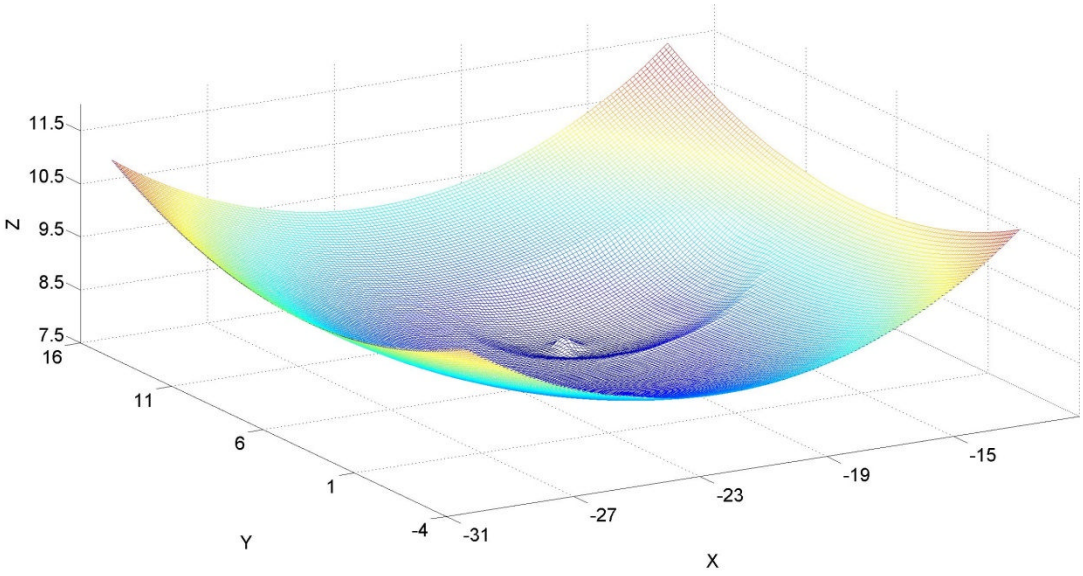

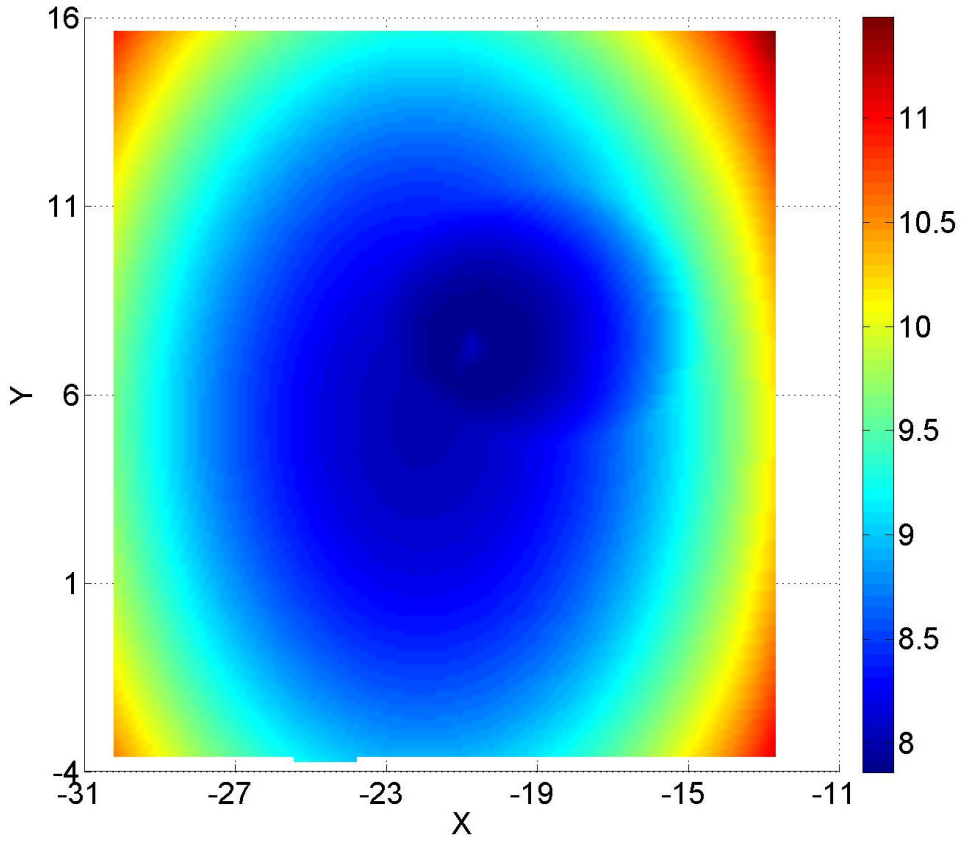

(d) physical volume removal test 4

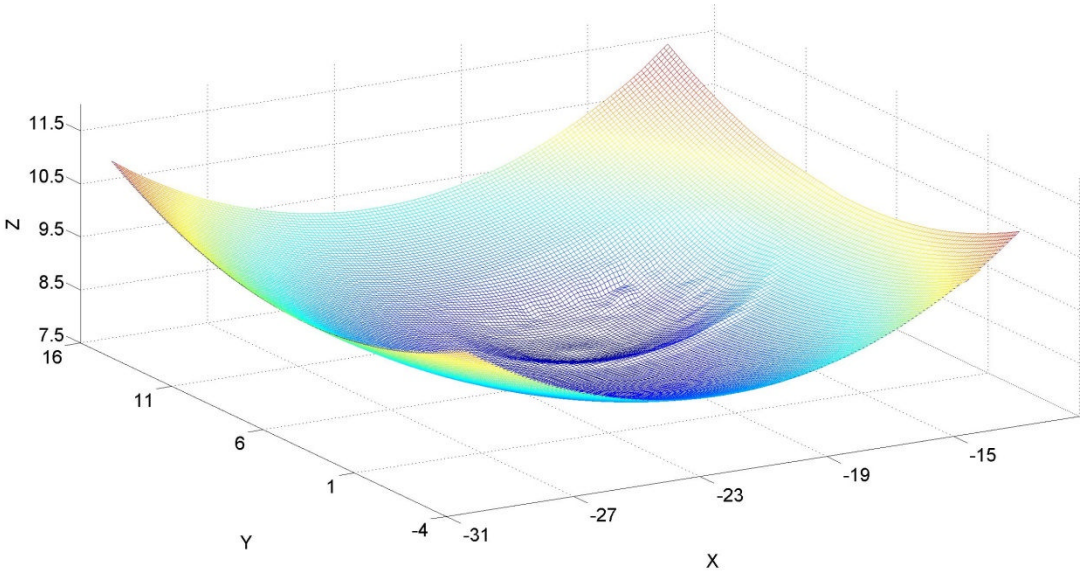

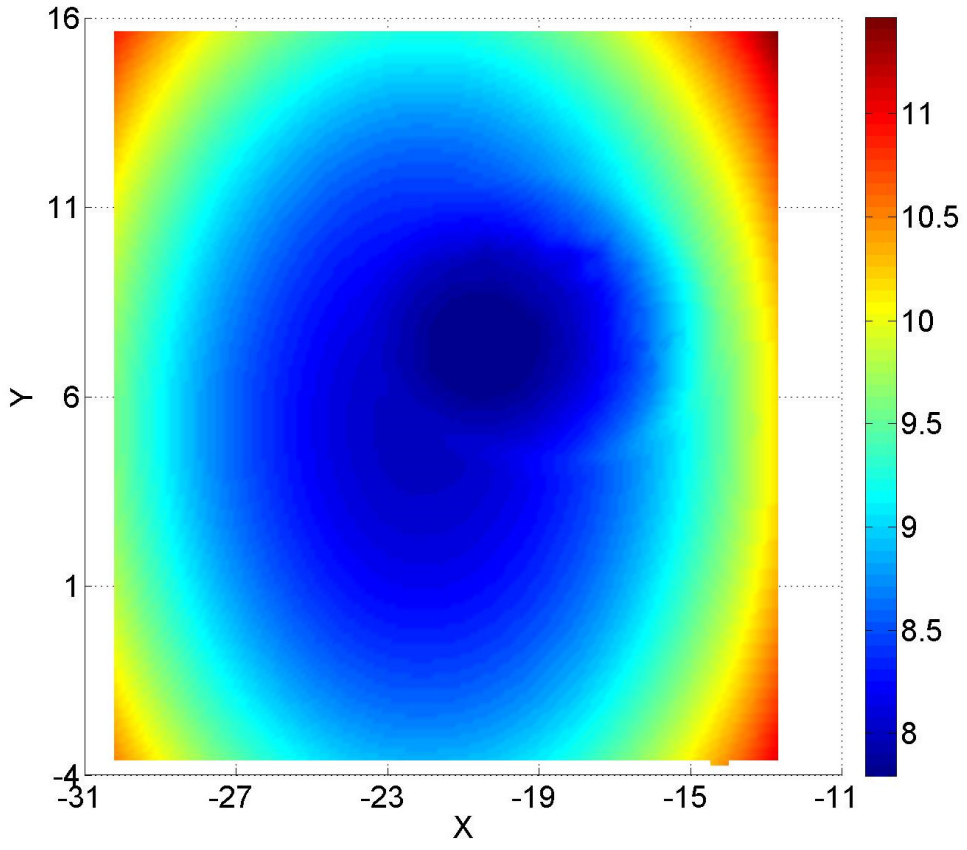

(e) physical volume removal test 5

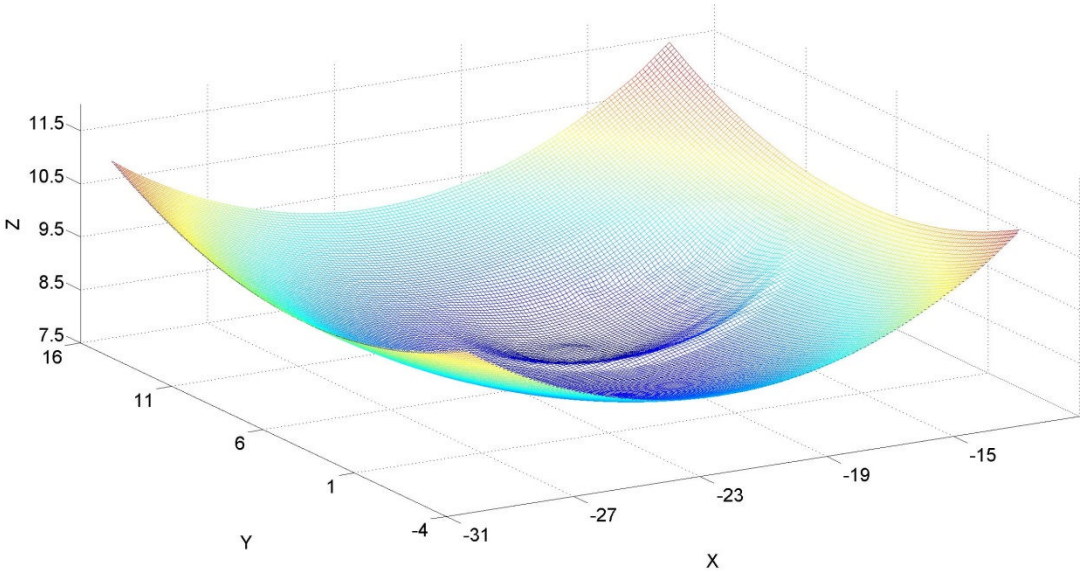

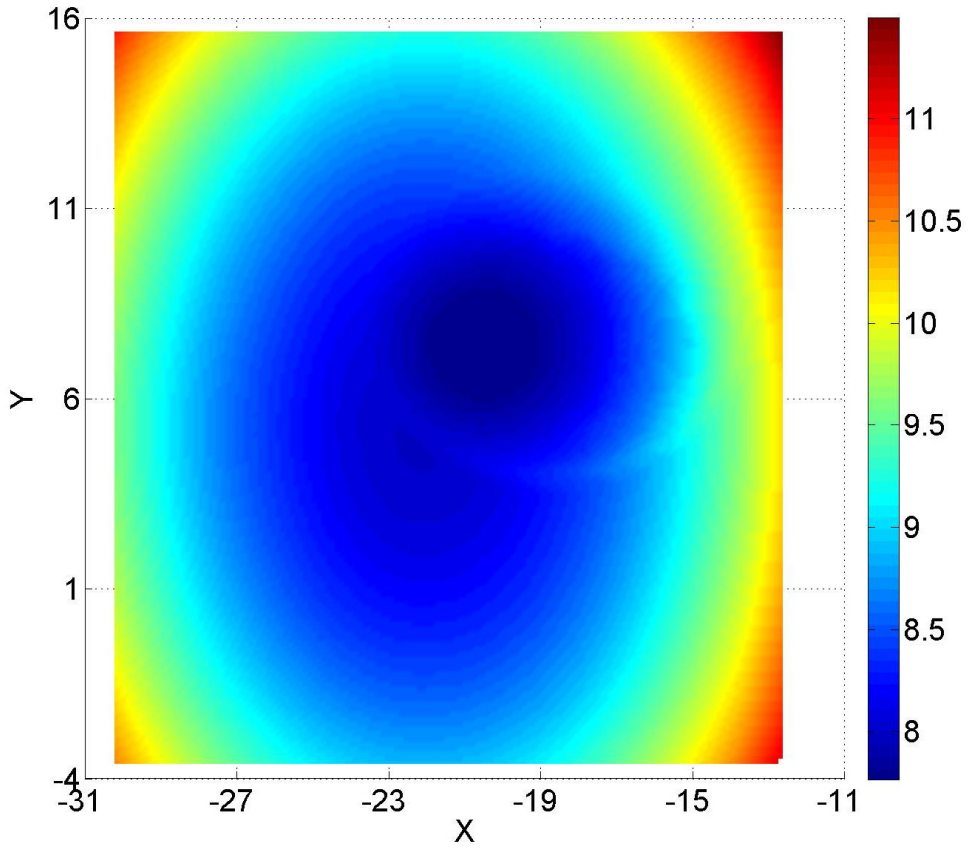

(f) physical volume removal test 6

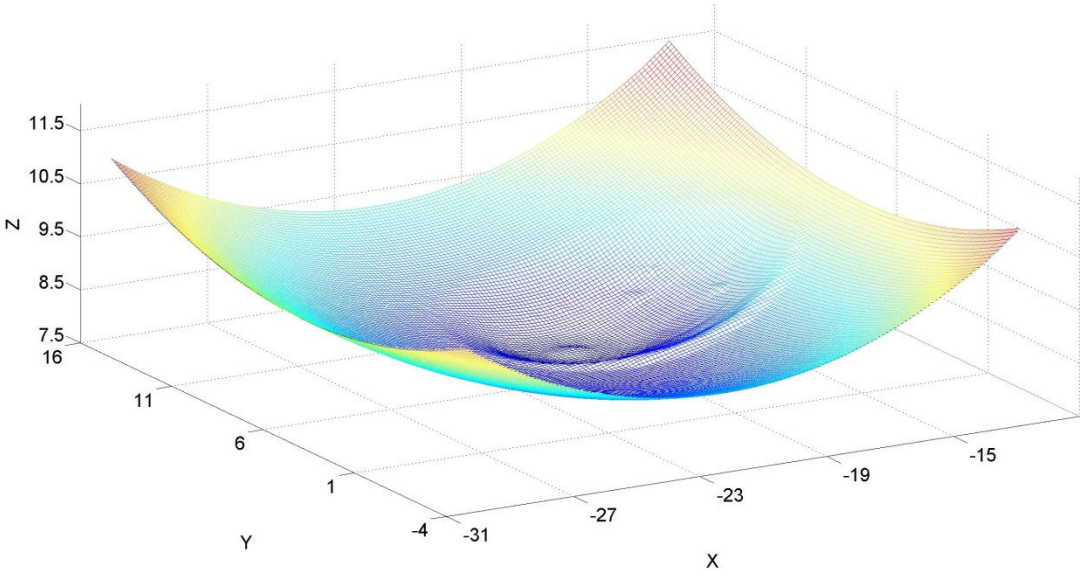

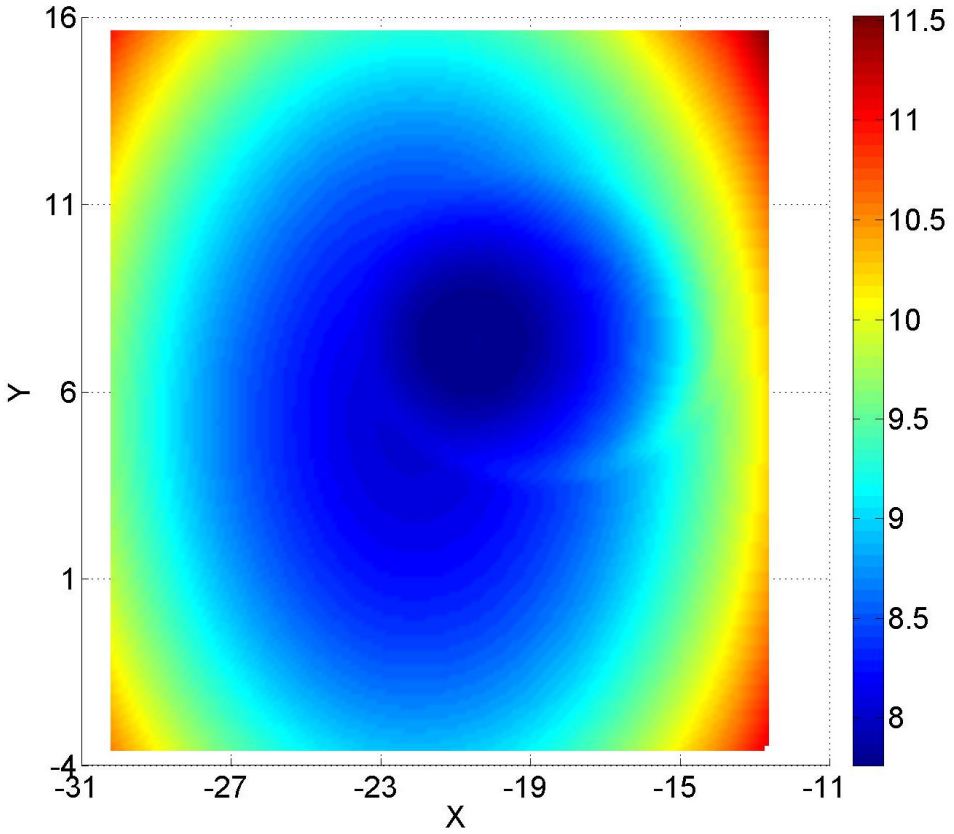

(g) physical volume removal test 7

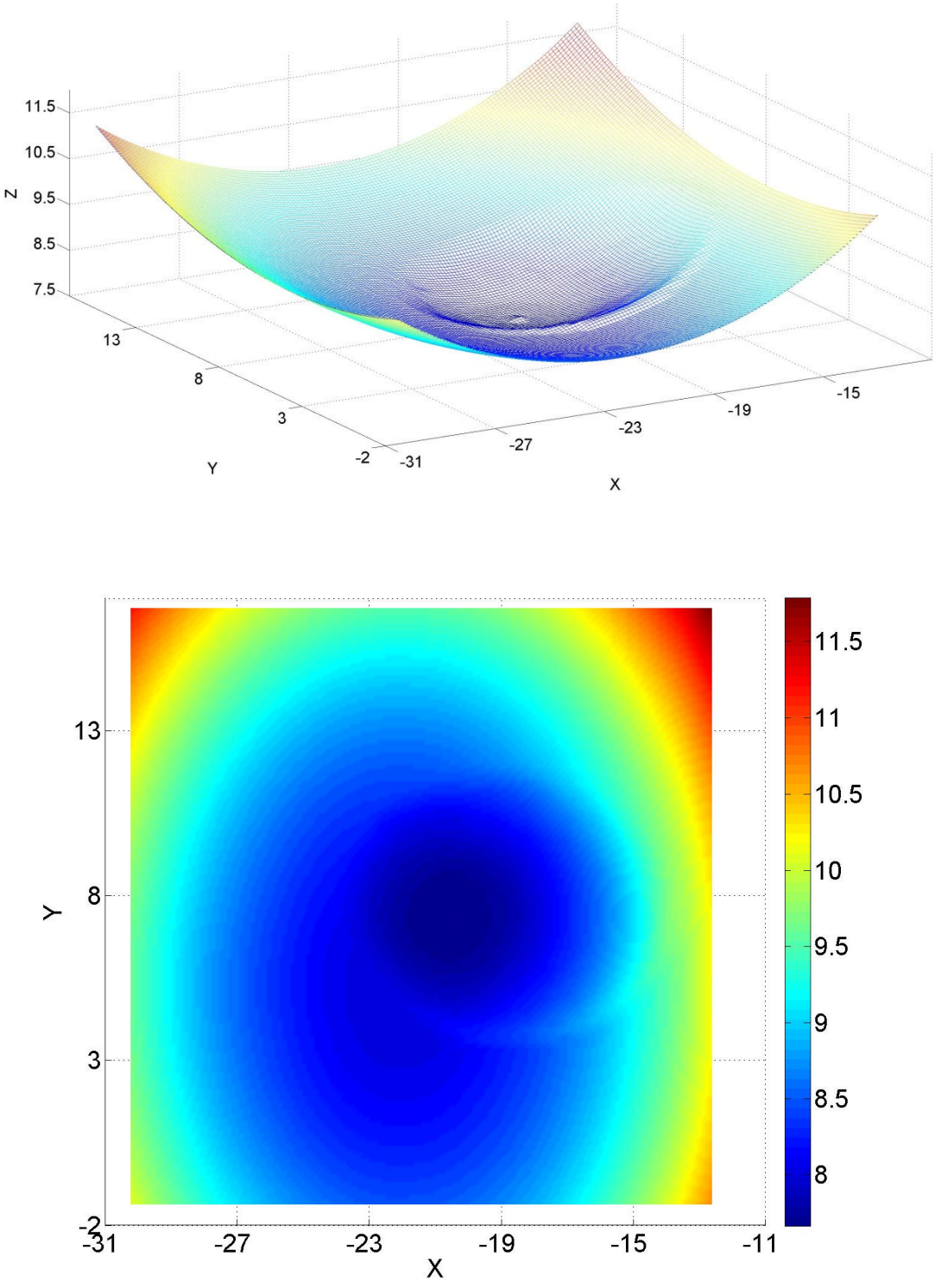

(h) physical volume removal test 8

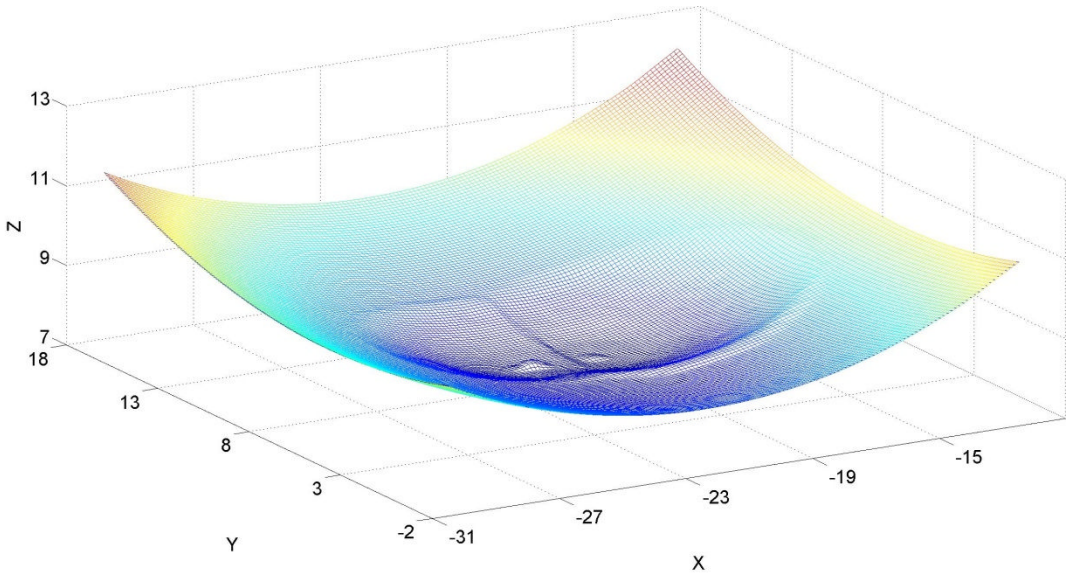

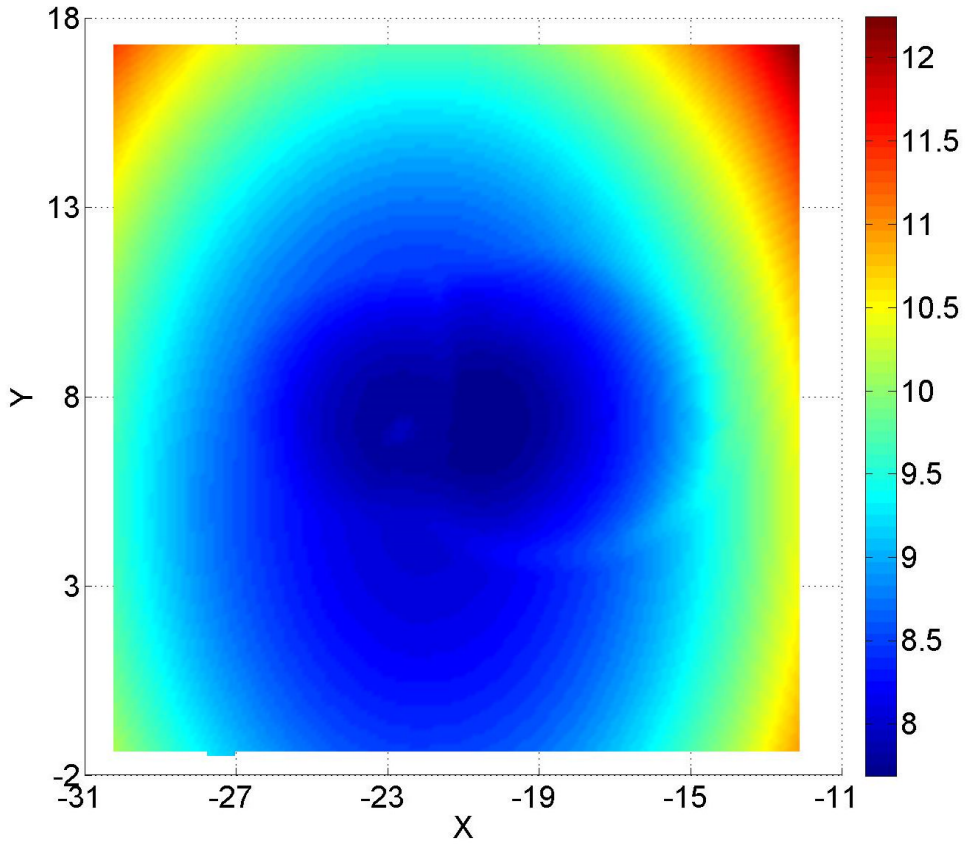

(i) physical volume removal test 9

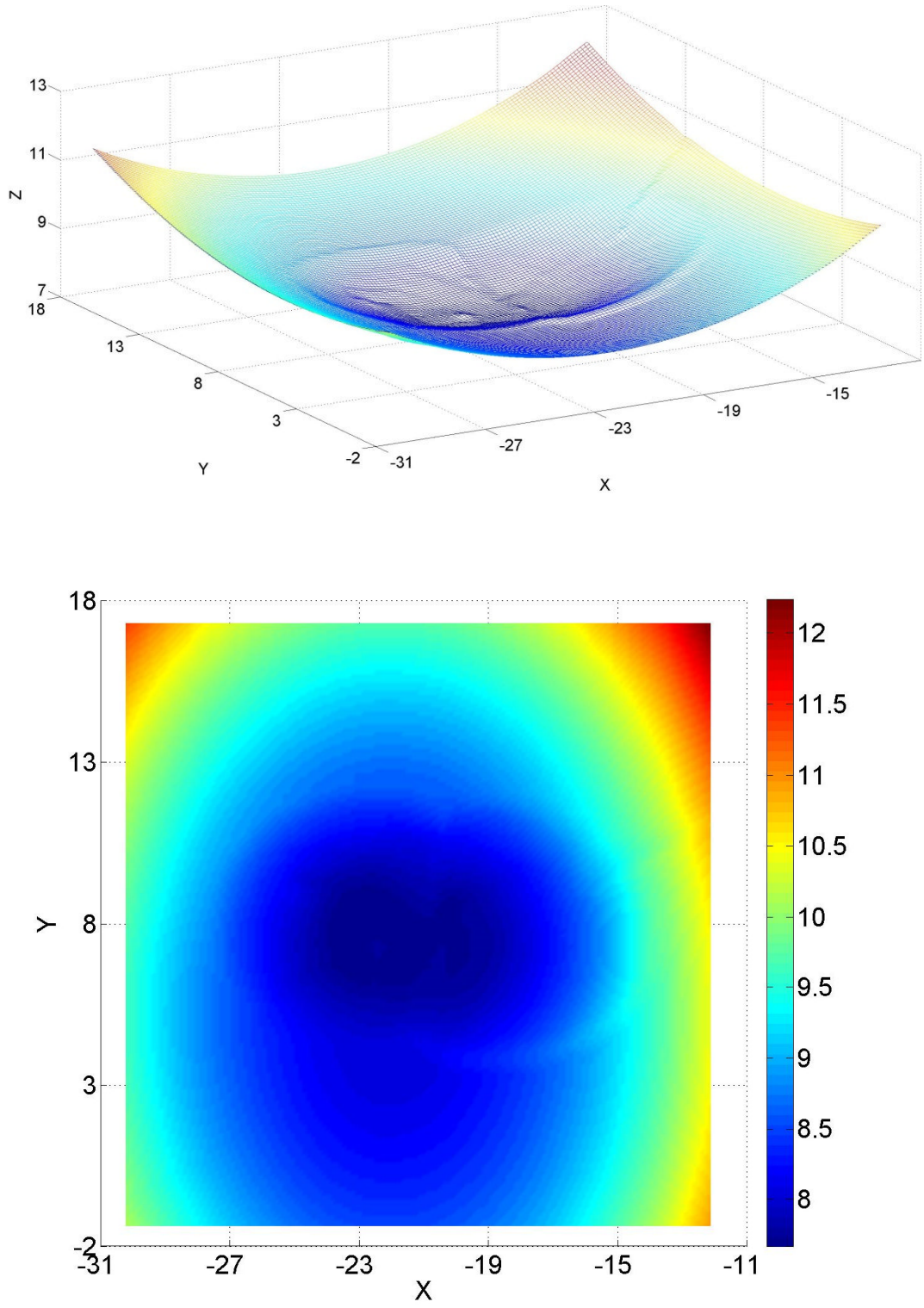

(j) physical volume removal test 10

Figure B Three-dimensional and X-Y images of each experimental wear test.